

Original research papers

-Part 1-

Paper I: Usefulness of *hsp65* marker as a complement to 16S rRNA sequences to demonstrate differences in Actinobacteria community according to anthropization of limestone caves and occurrence of visual marks in Lascaux Cave

1 **Usefulness of *hsp65* marker as a complement to 16S rRNA sequences to demonstrate**
2 **differences in *Actinobacteria* community according to anthropization of limestone caves and**
3 **occurrence of visual marks in Lascaux Cave**

4

5 Buresova Andrea^{1,2,3}, Kopecky Jan³, Sagova-Mareckova Marketa³, Alonso Lise¹, Vautrin Florian¹,
6 Moëgne-Loccoz Yvan¹, Rodriguez-Nava Veronica¹

7

8 ¹Univ Lyon, Université Claude Bernard Lyon 1, CNRS, INRAE, VetAgro Sup, UMR5557
9 Ecologie Microbienne, F-69622 Villeurbanne, France,

10 ²Department of Ecology, Faculty of Science, Charles University in Prague, Vinicna 7, Prague,
11 Czech Republic,

12 ³Laboratory for Diagnostics, Epidemiology and Ecology of Microorganisms, Crop Research
13 Institute, Drnovska 507, CZ-16106 Prague 6, Ruzyne, Czech Republic

14

15

16

17 **Abstract**

18 *Actinobacteria* are important cave inhabitants, but knowledge of how anthropization and
19 anthropization-related visual marks affect this community on cave walls is missing. We compared
20 *Actinobacteria* communities among four French limestone caves (Mouflon, Reille, Rouffignac,
21 and Lascaux) ranging from pristine to anthropized and within Lascaux Cave between marked and
22 unmarked areas on walls in different rooms (Sas-1, Passage, Apse, and Diaclase). In addition to
23 the 16S rRNA gene marker, 441-bp fragments of a heat shock protein gene (*hsp65*) were used for
24 the identification of *Actinobacteria* to the species level by Illumina MiSeq analysis. The *hsp65*
25 marker revealed higher resolution for species and richness (at 99% OTUs cutoff) assessment than
26 did 16S rRNA, which on the other hand identified more taxa on higher taxonomic ranks.
27 *Actinobacteria* communities varied between Mouflon and Reille (both pristine), Rouffignac
28 (anthropized/visited), and Lascaux (strongly anthropized and now closed to the public).
29 Rouffignac displayed high diversity of *Nocardia*, including species with potential pathogeny (i.e.
30 *N. carnea*, *N. paucivorans*, *N. abscessus*), and Lascaux high *Mycobacterium* abundance, whereas
31 *Gaiellales* were typical in pristine caves and the Diaclase i.e. the least affected room of Lascaux
32 Cave. Within Lascaux, the *Pseudonocardiaceae* dominated on unmarked walls and the
33 *Streptomycetaceae* (especially *Streptomyces mirabilis*) on marked surfaces, raising questions on
34 the possible role of *S. mirabilis* in the formation of visual marks. Our results show how the use of
35 the *hsp65* marker, well beyond the resolution provided by 16S rRNA sequences, enabled for the
36 first time to document species-level variations of the *Actinobacteria* community according to the
37 extent of anthropogenic pressure. This approach proved effective when comparing different
38 limestone caves or specific conditions within a cave.

39

40 Introduction

41

42 Limestone caves are considered to be rather isolated habitats that are extremely limited in
43 organic carbon (Barton et al., 2007), which leads to the development of microbial strategies
44 enabling adaptation to oligotrophic conditions and a high calcium content (Barton & Jurado, 2007;
45 De Mandal, Chatterjee, & Kumar, 2017; Ortiz et al., 2014). Some of these caves contain Paleolithic
46 artwork and thus are frequently visited by tourists (Alonso et al., 2019; Schabereiter-Gurtner, Saiz-
47 Jimenez, Pinar, Lubitz, & Rölleke, 2002). As a result, human-derived dispersion of endogenous as
48 well as exogenous nutrients and microorganisms inside the caves together with the human
49 metabolism may change their internal microclimatic and microbiological conditions (Hoyos,
50 Cañaveras, Sánchez-Moral, Sanz-Rubio, & Soler, 1998; Mulec, 2014). Microorganisms can be
51 resilient to changes to some extent (Johnston, Muench, Banks, & Barton, 2012; Tomczyk-Żak &
52 Zielenkiewicz, 2016). Community shifts may also take place, which deserves attention if it could
53 favor microorganisms with biodeterioration ability (F. Bastian, Jurado, Novakova, Alabouvette, &
54 Saiz-Jimenez, 2010; Fernandez-Cortes et al., 2011; Sánchez-Moral et al., 1999) or increase the
55 proportion of species harboring strains with pathogenic potential (Bercea, Năstase-Bucur,
56 Moldovan, Kenesz, & Constantin, 2019; Neral, Rajput, & Rai, 2015; Rajput, Rai, & Biswas, 2012).
57 If it were the case, such shifts could represent a threat for cave conservation and the health of
58 visitors, respectively.

59 *Actinobacteria* represent an important cave taxonomic group, from which many potentially
60 pathogenic (Valme Jurado et al., 2010), biotechnologically relevant (Bhullar et al., 2012; Hamedi,
61 Kafshnouchi, & Ranjbaran, 2019; Syiemiong & Jha, 2019) and novel (Fang et al., 2017; V. Jurado
62 et al., 2008; Valme Jurado, Kroppenstedt, et al., 2009; Rangseekaew & Pathom-aree, 2019) species
63 have been found in these environments. *Actinobacteria* can dominate both in anthropized

64 (Gonzalez-Pimentel et al., 2018) and pristine caves (De Mandal et al., 2017), but some
65 actinobacterial taxa are specific only one type of cave. For example, *Pseudonocardiaceae* are
66 known as indicators of urban contamination (Miller et al., 2018) and dominate in some anthropized
67 caves, but this dominance is most likely due to their ability to degrade exogenous organic
68 compounds (Lavoie et al., 2017; Porca, Jurado, Žgur-Bertok, Saiz-Jimenez, & Pašić, 2012). This
69 is partially true as well for *Streptomycetaceae*, which were also found among pristine cave
70 inhabitants (Maciejewska et al., 2017). Furthermore, these taxonomic groups seem to be prominent
71 in pigment-forming communities on the walls of certain show caves (Cuezva et al., 2012; Porca et
72 al., 2012). In contrast, *Euzebyales* (Gonzalez-Pimentel et al., 2018), *Nocardiaceae* (De Mandal et
73 al., 2017) and *Gaiellales* (Zhu et al., 2019) represent oligotrophic taxa that dominate in pristine
74 caves, most likely because of their ability to degrade complex compounds which are indigenously
75 present in the cave or fix CO₂.

76 *Actinobacteria* taxonomic identification in these environments has largely been based on
77 culture-dependent approaches and 16S rRNA sequencing (De Mandal et al., 2017; Yasir, 2018).
78 The culture-dependent approaches limits the coverage of the community and thus should be used
79 only as a supportive determinant with molecular approaches (Hamedi et al., 2019; Long et al.,
80 2019). The 16S rRNA gene is the marker most frequently used for bacterial systematics but
81 generally cannot resolve individual sequences at the species level (Fox, Wisotzkey, & Jurtschuk,
82 1992; Hirsch, Mauchline, & Clark, 2010). In addition, identical 16S rRNA gene sequences can be
83 found in different taxa or different 16S rRNA gene sequences in a single species (Větrovský &
84 Baldrian, 2013). Other protein-coding genes with high sequence polymorphisms (i.e., *rpoB*, *gyrB*,
85 *hsp65*) permit the distinction between closely-related strains. However, some of these protein-
86 coding markers may also have their limits as it is the case of *rpoB* gene who is present twice is

87 some genus belonging to Actinobacteria, they only target limited number of *Actinobacteria* or no
88 appropriate reference database is available for taxonomic identification (Gao & Gupta, 2012;
89 Takeda, Kang, Yazawa, Gono, & Mikami, 2010; Vos, Quince, Pijl, de Hollander, & Kowalchuk,
90 2012). Nevertheless, the gene of a molecular chaperone, the 65-kDa heat-shock protein (*hsp65*),
91 when amplified by specific primers (Telenti et al., 1993), has been used as a molecular marker for
92 identifying a large number of *Actinobacteria* isolates (Rodríguez-Nava et al., 2006, 2007). This
93 gene is present in *Actinobacteria* genomes as a single copy, unlike the 16S rRNA gene marker
94 (Colaco & MacDougall, 2014), and *hsp65* is considered to be a good candidate for making detailed
95 *Actinobacteria* community assessments from environmental DNA. Additionally, the amplified
96 fragment length of *hsp65* (441 bp) is sufficient for amplicon sequencing.

97 Lascaux Cave underwent several events of microbial outgrowth since the 1960s, as well as
98 (sometimes unsuccessful) chemical treatments, which resulted in the formation of various visual
99 marks (including stains) and threatened Paleolithic artwork (F. Bastian et al., 2010; Martin-
100 Sanchez, Miller, & Saiz-Jimenez, 2015). For the sake of cave conservation, Lascaux was closed
101 to the public in 1963. Although the few microbiological studies conducted in this cave suggest that
102 *Actinobacteria* is one of prevalent groups (Alonso et al., 2018, 2019; Martin-Sanchez, Nováková,
103 Bastian, Alabouvette, & Saiz-Jimenez, 2012), a more complete investigation of the *Actinobacteria*
104 community is lacking, especially at the species level. If we consider that key functional traits can
105 be related to precise species within the *Actinobacteria*, we can hypothesize that such an assessment
106 would allow a better discrimination of *Actinobacteria* communities according to ecological
107 conditions.

108 The objective of this work was to assess the usefulness of *hsp65* marker (as a complement
109 to 16S rRNA sequence data) for a deeper, species-level appraisal of the *Actinobacteria* community

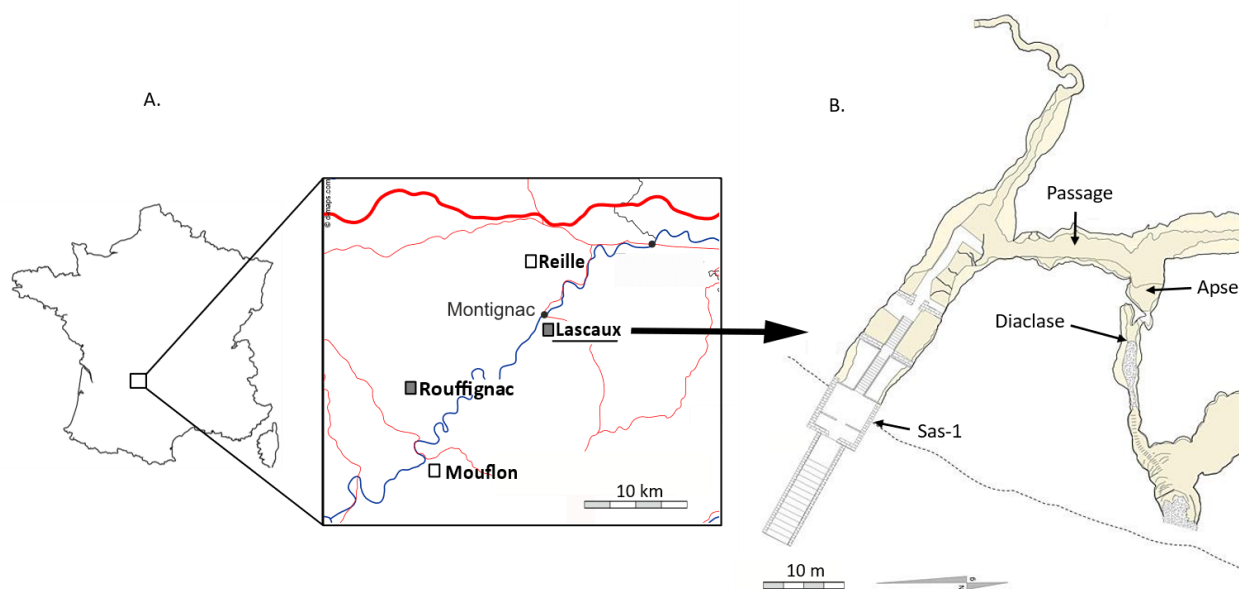
110 in caves, and to show variations according to cave conditions and especially human-induced
111 disturbances (Mammola, 2019). These aims were achieved by comparing *Actinobacteria*
112 communities in pristine limestone caves (Reille and Mouflon Caves) and anthropized caves
113 (Lascaux and Rouffignac Caves), and within Lascaux Cave of marked and unmarked areas in
114 different rooms (i.e., Sas-1, Passage, Apse, and Diaclase). To this end, *Actinobacteria* were
115 identified for the first time to the species level in cave environments, using metabarcoding analysis
116 of the *hsp65* gene marker.

117

118 **Materials and methods**

119 **Study site description and sample collection**

120 Samples were collected in May - June 2016 from the walls of four limestone caves located
121 in the Dordogne department of southwestern France: Lascaux (45°03'13" N 1°10'12"E, 235 m
122 length); Rouffignac (45°00'31"N 0°59'16"E, 8,000 m length); Reille (45°07'09.5"N 1°07'11.2"E,
123 2,000 m length) and Mouflon (44°55'N 1°5'E, 280 m length) (Fig. 1A).



124
125 Fig. 1. Map of A. Dordogne area with the cave locations (Lascaux, Rouffignac, Reille and
126 Mouflon; white squares – pristine and gray squares – anthropized). Map of B. Lascaux Cave
127 (entrance Sas-1, Passage, Apse, and Diaclase).

128
129 Lascaux and Rouffignac caves contain Paleolithic wall paintings and engravings and are
130 listed as UNESCO World Heritage Sites. Both caves are anthropized, Rouffignac being open for
131 touristic visits since 1959 (with up to 500 visitors per day) (5) and Lascaux being closed after 15
132 years of tourism (with up to 2000 visitors per day). Various visual marks have developed at
133 different times in Lascaux Cave, and extensive chemical treatments have been applied (13,42, 44,

134 45). Mouflon and Reille Caves are in a pristine state (5). The entrance of Mouflon Cave was locked
135 shortly after discovery, whereas Reille is occasionally explored by seasoned speleologists.

136 In Lascaux Cave, samples were taken from the walls of four distinct rooms representing
137 different cave environments that were located progressively farther from the entrance in the
138 following order: Sas-1, Passage, Apse and Diaclase (Fig. 1B). Sas-1 is a man-made, calcareous
139 airlock entrance and is isolated by doors from the cave interior and exterior. The Passage is a
140 central alley connecting different rooms of Lascaux Cave. In the Passage, samples were taken from
141 two mineral substrates: clay deposits (banks, later referred to as Passage B) and near-vertical
142 limestone walls (inclined planes, later referred to as Passage IP). In the Apse, samples were
143 collected from limestone inclined planes. The Diaclase is a distinct compartment located below
144 the main part of the cave and was least-affected by humans. It is separated from the Apse by a trap
145 door, received limited biocide treatments, and was never open to tourists. Samples originated from
146 limestone walls located immediately below the Apse, in an area of the Diaclase termed the Shaft
147 of the Dead Man.

148 Within each room, samples were collected from visual marks and unstained surfaces, as
149 described (Alonso et al., 2018). Approximately 50 mg of wall material samples (3-6 replicates)
150 were collected using sterile scalpels and placed in liquid nitrogen for transportation to the
151 laboratory, where they were stored at -80°C until DNA extraction. Overall, six samples from
152 Rouffignac, six from Mouflon, five from Reille and 41 from Lascaux (five from Sas-1, six from
153 Passage B, six from Passage IP, 18 from Apse and six from Diaclase) were used for subsequent
154 microbial analysis (Table S1). Sampling was performed in accordance with the caves' rules and
155 regulations.

156

157 **DNA extraction and amplicon sequencing**

158 DNA extraction was performed using the FastDNA SPIN Kit for Soil (MP Biomedicals,
159 Illkirch, France) following the manufacturer's instructions and was adapted to the low sample
160 amounts, as described (Alonso et al., 2018). The elution step was achieved using two volumes of
161 50 µl elution buffer for each sample.

162 For bacterial 16S rRNA gene amplification, we used the primers 341F
163 (CCTACGGGNGGCWGCAG) and 805R (GACTACHVGGGTATCTAATCC), which target the
164 V3-V4 region (428-bp fragments) (Herlemann et al., 2011). Amplification and sequencing were
165 carried out by the Fasteris Company (Geneva, Switzerland) using the Illumina MiSeq Reagent Kit
166 v3 (600 cycles) with the paired-end mode, resulting in 2×300 bp sequence reads, as described by
167 *Alonso et al.* (Alonso et al., 2018).

168 The 441-bp fragments of the 65-kDa heat shock protein gene (*hsp65*) were amplified by
169 PCR using the specific primers TB11 (ACCAACGATGGTGTGTCCAT) and TB12
170 (CTTGTCGAACCGCATACCCT) from *Telenti et al.* (Telenti et al., 1993). Amplification was
171 carried out in a reaction mixture with a total volume of 25 µl in packaged PCR tubes (Ready-to-
172 Go PCR Beads; Amersham Biosciences, Piscataway, NJ) (2.5 U of Taq polymerase puRe Taq, 10
173 mM Tris-HCl [pH 9], 50 mM KCl, 1.5 mM MgCl₂, and 200 µM of each deoxynucleoside
174 triphosphate) with primers (0.2 – 0.4 µM, depending on the template concentration) and DNA (1
175 – 40 ng). The PCR cycling protocol consisted of an initial denaturation at 94°C for 5 min, then 35
176 cycles of denaturation (94°C for 60 s), annealing (55°C for 60 s), and elongation (72°C for 60 s)
177 (Rodríguez-Nava et al., 2006). Sequencing was carried out (together with purification and quality
178 control) by the Biofidal Company (Biofidal, Vaulx-en-Velin, France – [lab.com](http://www.biofidal-
179 lab.com)) using the Illumina MiSeq Flow Cell V3 with the paired-end mode, resulting in 2 x 300

180 bp sequence reads. Overall, 50 samples for 16S rRNA gene and 45 samples for *hsp65* were
181 successfully sequenced, but sequences for both markers were obtained for only 37 samples (Table
182 S1).

183

184 **Processing and analysis of sequence data**

185 The paired sequence reads from sequencing were merged using FLASH (Fast Length
186 Adjustment of Short reads (Magoč & Salzberg, 2011)) with a maximum of 25% mismatches in the
187 overlapping region. The sequences were then filtered and aligned using reference alignments of
188 the *hsp65* gene sequences (this work) or using the 16S rRNA gene sequences from the Silva
189 database (Quast et al., 2012). Chimeric sequences were removed using the integrated Vsearch tool
190 (Rognes, Flouri, Nichols, Quince, & Mahé, 2016) according to the MiSeq standard operating
191 procedure (MiSeq SOP, February 2018) (Kozich, Westcott, Baxter, Highlander, & Schloss, 2013)
192 in Mothur v. 1.39.5 software (Schloss et al., 2009). Taxonomical assignments of sequence libraries
193 were performed in Mothur using the *hsp65* reference database for the *hsp65* sequences and the
194 recreated SEED database subset of the Silva Small Subunit rRNA Database, release 132 (Yilmaz
195 et al., 2014), adapted for use in Mothur (https://mothur.org/w/images/a/a4/Sylva.seed_v132.tgz),
196 as the reference database for the 16S rRNA gene sequences.

197 The sequences of plastids and mitochondria and those not classified in the domain Bacteria
198 (from the 16S rRNA sequence library), as well as sequences identified as homologs for *hsp65*
199 (*groEL*, in the database renamed as GROESL; see the *hsp65* reference database design section)
200 (from the *hsp65* sequence library), were discarded. The sequence library was clustered into
201 operational taxonomic units (OTUs) using the Uparse pipeline in Usearch v10.0.240 software
202 (OTUs at a 97% cutoff) (35) and Mothur (OTUs at a 99% cutoff). The OTU table was further

203 processed using tools implemented in Mothur. For 16S rRNA genes, only sequences
204 corresponding to *Actinobacteria* were used.

205 For comparison of *Actinobacteria* among the caves, 25 samples for *hsp65* and 24 samples
206 for 16S rRNA genes were used. Apse and Diaclase (both unmarked areas) were chosen as
207 representative samples for Lascaux Cave except for core microbiome analysis, for which all the
208 Lascaux Cave samples were included. To test the differences among locations in Lascaux Cave,
209 33 samples for *hsp65* and 38 samples for 16S rRNA were used. Among those, from marked areas
210 16 samples for *hsp65* and 20 samples for 16S rRNA were used. From unmarked areas 17 samples
211 for *hsp65* and 18 samples for 16S rRNA were used (Table S1). For 16S rRNA marker, Sas-1
212 unmarked area samples are missing for the analysis, because low number of replicates were
213 successfully sequenced. To obtain the highest number of replicates per sample, all samples, even
214 when they were not common to both markers, were included in the analysis. 37 common samples
215 for both markers were used for analyses comparing the usefulness of both markers (rarefaction
216 analysis, comparison of diversity indices and number of taxa recovered at different taxonomy
217 ranks).

218 Rarefaction analysis was performed to analyze the richness of the *Actinobacteria* OTUs
219 based on two cutoffs (i.e., 97% and 99%) as a function of sample number. The alpha diversity
220 indices (richness: Chao 1, evenness: Simpson Evenness, and diversity: Inverse Simpson) were
221 calculated in Mothur (97%, 99% OTU cutoff). Significant differences among samples were
222 calculated by ANOVA with Tukey's post hoc test ($P < 0.05$; Caves and locations in Lascaux Cave),
223 t tests and F tests ($P < 0.05$; marked/unmarked areas) in Past 4.02 software (Hammer, Harper, &
224 Ryan, 2001).

225 Bray-Curtis distance matrices describing the differences in bacterial community
226 composition among individual samples were calculated. The *Actinobacterial* communities in the
227 caves, in the different locations of Lascaux Cave, and between marked and unmarked areas within
228 each location were compared by nonmetric multidimensional scaling (NMDS) according to both
229 gene markers (97% OTU cutoff). Analysis of molecular variance (AMOVA) and homogeneity of
230 molecular variance (HOMOVA) were calculated in Mothur with 100,000 iterations for the same
231 factors (97% OTU cutoff).

232 Pairwise comparisons with Metastats (Segata et al., 2011) and biomarker searching
233 analysis with Lefse (Segata et al., 2011) were calculated to identify the *Actinobacteria* OTUs that
234 were significantly different among the respective caves, locations and marked/unmarked areas in
235 Lascaux Cave (99% OTU cutoffs). Metastats was also used to compare the relative abundances of
236 *Streptomyces* sequences among the marked/unmarked areas (*hsp65* marker). Venn diagrams were
237 created in Mothur to test the number of OTUs that encompassed the core microbiome for the
238 different caves and four rooms (e.g., Sas-1, Passage, Apse, and Diaclase) in Lascaux Cave (99%
239 OTU cutoff).

240 Taxonomical classification of OTUs was performed with Mothur by using the *hsp65* and
241 16S rRNA reference databases, and the *hsp65* marker was verified by BLASTN in the online
242 databases of the National Center for Biotechnology Information (NCBI; U.S. National Library of
243 Medicine, MD, USA). The taxonomical composition of the core microbiome was constructed
244 using the Krona tool (Ondov, Bergman, & Phillippy, 2011). The number of taxa recovered with
245 the common samples by *hsp65* and 16S rRNA at different taxonomic ranks were calculated and
246 displayed by Venn diagrams.

247 Co-occurrence networks were used to predict how marked/unmarked areas and different
248 locations influenced the relative abundances of *Actinobacteria* in Lascaux Cave. Spearman
249 correlation coefficients were computed in Mothur for Lascaux Cave OTUs and were categorized
250 according to their significantly different proportions in the marked/unmarked areas regardless of
251 the location in Lascaux Cave (Metastats) or for the Lascaux Cave locations (Lefse) (99% OTU
252 cutoff). Only significant ($P < 0.03$) correlations higher than 0.8/0.8 and lower than -0.35/-0.5 for
253 the *hsp65*/16S rRNA markers, respectively, were visualized in Gephi 0.9.2. (M. Bastian,
254 Heymann, & Jacomy, 2009) by Fruchterman-Reingold spatialization (Fruchterman & Reingold,
255 1991). The average degree, eigenvector centrality and modularity were computed, and the
256 minimum number of links was filtered to 5 (using a degree range filter).

257 Figures were plotted using the vegan package (Oksanen et al., 2018) in the R computing
258 environment (R Core Team, 2018) and in Inkscape (v0.92; <http://www.inkscape.org>).

259 The Illumina MiSeq 16S rRNA and *hsp65* gene amplicon sequences were deposited in the
260 NCBI Sequence Read Archive (www.ncbi.nlm.nih.gov/sra).

261

262 ***In silico* analysis**

263 Determination of the differences in the variability of the *hsp65* and 16S rRNA partial gene
264 sequences between pairs of *Actinobacteria* strains at different taxonomical levels (e.g., intraclass,
265 intraorder, intrafamily, and intragenus) was performed on genomes retrieved from the Integrated
266 Microbial Genomes and Microbiomes database (IMG; University of California, CA, USA,
267 <https://img.jgi.doe.gov/>). For the analysis, sequences from the available genomes of 47 species
268 from the order *Streptomyetales* (*Streptomyces*, *Kitakatospora*, Table S2) and 58 species from the
269 order *Corynebacteriales* (family *Corynebacteriaceae*: *Corynebacterium*; family *Gordoniaceae*:

270 *Gordonia*; family *Mycobacteriaceae*: *Mycobacterium*; family *Nocardiaceae*: *Nocardia*,
271 *Rhodococcus*; Table S2) were used. Sequences were aligned and trimmed to the amplified length
272 of both gene markers in BioEdit 7.2.5 software (Hall, Biosciences, & Carlsbad, 2011). The
273 pairwise distances between sequences were calculated in Mothur v. 1.39.5 software (Schloss et al.,
274 2009).

275

276 ***hsp65* reference database design**

277 For taxonomic assignment using the *hsp65* marker, the reference database of the
278 *Actinobacteria hsp65* gene was constructed similarly to that of the *rpoB* marker in the study of
279 Ogier et al. (2019) (Ogier, Pagès, Galan, Barret, & Gaudriault, 2019). Sequences homologous to
280 the 65-kDA heat shock protein (*hsp65*) of the reference strain *Nocardia asteroides* ATCC 14759
281 (Rodríguez-Nava et al., 2006) amplified by the TB11 and TB12 primers (Telenti et al., 1993) were
282 collected in the online databases of IMG and NCBI. Paralogs of heat shock proteins, such as *groEL*
283 genes from *Escherichia coli* (Colaco & MacDougall, 2014; Duchêne, Kieser, Hopwood,
284 Thompson, & Mazodier, 1994; C. M. S. Kumar, Mande, & Mahajan, 2015), were identified using
285 maximum-likelihood, FastTree 2.1 (Price, Dehal, & Arkin, 2010) and were kept in the reference
286 database (renamed as GROESL sequences) as an outgroup that enabled amplified sequences
287 belonging to this variant to be discarded.

288 The *hsp65* database contained 5,165 sequences, of which 1,782 sequences were denoted as
289 GROESL at the time of the analysis. Evaluation of the TB11 and TB12 primer complementarity
290 with the sequences from the reference database was performed using the OligoAnalyzer 3.1 tool
291 (<http://www.idtdna.com/calc/analyzer>). The percent coverage of the primers of *Actinobacteria*
292 genomes from different classes and orders was determined with primer BLAST using the RefSeq

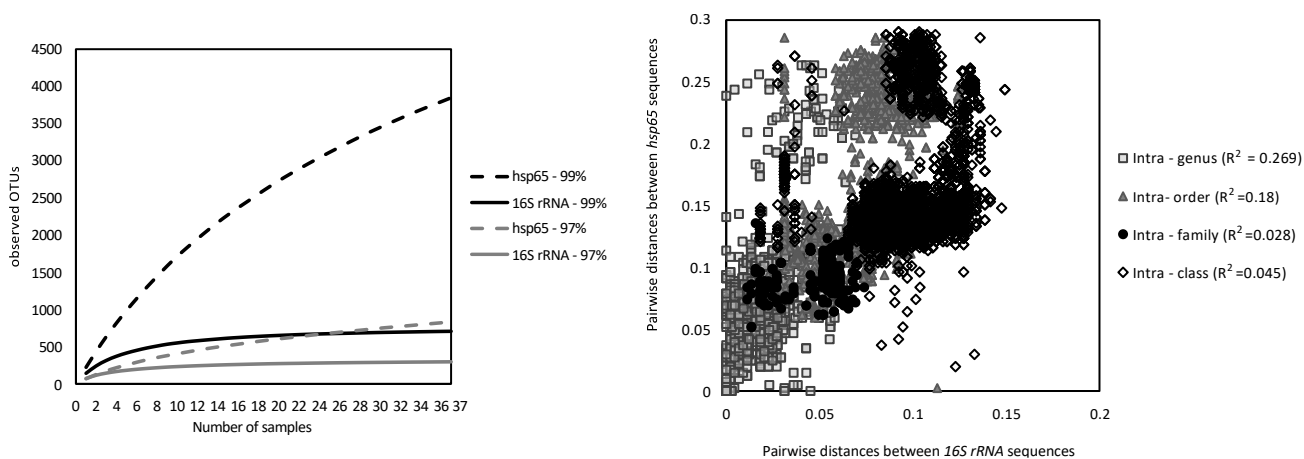
293 reference genomes (NCBI). Only targets with no mismatches for the last three nucleotides at the
294 3' end and no more than 4 overall mismatches were included.

295 **Results**

296 **Sequence polymorphism of *hsp65* versus 16S rRNA genes for cave *Actinobacteria***

297 A total of 1,799,680 *hsp65* and 1,919,236 16S rRNA gene sequence reads were obtained
298 for cave *Actinobacteria*. They were mapped to 968 (97% cutoff) and 4,265 OTUs (99% cutoff) for
299 *hsp65*, vs only 299 (97% cutoff) and 718 OTUs (99% cutoff) for 16S rRNA genes.

300 The curves of 16S rRNA genes for both cutoffs were more skewed and thus indicated an
301 accumulation of identical OTUs due to their repeated sampling, which did not increase with a
302 stricter cutoff, in contrast to *hsp65* (Fig. 2A). These results are in accordance with the *in silico*
303 analysis of *hsp65* and 16S rRNA partial gene sequences downloaded from genomes available on
304 IMG, where the pairwise distances between *hsp65* sequences, even for closely related species,
305 were higher than those between 16S rRNA genes (Fig. 2B).

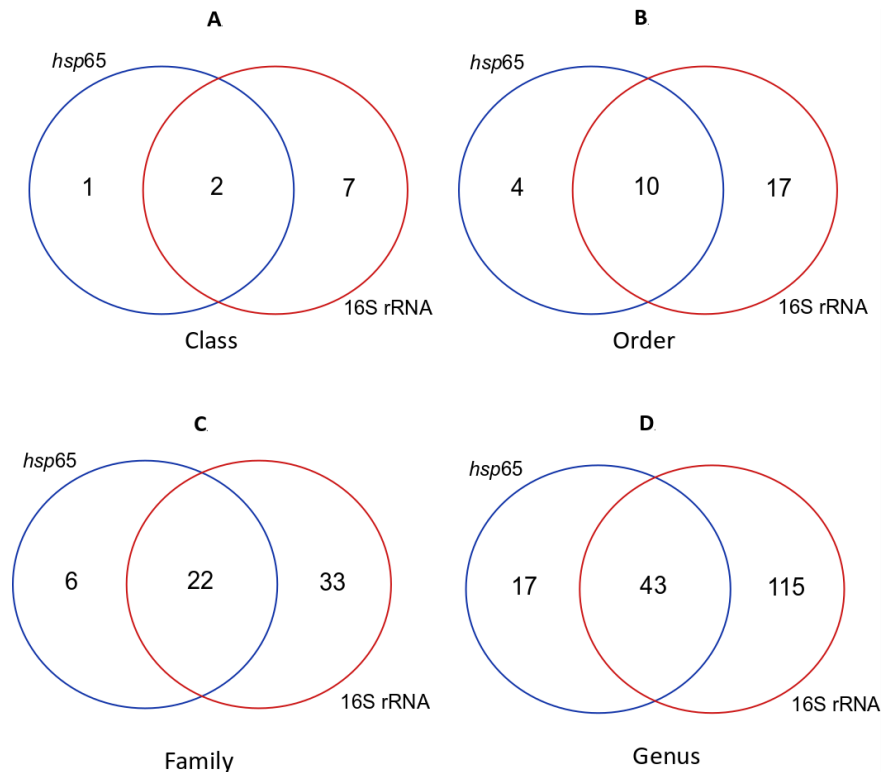


306 Fig. 2. A. Rarefaction curves for the 37 common samples of the *hsp65* and 16S rRNA genes at the
307 97% and 99% OTU cutoffs. The X-axis indicates the number of samples, and the Y-axis indicates
308 the number of OTUs. B. Pairwise molecular distances between sequences of the *hsp65* (Y axes)
309 and 16S rRNA (X axes) genes among *Actinobacteria* species from different taxonomical levels
310 with the R^2 level for each equation.

311

312 The *hsp65* primers targeted *hsp65* sequences from the reference database with lower
313 numbers of mismatches compared to the outgroup (i.e., distant homologs renamed in the database
314 as GROESL, *GroEl* of *Escherichia coli* and Chloroflexi members) (Table S3). However, the
315 primers targeted only selected groups from the class *Actinobacteria* as can be seen from analysis
316 with representative genomes from online database (Table S4). Moreover, the number of taxa
317 identified at class or lower categories is shown in a Fig. 3. At the class level, 20% of the detected
318 class with *hsp65* were also recovered with 16S rRNA, 32.3% it was for order 36.1% for family,
319 24.6% for genus-level taxa. Although the number of taxa detected uniquely by *hsp65* marker had
320 increasing trend with the lower taxonomic category, contrary to 16S rRNA, *hsp65* detected overall
321 lower number of taxa. However, on a species level overall 168 species were recovered only by
322 *hsp65* marker, where the highest species number were found for *Streptomyces*, *Mycobacterium*
323 and *Nocardia* genera (Table S5).

324



325 Fig 3. Venn diagrams showing the number of different Actinobacteria taxa recovered with *hsp65*
 326 (blue) or 16S rRNA (red) at different taxonomic ranks. (A) Class, (B) Order, (C) Family, (E)
 327 Genus.

328

329 This means that the 16S rRNA marker was more suited for broad taxonomic profiling of
 330 the *Actinobacteria* community. In comparison, the *hsp65* marker could distinguish between
 331 selected *Actinobacteria* species, which the 16S marker failed to achieve, and thus it completed the
 332 results from the 16S rRNA marker (Table S5).

333

334 *Actinobacteria* diversity in caves based on *hsp65* versus 16S rRNA genes

335 According to the diversity analysis based on 37 common samples of both markers, the
 336 *hsp65* marker recorded higher richness (Chao-1 index) and evenness (Simpson evenness index) only
 337 when considering the 99% OTU cutoff than 16S rRNA marker (Table S6). The diversity analysis

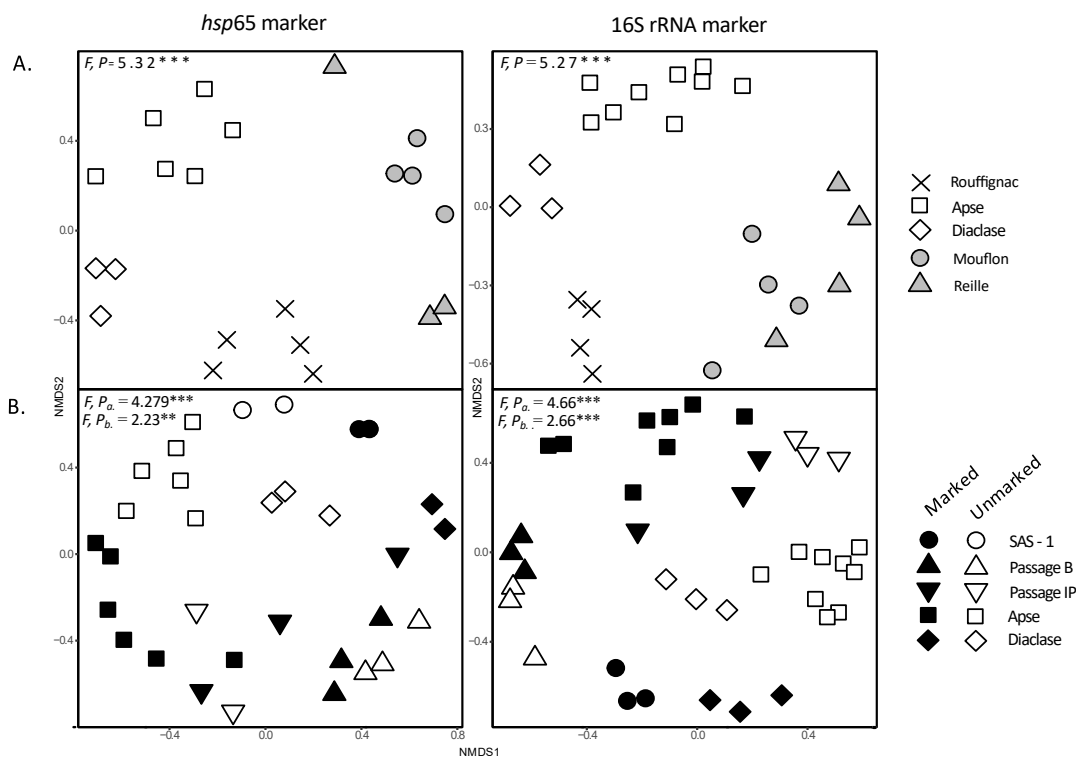
338 based on all samples indicated that Rouffignac Cave exhibited the highest *Actinobacteria* richness
339 (Chao 1 index, for the *hsp65* marker; Fig. S1) but lower evenness (Simpson evenness index; for
340 both markers; Fig. S1) as well as diversity (Inverse Simpson index; for the 16S rRNA marker; Fig.
341 S1) among other caves. In contrast, the Lascaux and Rouffignac Caves had lower evenness than
342 the pristine Reille (for the 16S rRNA marker) and the Mouflon Caves (for the *hsp65* marker; Fig.
343 S1). When comparing locations within Lascaux Cave, only the difference in *Actinobacteria*
344 richness between Sas-1 and Passage B was significant (for the 16S rRNA marker; Fig. S1). The
345 average diversity of the unmarked areas was higher than that of the marked areas for both markers,
346 (Fig. S1). Therefore, when documenting diversity *hsp65* might uncovered the high richness in
347 some of the samples which was not recorded by the 16S rRNA marker.

348

349 ***Actinobacteria* community structure in caves based on *hsp65* versus 16S rRNA genes**

350 NMDS analysis was conducted to compare the *Actinobacteria* communities in caves (97%
351 OTU cutoff). These communities did not differ significantly between pristine caves Reille and
352 Mouflon (AMOVA), based on *hsp65* and 16S rRNA genes. NMDS distinguished three groups of
353 communities corresponding to Lascaux, Rouffignac, and the two pristine caves Reille and
354 Mouflon, which was further supported by AMOVA (Table S7 A). The AMOVA comparison of
355 two groups: anthropized (Lascaux and Rouffignac) and pristine (Reille and Mouflon) caves
356 showed, that they significantly differed according to both markers (*hsp65*: $F= 3.986$, $p < 0.001$,
357 16S rRNA: $F=8.610$, $p < 0.001$). Within Lascaux Cave, the *Actinobacteria* communities differed
358 largely according to all locations (i.e. Sas-1, Passage B, Passage IP, Apse, Diaclase) with both
359 markers, except that differences between Passage IP, Sas-1 (both markers) and Diaclase (*hsp65*)
360 were not significant due to the low number of samples (Table S7 A). Overall, the effect of surface

361 alterations (i.e. marked vs unmarked areas) in Lascaux Cave was significant for both markers
 362 (Table S7 A), with higher *Actinobacteria* stability in unmarked than vs marked areas (Table S7
 363 B). Passage B had the highest community stability compared to Passage IP, Apse and Diacase
 364 (Table S7 B), which was reflected in the NMDS plot, where the marked and unmarked areas in
 365 Passage IP were the least separated from one another (Fig. 4).



366 Fig. 4. Sammon projection of nonmetric multidimensional scaling (NMDS) based on the Bray-
 367 Curtis distance matrices of the *hsp65* and 16S rRNA gene markers of A. different caves and B.
 368 Lascaux Cave locations and marked/unmarked areas. The F-values and P-values of overall
 369 AMOVA are indicated (a - locations, b - un/arked areas; 97% OTU cutoff).

370

371

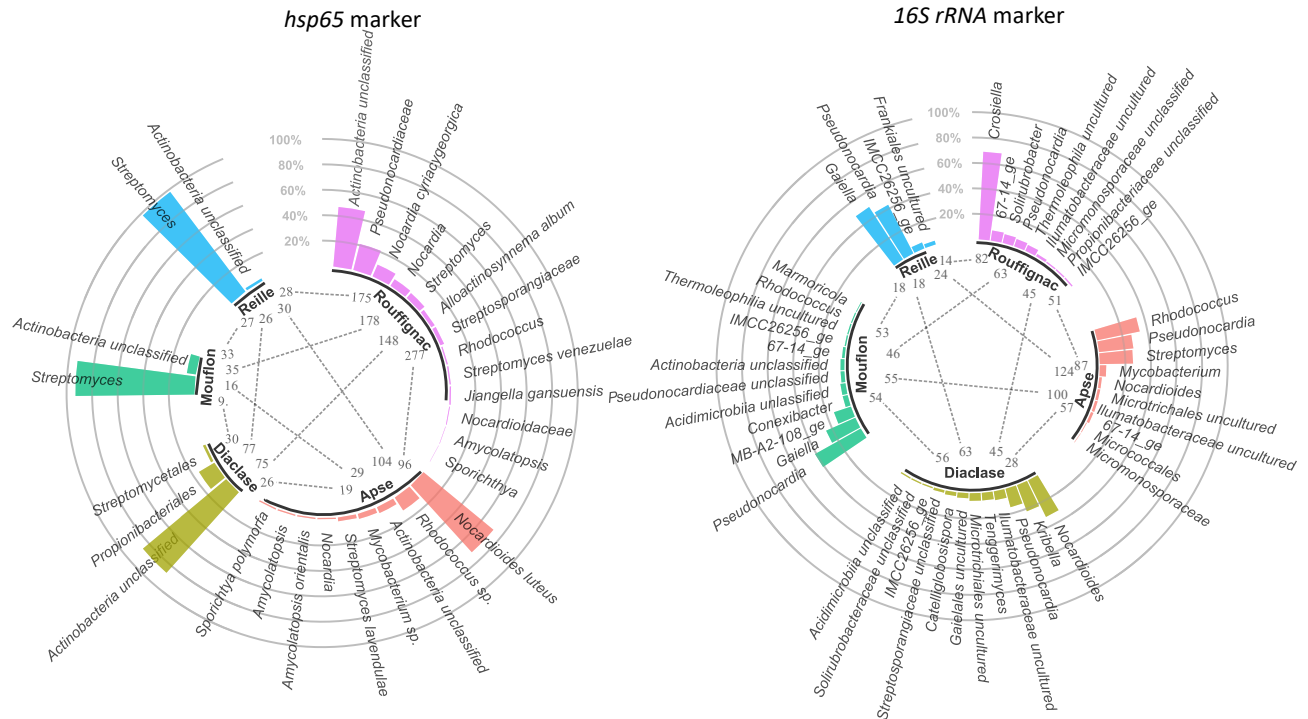
372

373 **Core and cave-specific *Actinobacteria* microbiomes based on *hsp65* versus 16S rRNA genes**

374 Venn diagrams indicated that the number of OTUs shared between different caves
375 (Rouffignac, Lascaux, Mouflon, Reille) was only 2 (0.04%) for the *hsp65* marker vs 72 (11%) for
376 the 16S rRNA marker (Fig. S2). Similarly, the number of OTUs shared between different Lascaux
377 rooms (Sas-1, Passage, Apse, Diaclase) reached 23 OTUs (0.89%) for the *hsp65* marker vs as
378 many as 88 (15.9%) for the 16S rRNA marker. The core microbiome was constituted especially
379 by *Pseudonocardiales* and *Streptomycetales*, as determined by *hsp65*, and *Gaiellales*,
380 *Pseudonocardiales* and strain IMCC26256_ge, as determined by 16S rRNA genes (Fig. S3).

381 The pairwise comparison of cave conditions (Rouffignac, Lascaux's Apse and Diaclase,
382 Mouflon, Reille) using significantly different OTUs (Metastats) showed that Rouffignac (based on
383 *hsp65*) and Lascaux's Apse (based on 16S rRNA genes) were most enriched in OTUs, separating
384 them from the other caves (Fig. 5). Among them, *Pseudonocardiaceae*, *Crosiella* and *Nocardia*
385 were the most abundant taxa that distinguished Rouffignac (for both markers), while *Nocardioides*,
386 *Rhodococcus*, *Pseudonocardia* distinguished Lascaux's Apse from the other caves and Diaclase.
387 *Mycobacterium* was uniquely found in Lascaux's Apse according to both markers. Pristine caves
388 were typified by *Streptomyces* (*hsp65* marker), *Gaiellales*, *Pseudonocardiales* and the
389 environmental clones MB-A2-108_ge and IMCC26256_ge (16S rRNA genes)(Fig. 5).

390



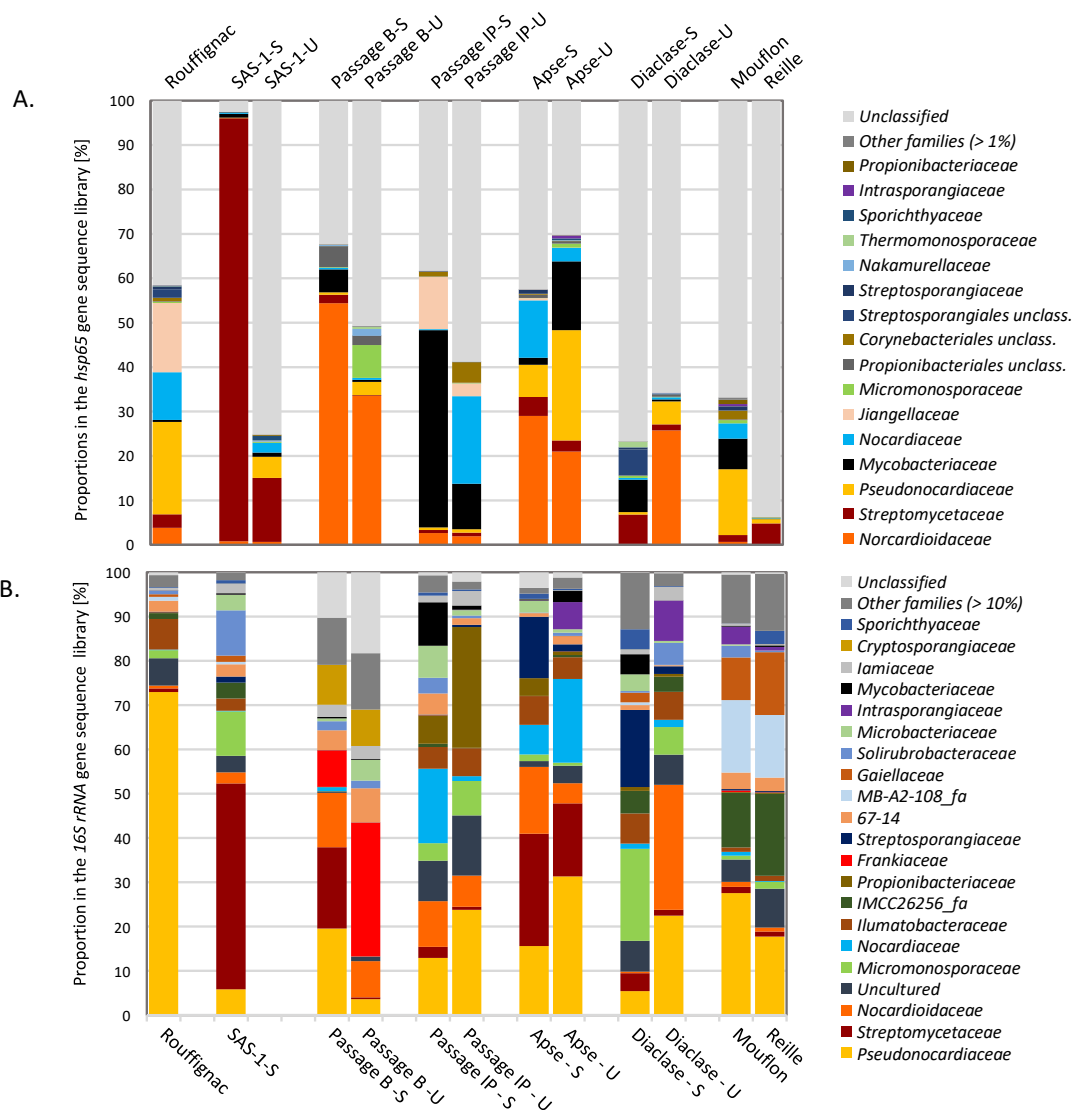
391 Fig. 5. Significantly different OTUs between pairs of caves (Metastats, $P < 0.005$). For each cave,
 392 the number of OTUs that proportionally differed from other caves and taxonomically assigned
 393 OTUs proportionally the most abundant in the respective cave are indicated (99% OTU cutoff).

394

395 **Proportions of cave *Actinobacteria* in sequences libraries based on *hsp65* versus 16S rRNA**
 396 **genes**

397 Taxonomical analysis showed that *Jiangellaceae*, *Actinobacteria incertae sedis*
 398 *Brevibacteriaceae*, *Nocardiopsaceae* and *Gordoniaceae* were uniquely identified by *hsp65* marker
 399 but not by 16S rRNA marker. *Nocardioidaceae*, *Streptomycetaceae* and *Pseudonocardiaceae*
 400 dominated the sequence libraries of both gene markers, when considering all cave conditions
 401 together. *Nocardioidaceae* and *Streptomycetaceae* (according to *hsp65*) while *Nocardiaceae* and
 402 *Streptomycetaceae* (according to 16S rRNA marker) were redundant especially in Lascaux Cave.
 403 According to both gene markers, *Streptomycetaceae* were in a higher proportion in marked areas
 404 than in unmarked areas of the Lascaux cave (Fig. 6). With a closer focus on *Streptomyces* using

405 only the *hsp65* marker, which contrary to 16S rRNA can identify the species, *S. mirabilis*, *S.*
406 *niveus*, and *S. fulvissimus* were the three species, which dominated in marked areas within Lascaux
407 Cave (Metastats $P < 0.005$; Fig. S4). The opposite result was found for *Pseudonocardiaceae*,
408 which were more proportionally abundant in Lascaux's unmarked areas than in marked areas
409 except for Passage IP (by *hsp65*) and Passage B (by 16S rRNA marker) (Fig. 6). *Mycobacteriaceae*
410 were found to be highly abundant in Lascaux Cave, and the *hsp65* marker also identified them in
411 Mouflon. *Jiangellaceae* was a group that was typical in Rouffignac and Passage IP (*hsp65* marker).
412 Closer analysis of *Nocardiaceae* with the *hsp65* marker uncovered the greatest richness of
413 *Nocardia* species in Rouffignac (including *N. carnea*, *N. paucivorans*, *N. abscessus*). Moreover,
414 high proportions of *N. jejuensis* in Lascaux and Mouflon, and *N. cummidelens* in Rouffignac, Apse
415 and Reille were found (Fig. S5). Both pristine caves had similar compositions of *Actinobacteria*
416 communities, especially *Gaiellaceae*, taxa related to the environmental clones MB-A2-108_fa and
417 IMCC26256_fa (16S rRNA marker), and high proportions of unclassified *Actinobacteria* (*hsp65*),
418 High proportions of unclassified *Actinobacteria* were similarly to pristine caves observed in
419 Diaclase (Fig. 6).



420

421 Fig. 6. Average proportions of families in the *Actinobacteria* A. *hsp65* and B. 16S rRNA amplicon
 422 sequence libraries from different caves (Rouffignac, Lascaux, Mouflon and Reille), Lascaux Cave
 423 locations (Sas-1, Passage-B, Passage - IP, Apse and Diaclase) and marked (S)/unmarked areas (U)
 424 within Lascaux.

425

426

427

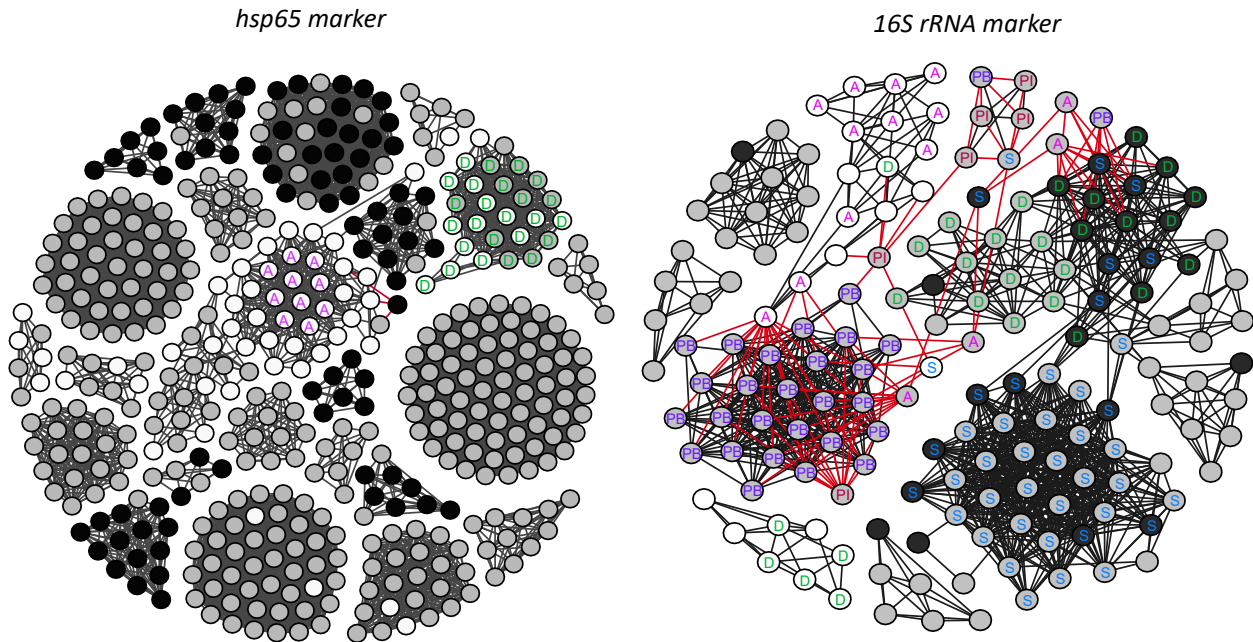
428

429 **Co-occurrence of *Actinobacteria* in Lascaux Cave based on *hsp65* versus 16S rRNA genes**

430 Co-occurrence networks showed the Spearman correlations between the relative
431 abundances of the *Actinobacteria* OTUs in Lascaux Cave (Fig. 7). The co-occurrence networks
432 identify OTUs significantly different for any of the Lascaux locations (calculated by Lefse) or for
433 marked/unmarked areas (calculated by Metastats). More co-occurrence connections were found
434 for *hsp65* than for 16S rRNA marker. For *hsp65* marker, more correlated OTUs were not indicated
435 by Lefse or Metastats as typical for any of the Lascaux location or marked/unmarked area,
436 respectively. Negative correlations between the OTUs revealed only 16S rRNA marker.

437 We found clusters of correlated OTUs dominating the unmarked areas that were also
438 significantly different in the Apse and Diaclase based on both gene markers (Fig. 7). Additionally,
439 OTUs clusters that dominated the marked areas were typical for the Diaclase and Sas-1 areas based
440 on the 16S rRNA marker. The OTUs from such distinct areas (Diaclase and Sas-1) correlated with
441 each other, suggesting that the marked areas factors affected the *Actinobacteria* communities in
442 both locations (Fig. 7). However, the *hsp65* gene marker showed that the OTU clusters typical of
443 marked areas were not typical for any of the Lascaux Cave locations. Finally, based on 16S rRNA
444 marker, the highest number of correlations between OTUs that did not differ between the marked
445 and unmarked areas was found for those that dominated in Passage B, Sas-1 and Diaclase (Fig. 7).
446 For those OTUs, the location factor was more influential than the marked/unmarked areas.
447 Networks based on both markers include variable actors (except the OTUs in unmarked areas of
448 Apse and in Diaclase regardless marked/unmarked areas) which show that each marker cover
449 different part of community and their interactions.

450



451 Fig. 7. Co-occurrence networks of *Actinobacteria* OTUs (A. *hsp65* marker, B. 16S rRNA
 452 marker) between OTUs that were significantly different between marked (black) and unmarked
 453 (white) areas in Lascaux Cave and those that did not differ between these areas (gray) using
 454 Metastats ($P < 0.05$). The letters indicate OTUs that were specific for the respective Lascaux Cave
 455 locations (S, Sas-1; PB, Passage banks; PI, Passage inclined planes; A, Apse; and D, Diaclase)
 456 using Lefse ($P < 0.03$). Strong significant connections (Spearman's correlation > 0.8 and < 0.5 for
 457 16S rRNA gene and < 0.35 for *hsp65* these thresholds are determined how?) are displayed (99%
 458 OTU cutoff).

459 Discussion

460 This study represents the first attempt to exploit the potential of *hsp65* as a taxonomic
461 marker more discriminant than the 16S rRNA gene to document *Actinobacteria* diversity at the
462 species level in cave environments. Indeed, Venn results showed a higher variability for *hsp65*
463 sequences than for *Actinobacteria* 16S rRNA sequences, and a higher OTU richness (at the 99%
464 cutoff) of *Actinobacteria* was obtained. Moreover, thanks to *hsp65* marker we evidenced 168
465 species which could not be identified by the same samples number of 16S rRNA marker.
466 Therefore, lower interspecific variation of 16S rRNA might underestimate the true diversity
467 which might be obtained by *hsp65* marker as was similarly found for other protein-coding gene,
468 (namely *rpoB*) (Vos et al., 2012). However, overall more taxa on higher taxonomic ranks were
469 identified by 16S rRNA than *hsp65* marker which might point on gaps in reference database which
470 prevent complete taxonomic assignment of *hsp65* sequences. Another reason might be a problem
471 with mismatch primers. As was shown by *in silico* analysis, the primers amplify the gene from
472 diverse *Actinobacteria* genomes, but targets without perfect homology might be amplified with
473 lower efficiency leading to underestimation of some taxa (Deagle, Jarman, Coissac, Pompanon, &
474 Taberlet, 2014). It confirms that *hsp65* marker is suitable complement for 16S rRNA in high
475 throughput sequencing methods, especially for specific taxonomic groups analysis into species
476 level, but possible primer biases might be taken into account especially for community analysis at
477 higher taxonomic ranks.

478 In this study, the combination of *hsp65* and 16S rRNA markers showed that *Actinobacteria*
479 diversity could vary according to anthropization in caves, at both higher (i.e., between caves) and
480 lower (i.e., between locations within one cave) spatial scales. Indeed, the actinobacterial
481 communities of anthropized (Lascaux and Rouffignac) and pristine caves (Reille and Mouflon)

482 differed. The occurrence of these caves in the same region and limestone vein probably facilitated
483 this observation, as geographic distance (Barraclough, Balbi, & Ellis, 2012) and geological type
484 (Zhu et al., 2019) are significant factors influencing cave communities. The core *Actinobacteria*
485 microbiome was relatively small (especially for *hsp65*) but it included typical pristine cave taxa,
486 indicating that at least part of the community was able to resist anthropogenic disturbances (Shade
487 et al., 2012).

488 Mouflon and Reille are pristine caves with evenly distributed taxa in the *Actinobacteria*
489 community, possibly as a result of their stable environments without man-made disturbances
490 (Mammola, 2019). Typical pristine cave taxa were evidenced in Mouflon and Reille, such as
491 *Gaiellales* (Zhu et al., 2019) and *Actinobacteria* related to the environmental clone MB-A2-
492 108_ge (A. DE Kumar et al., 2019; Zhang et al., 2019) according to the 16S rRNA marker. ~~vs~~
493 High proportions of *Streptomyces* and unclassified *Actinobacteria* based on *hsp65* data suggest
494 that each marker selectively identify partly a different *Actinobacteria* community. Environmental
495 selection in oligotrophic habitats may promote high molecular evolution (Kuo & Ochman, 2009a;
496 Sagova-Mareckova et al., 2015a) and result in a high number of novel species isolated from caves
497 (A. DE Kumar et al., 2019). A similar result was also found for *Streptomyces* genera (Hamm et
498 al., 2017), whose genomes may undergo a high evolution rate (Cheng et al., 2015). Interestingly,
499 similar results (i.e. high proportions of *Streptomyces*) to those for pristine caves were obtained
500 from Diaclose, which is an isolated site within the anthropized Lascaux Cave (Kuo & Ochman,
501 2009b; Sagova-Mareckova et al., 2015b), suggesting that it has remained at least partially
502 protected from human impacts. Therefore, not only individual caves but also less-exposed
503 locations within anthropized caves maintained a typical *Actinobacteria* cave community, which
504 probably include novel taxa not described so far (Rangseekaew & Pathom-Aree, 2019).

505 Contrary to a previous study based on whole bacterial community (Alonso et al., 2019), we
506 found a high richness but low evenness of *Actinobacteria* in the visited Rouffignac Cave compared
507 to the pristine caves based on *hsp65* marker. The high richness of Actinobacteria in this cave might
508 be a result of community response to a disturbance, since more diverse community is more resilient
509 to stressfull conditions (Shade et al., 2012). Our results are especially supported by the dominance
510 of *Pseudonocardiaceae* (based on 16S rRNA sequences), an indicator of human contamination
511 (Miller et al., 2018), as well as by the highest richness of *Nocardia* species (based on the *hsp65*
512 marker). More specifically, in Lascaux and Mouflon dominated *N. jejuensis*, the species firstly
513 isolated from a natural cave, while in Reille, Rouffignac and Apse dominated *N. cummidelens*, a
514 species previously isolated from rocks of Altamira cave (Valme Jurado, Fernandez-Cortes, et al.,
515 2009). However, *Nocardia* in Rouffignac uniquely included species with pathogenic potential,
516 such as *N. carnea* (Boiron, Provost, Chevrier, & Dupont, 1992), *N. paucivorans* (Watanabe et al.,
517 2006), *N. testacea* (Taj-Aldeen et al., 2013), and *N. abscessus* (Kageyama et al., 2004). Although
518 we cannot know if these environmental bacteria present any pathogenic potential, as those found
519 in human hosts, the enrichment of these species in caves points to a possible allochthonous input
520 by tourists. In turn, it raises the issue of potential health concerns, as proposed previously (Valme
521 Jurado et al., 2010), even though *Actinobacteria* disease problems related to cave frequentation
522 have never been reported. In contrast, *Jiangellaceae* are a typical pristine cave family
523 (Rangseekaew & Pathom-aree, 2019) and are another important group in Rouffignac Cave.
524 According to the intermediate disturbance hypothesis (Roxburgh, Shea, & Wilson, 2004), the
525 coexistence of typical pristine and anthropized taxa in one habitat may suggest that the cave is
526 under intermediate environmental pressure.

527 The actinobacterial communities in caves were highly specific even within very close
528 distances (81), since each Lascaux room hosted its own *Actinobacteria* populations. Lascaux Cave
529 was typified by high abundances of *Mycobacterium*. Similar to *Nocardia* in Rouffignac, this group
530 can signify external contamination (Valme Jurado et al., 2010; Modra et al., 2017). Confirming
531 the previous results from Alonso et al. (2018) that were based on the whole bacterial community
532 (Alonso et al., 2018), the different geological substrates of Lascaux's Passage had a stronger role
533 than the occurrence of marks, but marks there (black stains) had formed years before. However,
534 the effect of geological substrate contrasted with Diaclase and Apse because these two locations
535 contained significantly different *Actinobacteria*, especially in unmarked areas, as shown by
536 network analysis. It is possible that the isolation and distance from the cave entrance represent the
537 best filter for alien microorganisms and enable the maintenance of the cave oligotrophic
538 community, which is typical for unmarked areas (Cuezva, Sanchez-Moral, Saiz-Jimenez, &
539 Cañaveras, 2009; Mammola, 2019).

540 Our results show that the *Actinobacteria* community, mainly *Streptomyces*, varied
541 according to the presence of visual marks. Marked areas, where *Streptomycetaceae* dominated,
542 exhibited much lower diversity than unmarked zones, where *Pseudonocardiaceae* were prevalent.
543 Similarly to our study, the group *Pseudonocardiaceae* was confirmed as true cave rock dwellers
544 (Zhu et al., 2019). However, contrary to our results, this group was typically found in pigmented
545 zones of pristine caves (Lavoie et al., 2017). In addition, the members from the group
546 *Pseudonocardiaceae* are degraders of complex molecules and indicators of anthropogenic
547 contamination (Lavoie et al., 2017; Porca et al., 2012), which suggests that the unmarked areas
548 were not completely oligotrophic (Tomczyk-Żak & Zielenkiewicz, 2016). However, the higher
549 community diversity in unmarked areas than in marked areas indicates the prevalence of

550 cooperative relationships, which are typical for oligotrophic cave environments (Tomczyk-Żak &
551 Zielenkiewicz, 2016).

552 In contrast, the diversity of marked areas might be reduced due to the competitive
553 advantage of invading species (Hamm et al., 2017; Van Elsas et al., 2012). In isolated cave
554 systems, invasions are expected from the cave entrance, similar to Altamira Cave, where
555 *Streptomyces* is the most dominant group, especially in stains (Groth, Vettermann, Schuetze,
556 Schumann, & Saiz-Jimenez, 1999). Moreover, they are generally known to be competitively
557 effective because of their secondary metabolite production, which is supported by the prevalence
558 of the antimicrobial producers *S. mirabilis*, with gray mycelium (El-Sayed, 2012), *S. niveus*
559 (Kominek, 1972), and *S. fulvissimus* (Myronovskiy, Tokovenko, Manderscheid, Petzke, &
560 Luzhetskyy, 2013) in stains. Hypothetically, *Streptomyces* might also contribute to pigment
561 production, as indicated in different studies (Abdel-Haliem, Sakr, Ali, Ghaly, & Sohlenkamp,
562 2013; Cuezva et al., 2012), or might affect the pigment-forming fungi that are involved in black
563 stain formation in Lascaux Cave (De La Rosa et al., 2017; Frey-Klett et al., 2011). Another study
564 showed that *Streptomyces* cooperation with fungi in stains promoted mycelial extension and
565 secondary metabolite production of fungi (Frey-Klett et al., 2011). A previous study showed the
566 correlation between *Streptomyces* and pigment-forming fungi *Acremonium* and *Exophiala* in
567 Lascaux Cave, although only in unmarked areas (Alonso et al., 2018). Therefore, *Streptomyces*
568 role in black stains should be studied in more detail to evaluate if this group may represent a
569 missing chain for understanding stain development in Lascaux Cave.

570 To conclude, the *hsp65* marker can be reliably used for differentiating *Actinobacteria*
571 species present in environmental samples. However, in environmental studies, *hsp65* should
572 functionate as a complement for 16S rRNA gene, since 16S rRNA gene encompass larger part of

573 Actinobacteria community but cannot resolve species. the *Actinobacteria* community at different
574 spatial levels reflected the natural quality of the caves and different locations within Lascaux Cave.
575 Anthropization was shown to shape *Actinobacteria* communities, which altered typical cave
576 communities and was exhibited by the indicator *Actinobacteria*. We first found that the marked
577 areas of Lascaux Cave are an important factor shaping *Actinobacteria* communities, with particular
578 reference to the *Streptomyces*. Finally, the study revealed the linkage between *Actinobacteria* in
579 anthropized caves and marked areas and may help promote the conservation of

580 **References**

- 581 Abdel-Halim, M. E. F., Sakr, A. A., Ali, M. F., Ghaly, M. F., & Sohlenkamp, C. (2013). Characterization of
582 Streptomyces isolates causing colour changes of mural paintings in ancient Egyptian tombs. *Microbiological*
583 *Research*, 168(7), 428–437. doi: 10.1016/j.micres.2013.02.004
- 584 Alonso, L., Creuzé-des-Châtelliers, C., Trabac, T., Dubost, A., Moëgne-Loccoz, Y., & Pommier, T. (2018). Rock
585 substrate rather than black stain alterations drives microbial community structure in the passage of Lascaux
586 Cave. *Microbiome*, 6(1), 216. doi: 10.1186/s40168-018-0599-9
- 587 Alonso, L., Pommier, T., Kaufmann, B., Dubost, A., Chapulliot, D., Doré, J., ... Moëgne-Loccoz, Y. (2019).
588 Anthropization level of Lascaux Cave microbiome shown by regional-scale comparisons of pristine and
589 anthropized caves. *Molecular Ecology*, 28(14), 3383–3394. doi: 10.1111/mec.15144
- 590 Barraclough, T. G., Balbi, K. J., & Ellis, R. J. (2012). Evolving Concepts of Bacterial Species. *Evolution Biology*, 39,
591 148–157. doi: 10.1007/s11692-012-9181-8
- 592 Barton, H. A., & Jurado, V. (2007). *What's Up Down There? Microbial Diversity in Caves Microorganisms in caves*
593 *survive under nutrient-poor conditions and are metabolically versatile and unexpectedly diverse*. Retrieved
594 from
595 [https://pdfs.semanticscholar.org/cc59/ea424434255719237886aa7de76b3c99b24e.pdf?_ga=2.138095863.6183](https://pdfs.semanticscholar.org/cc59/ea424434255719237886aa7de76b3c99b24e.pdf?_ga=2.138095863.618314355.1561451191-1159738399.1560451939)
596 14355.1561451191-1159738399.1560451939
- 597 Barton, H. A., Taylor, N. M., Kreate, M. P., Springer, A. C., Oehrle, S. A., & Bertog, J. L. (2007). The Impact of Host
598 Rock Geochemistry on Bacterial Community Structure in Oligotrophic Cave Environments. *International*
599 *Journal of Speleology*, 36 (2), 93–104. Retrieved from www.ij.speleo.it
- 600 Bastian, F., Jurado, V., Novakova, A., Alabouvette, C., & Saiz-Jimenez, C. (2010). The microbiology of Lascaux
601 Cave. *Microbiology*, 156(3), 644–652. doi: 10.1099/mic.0.036160-0
- 602 Bastian, M., Heymann, S., & Jacomy, M. (2009). Gephi: An Open Source Software for Exploring and Manipulating
603 Networks. *Proceedings of the Third International ICWSM Conference (2009)*, 361–362. doi:
604 10.1136/qshc.2004.010033
- 605 Bercea, S., Năstase-Bucur, R., Moldovan, O. T., Kenezs, M., & Constantin, S. (2019). Yearly microbial cycle of
606 human exposed surfaces in show caves. *Subterranean Biology*, 31, 1–14. doi: 10.3897/subtbiol.31.34490
- 607 Bhullar, K., Waglechner, N., Pawlowski, A., Koteva, K., Banks, E. D., Johnston, M. D., ... Wright, G. D. (2012).
608 Antibiotic Resistance Is Prevalent in an Isolated Cave Microbiome. *PLoS ONE*, 7(4), e34953. doi:
609 10.1371/journal.pone.0034953
- 610 Boiron, P., Provost, F., Chevrier, G., & Dupont, B. (1992). Review of nocardial infections in France 1987 to 1990.
611 *European Journal of Clinical Microbiology & Infectious Diseases*, 11(8), 709–714. doi: 10.1007/BF01989975
- 612 Cheng, K., Rong, X., Pinto-Tomás, A. A., Fernández-Villalobos, M., Murillo-Cruz, C., & Huang, Y. (2015).
613 Population genetic analysis of Streptomyces albidoflavus reveals habitat barriers to homologous recombination
614 in the diversification of streptomycetes. *Applied and Environmental Microbiology*, 81(3), 966–975. doi:
615 10.1128/AEM.02925-14
- 616 Colaco, C. A., & MacDougall, A. (2014). Mycobacterial chaperonins: the tail wags the dog. *FEMS Microbiology*
617 *Letters*, 350(1), 20–24. doi: 10.1111/1574-6968.12276
- 618 Cuezva, S., Fernandez-Cortes, A., Porca, E., Pašić, L., Jurado, V., Hernandez-Marine, M., ... Saiz-Jimenez, C. (2012).
619 The biogeochemical role of Actinobacteria in Altamira Cave, Spain. *FEMS Microbiology Ecology*, 81(1), 281–
620 290. doi: 10.1111/j.1574-6941.2012.01391.x
- 621 Cuezva, S., Sanchez-Moral, S., Saiz-Jimenez, C., & Cañaveras, J. C. (2009). Microbial communities and associated
622 mineral fabrics in Altamira Cave, Spain. *International Journal of Speleology*, 38(1), 83–92. doi: 10.5038/1827-
623 806x.38.1.9
- 624 De La Rosa, J. M., Martin-Sanchez, P. M., Sanchez-Cortes, S., Hermosin, B., Knicker, H., & Saiz-Jimenez, C. (2017).

- 625 Structure of melanins from the fungi *Ochroconis lascauxensis* and *Ochroconis anomala* contaminating rock art
626 in the Lascaux Cave. *Scientific Reports*, 7(1), 1–11. doi: 10.1038/s41598-017-13862-7
- 627 De Mandal, S., Chatterjee, R., & Kumar, N. S. (2017). Dominant bacterial phyla in caves and their predicted functional
628 roles in C and N cycle. *BMC Microbiology*, 17(1), 1–9. doi: 10.1186/s12866-017-1002-x
- 629 Deagle, B. E., Jarman, S. N., Coissac, E., Pompanon, F., & Taberlet, P. (2014). DNA metabarcoding and the
630 cytochrome *c* oxidase subunit I marker: not a perfect match. *Biology Letters*, 10(9), 20140562. doi:
631 10.1098/rsbl.2014.0562
- 632 Duchêne, A.-M., Kieser, H. M., Hopwood, D. A., Thompson, C. J., & Mazodier, P. (1994). Characterization of two
633 groEL genes in *Streptomyces coelicolor* A3 (2). *Gene*, 144(1), 97–101. doi: 10.1016/0378-1119(94)90210-0
- 634 El-Sayed, M. H. (2012). Di-(2-ethylhexyl) Phthalate, a Major Bioactive Metabolite with Antimicrobial and Cytotoxic
635 Activity Isolated from the Culture Filtrate of Newly Isolated Soil *Streptomyces* (*Streptomyces mirabilis* Strain
636 NSQu-25). *World Applied Sciences Journal*, 20(9), 1202–1212. doi: 10.5829/idosi.wasj.2012.20.09.2868
- 637 Fang, B.-Z., Salam, N., Han, M.-X., Jiao, J.-Y., Cheng, J., Wei, D.-Q., ... Li, W.-J. (2017). Insights on the Effects of
638 Heat Pretreatment, pH, and Calcium Salts on Isolation of Rare Actinobacteria from Karstic Caves. *Frontiers in*
639 *Microbiology*, 8. doi: 10.3389/fmicb.2017.01535
- 640 Fernandez-Cortes, A., Cuezva, S., Sanchez-Moral, S., Cañaveras, J. C., Porca, E., Jurado, V., ... Saiz-Jimenez, C.
641 (2011). Detection of human-induced environmental disturbances in a show cave. *Environmental Science and*
642 *Pollution Research*, 18(6), 1037–1045. doi: 10.1007/s11356-011-0513-5
- 643 Fox, G. E., Wisotzkey, J. D., & Jurtschuk, P. (1992). How Close Is Close: 16S rRNA Sequence Identity May Not Be
644 Sufficient To Guarantee Species Identity. *Int. J. Syst. Bacteriol.*, 42(1), 166–170. doi: 10.1099/00207713-42-1-
645 166
- 646 Frey-Klett, P., Burlinson, P., Deveau, A., Barret, M., Tarkka, M., & Sarniguet, A. (2011). Bacterial-fungal
647 interactions: hyphens between agricultural, clinical, environmental, and food microbiologists. *Microbiology and*
648 *Molecular Biology Reviews* : MMBR, 75(4), 583–609. doi: 10.1128/MMBR.00020-11
- 649 Fruchterman, T. M. J., & Reingold, E. M. (1991). Graph drawing by force-directed placement. *Software: Practice and*
650 *Experience*, 21(11), 1129–1164. doi: 10.1002/spe.4380211102
- 651 Gao, B., & Gupta, R. (2012). Phylogenetic framework and molecular signatures for the main clades of the phylum
652 Actinobacteria. *Microbiology and Molecular Biology Reviews*, 76(1), 66–112. Retrieved from
653 <http://mmbbr.asm.org/content/76/1/66.short>
- 654 Gonzalez-Pimentel, J. L., Miller, A. Z., Jurado, V., Laiz, L., Pereira, M. F. C., & Saiz-Jimenez, C. (2018). Yellow
655 coloured mats from lava tubes of La Palma (Canary Islands, Spain) are dominated by metabolically active
656 Actinobacteria. *Sci. Rep.*, 8(1), 1–11. doi: 10.1038/s41598-018-20393-2
- 657 Groth, I., Vettermann, R., Schuetze, B., Schumann, P., & Saiz-Jimenez, C. (1999). Actinomycetes in Karstic caves of
658 northern Spain (Altamira and Tito Bustillo). *Journal of Microbiological Methods*, 36(1–2), 115–122. doi:
659 10.1016/S0167-7012(99)00016-0
- 660 Hall, T., Biosciences, I., & Carlsbad, C. (2011). BioEdit: An important software for molecular biology. *GERF Bulletin*
661 *of Biosciences*, 2(June), 60–61. doi: 10.1002/prot.24632
- 662 Hamed, J., Kafshnouchi, M., & Ranjbaran, M. (2019). A Study on actinobacterial diversity of Hampoel cave and
663 screening of their biological activities. *Saudi Journal of Biological Sciences*, 26(7), 1587–1595. doi:
664 10.1016/j.sjbs.2018.10.010
- 665 Hamm, P. S., Caimi, N. A., Northup, D. E., Valdez, E. W., Buecher, D. C., Dunlap, C. A., ... Porras-Alfaro, A. (2017).
666 *Western Bats as a Reservoir of Novel Streptomyces Species with Antifungal Activity*. doi: 10.1128/AEM.03057-
667 16
- 668 Hammer, Ø., Harper, D. A. T., & Ryan, P. D. (2001). *PAST: PALEONTOLOGICAL STATISTICS SOFTWARE*
669 *PACKAGE FOR EDUCATION AND DATA ANALYSIS*. 4(1), 1–9.

- 670 Herlemann, D. P. R., Labrenz, M., Jürgens, K., Bertilsson, S., Waniek, J. J., & Andersson, A. F. (2011). Transitions
671 in bacterial communities along the 2000 km salinity gradient of the Baltic Sea. *ISME Journal*, 5(10), 1571–
672 1579. doi: 10.1038/ismej.2011.41
- 673 Hirsch, P. R., Mauchline, T. H., & Clark, I. M. (2010). Culture-independent molecular techniques for soil microbial
674 ecology. *Soil Biol. Biochem.*, 42(6), 878–887. doi: 10.1016/j.soilbio.2010.02.019
- 675 Hoyos, M., Cañaveras, J. C., Sánchez-Moral, S., Sanz-Rubio, E., & Soler, V. (1998). Microclimatic characterization
676 of a karstic cave: human impact on microenvironmental parameters of a prehistoric rock art cave (Candamo
677 Cave, northern Spain). In *Environmental Geology* (Vol. 33). Springer-Verlag. Retrieved from Springer-Verlag
678 website: <https://link.springer.com/content/pdf/10.1007%2Fs002540050242.pdf>
- 679 Johnston, M. D., Muench, B. A., Banks, E. D., & Barton, H. A. (2012). Human urine in Lechuguilla cave: the
680 microbiological impact and potential for bioremediation. *Journal of Cave and Karst Studies*, 74(3), 278–291.
681 doi: 10.4311/2011MB0227
- 682 Jurado, V., Boiron, P., Kroppenstedt, R. M., Laurent, F., Couble, A., Laiz, L., ... Rodríguez-Nava, V. (2008). *Nocardia*
683 *altamirensis* sp. nov., isolated from Altamira cave, Cantabria, Spain. *International Journal of Systematic and*
684 *Evolutionary Microbiology*, 58(9), 2210–2214. doi: 10.1099/ijs.0.65482-0
- 685 Jurado, Valme, Fernandez-Cortes, A., Cuezva, S., Laiz, L., Cañaveras, J. C., Sanchez-Moral, S., & Saiz-Jimenez, C.
686 (2009). The fungal colonisation of rock-art caves: Experimental evidence. *Naturwissenschaften*, 96(9), 1027–
687 1034. doi: 10.1007/s00114-009-0561-6
- 688 Jurado, Valme, Kroppenstedt, R. M., Saiz-Jimenez, C., Klenk, H. P., Mounié, D., Laiz, L., ... Rodríguez-Nava, V.
689 (2009). *Hoyosella altamirensis* gen. nov., sp. nov., a new member of the order Actinomycetales isolated from a
690 cave biofilm. *International Journal of Systematic and Evolutionary Microbiology*, 59(12), 3105–3110. doi:
691 10.1099/ijs.0.008664-0
- 692 Jurado, Valme, Laiz, L., Rodríguez-Nava, V., Boiron, P., Hermosin, B., Sanchez-Moral, S., & Saiz-Jimenez, C.
693 (2010). Pathogenic and opportunistic microorganisms in caves. *International Journal of Speleology*, 39 (1), 15–
694 24. Retrieved from www.ijs.speleo.it
- 695 Kageyama, A., Yazawa, K., Kudo, T., Taniguchi, H., Nishimura, K., & Mikami, Y. (2004). First Isolates of *Nocardia*
696 abscessus from Humans and Soil in Japan. *Nippon Ishinkin Gakkai Zasshi*, 45(1), 17–21. doi:
697 10.3314/jjmm.45.17
- 698 Kominek, L. A. (1972). Biosynthesis of novobiocin by *Streptomyces niveus*. *Antimicrobial Agents and*
699 *Chemotherapy*, 1(2), 123–134. doi: 10.1128/AAC.1.2.123
- 700 Kozich, J. J., Westcott, S. L., Baxter, N. T., Highlander, S. K., & Schloss, P. D. (2013). Development of a dual-index
701 sequencing strategy and curation pipeline for analyzing amplicon sequence data on the miseq illumina
702 sequencing platform. *Appl. Environ. Microbiol.*, 79(17), 5112–5120. doi: 10.1128/AEM.01043-13
- 703 Kumar, C. M. S., Mande, S. C., & Mahajan, G. (2015). Multiple chaperonins in bacteria--novel functions and non-
704 canonical behaviors. *Cell Stress & Chaperones*, 20(4), 555–574. doi: 10.1007/s12192-015-0598-8
- 705 Kumar, A. DE, Muthiyan, R., Sunder, J., Bhattacharya, D., Kundu, A., & Dam Roy, S. (2019). *Profiling Bacterial*
706 *Diversity of B2 Cave, A Limestone Cave of Baratang, Andaman and Nicobar Islands, India*. doi:
707 10.16943/ptinsa/2019/49589
- 708 Kuo, C. H., & Ochman, H. (2009a). Inferring clocks when lacking rocks: The variable rates of molecular evolution in
709 bacteria. *Biology Direct*, 4(1), 35. doi: 10.1186/1745-6150-4-35
- 710 Kuo, C. H., & Ochman, H. (2009b). Inferring clocks when lacking rocks: The variable rates of molecular evolution in
711 bacteria. *Biology Direct*, 4(1), 35. doi: 10.1186/1745-6150-4-35
- 712 Lavoie, K. H., Winter, A. S., Read, K. J. H., Hughes, E. M., Spilde, M. N., & Northup, D. E. (2017). Comparison of
713 bacterial communities from lava cave microbial mats to overlying surface soils from Lava Beds National
714 Monument, USA. *PLoS One*, 12(2). doi: 10.1371/journal.pone.0169339

- 715 Long, Y., Jiang, J., Hu, X., Zhou, J., Hu, J., & Zhou, S. (2019). Actinobacterial community in Shuanghe Cave using
716 culture-dependent and -independent approaches. *World Journal of Microbiology and Biotechnology*, 35(10).
717 doi: 10.1007/s11274-019-2713-y
- 718 Maciejewska, M., Adam, D., Naômé, A., Martinet, L., Tenconi, E., Calusinska, M., ... Rigali, S. (2017). Assessment
719 of the potential role of Streptomyces in cave moonmilk formation. *Front. Microbiol.*, 8(JUN), 1–18. doi:
720 10.3389/fmicb.2017.01181
- 721 Maciejewska, M., Całusińska, M., Cornet, L., Adam, D., Pessi, I., Malchair, S., ... Rigali, S. (2018). High-Throughput
722 Sequencing Analysis of the Actinobacterial Spatial Diversity in Moonmilk Deposits. *Antibiotics*, 7(2), 27. doi:
723 10.3390/antibiotics7020027
- 724 Magoč, T., & Salzberg, S. L. (2011). FLASH: Fast length adjustment of short reads to improve genome assemblies.
725 *Bioinformatics*, 27(21), 2957–2963. doi: 10.1093/bioinformatics/btr507
- 726 Mammola, S. (2019). Finding answers in the dark: caves as models in ecology fifty years after Poulson and White.
727 *Ecography*, 42(7), 1331–1351. doi: 10.1111/ecog.03905
- 728 Martin-Sanchez, P. M., Miller, A. Z., & Saiz-Jimenez, C. (2015). Lascaux Cave: An Example of Fragile Ecological
729 Balance in Subterranean Environments. *Microbial Life of Cave Systems*. doi: 10.1515/9783110339888-015
- 730 Martin-Sanchez, P. M., Nováková, A., Bastian, F., Alabouvette, C., & Saiz-Jimenez, C. (2012). Use of Biocides for
731 the Control of Fungal Outbreaks in Subterranean Environments: The Case of the Lascaux Cave in France.
732 *Environmental Science & Technology*, 46(7), 3762–3770. doi: 10.1021/es2040625
- 733 Miller, A. Z., Garcia-Sanchez, A. M., Martin-Sanchez, P. M., Costa Pereira, M. F., Spangenberg, J. E., Jurado, V., ...
734 Saiz-Jimenez, C. (2018). Origin of abundant moonmilk deposits in a subsurface granitic environment.
735 *Sedimentology*, 65(5), 1482–1503. doi: 10.1111/sed.12431
- 736 Modra, H., Bartos, M., Hribova, P., Ulmann, V., Hubelova, D., Konecny, O., ... Pavlik, I. (2017). Detection of
737 mycobacteria in the environment of the Moravian Karst (Bull Rock Cave and the relevant water catchment area):
738 the impact of water sediment, earthworm castings and bat guano. *Veterinárni Medicína*, 62 (2017)(No. 3), 153–
739 168. doi: 10.17221/126/2016-VETMED
- 740 Mulec, J. (2014). Human impact on underground cultural and natural heritage sites, biological parameters of
741 monitoring and remediation actions for insensitive surfaces: Case of Slovenian show caves. *Journal for Nature
742 Conservation*, 22(2), 132–141. doi: 10.1016/J.JNC.2013.10.001
- 743 Myronovskyi, M., Tokovenko, B., Manderscheid, N., Petzke, L., & Luzhetskyy, A. (2013). Complete genome
744 sequence of *Streptomyces fulvissimus*. *Journal of Biotechnology*, 168(1), 117–118. doi:
745 10.1016/j.jbiotec.2013.08.013
- 746 Neral, A., Rajput, Y., & Rai, V. (2015). Genotypic and Serotypic confirmations of Bacterial community to Kotumsar
747 cave for occupational safety of cave workers and visitors from pathogenic threats. *International Journal of
748 Occupational Safety and Health*, 5(1), 22–27. doi: 10.3126/ijosh.v5i1.16631
- 749 Ogier, J. C., Pagès, S., Galan, M., Barret, M., & Gaudriault, S. (2019). RpoB, a promising marker for analyzing the
750 diversity of bacterial communities by amplicon sequencing. *BMC Microbiology*, 19(1). doi: 10.1186/s12866-
751 019-1546-z
- 752 Oksanen, J., Blanchet, F. G., Friendly, M., Kindt, R., Legendre, P., Mcglinn, D., ... Maintainer, H. W. (2018). *Package
753 “vegan” Title Community Ecology Package.* Retrieved from
754 <https://cran.ism.ac.jp/web/packages/vegan/vegan.pdf>
- 755 Ondov, B. D., Bergman, N. H., & Phillippy, A. M. (2011). Interactive metagenomic visualization in a Web browser.
756 *BMC Bioinformatics*, 12(1), 385. doi: 10.1186/1471-2105-12-385
- 757 Ortiz, M., Legatzki, A., Neilson, J. W., Fryslie, B., Nelson, W. M., Wing, R. A., ... Maier, R. M. (2014). Making a
758 living while starving in the dark: metagenomic insights into the energy dynamics of a carbonate cave. *The ISME
759 Journal*, 8(2), 478–491. doi: 10.1038/ismej.2013.159

- 760 Porca, E., Jurado, V., Žgur-Bertok, D., Saiz-Jimenez, C., & Pašić, L. (2012). Comparative analysis of yellow microbial
761 communities growing on the walls of geographically distinct caves indicates a common core of microorganisms
762 involved in their formation. *FEMS Microbiology Ecology*, *81*(1), 255–266. doi: 10.1111/j.1574-
763 6941.2012.01383.x
- 764 Price, M. N., Dehal, P. S., & Arkin, A. P. (2010). FastTree 2 – Approximately Maximum-Likelihood Trees for Large
765 Alignments. *PLoS ONE*, *5*(3), e9490. doi: 10.1371/journal.pone.0009490
- 766 Quast, C., Pruesse, E., Yilmaz, P., Gerken, J., Schweer, T., Yarza, P., ... Glöckner, F. O. (2012). The SILVA ribosomal
767 RNA gene database project: improved data processing and web-based tools. *Nucleic Acids Research*, *41*(D1),
768 D590–D596. doi: 10.1093/nar/gks1219
- 769 R Core Team. (2018). R Core Team, R: A language and environment for statistical computing. *R Foundation for*
770 *Statistical Computing, Vienna, Austria*, R Foundation for Statistical Computing.
- 771 Rajput, Y., Rai, V., & Biswas, J. (2012). Screening of Bacterial Isolates from Various Microhabitat Sediments of
772 Kotumsar Cave: A Cogitation on Their Respective Benefits and Expected Threats for Complete Biosphere and
773 Tourists. *Research Journal of Environmental Toxicology*, *6*(1), 13–24.
- 774 Rangseekaew, P., & Pathom-aree, W. (2019). Cave Actinobacteria as Producers of Bioactive Metabolites. *Frontiers*
775 *in Microbiology*, *10*, 387. doi: 10.3389/fmicb.2019.00387
- 776 Rangseekaew, P., & Pathom-Aree, W. (2019). Cave Actinobacteria as Producers of Bioactive Metabolites. *Frontiers*
777 *in Microbiology*, *10*, 387. doi: 10.3389/fmicb.2019.00387
- 778 Rodríguez-Nava, V., Couble, A., Devulder, G., Flandrois, J.-P., Boiron, P., & Laurent, F. (2006). Use of PCR-
779 restriction enzyme pattern analysis and sequencing database for hsp65 gene-based identification of *Nocardia*
780 species. *Journal of Clinical Microbiology*, *44*(2), 536–546. doi: 10.1128/JCM.44.2.536-546.2006
- 781 Rodríguez-Nava, V., Khan, Z. U., Pötter, G., Kroppenstedt, R. M., Boiron, P., & Laurent, F. (2007). *Nocardia*
782 *coupleae* sp. nov., isolated from oil-contaminated Kuwaiti soil. doi: 10.1099/ijs.0.64815-0
- 783 Rognes, T., Flouri, T., Nichols, B., Quince, C., & Mahé, F. (2016). VSEARCH: a versatile open source tool for
784 metagenomics. *PeerJ*, *4*, e2584. doi: 10.7717/peerj.2584
- 785 Roxburgh, S. H., Shea, K., & Wilson, J. B. (2004). The intermediate disturbance hypothesis: Patch dynamics and
786 mechanisms of species coexistence. *Ecology*, *85*(2), 359–371. doi: 10.1890/03-0266
- 787 Sagova-Mareckova, M., Ulanova, D., Sanderova, P., Omelka, M., Kamenik, Z., Olsovska, J., & Kopecky, J. (2015a).
788 Phylogenetic relatedness determined between antibiotic resistance and 16S rRNA genes in actinobacteria
789 Ecological and evolutionary microbiology. *BMC Microbiology*, *15*(1), 81. doi: 10.1186/s12866-015-0416-6
- 790 Sagova-Mareckova, M., Ulanova, D., Sanderova, P., Omelka, M., Kamenik, Z., Olsovska, J., & Kopecky, J. (2015b).
791 Phylogenetic relatedness determined between antibiotic resistance and 16S rRNA genes in actinobacteria
792 Ecological and evolutionary microbiology. *BMC Microbiology*, *15*(1), 81. doi: 10.1186/s12866-015-0416-6
- 793 Sánchez-Moral, S., Soler, V., Cañaveras, J. ., Sanz-Rubio, E., Van Grieken, R., & Gysels, K. (1999). Inorganic
794 deterioration affecting the Altamira Cave, N Spain: quantitative approach to wall-corrosion (solutional etching)
795 processes induced by visitors. *Science of The Total Environment*, *243–244*, 67–84. doi: 10.1016/S0048-
796 9697(99)00348-4
- 797 Schabereiter-Gurtner, C., Saiz-Jimenez, C., Pinar, G., Lubitz, W., & Rölleke, S. (2002). Altamira cave Paleolithic
798 paintings harbor partly unknown bacterial communities. *FEMS Microbiology Letters*, *211*(1), 7–11. doi:
799 10.1111/j.1574-6968.2002.tb11195.x
- 800 Schloss, P. D., Westcott, S. L., Ryabin, T., Hall, J. R., Hartmann, M., Hollister, E. B., ... Weber, C. F. (2009).
801 Introducing mothur: Open-source, platform-independent, community-supported software for describing and
802 comparing microbial communities. *Appl. Environ. Microbiol.*, *75*(23), 7537–7541. doi: 10.1128/AEM.01541-
803 09
- 804 Segata, N., Izard, J., Waldron, L., Gevers, D., Miropolsky, L., Garrett, W. S., & Huttenhower, C. (2011). Metagenomic

- 805 biomarker discovery and explanation. *Genome Biology*, 12(6), R60. doi: 10.1186/gb-2011-12-6-r60
- 806 Shade, A., Peter, H., Allison, S. D., Baho, D. L., Berga, M., Bürgmann, H., ... Gilbert, J. (2012). *Fundamentals of*
807 *microbial community resistance and resilience*. doi: 10.3389/fmicb.2012.00417
- 808 Syiemiong, D., & Jha, D. K. (2019). Antibacterial potential of Actinobacteria from a Limestone Mining Site in
809 Meghalaya, India. *Journal of Pure and Applied Microbiology*, 13(2), 789–802. doi: 10.22207/JPAM.13.2.14
- 810 Taj-Aldeen, S. J., Deshmukh, A., Doiphode, S., Wahab, A. A., Allangawi, M., Muzrkchi, A. Al, ... Meis, J. J. (2013).
811 Molecular Identification and Susceptibility Pattern of Clinical Nocardia Species: Emergence of Nocardia
812 crassostreae as an Agent of Invasive Nocardiosis. *Canadian Journal of Infectious Diseases and Medical*
813 *Microbiology*, 24(2), e33–e38. Retrieved from <https://www.hindawi.com/journals/cjidmm/2013/256025/>
- 814 Takeda, K., Kang, Y., Yazawa, K., Gono, T., & Mikami, Y. (2010). Phylogenetic studies of Nocardia species based
815 on gyrB gene analyses. *Journal of Medical Microbiology*, 59(2), 165–171. doi: 10.1099/jmm.0.011346-0
- 816 Telenti, A., Marchesi, F., Balz, M., Bally, F., Bottger, E. C., & Bodmer, T. (1993). Rapid identification of
817 mycobacteria to the species level by polymerase chain reaction and restriction enzyme analysis. *Journal of*
818 *Clinical Microbiology*, 31(2), 175–178.
- 819 Tomczyk-Żak, K., & Zielenkiewicz, U. (2016). Microbial Diversity in Caves. *Geomicrobiol. J.*, 33(1), 20–38. doi:
820 10.1080/01490451.2014.1003341
- 821 Van Elsland, J. D., Chiurazzi, M., Mallon, C. A., Elhottova, D., Křišťůfek, V., & Salles, J. F. (2012). Microbial diversity
822 determines the invasion of soil by a bacterial pathogen. *Proceedings of the National Academy of Sciences of the*
823 *United States of America*, 109(4), 1159–1164. doi: 10.1073/pnas.1109326109
- 824 Větrovský, T., & Baldrian, P. (2013). The Variability of the 16S rRNA Gene in Bacterial Genomes and Its
825 Consequences for Bacterial Community Analyses. *PLoS ONE*, 8(2), e57923. doi:
826 10.1371/journal.pone.0057923
- 827 Vos, M., Quince, C., Pijl, A. S., de Hollander, M., & Kowalchuk, G. A. (2012). A comparison of rpoB and 16S rRNA
828 as markers in pyrosequencing studies of bacterial diversity. *PLoS ONE*, 7(2). doi:
829 10.1371/journal.pone.0030600
- 830 Watanabe, K., Shinagawa, M., Amishima, M., Iida, S., Yazawa, K., Kageyama, A., ... Mikami, Y. (2006). First
831 Clinical Isolates of Nocardia carnea, Nocardia elegans, Nocardia paucivorans, Nocardia puris and Nocardia
832 takedensis in Japan. *Nippon Ishinkin Gakkai Zasshi*, 47(2), 85–89. doi: 10.3314/jjmm.47.85
- 833 Yasir, M. (2018). Analysis of bacterial communities and characterization of antimicrobial strains from cave
834 microbiota. *Brazilian Journal of Microbiology*, 49(2), 248–257. doi: 10.1016/j.bjm.2017.08.005
- 835 Yilmaz, P., Parfrey, L. W., Yarza, P., Gerken, J., Pruesse, E., Quast, C., ... Glöckner, F. O. (2014). The SILVA and
836 “all-species Living Tree Project (LTP)” taxonomic frameworks. *Nucleic Acids Research*, 42(D1), 643–648. doi:
837 10.1093/nar/gkt1209
- 838 Zhang, B., Wu, X., Tai, X., Sun, L., Wu, M., Zhang, W., ... Dyson, P. (2019). Variation in Actinobacterial Community
839 Composition and Potential Function in Different Soil Ecosystems Belonging to the Arid Heihe River Basin of
840 Northwest China. *Frontiers in Microbiology*, 10, 2209. doi: 10.3389/fmicb.2019.02209
- 841 Zhu, H. Z., Zhang, Z. F., Zhou, N., Jiang, C. Y., Wang, B. J., Cai, L., & Liu, S. J. (2019). Diversity, distribution and
842 co-occurrence patterns of bacterial communities in a karst cave system. *Frontiers in Microbiology*, 10(JULY).
843 doi: 10.3389/fmicb.2019.01726

844

Supplementary Information for:

Usefulness of *hsp65* marker as a complement to 16S rRNA sequences to demonstrate differences in *Actinobacteria* community according to anthropization of limestone caves and occurrence of visual marks in Lascaux Cave

Buresova Andrea^{1,2,3}, Kopecky Jan³, Sagova-Mareckova Marketa³, Alonso Lise¹, Vautrin Florian¹, Moëgne-Loccoz Yvan¹, Rodriguez-Nava Veronica¹

¹Univ Lyon, Université Claude Bernard Lyon 1, CNRS, INRAE, VetAgro Sup, UMR5557 Ecologie Microbienne, F-69622 Villeurbanne, France

²Department of Ecology, Faculty of Science, Charles University in Prague, Vinicna 7, Prague, Czech Republic,

³Laboratory for Diagnostics and Epidemiology of Microorganisms, Crop Research Institute, Drnovska 507, CZ-16106 Prague 6, Ruzyně, Czech Republic

This PDF file includes:

Figs. S1 to S5

Tables S1 to S7

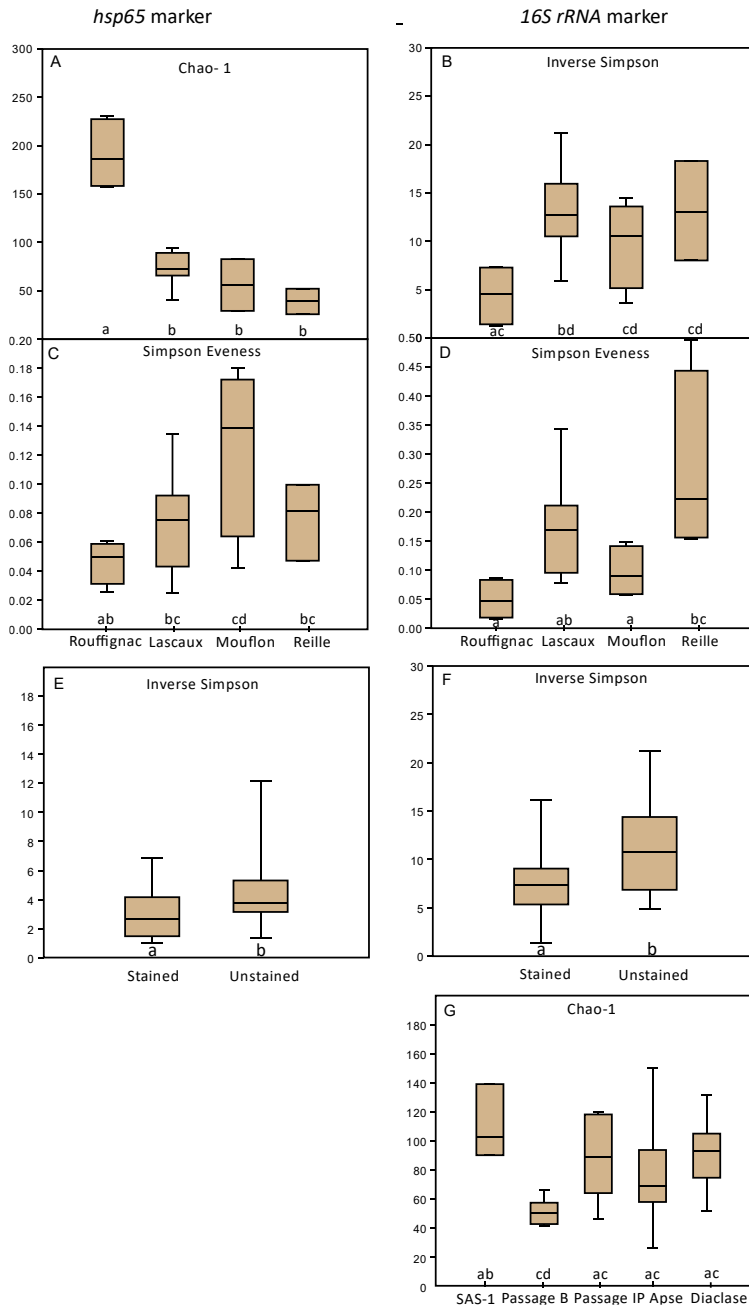


Fig. S1. Indices of alpha diversity (richness: Chao 1, evenness: Simpson evenness, diversity: inverse Simpson) for *Actinobacteria* communities among caves, different locations within Lascaux Cave, and marked/unmarked areas. Significant differences between groups are shown with letters (ANOVA and Tukey post hoc test; $P < 0.05$; 97% OTU cutoff).

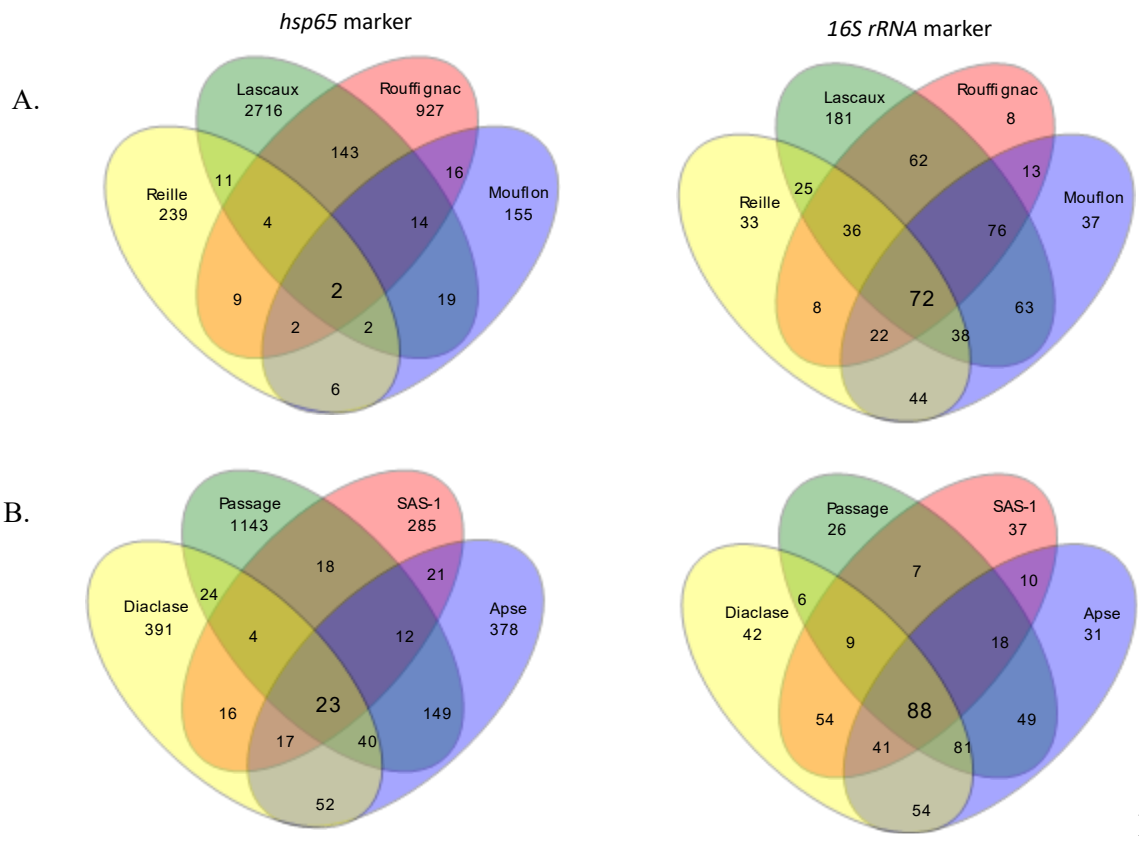


Fig.

Fig S2. Venn diagrams showing unique and shared OTUs between A. different caves and B. different locations within Lascaux Cave based on *hsp65* and *16S rRNA* gene markers (99% OTU cutoff).

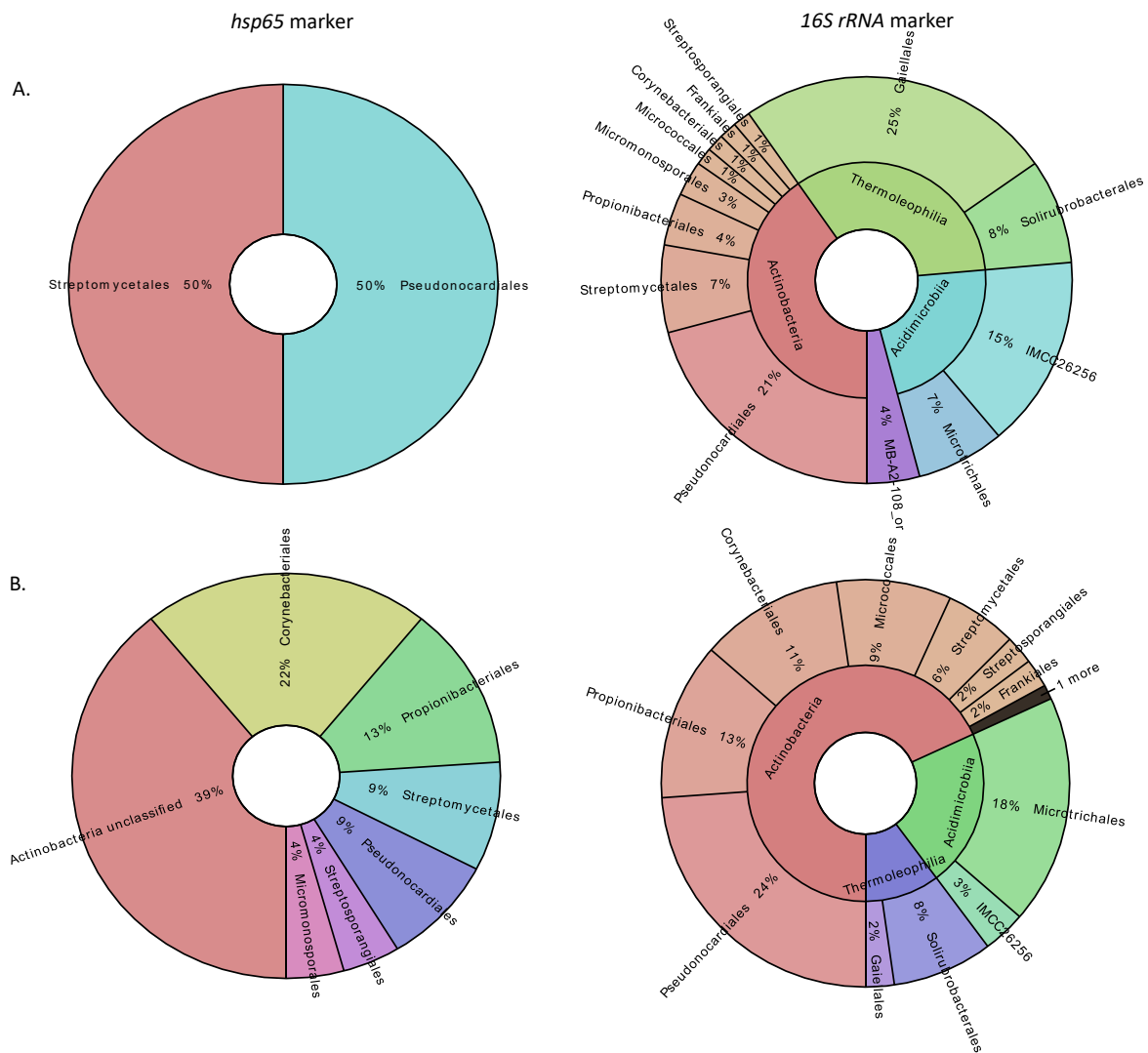


Fig. S3. Taxonomical compositions of the core microbiome between A. caves and B. different locations within Lascaux Cave based on the *hsp65* and 16S rRNA gene markers (99% OTU cutoff).

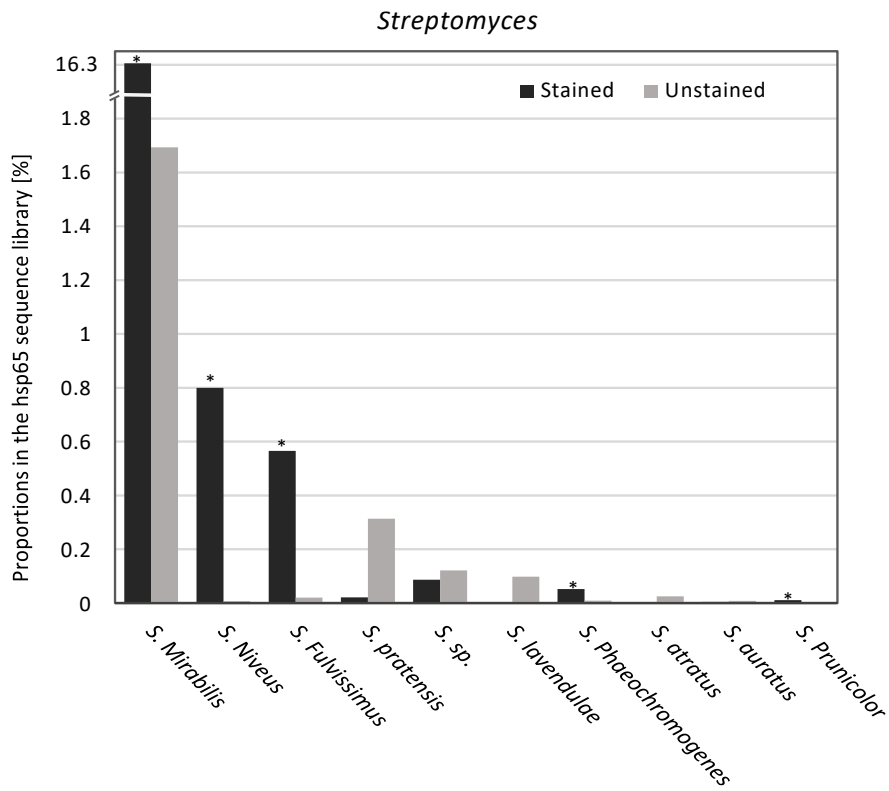


Fig. S4. Average proportions of species within the genus *Streptomyces* in the *Actinobacteria* *hsp65* amplicon sequence libraries significantly different in marked (S) and unmarked areas (U) of Lascaux Cave (metastats, $P < 0.05$).

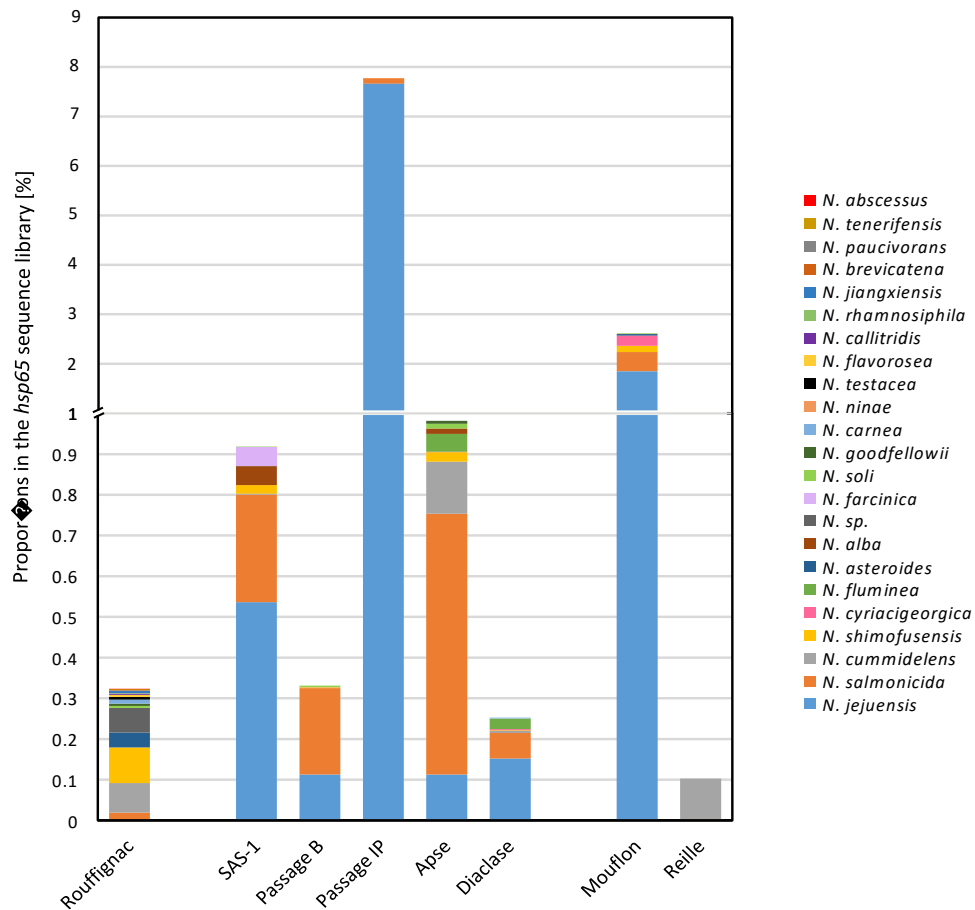


Fig. S5. Average proportions of genus *Nocardia* in the *Actinobacteria hsp65* gene amplicon sequence libraries in different caves (Rouffignac, Lascaux, Mouflon and Reille) and different locations within Lascaux Cave (Sas-1, Passage-B, Passage-IP, Apse and Diaclose).

Table S1. Location of cave samples and list of gene markers sequenced using Illumina MiSeq

Sample ID	Cave name	Room	Area	Obtained sequences
Apse-S1	Lascaux	Apse		16S rRNA gene
Apse-S2	Lascaux	Apse	Visual mark	<i>hsp65</i> , 16S rRNA gene
Apse-S3	Lascaux	Apse		<i>hsp65</i> , 16S rRNA gene
Apse-U1	Lascaux	Apse		<i>hsp65</i> , 16S rRNA gene
Apse-U2	Lascaux	Apse	Unmarked area	<i>hsp65</i> , 16S rRNA gene
Apse-U3	Lascaux	Apse		<i>hsp65</i> , 16S rRNA gene
Apse-DZ1	Lascaux	Apse		16S rRNA gene
Apse-DZ2	Lascaux	Apse		<i>hsp65</i>
Apse-DZ3	Lascaux	Apse	Visual mark	<i>hsp65</i> , 16S rRNA gene
Apse-DZ4	Lascaux	Apse		16S rRNA gene
Apse-DZ5	Lascaux	Apse		<i>hsp65</i> , 16S rRNA gene
Apse-DZ6	Lascaux	Apse		<i>hsp65</i> , 16S rRNA gene
Apse-UDZ1	Lascaux	Apse		16S rRNA gene
Apse-UDZ2	Lascaux	Apse		16S rRNA gene
Apse-UDZ3	Lascaux	Apse	Unmarked area	<i>hsp65</i> , 16S rRNA gene
Apse-UDZ4	Lascaux	Apse		<i>hsp65</i> , 16S rRNA gene
Apse-UDZ5	Lascaux	Apse		16S rRNA gene
Apse-UDZ6	Lascaux	Apse		<i>hsp65</i> , 16S rRNA gene
Dia-S1	Lascaux	Diaclase		<i>hsp65</i> , 16S rRNA gene
Dia-S2	Lascaux	Diaclase	Visual mark	<i>hsp65</i> , 16S rRNA gene
Dia-S3	Lascaux	Diaclase		16S rRNA gene
Dia-U1	Lascaux	Diaclase		<i>hsp65</i> , 16S rRNA gene
Dia-U2	Lascaux	Diaclase	Unmarked area	<i>hsp65</i> , 16S rRNA gene
Dia-U3	Lascaux	Diaclase		<i>hsp65</i> , 16S rRNA gene
Passage B-S1	Lascaux	Passage banks		<i>hsp65</i> , 16S rRNA gene
Passage B-S2	Lascaux	Passage banks	Visual mark	<i>hsp65</i> , 16S rRNA gene
Passage B-S3	Lascaux	Passage banks		<i>hsp65</i> , 16S rRNA gene
Passage B-U1	Lascaux	Passage banks		<i>hsp65</i> , 16S rRNA gene
Passage B-U2	Lascaux	Passage banks	Unmarked area	<i>hsp65</i> , 16S rRNA gene
Passage B-U3	Lascaux	Passage banks		<i>hsp65</i> , 16S rRNA gene
Passage IP-S1	Lascaux	Passage inclined planes		<i>hsp65</i> , 16S rRNA gene
Passage IP-S2	Lascaux	Passage inclined planes	Visual mark	<i>hsp65</i> , 16S rRNA gene
Passage IP-S3	Lascaux	Passage inclined planes		<i>hsp65</i> , 16S rRNA gene
Passage IP-U1	Lascaux	Passage inclined planes		<i>hsp65</i> , 16S rRNA gene
Passage IP-U2	Lascaux	Passage inclined planes	Unmarked area	<i>hsp65</i> , 16S rRNA gene
Passage IP-U3	Lascaux	Passage inclined planes		16S rRNA gene
SAS-1-S1	Lascaux	Sas-1 (airlock-1 entrance zone, compartment 2)		<i>hsp65</i> , 16S rRNA gene
SAS-1-S2	Lascaux	Sas-1 (airlock-1 entrance zone, compartment 2)	Visual mark	<i>hsp65</i> , 16S rRNA gene
SAS-1-S3	Lascaux	Sas-1 (airlock-1 entrance zone, compartment 2)		<i>hsp65</i> , 16S rRNA gene
SAS-U1	Lascaux	Sas-1 (airlock-1 entrance zone, compartment 2)		<i>hsp65</i>
SAS-U3	Lascaux	Sas-1 (airlock-1 entrance zone, compartment 2)	Unmarked area	<i>hsp65</i>
Rouf1	Rouffignac			<i>hsp65</i> , 16S rRNA gene
Rouf2	Rouffignac			<i>hsp65</i>
Rouf3	Rouffignac	x	x	<i>hsp65</i>
Rouf4	Rouffignac			<i>hsp65</i> , 16S rRNA gene
Rouf5	Rouffignac			<i>hsp65</i> , 16S rRNA gene
Rouf6	Rouffignac			16S rRNA gene
Mouf1	Mouflon			16S rRNA gene
Mouf2	Mouflon			<i>hsp65</i> , 16S rRNA gene
Mouf3	Mouflon	x	x	<i>hsp65</i>
Mouf4	Mouflon			<i>hsp65</i> , 16S rRNA gene
Mouf5	Mouflon			<i>hsp65</i>
Mouf6	Mouflon			16S rRNA gene
Reil1	Reille			<i>hsp65</i>
Reil2	Reille			16S rRNA gene
Reil3	Reille	x	x	<i>hsp65</i> , 16S rRNA gene
Reil4	Reille			<i>hsp65</i> , 16S rRNA gene
Reil5	Reille			16S rRNA gene

Table S3. Percentage of complementarity between the hsp65-specific forward (TB11) and reverse (TB12) primers and the hsp65 sequence database with respect to the number of mismatches.

	Number of mismatches	Match to <i>hsp65</i> [%]	Match to GROESL [%]
Forward primer	0	30.8	0
	1	74.8	0
	2	86	4.2
	3	98.1	56.2
	4	99.1	85.4
	5	100	100
Reverse primer	0	6.5	0
	1	44.9	0
	2	89.7	52.1
	3	96.3	64.6
	4	100	81.2
	5	100	89.6

Class	Order	Numb. of RefSeq representative genomes	Percentual primer matches
Acidimicrobiia		8	38
Coriobacteriia		63	10
Nitriliruptoria		5	0
Rubrobacteria		7	43
Thermoleophilia		7	14
Actinobacteria			
	Acidothermales	1	0
	Actinomycetales	75	27
	Actinopolysporales	8	100
	Bifidobacteriales	87	68
	Catenulisporales	3	100
	Corynebacteriales	473	83
	Frankiales	18	94
	Geodermatophilales	34	100
	Glycomycetales	13	77
	Kineosporiales	5	80
	Micrococcales	482	53
	Micromonosporales	106	100
	Nakamurellales	5	20
	Propionibacteriales	120	63
	Pseudonocardiales	151	74
	Streptomycetales	348	95
	Streptosporangiales	112	88

Table S5. Number of identified Actinobacteria species by hsp65 marker for respective genus

Family	Genus (number of recovered species)			
<i>Nocardiaceae</i>	<i>Nocardia</i> (24)	<i>Rhodococcus</i> (10)		
<i>Streptomycetaceae</i>	<i>Streptomyces</i> (30)	<i>Kitasatospora</i> (1)		
<i>Mycobacteriaceae</i>	<i>Mycobacterium</i> (26)			
<i>Pseudonocardiaceae</i>	<i>Amycolatopsis</i> (7) <i>Kibdelosporangium</i> (1) <i>Sciscionella</i> (1)	<i>Pseudonocardia</i> (4) <i>Thermocrispum</i> (1) <i>Actinoalloteichus</i> (1)	<i>Lentzea</i> (2) <i>Saccharothrix</i> (1) <i>Actinokineospora</i> (1)	<i>Actinomycetospora</i> (1) <i>Alloactinosynnema</i> (1)
<i>Norcardioidaceae</i>	<i>Nocardioides</i> (6) <i>Marmoricola</i> (1)	<i>Kribbella</i> (2) <i>Aeromicrobium</i> (1)	<i>Pimelobacter</i> (1)	
<i>Streptosporangiaceae</i>	<i>Microbispora</i> (1) <i>Sinosporangium</i> (1)	<i>Microtetraspora</i> (1) <i>Streptosporangium</i> (1)	<i>Nonomuraea</i> (1)	<i>Planomonospora</i> (1)
<i>Micromonosporaceae</i>	<i>Micromonospora</i> (3)	<i>Longispora</i> (1)	<i>Catelliglobospora</i> (1)	<i>Plantactinospora</i> (1)
<i>Intrasporangiaceae</i>	<i>Janibacter</i> (3)	<i>Knoellia</i> (1)		
<i>Actinomycetaceae</i>	<i>Actinomyces</i> (3)			
<i>Jiangellaceae</i>	<i>Jaingella</i> (3)			
<i>Microbacteriaceae</i>	<i>Agromyces</i> (1)	<i>Microcella</i> (1)		
<i>Propionibacteriaceae</i>	<i>Cutibacterium</i> (1)	<i>Propionibacterium</i> (1)		
<i>Geodermatophilaceae</i>	<i>Geodermatophilus</i> (1)	<i>Modestobacter</i> (1)		
<i>Micrococcaceae</i>	<i>Micrococcus</i> (1)	<i>Rothia</i> (1)		
<i>Dermabacteraceae</i>	<i>Brachybacterium</i> (2)			
<i>Brevibacteriaceae</i>	<i>Brevibacterium</i> (2)			
<i>Corynebacteriaceae</i>	<i>Corynebacterium</i> (2)			
<i>Catenulisporaceae</i>	<i>Catenulispora</i> (1)			
<i>Dermacoccaceae</i>	<i>Kytococcus</i> (1)			
<i>Actinobacteria_incertae_sedis</i>	<i>Thermobispora</i> (1)			
<i>Nakamurellaceae</i>	<i>Nakamurella</i> (1)			
<i>Sporichthyaceae</i>	<i>Sporichthya</i> (1)			
<i>Nocardiopsaceae</i>	<i>Thermobifida</i> (1)			

Table S6. T test and F test for comparison of means and variation of diversity indices for 37 common samples of *hsp 65* and 16S rRNA markers at 97% and 99% OTUs cutoffs. For each marker averages and standard deviations are indicated.

	<i>hsp 65</i>	16S rRNA	t test		F test	
			t	P-value	F	P-value
99% OTU						
Chao-1	260.78 ± 137.051	182.17 ± 82.018	2.984	0.003	2.745	0.017
Simpson evenness	0.286 ± 0.246	0.089 ± 0.048	4.72	<0.001	26.81	<0.001
Inverse Simpson	6.57 ± 4.974	14.07 ± 6.289	5.664	<0.001	1.597	0.153
97% OTU						
Chao-1	75.74 ± 42.262	89.115 ± 36.349	1.45	0.148	1.315	0.588
Simpson evenness	0.38 ± 0.264	0.148 ± 0.105	4.908	<0.001	6.281	0.002
Inverse Simpson	4.089 ± 2.742	9.106 ± 4.443	5.824	<0.001	2.637	0.013

Table S7. Differences between Actinobacteria communities between A. caves, B. different locations within Lascaux Cave, and marked and unmarked areas calculated by analysis of molecular variance (AMOVA) and homogeneity of molecular variance (HOMOVA) for the hsp65 and 16S rRNA gene markers (97% OTUs cutoff).

A. AMOVA				Lascaux cave location				Surface area					
<i>hsp 65</i>				<i>hsp 65</i>				<i>hsp 65</i>					
Cave				Lascaux cave location				Surface area					
Lascaux		Rouffignac		Reille		Sas-1		Passage IP		Apse			
Df	F, p	Df	F, p	Df	F, p	Df	F, p	Df	F, p	Df	F, p		
Rouffignac	13	5.72***						Passage B	10	7.858**			
Reille	11	3.614**	7	4.617			Passage IP	9	3.978	10	4.419**		
Moufflon	12	6.265**	8	8.033*	6	4.736	Apse	16	4.505***	17	5.903***		
							Diaclase	9	4.518	10	5.635**		
Overall	20	5.317***					Overall	32	4.279***		3.193***		
16S rRNA				16S rRNA				16S rRNA		16S rRNA			
<i>hsp 65</i>				<i>hsp 65</i>				<i>hsp 65</i>		<i>hsp 65</i>			
Cave				Lascaux cave location				Surface area		Surface area			
Lascaux		Rouffignac		Reille		Sas-1		Passage B		Passage IP		Apse	
Df	F, p	Df	F, p	Df	F, p	Df	F, p	Df	F, p	Df	F, p	Df	F, p
Rouffignac	15	5.79***					Passage B	8	10.063				
Reille	15	5.43***	7	6.263			Passage IP	8	4.863	11	9.013**		
Moufflon	15	5.36**	7	6.329	7	2.260	Apse	19	4.09***	22	8.115***	22	2.788**
							Diaclase	8	2.723	11	5.79**	11	2.902**
Overall	23	5.274***					Overall	37	4.656***				3.005***
Bonferonni pair-wise err. rate: 0.008				Bonferonni pair-wise err. rate: 0.005				Bonferonni pair-wise err. rate: 0.005		Bonferonni pair-wise err. rate: 0.005		Bonferonni pair-wise err. rate: 0.005	
0.008 > * P > 0.005 > ** P > 0.001 > P***				0.008 > * P > 0.005 > ** P > 0.001 > P***				0.005 > * P > 0.0025 > ** P > 0.001 > P***		0.005 > * P > 0.0025 > ** P > 0.001 > P***		0.05 > * P > 0.01 > ** P > 0.001 > P	
B. HOMOVA				B. HOMOVA				B. HOMOVA		B. HOMOVA		B. HOMOVA	
<i>hsp 65</i>				<i>hsp 65</i>				<i>hsp 65</i>		<i>hsp 65</i>		<i>hsp 65</i>	
Cave				Lascaux cave location				Surface area		Surface area		Surface area	
Lascaux		Rouffignac		Reille		Sas-1		Passage B		Passage IP		Apse	
Df	F, p	Df	F, p	Df	F, p	Df	F, p	Df	F, p	Df	F, p	Df	F, p
Rouffignac	(0.193)						Sas-1	(0.229)					
Lascaux	(0.303)	0.235*					Passage B	(0.212)	0.006				
Reille	(0.342)	0.193	0.010				Passage IP	(0.388)	0.246	0.367			
Moufflon	(0.160)	0.026	0.359	0.295			Apse	(0.364)	0.270*	0.433*	0.005		
							Diaclase	(0.333)	0.126	0.206	0.020	0.010	
Overall			0.573*				Overall				0.693*		
Rouffignac		Lascaux		Reille		Sas-1		Passage B		Passage IP		Apse	
Rouffignac	(0.145)						Sas-1	(0.153)					
Lascaux	(0.276)	0.380					Passage B	(0.133)	0.012				
Reille	(0.23)	0.133	0.034				Passage IP	(0.133)	0.166	0.531*			
Moufflon	(0.199)	0.062	0.105	0.014			Apse	(0.328)	0.364	1.227*	0.079		
							Diaclase	(0.374)	0.415	1.166*	0.134*	0.031	
Overall			0.432*				Overall				1.689*		
Bonferonni pair-wise err. rate: 0.008 > P*				Bonferonni pair-wise err. rate: 0.005 > P*				Bonferonni pair-wise err. rate: 0.005 > P*		Bonferonni pair-wise err. rate: 0.005 > P*		Bonferonni pair-wise err. rate: 0.05 > P*	

-Part 2-

Paper II: Succession of microbial decomposers is determined by litter type but sites conditions drive decomposition rate



Succession of Microbial Decomposers Is Determined by Litter Type, but Site Conditions Drive Decomposition Rates

A. Buresova,^{a,b,c} J. Kopecky,^a V. Hrdinkova,^a Z. Kamenik,^d M. Omelka,^e M. Sagova-Mareckova^{a,f}

^aEpidemiology and Ecology of Microorganisms, Crop Research Institute, Prague, Czech Republic

^bDepartment of Ecology, Faculty of Science, Charles University, Prague, Czech Republic

^cEcologie Microbienne, Université Claude Bernard Lyon 1, Villeurbanne, France

^dLaboratory for Biology of Secondary Metabolism, Institute of Microbiology, Academy of Sciences of the Czech Republic, Prague, Czech Republic

^eDepartment of Probability and Mathematical Statistics, Faculty of Mathematics and Physics, Charles University in Prague, Prague, Czech Republic

^fDepartment of Microbiology, Nutrition and Dietetics, Faculty of Agrobiological Sciences, Food and Natural Resources, Czech University of Life Science in Prague, Prague, Czech Republic

ABSTRACT Soil microorganisms are diverse, although they share functions during the decomposition of organic matter. Thus, preferences for soil conditions and litter quality were explored to understand their niche partitioning. A 1-year-long litterbag transplant experiment evaluated how soil physicochemical traits of contrasting sites combined with chemically distinct litters of sedge (S), milkvetch (M) from a grassland, and beech (B) from forest site decomposition. Litter was assessed by mass loss; C, N, and P contents; and low-molecular-weight compounds. Decomposition was described by the succession of fungi, *Actinobacteria*, *Alphaproteobacteria*, and *Firmicutes*; bacterial diversity; and extracellular enzyme activities. The M litter decomposed faster at the nutrient-poor forest site, where the extracellular enzymes were more active, but microbial decomposers were not more abundant. *Actinobacteria* abundance was affected by site, while *Firmicutes* and fungi by litter type and *Alphaproteobacteria* by both factors. *Actinobacteria* were characterized as late-stage substrate generalists, while fungi were recognized as substrate specialists and site generalists, particularly in the grassland. Overall, soil conditions determined the decomposition rates in the grassland and forest, but successional patterns of the main decomposers (fungi and *Actinobacteria*) were determined by litter type. These results suggest that shifts in vegetation mostly affect microbial decomposer community composition.

IMPORTANCE Anthropogenic disturbance may cause shifts in vegetation and alter the litter input. We studied the decomposition of different litter types under soil conditions of a nutrient-rich grassland and nutrient-poor forest to identify factors responsible for changes in the community structure and succession of microbial decomposers. This will help to predict the consequences of induced changes on the abundance and activity of microbial decomposers and recognize if the decomposition process and resulting quality and quantity of soil organic matter will be affected at various sites.

KEYWORDS succession, enzyme activities, forest, grassland, organic matter

Microbial community structure and activity reflect changes of biotic (soil biota) and abiotic (climate, soil chemistry, and litter quality) factors as well as ecosystem functioning (1, 2). In particular, the complex environmental characteristics of a given site influence the pool of microbial species at the regional scale, while litter quality affects the dynamics of microorganisms coming from that pool at the local scale (3, 4).

It is still debatable whether environmental conditions or litter quality plays a larger role in decomposition (5). The transfer of litter between sites can differentiate between

Citation Buresova A, Kopecky J, Hrdinkova V, Kamenik Z, Omelka M, Sagova-Mareckova M. 2019. Succession of microbial decomposers is determined by litter type, but site conditions drive decomposition rates. *Appl Environ Microbiol* 85:e01760-19. <https://doi.org/10.1128/AEM.01760-19>.

Editor Claire Vieille, Michigan State University

Copyright © 2019 American Society for Microbiology. All Rights Reserved.

Address correspondence to M. Sagova-Mareckova, marketa.sagova@gmail.com.

Received 31 July 2019

Accepted 3 October 2019

Accepted manuscript posted online 11 October 2019

Published 27 November 2019

these two factors because site will have a predominant effect on decomposition if the local communities decompose the litter to which they are preadapted faster (6). Yet, if the litter type affects decomposition regardless of the site, the microbes are functionally redundant with respect to litter type (7). Therefore, to understand the factors driving microbial decomposition, connections between local and regional scales need to be considered over time, together with various litter types and origin (5, 8).

The roles of biotic and abiotic factors change over time as the litter is sequentially decomposed. As the chemical composition of litter changes, the associated microbial community and extracellular enzyme activities also change (9–11). The differential response of microbes to the changing litter chemistry is the basis for sorting microbes into specific guilds (10, 12). More specifically, a nutritious organic substrate is connected to a wide range of nonspecialized microbes, while recalcitrant organic substrates are decomposed only by a limited number of taxa, which can break the resistant organic structures (3, 13). It has been proposed that the identification of microbes from the late stage and/or specialized guilds should be the first step in predicting the consequences of environmental change connected to decomposition processes in temperate areas (5, 14).

Fungi have long been considered the main microbial decomposers catalyzing the decomposition of complex substrates (9, 15). Most studies focused on their decomposing abilities, while factors affecting them were found to be variable (10, 16, 17). However, the role of bacteria in decomposition has also been recently highlighted (7, 11). Particularly, *Actinobacteria*, *Proteobacteria*, *Firmicutes*, and *Bacteroidetes* produce extracellular enzymes and are active in substrate degradation (5, 18). Moreover, *Actinobacteria* are able to produce lignolytic enzymes and secondary metabolites and form filaments, which are strategies similar to those of fungi (19–23). Therefore, *Actinobacteria* may compete with fungi (15), but those two groups have rarely been studied together during the decomposition process. Their coexistence patterns, such as niche overlap and/or separation (3, 15) under the influence of various abiotic factors, could be a missing biotic predictor of decomposition (5, 15, 24).

The aim of this study was to explore the interplay of factors affecting the abundances and succession of main decomposers. We hypothesized that main decomposers will be site specific but will selectively inhabit different litter and shift their enzyme activities during the decomposition stages. In particular, we wanted to determine the importance of cross-kingdom coexistence and successional patterns of microbial communities in influencing the effects of litter type and soil condition on decomposition processes.

RESULTS

Low-molecular-weight compounds (measured by high-performance liquid chromatography [HPLC]) shifted over time (Fig. 1A). In January and March 2011, compounds were separated according to litter type, while in later months they were separated according to sites. The HPLC profiles of the milkvetch (M) litter type in January and March 2011 significantly correlated with C content ($R = 6.377$, $P < 0.001$) and most extracellular enzymes, such as β -glucosidase ($R = 7.491$, $P < 0.001$), acid phosphatase ($R = 7.776$, $P < 0.001$), and chitinase ($R = 6.152$, $P < 0.001$), according to the permutation test. Of all bacterial groups, the abundance of *Actinobacteria* most strongly correlated with the late-stage HPLC profile ($R = 10.569$, $P < 0.001$). *Actinobacteria* significantly correlated with soil water potential ($R = 2.347$, $P = 0.004$) and temperature ($R = 4.871$, $P < 0.001$).

Bacterial communities on the beech (B) and sedge (S) litter types separated from that on the M litter type, especially in January and March 2011 (Fig. 1B). Bacterial communities also shifted from the initial to late stages of decomposition (confirmed by Sammon's multidimensional scaling; see Fig. S1 in the supplemental material). Bacterial communities from a later month of decomposition significantly correlated with the abundances of *Actinobacteria* ($R = 2.5940$, $P < 0.001$), *Firmicutes* ($R = 1.2363$, $P < 0.001$), and bacterial diversity ($R = 0.9875$, $P < 0.001$) according to the permutation test. From January

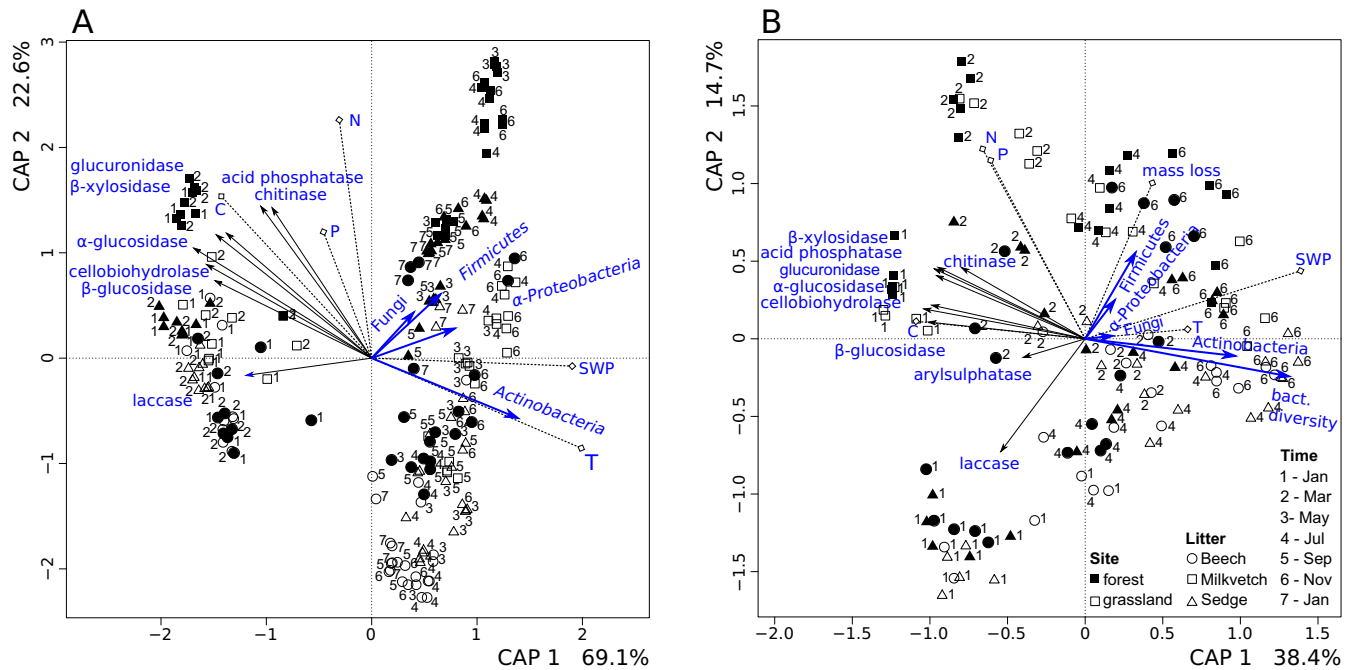


FIG 1 RDA of low-molecular-weight compounds (A, Manhattan distance) and bacterial communities (B, Bray-Curtis distance) from beech (circle), milkvetch (square), and sedge (triangle) litters at the forest (full symbol) and grassland (empty symbol) sites during the decomposition experiment (5 replicates). Vectors correspond to the statistically significant linear variables. Numbers 1 to 7 (1 to 4, respectively, for bacterial communities) correspond to sampling months (1, January 2011; 2, March 2011; 3, May 2011; 4, July 2011; 5, September 2011; 6, November 2011; 7, January 2012). Blue arrows represent extracellular enzyme activities.

2011, bacterial communities on the M litter type were significantly correlated with C ($R = 1.3441$, $P < 0.001$) and most extracellular enzyme activities, such as β -glucosidase ($R = 1.3134$, $P < 0.001$), cellobiohydrolase ($R = 0.5805$, $P < 0.001$), chitinase ($R = 0.5606$, $P < 0.001$), and acid phosphatase ($R = 0.4410$, $P = 0.007$). Bacterial communities on the B and S litter types in January 2011 significantly correlated with laccase ($R = 0.8082$, $P < 0.001$). The bacterial communities on the M litter from March significantly correlated with N ($R = 0.7699$, $P < 0.001$) and P ($R = 0.5463$, $P = 0.002$). Late-stage bacterial communities significantly correlated with soil water tension ($R = 0.7697$, $P < 0.001$) and temperature ($R = 0.3895$, $P = 0.007$).

Litter mass loss. Loss of dry mass significantly differed between sites in all decomposition stages. At the forest site (F), the average residual dry mass was about 0.5 g lower than the grassland site (G) (ANOVA, $P < 0.001$) (see Table S1 in the supplemental material). Milkvetch (M) had the highest average mass loss (ANOVA, $P < 0.001$) (Table S1), while that of sedge (S) was significantly higher than beech (B) (ANOVA, $P < 0.001$) (Table S1) at both sites. Time courses of dry mass loss were similar for the same litter type regardless of the site (Fig. 2, P_{perm} [i.e., the P value from permutational multivariate analysis of variance using distance matrices {PERMANOVA}] < 0.001 , Table S1), while dispersion did not differ between the litter types (Fig. 2; Table S1) (P_{Disp} [i.e., the P value from homogeneity of multivariate dispersions using dissimilarity measures] = 0.382). No significant differences were observed between the indigenous and exogenous origin of the litter (i.e., M and S litters did not decompose faster than B litter in the grassland and B litter did not decompose faster than M and S litters in the forest).

Carbon, nitrogen, and phosphorus contents in the litter. Carbon (C), nitrogen (N), and phosphorus (P) contents in litter significantly differed between the forest and grassland sites during decomposition (see Fig. S2 in the supplemental material). The N and C contents in all litter types were significantly higher at the forest site than the grassland site (ANOVA, $P < 0.001$) (Table S1), while P content showed the opposite relationship (ANOVA, $P = 0.001$) (Table S1). C content did not differ between litter types

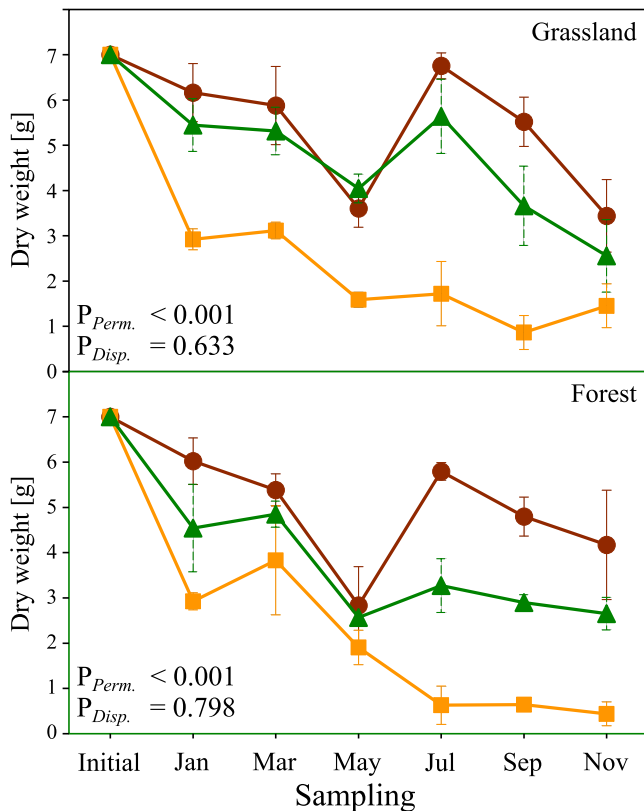


FIG 2 Average dry mass of beech (brown), milkvetch (yellow), and sedge (green) litters at the grassland and forest sites during the decomposition experiment (\pm SD, 5 replicates). The x axis indicates sampling months (i.e., initial, before litterbag burial in November 2010 and then in 2-month periods from January 2011; overall, 12 months). The P values indicate differences between profiles' distances (PERMANOVA; P_{Perm}) and dispersion (dispersion test, P_{Disp}).

at both sites, while N and P contents significantly differed, with the highest content measured for the M litter ($P < 0.001$ for N, $P < 0.001$ for P) (Table S1).

HPLC analysis of extractable low-molecular-weight compounds. HPLC profiles significantly differed between sites and litter types within each site ($P < 0.001$ for all sampling times and litter types) (Table S2).

Extracellular enzyme activities. Overall, the activities of extracellular enzymes were significantly higher in the forest than in the grassland (ANOVA, β -glucosidase, $P < 0.001$; cellobiohydrolase, $P = 0.001$; β -xylosidase, $P < 0.001$; chitinase, $P < 0.001$; glucuronidase, $P = 0.003$; acid phosphatase, $P < 0.001$; arylsulfatase, $P < 0.001$; α -glucosidase, $P = 0.001$; laccase, $P = 0.007$). Manganese peroxidase activity did not differ between the sites. Overall, higher enzyme activities were measured for the M than the S or B litters for β -glucosidase ($M > B$ and S , $P < 0.001$), cellobiohydrolase ($M > S$, $P < 0.005$; $M > B$, $P < 0.001$; $S > B$, $P < 0.001$), β -xylosidase ($M > S$, $P = 0.015$; $M > B$, $P < 0.001$; $S > B$, $P < 0.001$), and acid phosphatase ($M > B$ and S , $P < 0.001$). The activities on the M and S litters were not statistically different but were higher than those of the B litter for chitinase ($P < 0.001$), glucuronidase ($P < 0.001$), and α -glucosidase ($P < 0.001$). The S litter had the highest laccase activity ($P = 0.007$) (Table S1; Fig. 3).

Time courses of enzyme activities for chitinase, arylsulfatase, laccase, and manganese peroxidase were similar for the same litter type regardless of the site, while dispersion did not differ between the litter types (chitinase, $P_{Perm} = 0.005$, $P_{Disp} = 0.914$; arylsulfatase, $P_{Perm} = 0.004$, $P_{Disp} = 0.052$; laccase, $P_{Perm} = 0.009$, $P_{Disp} = 0.796$; and manganese peroxidase, $P_{Perm} < 0.001$, $P_{Disp} = 0.385$) (Table S1).

Bacterial communities. A total of 9,366,330 16S rRNA gene sequences were obtained, of which 6,898,021 (i.e., 73.6%) were mapped to 13,987 operational taxo-

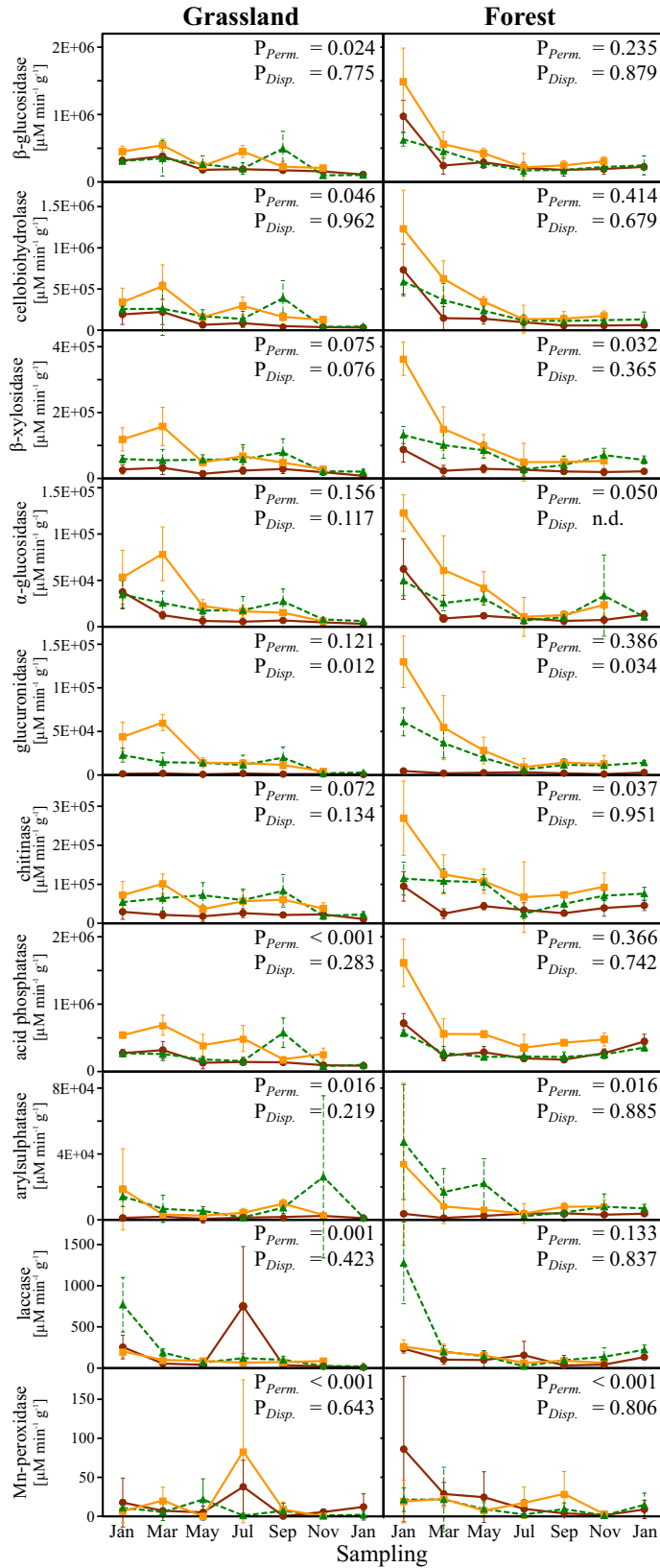


FIG 3 Extracellular enzyme activities on beech (brown), milkvetch (yellow), and sedge (green) litters at the forest and grassland sites during the decomposition experiment (\pm SD, 5 replicates). The x axes indicate sampling months (January 2011 to January 2012, i.e., 2 to 14 months after litterbag burial). The P values indicate differences between profiles' distances (PERMANOVA; P_{Perm}) and dispersion (dispersion test, P_{Disp}).

Downloaded from <http://aem.asm.org/> on December 3, 2020 by guest

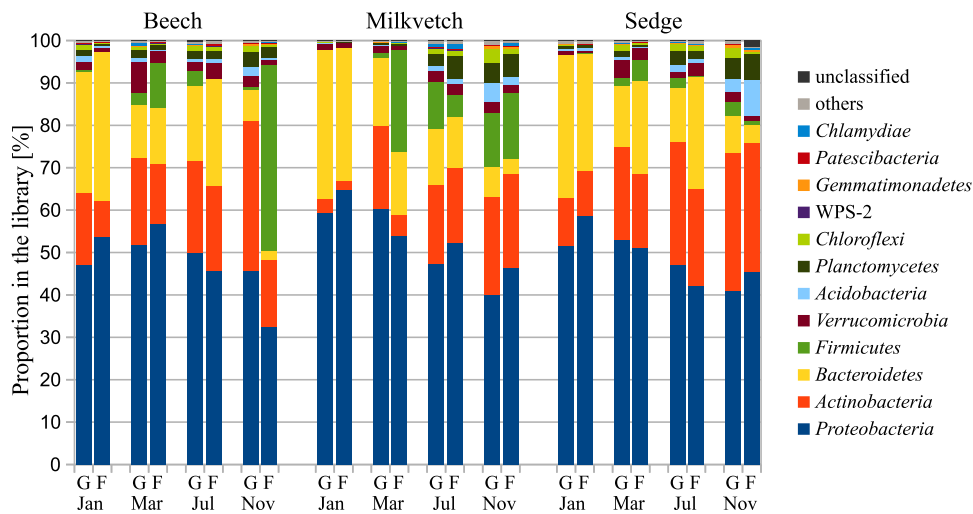


FIG 4 Average proportions of phyla in the bacterial 16S rRNA gene amplicon sequence libraries (5 replicates). Labels on the horizontal axis indicate sampling months (January to November 2011, i.e., 2 to 12 months after litterbag burial) and experimental site (G, grassland; F, forest).

nomic units (OTUs). The numbers per sample ranged between 12,630 and 78,406 sequences, with a median at 41,137 sequences.

Bacterial communities differed significantly between the forest and grassland sites in the first two sampling months for the M litter ($P = 0.009$ in January 2011, $P = 0.008$ in March) (Table S3) and in the last two sampling months for the B and S litters ($P = 0.008$ and $P = 0.006$, respectively, in July, and both species $P = 0.009$ in November 2011) (see Table S3 in the supplemental material). The bacterial community on the M litter significantly differed from that on the B and S litters (analysis of molecular variance [AMOVA], $P < 0.001$ and $P = 0.003$ at the grassland and forest sites, respectively, for both litter types) (see Table S4 in the supplemental material), with the bacterial communities not differing between the latter two litter types.

The proportions of phyla in the bacterial 16S rRNA gene amplicon sequence libraries were the highest for *Proteobacteria*, followed by *Actinobacteria*, *Bacteroidetes*, *Firmicutes*, and *Verrucomicrobia* (Fig. 4). These proportions increased over time for *Actinobacteria* (except on the B litter in November 2011 in the forest) and *Firmicutes* (especially from January to March 2011) and decreased for *Proteobacteria* and *Bacteroidetes* from January to November 2011 (Fig. 4). *Acidobacteria* proportions were the highest in the late sampling months on the M and S litters (Fig. 4) and in soil (see Fig. S3 in the supplemental material) in January and November 2011. *Verrucomicrobia* proportions were the highest in the middle sampling months (Fig. 4). Within the phylum *Actinobacteria* (see Fig. S4 in the supplemental material), the families *Streptomycetaceae* (mostly on S plants) and *Mycobacteriaceae* increased at both sites, while the proportions of *Pseudonocardiaceae*, *Gaiellaceae*, and *Promicromonosporaceae* increased mostly in the grassland, and the order *Frankiales* increased in the forest. The Trebon clade proportion increased in November 2011 on the S litter in the forest (Fig. 4).

The number of OTUs (cutoff, 97%) significantly contributing to differences between the sites was the lowest for the B litter and the highest for the M litter at both sites according to metastats (see Fig. S5 in the supplemental material). According to the rarefaction curves, the highest number of OTUs in January and March 2011 was found at the grassland site, especially for the B and S litter types. The number of OTUs was similar for all litter types for both sites in July, while the highest number of OTUs in November was measured for the M followed by S and B litter types at the grassland site (see Fig. S6 in the supplemental material). Rarefaction analysis showed that bacterial diversity differed between the sites (ANOVA; $F = 12.86$, $P < 0.001$). Bacterial diversity

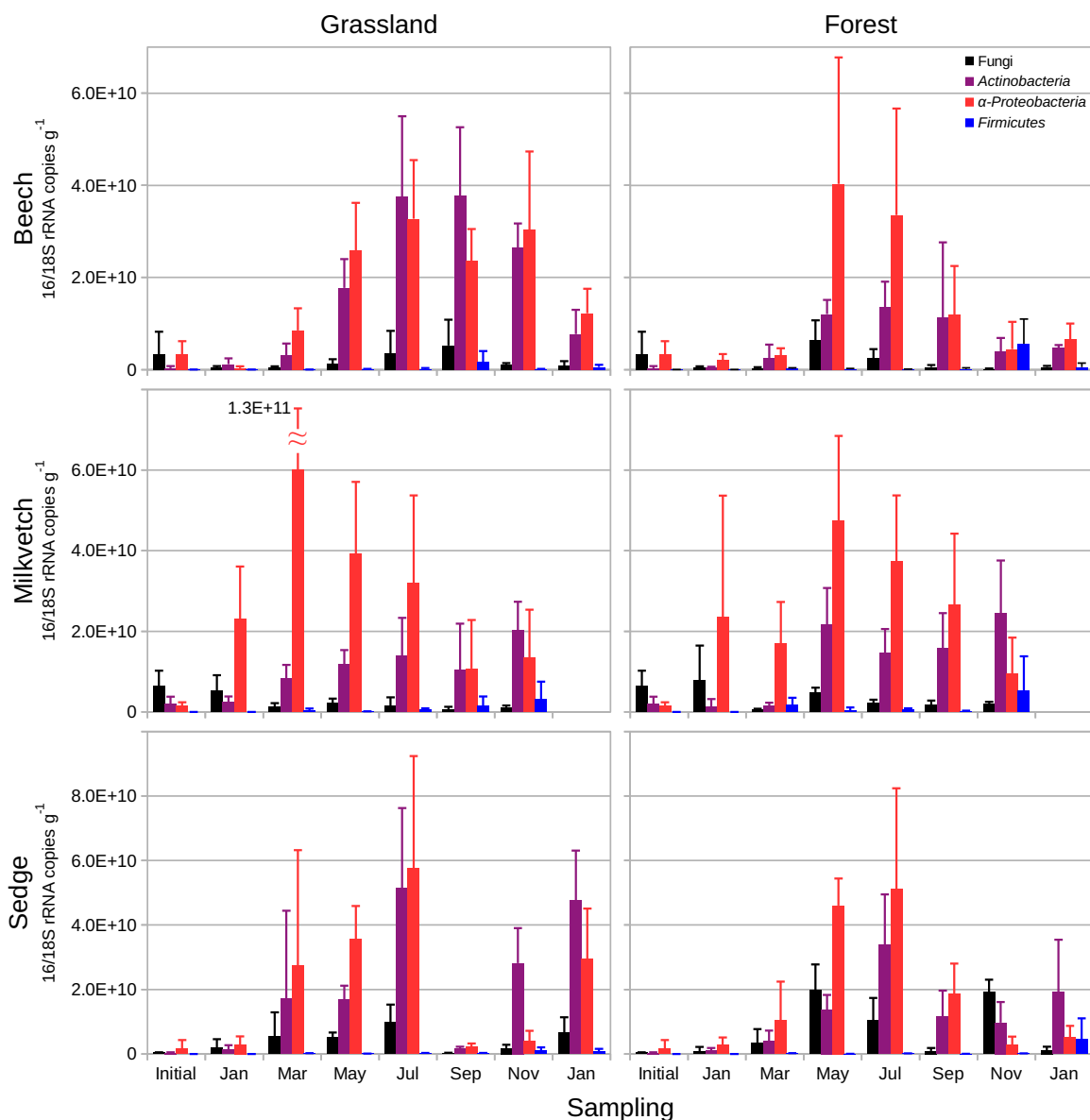


FIG 5 Abundances of fungi (18S rRNA genes), *Actinobacteria*, *Alphaproteobacteria*, and *Firmicutes* (16S rRNA genes) assayed by qPCR on beech, milkvetch, and sedge at the forest and grassland sites during the decomposition experiment (\pm SD, 5 replicates). The x axes indicate sampling months (i.e., initial in November 2010 and then in 2-month periods from January 2011; overall, 14 months).

increased on all litter types over decomposition except for the S and B litters in the forest, where the diversity declined from July to November 2011 (see Fig. S7 in the supplemental material).

Abundance of soil microorganisms. Overall, *Alphaproteobacteria* gene copies (16S rRNA) were more abundant in the grassland than at the forest but only for January and March 2011 (ANOVA, $P = 0.009$) (Table S1) and on the M than the B and S litters (both $P < 0.001$). *Actinobacteria* gene copies (16S rRNA) were more abundant in the grassland than at the forest (ANOVA, $P < 0.001$) (Table S1) but did not differ between litter types. Fungi (18S rRNA) and *Firmicutes* (16S rRNA) gene copies did not differ between the sites. *Firmicutes* were more abundant on the M than the B and S litters (ANOVA, both $P < 0.001$) (Table S1). Fungi were the least abundant on the B litter compared with both the S (ANOVA, $P < 0.001$) (Table S1) and M litters ($P = 0.015$) (Fig. 5).

The time courses of *Actinobacteria* ($P_{Perm} = 0.021$; $P_{Disp} = 0.387$) and fungi ($P_{Perm} < 0.001$; $P_{Disp} = 0.505$) were similar for the same litter type regardless of site, while dispersion did not differ between the litter types.

DISCUSSION

Decomposition rate, extracellular enzyme activities, and litter chemistry were specific according to sites and within both sites according to litter type but not litter origin. Fungi, *Actinobacteria*, *Firmicutes*, *Proteobacteria*, *Bacteroidetes*, *Acidobacteria*, and *Verrucomicrobia* each had its own role in the decomposition process. Their successional patterns differed based on their requirements for site conditions or litter type. *Actinobacteria* were identified as late-stage site-specific substrate generalists, which was the opposite pattern to fungi. The dynamics of these two groups together with bacterial community composition were driven by litter type and were synchronized with the mass loss of the most nutritious litter of milkvetch (M).

Overall, the forest site had higher decomposition rates and enzyme activities than the grassland site. The beech forest soils are considered to be an environment limited by low soil N and P (25). Thus, nutrient limitations might stimulate microbes to produce enzymes to gain the deficient nutrients from complex substrates (26). This is also supported by our finding that P acquisition for all substrates, as well as enzyme activities, was significantly higher at the forest site (27, 28). In contrast, the nutrient-rich but warmer and drier soil with diverse sources of litter at the grassland site (29) probably sufficiently covered the demands of soil microbes (30). Consequently, a higher diversity of bacterial communities was found on the grassland litter. (31).

The profiles of the low-molecular-weight compounds derived from the litter substrates represented the molecular environment during decomposition and were characteristic of each site (29) and as well as each decomposition stage within a site (32). Over time, the litter types separated mostly according to the site as opposed to the litter types (redundancy analysis [RDA]), which demonstrates how decomposition transforms litter to a humus type specific for a given site (33).

The bacterial communities for the sedge (S) and beech (B) litters considerably diverged between sites but only in the later stages of decomposition when they were composed mostly of bacteria representing the indigenous soil communities of the sites. In contrast, the associated bacterial communities on the M litter at the two sites converged over time as the nutrient-rich M litter was sequentially exhausted (4, 10). A uniform community, therefore, reflected the final stage of decomposition for the M litter, while it possibly represented only the initial depolymerization of lignin for the S and B litters (34). Furthermore, the higher-quality M litter showed the largest shifts in bacterial OTUs over time, as well as the higher decomposition rates and highest activity of hydrolytic enzymes compared with the B and S litters across both sites (35). Thus, local-scale decomposition was driven by the local community according to the litter type (33) without any effect of endogenous or exogenous litter origin (i.e., M and S litters originating at the grassland site and beech at the forest site), contrary to the home-field advantage theory (31).

Quantitative analysis based on 16S and 18S rRNA gene abundances suggested discriminating driving factors for various microbial groups during litter decomposition. Specifically, *Firmicutes* and *Alphaproteobacteria* preferentially colonized the M litter, but colonized *Firmicutes* at both sites and *Alphaproteobacteria* (only for January and March 2011) at the grassland site. Fungi were affected more and *Actinobacteria* less by litter quality, similarly as in boreal peat soil (36). Therefore, *Actinobacteria* are substrate generalists influenced by environmental conditions, and consequently, they can specifically reflect site soil characteristics (37). In contrast, the site generalism of fungi supports this group's resiliency to environmental factors (17). However, that contrasts with the generally acknowledged assumption of fungi sensitivity to soil pH (38). Thus, in this study, the relationship between fungi and bacteria was probably neutral because fungi were pH dependent only if they grew in competition with bacteria (39).

The dynamics of *Actinobacteria* and fungi, certain enzymatic activities (arylsulfatase, chitinase, laccase, and manganese peroxidase), and mass loss were more similar for one

litter type between sites than the three litter types were similar within each site. Most of those enzymes target complex organic substrates and were found to be (except manganese peroxidase) produced by both *Actinobacteria* and fungi (20, 40–42). The ability of different soil communities to carry out decomposition of the same substrate over time regardless of the site implies functional redundancy (43). Such dynamics were, however, not the case for *Alphaproteobacteria* and *Firmicutes*, which are, therefore, likely functionally distinct (7). The results indirectly suggest that the dynamics of *Actinobacteria* and fungi were driven by the same factor, i.e., litter type (19).

The decomposition process is often considered to be separated into three stages characterized by typical microbial guilds and their functions (11). In the present study, the initial stage (from January to March 2011) was characterized by high extracellular enzyme activities, especially at the forest site. The bacterial communities on the M litter type were positively affected by available N and P, suggesting that bacteria require a lower C:N but higher N:P ratio (44), especially after intense enzyme production which likely leads to substantial losses of C and N (9). In this stage, a specific form of low-molecular-weight compounds was recorded on the M litter (45). In addition, the nutrient-rich M litter had the most dynamic bacterial communities, with high incidences of fungi and *Alphaproteobacteria* (according to quantitative PCR [qPCR]). Since fungi and *Alphaproteobacteria* are known for their ability to depolymerize recalcitrant compounds (46), their initial dominance may correspond with carbon depolymerization of the M litter. Meanwhile, *Bacteroidetes* (according to amplicon sequencing) occurred on all litter types at both sites. *Bacteroidetes* are also known for their decomposing activity, and their presence in all litter types suggested promotion by litter addition (47) regardless of its quality and origin.

The middle stage of decomposition was prevalently characterized by cellulose decomposition (48), even though in the current study it was documented only at grassland site from the increased activity of cellulolytic enzymes in May for the M litter and in July for the S litter. In this stage, *Verrucomicrobia* and *Proteobacteria* make up the highest proportion of taxa on all litter types, which suggests that they are substrate generalists and polysaccharide decomposers (49). Fungi decreased and were replaced by bacteria at both sites possibly because bacteria are scavengers benefitting from the initial cellulose degradation by fungi (48).

Finally, bacterial diversity increased especially on the M litter type over time, which suggested an increased number of ecological niches when the soil and litter communities combine (9, 50). The gradual incorporation of litter to the soil is supported by the relative increase of *Acidobacteria* and *Actinobacteria*, also increased later in the decomposition process, which corresponds to their relative abundance in soil, especially *Actinobacteria* (51). The increase of *Actinobacteria*, as well as *Firmicutes*, on the M and S litter types (according to both qPCR and relative proportion in sequence libraries) implies that late-stage decomposition is associated with Gram-positive K-strategist microbial groups (10, 52).

Actinobacteria were substrate generalists that adapt to litter of different decomposability (19, 53). *Actinobacteria* quantity, together with overall bacterial diversity, was positively correlated with the structure of the late-stage bacterial communities, suggesting they have a specific function in that decomposition stage. This conclusion was also supported by the late proportional increase of the *Actinobacteria* families *Mycobacteriaceae* and *Streptomyetaceae*, of which some genera are soil saprotrophs (54) or known for lignin breakdown (46). These families are also recognized for antimicrobial activity, which may be utilized for competitor suppression or as a synergic communication to overcome the small energetic return from recalcitrant compounds (15, 23). The relative abundance of *Frankiales* also increased in the late stages but only at the forest site, suggesting the advantage of the N fixation metabolism typical for this group in decomposing recalcitrant substrates in infertile soil (53). Interestingly, we also found an increase in the proportion of the Trebon clade later in decomposition at the forest site but only on the S litter, supporting previous findings of that clade's adaptation to low pH forest soil with recalcitrant humus (55). Finally, *Actinobacteria* might have a strong impact on litter-derived humus formation through modulation of the molecular environment and interactions within the decomposer community.

Niche partitioning is related to changes in environmental conditions (35) and might result from previous competition between species regulating their coexistence (56). This may be demonstrated by the different abundance maxima of the studied microbial groups, especially fungi and *Actinobacteria*, on the rich M litter (57). On the poorer B and S litters, the abundance curves of *Actinobacteria*, fungi, and *Alphaproteobacteria* were congruent, which may represent a synergistic interaction (58, 59). In spite of fungi being the initial decomposers, they dominated over *Actinobacteria* in the later stages at the forest site on the S litter, habitats favorable for fungi and unfavorable for *Actinobacteria*. This is in accordance with the higher fitness of specialists (fungi) at their optimal environmental conditions relative to generalists (*Actinobacteria*) at the same site (60). The S litter at the grassland site represents a niche overlap for *Actinobacteria* and fungi since it is the most favorable habitat of both. Interestingly, in this situation, *Actinobacteria* dominated over fungi, which might suggest a greater contribution of *Actinobacteria* to ecosystem functioning (61).

Site conditions had the biggest impact on the progress of decomposition, measured as litter mass loss, litter chemistry, and enzyme activities. The site conditions also determined bacterial diversity, although the litter seemed to create specific niches according to the type and stage of decomposition. Finally, the site conditions were most important for the total abundance of *Actinobacteria*. In contrast, litter type determined the abundance of fungi, while the abundance of *Alphaproteobacteria* was related to both factors. Also, litter type influenced the succession of fungi and *Actinobacteria* regardless of the site. Consequently, the observed patterns revealed that the decomposition process is independent of litter type and, therefore, may be relatively stable with respect to shifts of vegetation due to disturbance. However, the niches created by various litter types and decomposition stages may have an impact on the dynamics of the main microbial decomposers and that may lead to changes in organic matter quality and sequestration.

MATERIALS AND METHODS

Litterbag experiment. A grassland site situated on the western slope of Oblik Hill in the Bohemian Massif Central, Czech Republic, and a forest site in Dorotheer Wald, Neustift near Vienna, Austria, were chosen for the litterbag experiment. Soil humidity and temperature differed between the sites (see Fig. S8 in the supplemental material). The forest site was dominated by beech (*Fagus sylvatica*), with acidic soil (pH 5.3) and soil organic matter content of 11.7%. The grassland site was dominated by diverse forbs (29), with alkaline soil (pH 7.9) and soil organic matter content of 11.0%.

For the litter transplant experiment, we used beech leaves (B), collected in November 2010 at the forest site from beech trees before litter fall, and aboveground parts of a sedge (S; *Carex humilis*) and milkvetch (M; *Astragalus exscapus*) both cut from living plants in November 2010 at the grassland site. We chose these litter types according to their quality and decomposability as described by their C:N:P ratio. B had the highest, M the lowest, and S an intermediate C:N:P ratio (Fig. S2). Polyester litterbags of size 10 × 10 cm with a mesh size of 1 mm were filled with 7 g of dried litter, with 70 litterbags prepared for each litter type. The remaining litter was stored at -70°C for future analysis and was considered the initial sampling time (initial). Overall, 105 litterbags (35 litterbags from each litter type) were placed under the top 5 cm of the soil organic layer at each site in November 2010 (Fig. 6).

A total of 50 ml of surrounding soil and litterbag samples were collected in 2-month intervals; overall, 7 samplings were performed (January, March, May, July, September, and November 2011; and January 2012). Each litterbag was weighed to assess the weight loss during the decomposition process. The M litter was completely decomposed by January 2012 and no material remained in the litterbags. Therefore, analysis of the M litter type for this sampling time is missing (Fig. 6).

The soil and litter samples were cooled during transportation and homogenized and divided into subsamples upon arrival at the laboratory. Litter water content was assessed by the gravimetric method with oven drying (62). For microbial analysis, the soil and litter samples were placed in 2-ml sterile plastic tubes and stored at -70°C until further analysis. For high-performance liquid chromatography (HPLC) analysis, 100-ml glass bottles were filled with the soil and litter samples, overlaid with a methanol-water-acetic acid mixture (80:19:1 [vol/vol/vol]), and stored at -20°C. The remaining soil and litter samples were placed in plastic bags for an analysis of pH; organic carbon content (soil samples); and C, N, and P contents (litter samples) (Fig. 6).

Soil analysis. Soil moisture tension and temperature were recorded at both sites by a Microlog SP1 datalogger (EMS, Brno, Czech Republic) equipped with a gypsum block sensor. From the recorded values, mean temperature and humidity were calculated for every month from November 2010 to March 2012. Soil pH was measured by a Multi 350 WTW glass electrode in a soil water extract (5 g of soil was extracted with 20 ml of distilled water and set for 12 hours at room temperature). Soil organic matter content was estimated by combustion in an oven at 550°C to a constant weight.

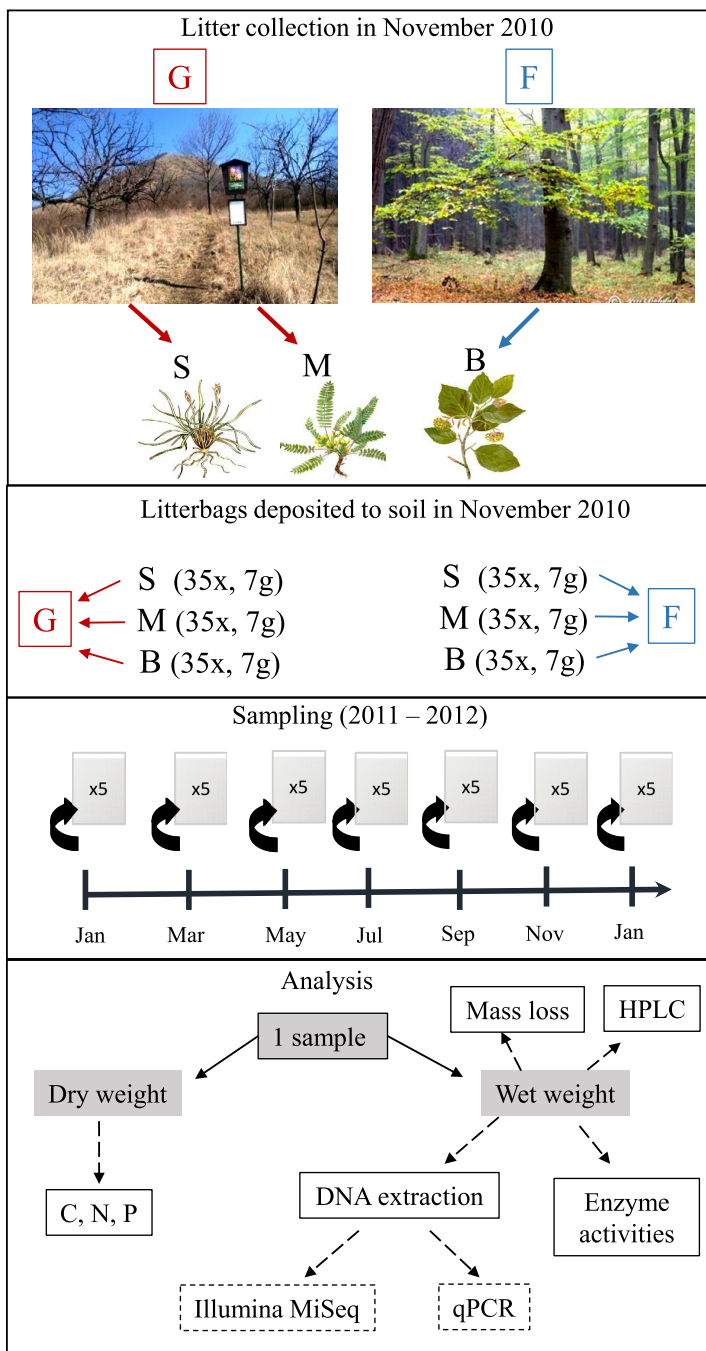


FIG 6 Diagram showing the design of the litterbag experiment on decomposition of beech (B), milkvetch (M), and sedge (S) at the grassland (G) and forest (F) sites over 1 year (January to November 2011, i.e., 2 to 12 months after litterbag burial).

Carbon, nitrogen, and phosphorus analysis in the litter. Total phosphorus (P) content was determined colorimetrically in 20 mg of dried plant litter sequentially decomposed with HNO₃ and HClO₄ using the ammonium molybdate-ascorbic acid method on a QuikChem 8500 flow injection analysis system (Lachat Instruments, Hach Company, Loveland, CO, USA) at the Botanical Institute in Třeboň, Czech Republic (63). Total carbon (C) and nitrogen (N) contents were determined in 2 g of dried litter by high-temperature combustion, followed by gas separation in a Vario Max CNS element analyzer (Elementar Analysensysteme, Hanau, Germany) by Aquatest a.s. (Prague, Czech Republic).

HPLC analysis of soluble low-molecular-weight soil metabolites. Low-molecular-weight compounds of the soil and litter samples were analyzed by high performance liquid chromatography (HPLC) (64). The compounds were extracted in methanol-water-acetic acid (80:19:1 [vol/vol/vol]) and then filtered and vacuum concentrated. The concentrated solution was fractionated using Amberlite XAD

TABLE 1 Primers used for qPCR and for MiSeq Illumina sequencing

Procedure	Primer	Sequence, 5'–3'	Concn (μM)	Target	Annealing temp (°C)	Reference
qPCR	EUB518 ^a	ATTACCGCGGCTGCTGG	0.2	Bacteria, 16S rRNA	56	76
	Act235	CGCGGCTATCAGCTTGTTG	0.2	Actinobacteria, 16S rRNA	56	77
	S-C-aProt-0528-a-S-19	CGGTAATACGRAGGGRGYT	0.4	Alphaproteobacteria, 16S rRNA	61	67
	S-C-aProt-0689-a-A-21	CBAATATCTACGAATTYCACCT	0.4	Alphaproteobacteria, 16S rRNA	61	67
	S-P-Firm-0352-a-S-18	CAGCAGTAGGGAATCTTC	0.2	Firmicutes, 16S rRNA	57	67
	S-P-Firm-0525-a-A-18	ACCTACGTATTACGCGG	0.2	Firmicutes, 16S rRNA	57	67
	FF390	CGATAACGAACGAGACCT	0.6	Fungi, 18S rRNA	50	78
	FR1	AICCATCAATCGGTAIT	0.6	Fungi, 18S rRNA	50	78
	Sequencing	CS1-515F	ACACTGACGACATGGTTCTA- CAGTGCCAGCMGCCGCGGTAA		Bacteria, 16S rRNA	
CS2-806R		TACGGTAGCAGAGACTTGGT CTGGACTACHVGGGTWTCTAAT		Bacteria, 16S rRNA		68

^aEub518 was used as a reverse primer for Act235.

1180 (5 g aqueous suspension; 2-cm-diameter glass column, equilibrated with water). A total of 50 ml of water (MilliQ quality) was used as the effluent for the first (hydrophilic) fraction and 50 ml of absolute ethanol for the second (lipophilic) fraction. The ethanolic fraction was evaporated and diluted in methanol at a concentration of 5 mg ml⁻¹. The analysis was performed using the Acquity ultraperformance liquid chromatography (UPLC) system with a 2996 photodiode array (PDA) detector (Waters, Milford, MA, USA) with a Phenomenex Luna column (5 mm, C18[2], 100 Å, 100 × 4.6 mm) equipped with a SecurityGuard cartridge (C18, 4 × 3.0-mm internal diameter [ID]; Phenomenex, Torrance, CA, USA). The separation was run in an air-conditioned room at 20°C, with a flow rate of 1.0 ml min⁻¹. Solvent A was ultrapure water, while solvent B was acetonitrile. The gradient started with 10% of solvent B for 1 min and then increased linearly to 100% of B within 8 min. The final concentration was held for a further 3.5 min. A total of 20 μl of each sample was injected. The spectra were recorded from 194 to 800 nm in 1-nm intervals. Data points were recorded twice per second and downloaded using MassLynx software (Waters) in text format for further processing.

Enzyme extraction and assays. The activities of the extracellular hydrolytic enzymes α-glucosidase (EC 3.2.1.3), 1,4-β-xylosidase (EC 3.2.1.37), 1,4-β-glucosidase (EC 3.2.1.21), acid phosphatase (EC 3.1.3.1), chitinase (EC 3.2.1.52), cellobiohydrolase (EC 3.2.1.91), glucuronidase (EC 3.2.1.31), and arylsulfatase (EC 3.1.6.1) were directly measured using methylumbelliferone-derived fluorogenic substrates in aliquots of litter samples homogenized in 50 mM sodium acetate buffer at pH 5.0 (65).

For the extracellular oxidative enzymes laccase (EC 1.10.3.2) and manganese peroxidase (EC 1.11.1.13), aliquots were desalted to separate inhibitory molecules. The activity of laccase was measured by monitoring the oxidation of 2,20-azinobis-3-ethylbenzothiazoline-6-sulfonic acid in a citrate-phosphate buffer (pH 5.0) (66). Manganese peroxidase activity was assayed in a succinate-lactate buffer (100 mM, pH 4.5) using 3-methyl-2-benzothiazolinone hydrazone and 3,3-dimethylaminobenzoic acid, which were oxidatively coupled by the enzyme. The results were compared to the activities of samples without manganese (for manganese peroxidase, the addition of manganese sulfate was substituted by an equimolar amount of EDTA). One unit of enzyme activity is defined as the amount of enzyme forming 1 μM reaction product per minute. Enzyme activities were measured in three analytical replicates and expressed per gram of plant litter dry mass (48).

DNA extraction and microbial community analysis. DNA was extracted from litter and soil samples according to Sagova-Mareckova et al. (67). The method is based on bead beating and phenol-chloroform extraction. The samples were purified by incubation with acetyltrimethylammonium bromide, followed by chloroform extraction and incubation with CaCl₂, and finally cleaned with the GeneClean turbo kit (MP Biomedicals, Santa Ana, CA, USA). DNA extracts were stored at -70°C until further analysis.

Illumina MiSeq and data processing. Bacterial 16S rRNA gene fragments, including the variable region V4, were amplified by PCR using universal primers with overhang adapters (Table 1) (68). The construction of amplicon libraries and sequencing using the MiSeq sequencer (Illumina, San Diego, CA, USA) were done at the DNA Services Facility, Research Resources Center, University of Illinois (Chicago, IL, USA). The resulting paired sequence reads were merged, filtered, and aligned using a reference alignment from the Silva database (69) and chimera checked using the integrated Vsearch tool (70) according to the MiSeq standard operation procedure (MiSeq standard operating procedure [SOP], February 2018 [68] in Mothur v. 1.39.5 [70]). A taxonomical assignment of sequence libraries was performed in Mothur using the nonredundant subset of the SILVA small subunit rRNA database, release 132 (71), adapted for use in Mothur (https://mothur.org/w/images/3/32/Silva.nr_v132.tgz), as the reference database. Sequences of plastids and mitochondria and those not classified in the domain *Bacteria* were discarded.

The sequence library was clustered into OTUs (97%) using Usearch v. 10.0.240 (72), and the OTU table was further processed using tools implemented in Mothur. Distance matrices describing the differences in community composition between individual samples were calculated using Bray-Curtis dissimilarity (73). Analysis of molecular variance (AMOVA) (74) was based on a matrix of the Bray-Curtis distances. Metastats (75) analyses were used to detect differentially represented OTUs. Rarefaction analysis was performed with the rarefaction.single function in Mothur, and areas under the rarefaction curves were

calculated using the trapezoidal rule in R version 3.4.4 (76). Figures were created using Inkscape (v. 0.92; <http://www.inkscape.org>).

Quantitative real-time PCR. Quantification of the 16S rRNA gene in *Actinobacteria*, *Alphaproteobacteria*, and *Firmicutes* and the 18S rRNA gene of fungi in the DNA extracted from litter samples was performed with the primers listed in Table 1 (77–79).

Quantitative PCR was performed using the StepOnePlus real-time PCR system (Applied Biosystems, Foster City, CA, USA) using 96-well plates with GoTaq qPCR master mix (Promega, Madison, WI, USA) containing SYBR green as a double-stranded DNA (dsDNA) binding dye. The reaction mixture contained in total a volume of 15 μ l with 1 \times GoTaq qPCR master mix, primers (for concentrations see Table 1), and 2-ng DNA sample. For all microbial groups, the PCR cycling protocol consisted of initial denaturation at 95°C for 10 min, followed by 45 cycles of denaturation (95°C for 15 s), annealing (for respective temperature see Table 1), and elongation (72°C for 30 s). Standards containing a known number of copies of the target genes 16S rRNA from *Streptomyces europaeiscabiei* DSM 41802 (for *Actinobacteria*), *Bartonella*-like clone (for *Alphaproteobacteria*), and *Paenibacillus* clone (for *Firmicutes*) and 18S rRNA from a *Penicillium* sp. clone (for fungi) were serially diluted to calibrate each qPCR melting curve and were recorded to ensure qPCR specificity. Baseline and threshold calculations were performed with StepOne v. 2.2.2. Inhibition was tested by serial DNA dilutions from each site. All qPCR measurements were done in duplicate.

Statistical analysis. All statistical calculations were done in the R computing environment (76). The effect of sites and litter types on bacterial community composition and the litter molecular parameters during the decomposition process were measured as the relationship between the distance matrices of the HPLC profiles of low-molecular-weight compounds (HPLC) and bacterial communities using a generalized distance covariance (80). The HPLC profiles were baseline corrected using the PTW package (81), and distances between profiles were calculated using Manhattan metrics. The distance matrices of the HPLC profiles and bacterial communities (exported from Mothur) were plotted by RDA projection and Sammon's multidimensional scaling using the MASS package (82). Correlations between linear variables, bacterial community, and HPLC profiles were analyzed by permutation test for capscale under a reduced model using the Bray-Curtis (bacterial communities) and Manhattan (HPLC) dissimilarities (with 999 permutations) in the VEGAN package in R (83).

To analyze the overall quantitative differences of linear variabilities (dry mass loss; abundances of microbial groups; enzyme activities; and C, N, and P contents in litter) between sites and litter types (within sites), a linear model with the additive effect of time, site, and litter type was calculated (84).

We used two tests based on the distance between the profiles as measured by correlation coefficients (see p. 319 of reference 85) to analyze the qualitative similarities between the linear variables. Permutational multivariate analysis of variance (PERMANOVA; significance values denoted here as P_{perm}) (86) tests whether the within-group distances (same litter type) are on average shorter than the between-group distances (between different litter types, aimed at detection of different mean profiles). The dispersion test (significance values denoted here as P_{disp}), introduced in Gijbels and Omelka (87), checks whether the average within-group distances differ among groups (aiming at detecting different dispersions of the samples). For manganese peroxidase, a Manhattan distance instead of the distance based on the correlation coefficient was used due to zero values in some profiles.

All linear variables (dry mass loss; microbial gene quantities; C, N, and P content; and enzyme activities, except manganese peroxidase) were logarithmically transformed (with negative values of enzymes replaced by 1 before transformation) to make their distribution more similar to a normal distribution.

Data availability. The Illumina MiSeq 16S rRNA gene amplicon sequences have been deposited in the NCBI Sequence Read Archive under accession no. [SRP158384](https://www.ncbi.nlm.nih.gov/submit/seq/srp158384) and are available under BioProject accession number [PRJNA485178](https://www.ncbi.nlm.nih.gov/bioproject/PRJNA485178).

SUPPLEMENTAL MATERIAL

Supplemental material for this article may be found at <https://doi.org/10.1128/AEM.01760-19>.

SUPPLEMENTAL FILE 1, PDF file, 0.8 MB.

ACKNOWLEDGMENTS

The work was funded by the Czech Science Foundation (grant number 15-01312S); Ministry of Education, Youth and Sports of the Czech Republic, European Regional Development Fund-Project number CZ.02.1.01/0.0/0.0/16_019/0000845 and grant number LTC17075; and Ministry of Agriculture of the Czech Republic, institutional support number MZE-RO0418.

We declare no conflict of interest.

REFERENCES

1. Purahong W, Krüger D, Buscot F, Wubet T. 2016. Correlations between the composition of modular fungal communities and litter decomposition-associated ecosystem functions. *Fungal Ecol* 22:106–114. <https://doi.org/10.1016/j.funeco.2016.04.009>.
2. Lladó S, López-Mondéjar R, Baldrian P. 2017. Forest soil bacteria: diversity, involvement in ecosystem processes, and response to global change. *Microbiol Mol Biol Rev* 81:e00063-16. <https://doi.org/10.1128/MMBR.00063-16>.

3. Fukami T. 2015. Historical contingency in community assembly: integrating niches, species pools, and priority effects. *Annu Rev Ecol Evol Syst* 46:1–23. <https://doi.org/10.1146/annurev-ecolsys-110411-160340>.
4. McGuire KL, Treseder KK. 2010. Microbial communities and their relevance for ecosystem models: decomposition as a case study. *Soil Biol Biochem* 42:529–535. <https://doi.org/10.1016/j.soilbio.2009.11.016>.
5. Bani A, Pioli S, Ventura M, Panzacchi P, Borruso L, Tognetti R, Tonon G, Brusetti L. 2018. The role of microbial community in the decomposition of leaf litter and deadwood. *Appl Soil Ecol* 126:75–84. <https://doi.org/10.1016/j.apsoil.2018.02.017>.
6. Fraser LH, Hockin AD. 2013. Litter decomposition rates of two grass species along a semi-arid grassland-forest ecocline. *J Arid Environ* 88: 125–129. <https://doi.org/10.1016/j.jaridenv.2012.07.009>.
7. Glassman SI, Weihe C, Li J, Albright MBN, Looby CI, Martiny AC, Treseder KK, Allison SD, Martiny JBH. 2018. Decomposition responses to climate depend on microbial community composition. *Proc Natl Acad Sci U S A* 115:11994–11999. <https://doi.org/10.1073/pnas.1811269115>.
8. García-Palacios P, Shaw EA, Wall DH, Hättenschwiler S. 2016. Temporal dynamics of biotic and abiotic drivers of litter decomposition. *Ecol Lett* 19:554–563. <https://doi.org/10.1111/ele.12590>.
9. Purahong W, Wubet T, Lentendu G, Schloter M, Pecyna MJ, Kapturska D, Hofrichter M, Krüger D, Buscot F. 2016. Life in leaf litter: novel insights into community dynamics of bacteria and fungi during litter decomposition. *Mol Ecol* 25:4059–4074. <https://doi.org/10.1111/mec.13739>.
10. Bray SR, Kitajima K, Mack MC. 2012. Temporal dynamics of microbial communities on decomposing leaf litter of 10 plant species in relation to decomposition rate. *Soil Biol Biochem* 49:30–37. <https://doi.org/10.1016/j.soilbio.2012.02.009>.
11. Tlaskal V, Voříšková J, Baldrian P. 2016. Bacterial succession on decomposing leaf litter exhibits a specific occurrence pattern of cellulolytic taxa and potential decomposers of fungal mycelia. *FEMS Microbiol Ecol* 92:fw177. <https://doi.org/10.1093/femsec/fw177>.
12. Wertz S, Degrange V, Prosser JI, Poly F, Commaux C, Freitag T, Guillaumeud N, Roux XL. 2006. Maintenance of soil functioning following erosion of microbial diversity. *Environ Microbiol* 8:2162–2169. <https://doi.org/10.1111/j.1462-2920.2006.01098.x>.
13. Purahong W, Schloter M, Pecyna MJ, Kapturska D, Däumlich V, Mital S, Buscot F, Hofrichter M, Gutknecht JLM, Krüger D. 2014. Uncoupling of microbial community structure and function in decomposing litter across beech forest ecosystems in Central Europe. *Sci Rep* 4:7014. <https://doi.org/10.1038/srep07014>.
14. Moorhead DL, Sinsabaugh RL. 2006. A theoretical model of litter decay and microbial interaction. *Ecol Monogr* 76:151–174. [https://doi.org/10.1890/0012-9615\(2006\)076\[0151:ATMOLD\]2.0.CO;2](https://doi.org/10.1890/0012-9615(2006)076[0151:ATMOLD]2.0.CO;2).
15. De Boer W, Folman LB, Summerbell RC, Boddy L. 2005. Living in a fungal world: impact of fungi on soil bacterial niche development. *FEMS Microbiol Rev* 29:795–811. <https://doi.org/10.1016/j.femsre.2004.11.005>.
16. Baldrian P, Zrůstová P, Tlaskal V, Davidová A, Merhautová V, Vrška T. 2016. Fungi associated with decomposing deadwood in a natural beech-dominated forest. *Fungal Ecol* 23:109–122. <https://doi.org/10.1016/j.funeco.2016.07.001>.
17. A'Bear AD, Jones TH, Kandler E, Boddy L. 2014. Interactive effects of temperature and soil moisture on fungal-mediated wood decomposition and extracellular enzyme activity. *Soil Biol Biochem* 70:151–158. <https://doi.org/10.1016/j.soilbio.2013.12.017>.
18. Fierer N, Bradford MA, Jackson RB. 2007. Toward an ecological classification of soil bacteria. *Ecology* 88:1354–1364. <https://doi.org/10.1890/05-1839>.
19. Větrovský T, Steffen KT, Baldrian P. 2014. Potential of cometabolic transformation of polysaccharides and lignin in lignocellulose by soil Actinobacteria. *PLoS One* 9:e89108. <https://doi.org/10.1371/journal.pone.0089108>.
20. Fernandes ART, da Silveira WB, Passos MLF, Zucchi TD. 2014. Laccases from Actinobacteria—what we have and what to expect. *Adv Microbiol* 04:285–296. <https://doi.org/10.4236/aim.2014.46035>.
21. Sagova-Mareckova M, Zadorova T, Penizek V, Omelka M, Tejnecky V, Pruchova P, Chuman T, Drabek O, Buresova A, Vanek A, Kopecky J. 2016. The structure of bacterial communities along two vertical profiles of a deep colluvial soil. *Soil Biol Biochem* 101:65–73. <https://doi.org/10.1016/j.soilbio.2016.06.026>.
22. Abdelmohsen UR, Grkovic T, Balasubramanian S, Kamel MS, Quinn RJ, Hentschel U. 2015. Elicitation of secondary metabolism in Actinomycetes. *Biotechnol Adv* 33:798–811. <https://doi.org/10.1016/j.biotechadv.2015.06.003>.
23. Sharma M, Dangi P, Choudhary M. 2014. Actinomycetes: source, identification, and their applications. *Int J Curr Microbiol Appl Sci* 3:801–832.
24. Fukami T, Dickie IA, Paula Wilkie J, Paulus BC, Park D, Roberts A, Buchanan PK, Allen RB. 2010. Assembly history dictates ecosystem functioning: evidence from wood decomposer communities. *Ecol Lett* 13:675–684. <https://doi.org/10.1111/j.1461-0248.2010.01465.x>.
25. Schmidt M, Veldkamp E, Corre MD. 2015. Tree species diversity effects on productivity, soil nutrient availability and nutrient response efficiency in a temperate deciduous forest. *For Ecol Manage* 338:114–123. <https://doi.org/10.1016/j.foreco.2014.11.021>.
26. Fontaine S, Mariotti A, Abbadie L. 2003. The priming effect of organic matter: a question of microbial competition? *Soil Biol Biochem* 35: 837–843. [https://doi.org/10.1016/S0038-0717\(03\)00123-8](https://doi.org/10.1016/S0038-0717(03)00123-8).
27. Mokany K, Raison RJ, Prokushkin AS. 2006. Critical analysis of root:shoot ratios in terrestrial biomes. *Glob Chang Biol* 12:84–96. <https://doi.org/10.1111/j.1365-2486.2005.001043.x>.
28. Lange M, Eisenhauer N, Sierra CA, Bessler H, Engels C, Griffiths RI, Mellado-Vázquez PG, Malik AA, Roy J, Scheu S, Steinbeiss S, Thomson BC, Trumbore SE, Gleixner G. 2015. Plant diversity increases soil microbial activity and soil carbon storage. *Nat Commun* 6:6707. <https://doi.org/10.1038/ncomms7707>.
29. Sagova-Mareckova M, Omelka M, Cermak L, Kamenik Z, Olsovska J, Hackl E, Kopecky J, Hadacek F. 2011. Microbial communities show parallels at sites with distinct litter and soil characteristics. *Appl Environ Microbiol* 77:7560–7567. <https://doi.org/10.1128/AEM.00527-11>.
30. McDaniel MD, Grandy AS, Tiemann LK, Weintraub MN. 2014. Crop rotation complexity regulates the decomposition of high and low quality residues. *Soil Biol Biochem* 78:243–254. <https://doi.org/10.1016/j.soilbio.2014.07.027>.
31. John MGS, Orwin KH, Dickie IA. 2011. No “home” versus “away” effects of decomposition found in a grassland-forest reciprocal litter transplant study. *Soil Biol Biochem* 43:1482–1489. <https://doi.org/10.1016/j.soilbio.2011.03.022>.
32. Ristok C, Leppert KN, Franke K, Scherer-Lorenzen M, Niklaus PA, Wess-johann LA, Bruehlheide H. 2017. Leaf litter diversity positively affects the decomposition of plant polyphenols. *Plant Soil* 419:305–317. <https://doi.org/10.1007/s11104-017-3340-8>.
33. Solly EF, Schöning I, Boch S, Kandler E, Marhan S, Michalzik B, Müller J, Zscheischler J, Trumbore SE, Schirmpf M. 2014. Factors controlling decomposition rates of fine root litter in temperate forests and grasslands. *Plant Soil* 382:203–218. <https://doi.org/10.1007/s11104-014-2151-4>.
34. Dungait JAJ, Hopkins DW, Gregory AS, Whitmore AP. 2012. Soil organic matter turnover is governed by accessibility not recalcitrance. *Glob Chang Biol* 18:1781–1796. <https://doi.org/10.1111/j.1365-2486.2012.02665.x>.
35. Kielak AM, Scheublin TR, Mendes LW, Van Veen JA, Kuramae EE. 2016. Bacterial community succession in pine-wood decomposition. *Front Microbiol* 7:231. <https://doi.org/10.3389/fmicb.2016.00231>.
36. Peltoniemi K, Straková P, Fritze H, Iráizoz PA, Pennanen T, Laiho R. 2012. How water-level drawdown modifies litter-decomposing fungal and actinobacterial communities in boreal peatlands. *Soil Biol Biochem* 51: 20–34. <https://doi.org/10.1016/j.soilbio.2012.04.013>.
37. Sagova-Mareckova M, Cermak L, Omelka M, Kyselkova M, Kopecky J. 2015. Bacterial diversity and abundance of a creek valley sites reflected soil pH and season. *Open Life Sci* 10:61–70. <https://doi.org/10.1515/biol-2015-0007>.
38. Högborg MN, Högborg P, Myrold DD. 2007. Is microbial community composition in boreal forest soils determined by pH, C-to-N ratio, the trees, or all three? *Oecologia* 150:590–601. <https://doi.org/10.1007/s00442-006-0562-5>.
39. Rousk J, Brookes PC, Bååth E. 2009. Contrasting soil pH effects on fungal and bacterial growth suggest functional redundancy in carbon mineralization. *Appl Environ Microbiol* 75:1589–1596. <https://doi.org/10.1128/AEM.02775-08>.
40. Malý S, Fiala P, Reininger D, Obdržálková E. 2014. The relationships among microbial parameters and the rate of organic matter mineralization in forest soils, as influenced by forest type. *Pedobiologia (Jena)* 57:235–244. <https://doi.org/10.1016/j.pedobi.2014.09.003>.
41. Chen H, Liu J, Li D, Xiao K, Wang K. 2019. Controls on soil arylsulfatase activity at a regional scale. *Eur J Soil Biol* 90:9–14. <https://doi.org/10.1016/j.ejsobi.2018.11.001>.
42. Vrsanska M, Voberkova S, Langer V, Palovcikova D, Moullick A, Adam V, Kopel P, Vrsanska M, Voberkova S, Langer V, Palovcikova D, Moullick A, Adam V, Kopel P. 2016. Induction of laccase, lignin peroxidase and

- manganese peroxidase activities in white-rot fungi using copper complexes. *Molecules* 21:1553. <https://doi.org/10.3390/molecules21111553>.
43. Banerjee S, Kirkby CA, Schmutter D, Bissett A, Kirkegaard JA, Richardson AE. 2016. Network analysis reveals functional redundancy and keystone taxa amongst bacterial and fungal communities during organic matter decomposition in an arable soil. *Soil Biol Biochem* 97:188–198. <https://doi.org/10.1016/j.soilbio.2016.03.017>.
 44. Güsewell S, Gessner MO. 2009. N:P ratios influence litter decomposition and colonization by fungi and bacteria in microcosms. *Funct Ecol* 23: 211–219. <https://doi.org/10.1111/j.1365-2435.2008.01478.x>.
 45. van Hees PAW, Jones DL, Finlay R, Godbold DL, Lundström US. 2005. The carbon we do not see—the impact of low molecular weight compounds on carbon dynamics and respiration in forest soils: a review. *Soil Biol Biochem* 37:1–13. <https://doi.org/10.1016/j.soilbio.2004.06.010>.
 46. Bugg TDH, Ahmad M, Hardiman EM, Singh R. 2011. The emerging role for bacteria in lignin degradation and bio-product formation. *Curr Opin Biotechnol* 22:394–400. <https://doi.org/10.1016/j.copbio.2010.10.009>.
 47. Sauvadet M, Chauvat M, Cluzeau D, Maron PA, Villenave C, Bertrand I. 2016. The dynamics of soil micro-food web structure and functions vary according to litter quality. *Soil Biol Biochem* 95:262–274. <https://doi.org/10.1016/j.soilbio.2016.01.003>.
 48. Šnajdr J, Cajthaml T, Valášková V, Merhautová V, Petráňková M, Spetz P, Leppänen K, Baldrian P. 2011. Transformation of *Quercus petraea* litter: successive changes in litter chemistry are reflected in differential enzyme activity and changes in the microbial community composition. *FEMS Microbiol Ecol* 75:291–303. <https://doi.org/10.1111/j.1574-6941.2010.00999.x>.
 49. Cardman Z, Arnosti C, Durbin A, Ziervogel K, Cox C, Steen AD, Teske A. 2014. Verrucomicrobia are candidates for polysaccharide-degrading bacterioplankton in an arctic fjord of Svalbard. *Appl Environ Microbiol* 80:3749–3756. <https://doi.org/10.1128/AEM.00899-14>.
 50. Jackson CR. 2003. Changes in community properties during microbial succession. *Oikos* 101:444–448. <https://doi.org/10.1034/j.1600-0706.2003.12254.x>.
 51. Štursová M, Žifčáková L, Leigh MB, Burgess R, Baldrian P. 2012. Cellulose utilization in forest litter and soil: identification of bacterial and fungal decomposers. *FEMS Microbiol Ecol* 80:735–746. <https://doi.org/10.1111/j.1574-6941.2012.01343.x>.
 52. Bastian F, Bouziri L, Nicolardot B, Ranjard L. 2009. Impact of wheat straw decomposition on successional patterns of soil microbial community structure. *Soil Biol Biochem* 41:262–275. <https://doi.org/10.1016/j.soilbio.2008.10.024>.
 53. Gao B, Gupta R. 2012. Phylogenetic framework and molecular signatures for the main clades of the phylum Actinobacteria. *Microbiol Mol Biol Rev* 76:66–112. <https://doi.org/10.1128/MMBR.05011-11>.
 54. Kopecky J, Kyselkova M, Omelka M, Cermak L, Novotna J, Grundmann G, Moëgne-Loccoz Y, Sagova-Mareckova M. 2011. Environmental mycobacteria closely related to the pathogenic species evidenced in an acidic forest wetland. *Soil Biol Biochem* 43:697–700. <https://doi.org/10.1016/j.soilbio.2010.11.033>.
 55. Kopecky J, Kyselkova M, Omelka M, Cermak L, Novotna J, Grundmann GL, Moëgne-Loccoz Y, Sagova-Mareckova M. 2011. Actinobacterial community dominated by a distinct clade in acidic soil of a waterlogged deciduous forest. *FEMS Microbiol Ecol* 78:386–394. <https://doi.org/10.1111/j.1574-6941.2011.01173.x>.
 56. Leibold M, McPeck M. 2006. Coexistence of the niche and neutral perspectives in community ecology. *Ecology* 87:1399–1410. [https://doi.org/10.1890/0012-9658\(2006\)87\[1399:COTNAN\]2.0.CO;2](https://doi.org/10.1890/0012-9658(2006)87[1399:COTNAN]2.0.CO;2).
 57. Rousk J, Demoling LA, Bahr A, Bååth E. 2008. Examining the fungal and bacterial niche overlap using selective inhibitors in soil. *FEMS Microbiol Ecol* 63:350–358. <https://doi.org/10.1111/j.1574-6941.2008.00440.x>.
 58. Johnston SR, Boddy L, Weightman AJ. 2016. Bacteria in decomposing wood and their interactions with wood-decay fungi. *FEMS Microbiol Ecol* 92:fiw179. <https://doi.org/10.1093/femsec/fiw179>.
 59. Meidute S, Demoling F, Bååth E. 2008. Antagonistic and synergistic effects of fungal and bacterial growth in soil after adding different carbon and nitrogen sources. *Soil Biol Biochem* 40:2334–2343. <https://doi.org/10.1016/j.soilbio.2008.05.011>.
 60. Monard C, Gantner S, Bertilsson S, Hallin S, Stenlid J. 2016. Habitat generalists and specialists in microbial communities across a terrestrial-freshwater gradient. *Sci Rep* 6:37719. <https://doi.org/10.1038/srep37719>.
 61. Strickland MS, Rousk J. 2010. Considering fungal:bacterial dominance in soils—methods, controls, and ecosystem implications. *Soil Biol Biochem* 42:1385–1395. <https://doi.org/10.1016/j.soilbio.2010.05.007>.
 62. Carter MR, Gregorich EG. 2008. Soil sampling and methods of analysis, second ed. Taylor & Francis Group, LLC, USA.
 63. Olsen SR. 1954. Estimation of available phosphorus in soils by extraction with sodium bicarbonate. US Department of Agriculture, Washington, DC.
 64. Kameník Z, Hadacek F, Marečková M, Ulanova D, Kopecký J, Chobot V, Plháčková K, Olšovská J. 2010. Ultra-high-performance liquid chromatography fingerprinting method for chemical screening of metabolites in cultivation broth. *J Chromatogr A* 1217:8016–8025. <https://doi.org/10.1016/j.chroma.2010.08.031>.
 65. Baldrian P. 2009. Microbial enzyme-catalyzed processes in soils and their analysis. *Plant Soil Environ* 55:370–378. <https://doi.org/10.17221/134/2009-PSE>.
 66. Bourbonnais R, Paice MG. 1990. Oxidation of non-phenolic substrates. *FEBS Lett* 267:99–102. [https://doi.org/10.1016/0014-5793\(90\)80298-w](https://doi.org/10.1016/0014-5793(90)80298-w).
 67. Sagova-Mareckova M, Cermak L, Novotna J, Plhacova K, Forstova J, Kopecky J. 2008. Innovative methods for soil DNA purification tested in soils with widely differing characteristics. *Appl Environ Microbiol* 74: 2902–2907. <https://doi.org/10.1128/AEM.02161-07>.
 68. Kozich JJ, Westcott SL, Baxter NT, Highlander SK, Schloss PD. 2013. Development of a dual-index sequencing strategy and curation pipeline for analyzing amplicon sequence data on the MiSeq Illumina sequencing platform. *Appl Environ Microbiol* 79:5112–5120. <https://doi.org/10.1128/AEM.01043-13>.
 69. Quast C, Pruesse E, Yilmaz P, Gerken J, Schweer T, Yarza P, Peplies J, Glöckner FO. 2013. The SILVA ribosomal RNA gene database project: improved data processing and Web-based tools. *Nucleic Acids Res* 41:D590–D596. <https://doi.org/10.1093/nar/gks1219>.
 70. Rognes T, Flouri T, Nichols B, Quince C, Mahé F. 2016. VSEARCH: a versatile open source tool for metagenomics. *PeerJ* 4:e2584. <https://doi.org/10.7717/peerj.2584>.
 71. Yilmaz P, Parfrey LW, Yarza P, Gerken J, Pruesse E, Quast C, Schweer T, Peplies J, Ludwig W, Glöckner FO. 2014. The SILVA and “all-species Living Tree Project (LTP)” taxonomic frameworks. *Nucleic Acids Res* 42: D643–D648. <https://doi.org/10.1093/nar/gkt1209>.
 72. Edgar RC. 2013. UPARSE: highly accurate OTU sequences from microbial amplicon reads. *Nat Methods* 10:996–998. <https://doi.org/10.1038/nmeth.2604>.
 73. Bray JR, Curtis JT. 1957. An ordination of the upland forest communities of southern Wisconsin. *Ecol Monogr* 27:325–349. <https://doi.org/10.2307/1942268>.
 74. Martin AP. 2002. Phylogenetic approaches for describing and comparing the diversity of microbial phylogenetic approaches for describing and comparing the diversity of microbial communities. *Appl Environ Microbiol* 68:3673–3682. <https://doi.org/10.1128/aem.68.8.3673-3682.2002>.
 75. White JR, Nagarajan N, Pop M. 2009. Statistical methods for detecting differentially abundant features in clinical metagenomic samples. *PLoS Comput Biol* 5:e1000352. <https://doi.org/10.1371/journal.pcbi.1000352>.
 76. R Core Team. 2018. R: a language and environment for statistical computing. R Foundation for Statistical Computing, Vienna, Austria.
 77. Muyzer G, de Waal EC, Uitterlinden AG. 1993. Profiling of complex microbial populations by denaturing gradient gel electrophoresis analysis of polymerase chain reaction-amplified genes coding for 16S rRNA. *Appl Environ Microbiol* 59:695–700.
 78. Stach JEM, Maldonado LA, Ward AC, Goodfellow M, Bull AT. 2003. New primers for the class Actinobacteria: application to marine and terrestrial environments. *Environ Microbiol* 5:828–841. <https://doi.org/10.1046/j.1462-2920.2003.00483.x>.
 79. Prévost-Bouré CN, Christen R, Dequiedt S, Mougé C, Lelièvre M, Jolivet C, Shahbazkia HR, Guillou L, Arrouays D, Ranjard L. 2011. Validation and application of a PCR primer set to quantify fungal communities in the soil environment by real-time quantitative PCR. *PLoS One* 6:e24166. <https://doi.org/10.1371/journal.pone.0024166>.
 80. Omelka M, Hudecová Š. 2013. A comparison of the Mantel test with a generalised distance covariance test. *Environmetrics* 24:449–460. <https://doi.org/10.1002/env.2238>.
 81. Bloemberg TG, Gerretzen J, Lunshof A, Wehrens R, Buydens L. 2013. Warping methods for spectroscopic and chromatographic signal alignment: a tutorial. *Anal Chim Acta* 781:14–32. <https://doi.org/10.1016/j.jca.2013.03.048>.
 82. Venables WN, Ripley BD. 2002. Random and mixed effects, p 271–300. *In* Modern applied statistics with S. Springer, New York, NY.
 83. Oksanen J, Blanchet FG, Friendly M, Kindt R, Legendre P, McGlenn D, Minchin PR, O'Hara RB, Simpson GL, Solymos P, Stevens MHH, Szocs E,

- Wagner H. 2019. vegan: community ecology package. R package version 2.5-6. <https://CRAN.R-project.org/package=vegan>.
84. Hothorn T, Everitt BS. 2014. A handbook of statistical analyses using R. Chapman and Hall/CRC, New York, NY. <https://doi.org/10.1201/b17081>.
85. Legendre P, Legendre L. 2012. Numerical ecology, 3rd English ed. Elsevier Science BV, Amsterdam, the Netherlands.
86. McArdle BH, Anderson MJ. 2001. Fitting multivariate models to community data: a comment on distance-based redundancy analysis. *Ecology* 82:290–297. <https://doi.org/10.2307/2680104>.
87. Gijbels I, Omelka M. 2013. Testing for homogeneity of multivariate dispersions using dissimilarity measures. *Biometrics* 69:137–145. <https://doi.org/10.1111/j.1541-0420.2012.01797.x>.

Supplementary Information for

Decomposition was driven by site conditions, while dynamics of *Actinobacteria* and fungi reflected a litter type

Buresova A., Kopecky J., Hrdinkova V., Kamenik Z., Omelka M., Sagova-Mareckova M.

Corresponding author: Marketa Sagova-Mareckova
Email: marketa.sagova@gmail.com

This PDF file includes:

Supplementary text
Figs. S1 to S10
Tables S1 to S5
References for supplementary text citations

Supplementary Text

Materials and Methods

Litterbag experiment

A grassland site (G) situated at the western slope of Oblik hill in Bohemian Massive Central, Czech Republic and a forest site (F) in Dorotheer Wald, Neustift near Wien, Austria were chosen for the litterbag experiment. Soil pH, vegetation, soil organic carbon content, soil humidity and temperature contrasted the sites (Fig. S1.). The F site was dominated by beech (*Fagus sylvatica*), with acidic soil (pH 5.3) and soil organic matter content 11.7%. The G site was dominated by diverse forbs (1), with alkaline soil (pH 7.9) and soil organic matter content 11.0%.

For the experiment, we used leaves of beech (B, *Fagus sylvatica*) from *Fagaceae* family (collected in November 2010 at the forest site), and aboveground parts of sedge (S, *Carex humilis*) from *Cyperaceae* family, and milkvetch (M, *Astragalus exscapus*) from *Fabaceae* family (both collected in November 2010 at the grassland site). We chose these litter types according to their quality and decomposability described by C:N:P ratio. B disposed of the highest, M the lowest and S the intermediate C:N:P ratio in its tissues (Fig. S2).

The soil and litterbag samples were collected in two-month intervals; overall 7 samplings were performed (January 2011, March 2011, May 2011, July 2011, September 2011, November 2011 and January 2012). Each litterbag was weighted to assess the weight loss during the decomposition process. M litter was completely decomposed in January 2012 and no material remained in the litterbags. Therefore, analysis for this sampling time for M litter type are missing.

The soil and litter samples were cooled during transportation, homogenized and divided into subsamples upon arrival to the laboratory. For microbial analysis, the soil and litter samples were placed in 2 ml sterile plastic tubes and stored at -70°C until a further analysis. For high performance liquid chromatography (HPLC) analysis 100 ml glass bottles were filled with the soil and litter samples, overlaid with a mixture of methanol-water-acetic acid (80:19:1, vol/vol/vol) and stored in -20°C. The remaining soil and litter samples were placed in plastic bags for analysis of pH, organic carbon content (soil samples) and C, N and P contents (litter samples).

Soil analysis

Soil moisture tension and temperature were recorded at both sites by a datalogger Microlog SP1 (EMS, Brno, Czech Republic) equipped with a gypsum block sensor. From recorded values, mean temperature and humidity for every month from November 2010 to March 2012 were calculated. The soil pH was measured by a Multi 350 WTW glass electrode in a soil water extract (5 g of soil was extracted with 20 ml of distilled water and set for 12 hours at a room temperature). The soil organic matter content was estimated by combustion in an oven at 550°C to the constant weight.

HPLC analysis of soluble low-molecular-weight soil metabolites

The extracts of soil and litter samples in a methanol-water-acetic acid were filtered and vacuum concentrated. The concentrated solution was fractionated using Amberlite XAD 1180 (5 g of aqueous suspension; 2 cm diameter of a glass column, equilibrated with water). 50 ml of water (MilliQ quality) was used as the effluent for the first (hydrophilic) fraction; 50 ml of absolute ethanol was used for the second (lipophilic) fraction. The ethanolic fraction was evaporated and diluted in a methanol at a concentration of 5 mg ml⁻¹. The analysis was performed using Acquity UPLC system with the 2996 PDA detector (Waters, Milford, MA, USA). The column was a Phenomenex Luna 5 mm C18(2) 100 Å, 100 × 4.6 mm, equipped with a SecurityGuard cartridge C18, 4 × 3.0 mm ID (Phenomenex, Torrance, CA, USA). The separation was run in the air-conditioned room at 20°C, and the flow rate was 1.0 ml min⁻¹. Solvent A was ultrapure water; solvent B was acetonitrile. The gradient started with 10% of solvent B for 1 min and then increased linearly to 100% of B within 8 min. The final concentration was held for further 3.5 min. 20 µl of each sample were injected. The spectra were recorded from 194 to 800 nm in 1 nm intervals. Data points recorded twice per second were exported from a MassLynx software (Waters) in a text format for further processing.

Enzyme extraction and assays

The activities of extracellular hydrolytic enzymes α – glucosidase (3.2.1.3), 1,4- β - xylosidase (EC 3.2.1.37), 1,4- β -glucosidase (EC 3.2.1.21), acid phosphatase (EC 3.1.3.1), chitinase (EC 3.2.1.52), cellobiohydrolase (EC 3.2.1.91), glucuronidase

(3.2.1.31) and arylsulphatase (3.1.6.1) were measured using methylumbellyferone-derived fluorogenic substrates directly in aliquots of litter samples homogenized in 50 mM sodium acetate buffer at pH 5.0 (2).

For extracellular oxidative enzymes laccase (EC 1.10.3.2) and manganese peroxidase (EC 1.11.1.13), aliquots were desalted to separate inhibitory molecules. The activity of laccase was measured by monitoring the oxidation of 2,20-azinobis-3-ethylbenzothiazoline-6-sulfonic acid in a citrate-phosphate buffer (pH 5.0) (3). The manganese peroxidase activity was assayed in a succinate-lactate buffer (100 mM, pH 4.5) using 3-Methyl-2-benzothiazolinone hydrazone and 3,3-dimethylaminobenzoic acid, which were oxidatively coupled by the enzyme. The results were corrected by activities of samples without manganese (for MnP) – the addition of manganese sulphate was substituted by an equimolar amount of EDTA. One unit of enzyme activity is defined as the amount of enzyme forming 1 μ M of reaction product per min. Enzyme activities were measured in three analytical replicates and expressed per g plant litter dry mass (4).

DNA extraction and purification

DNA was extracted from 0.1 g of homogenized litter and 0.5 g of soil samples (only from those collected in January 2011 and November 2011) by method SK described by Sagova-Mareckova *et al.* (2008). The method is based on bead-beating and phenol/chloroform extraction. The samples were purified by incubation with acetyltrimethylammonium bromide followed by chloroform extraction and incubation with CaCl_2 , and finally cleaned with GeneClean Turbo kit (MP Biomedicals, Santa Ana, CA, USA). DNA extracts were stored at -70°C until the further analysis.

Quantitative real-time PCR

Quantification of 16S rRNA gene of *Actinobacteria*, *Alphaproteobacteria*, *Firmicutes* and 18S rRNA gene of fungi in the extracted DNA from litter samples were performed with primers listed in Table S1(6–8).

Quantitative PCR were performed using a StepOnePlus Real-Time PCR System (Applied Biosystems, Foster City, CA, USA) using 96-well plates with GoTaq qPCR Master Mix (Promega, Madison, WI, USA) containing SYBR Green as a double-stranded DNA (dsDNA) binding dye. The reaction mixture contained in a total

volume of 15 μ l: 1 \times GoTaq qPCR Master Mix, primers (for concentrations see Table S1.) and 2 ng DNA sample. For all microbial groups the PCR cycling protocol consisted of initial denaturation at 95°C for 10 min, followed by 45 cycles of denaturation (95°C for 15s), annealing (for respective temperature see Table S1.) and elongation (72°C for 30s). Standards containing known number of copies of the target genes 16S rRNA from *Streptomyces europaeiscabiei* DSM 41802 (for *Actinobacteria*), *Bartonella-like* clone (for *Alphaproteobacteria*), *Paenibacillus* clone (for *Firmicutes*) and 18S rRNA from *Penicillium sp.* clone (for fungi), were serially diluted to calibrate each qPCR melting curve and were recorded to ensure qPCR specificity. Baseline and threshold calculations were performed with the StepOne v. 2.2.2 software. The inhibition was tested by serial DNA dilutions from each site. All qPCR measurements were done in duplicate.

Illumina MiSeq and data processing

Bacterial 16S rRNA gene fragments including the variable region V4 were amplified by PCR using universal primers with overhang adapters (Table S1.) (9). Construction of amplicon libraries and sequencing using the MiSeq sequencer (Illumina, San Diego, USA) were done at the DNA Services Facility, Research Resources Center, University of Illinois (Chicago, USA). The resulting paired sequence reads were merged, filtered, aligned using a reference alignment from the Silva database (10), and chimera checked using integrated Vsearch tool [12] according to the MiSeq standard operation procedure (Miseq SOP, February 2018; (9)) in Mothur v. 1.39.5 software (11). A taxonomical assignment of sequence libraries was performed in Mothur using the non-redundant subset of Silva Small Subunit rRNA Database, release 132 (12) adapted for use in Mothur (https://mothur.org/w/images/3/32/Silva.nr_v132.tgz) as the reference database. Sequences of plastids, mitochondria, and those not classified in the domain *Bacteria* were discarded.

The sequence library was clustered into OTUs using the Usearch v10.0.240 software (13), and the OTU table was further processed using tools implemented in the Mothur software. Distance matrices describing the differences in community composition between individual samples were calculated using the Yue-Clayton theta calculator (14). Analysis of molecular variance (AMOVA; (15)) was based on a

matrix of Yue-Clayton theta distances. Metastats (16) analyses were used to detect differentially represented OTUs. Rarefaction analysis was performed with rarefaction.single function in Mothur, and areas under the rarefaction curves were calculated using trapezoidal rule in the R version 3.4.4 software (17). Figures were created using Inkscape (v0.92; <http://www.inkscape.org>).

The Illumina MiSeq 16S rRNA gene amplicon sequences have been deposited in the NCBI Sequence Read Archive under accession no. SRP158384 (<https://www.ncbi.nlm.nih.gov/sra/SRP158384>) and are available under BioProject no. PRJNA485178.

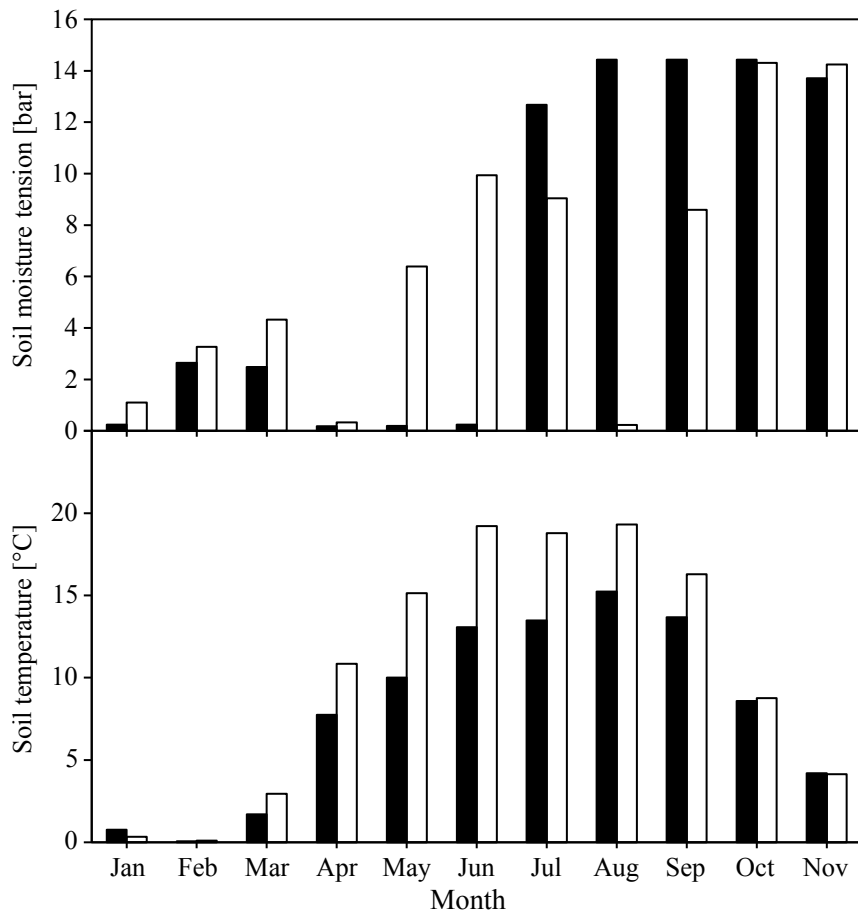


Fig. S1. Monthly averages of soil moisture tension and soil temperature measured by datalogger during litterbag experiment at the forest (black) and the grassland (white) sites.

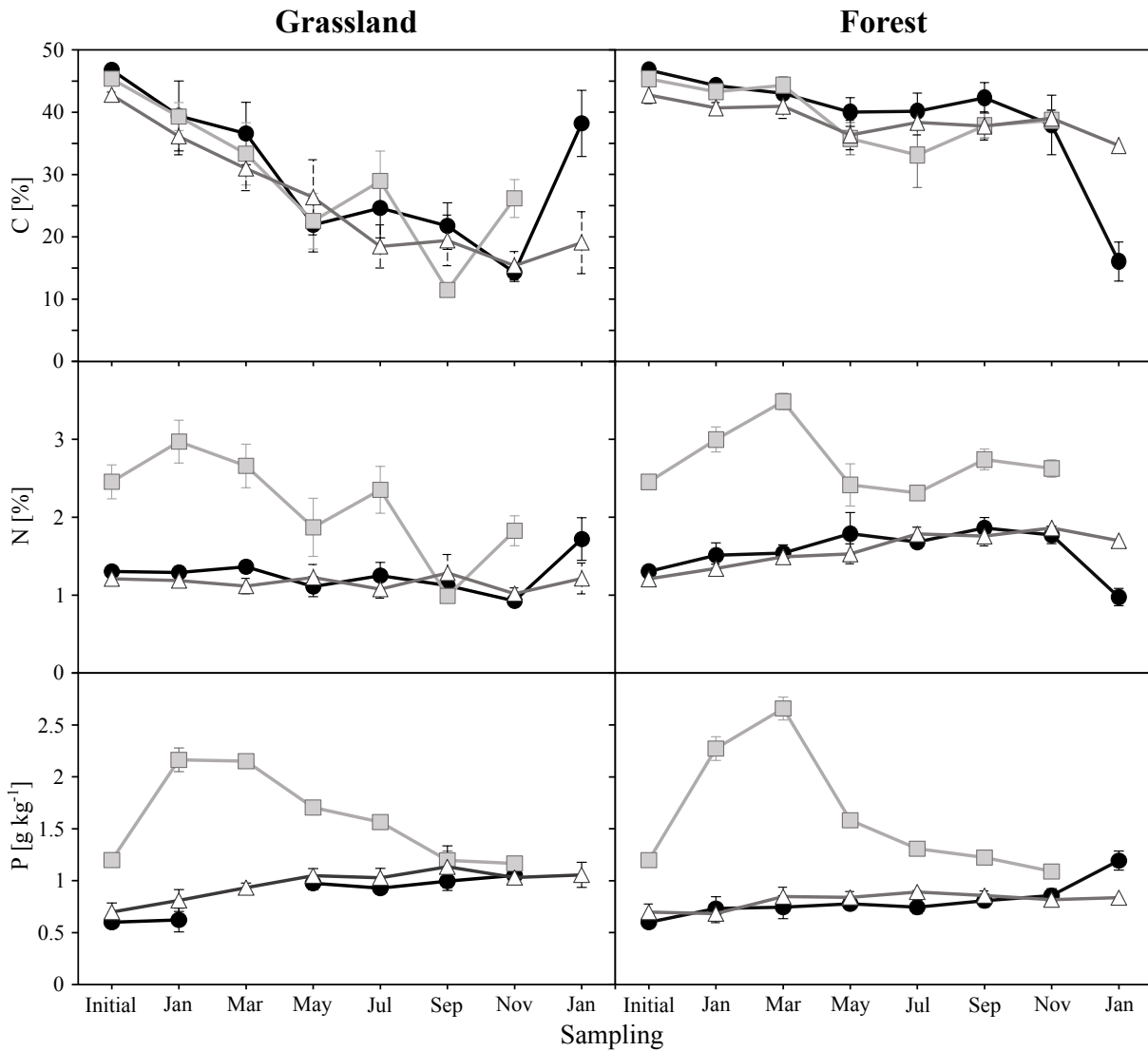


Fig. S2. Carbon, nitrogen and phosphorus content in dry weight of beech (black circles), milkvetch (grey squares) and sedge (white triangles) at the forest and the grassland sites during decomposition experiment \pm SD (5 replicates). The x axes indicate sampling time (Initial - Jan, i.e. initial C,N and P content and litterbag sampling after 2 - 14 months).

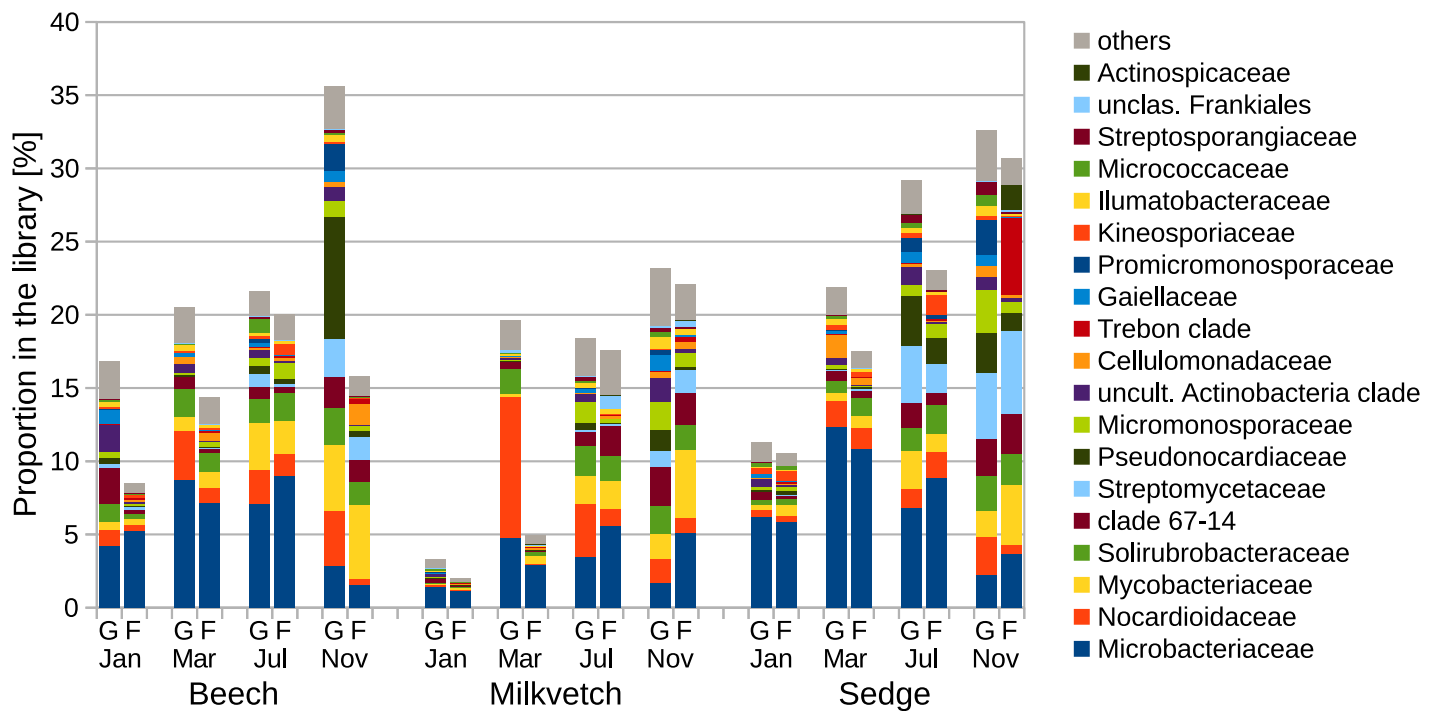


Fig. S3. Average proportions of families within the phylum *Actinobacteria* in the bacterial 16S rRNA gene amplicon sequence libraries (5 replicates).

Labels at the horizontal axis indicate type of sampled plant litter (beech, milkvetch, and sedge), sampling time (Jan - Nov, i.e. after 2 - 12 months), and experimental site (G - grassland, F - forest).

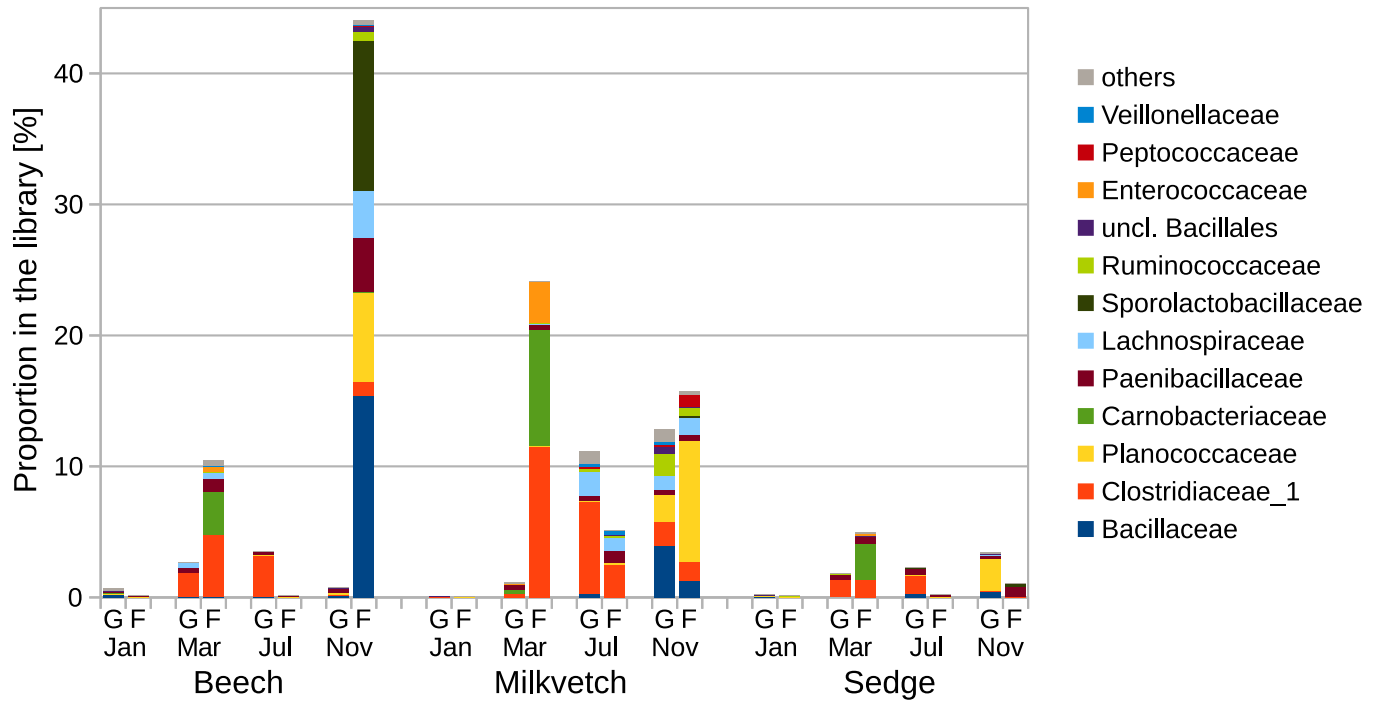


Fig. S4. Average proportions of families within the phylum *Firmicutes* in the bacterial 16S rRNA gene amplicon sequence libraries (5 replicates).

Labels at the horizontal axis indicate type of sampled plant litter (beech, milkvetch, and sedge), sampling time (Jan - Nov, i.e. after 2 - 12 months), and experimental site (G - grassland, F - forest).

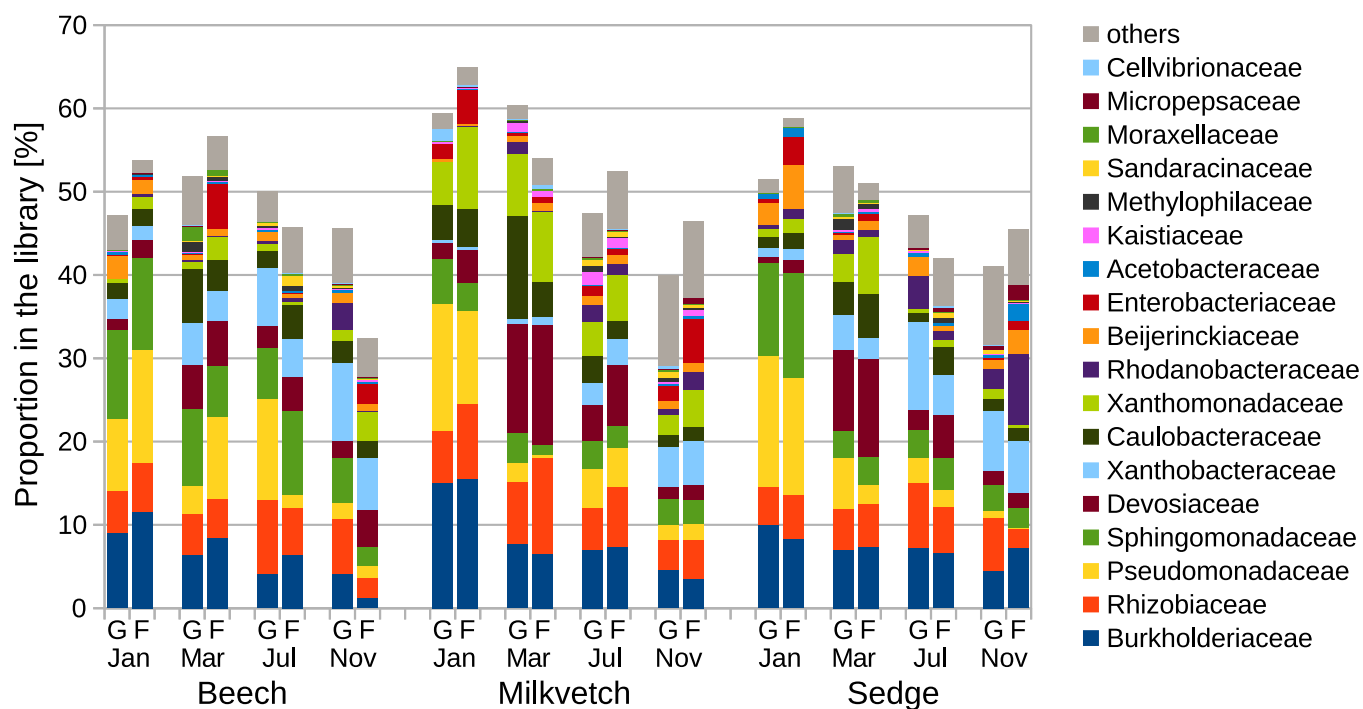


Fig. S5. Average proportions of families within the phylum *Proteobacteria* in the bacterial 16S rRNA gene amplicon sequence libraries (5 replicates) .

Labels at the horizontal axis indicate type of sampled plant litter (beech, milkvetch, and sedge), sampling time (Jan - Nov, i.e. after 2 - 12 months), and experimental site (G - grassland, F - forest).

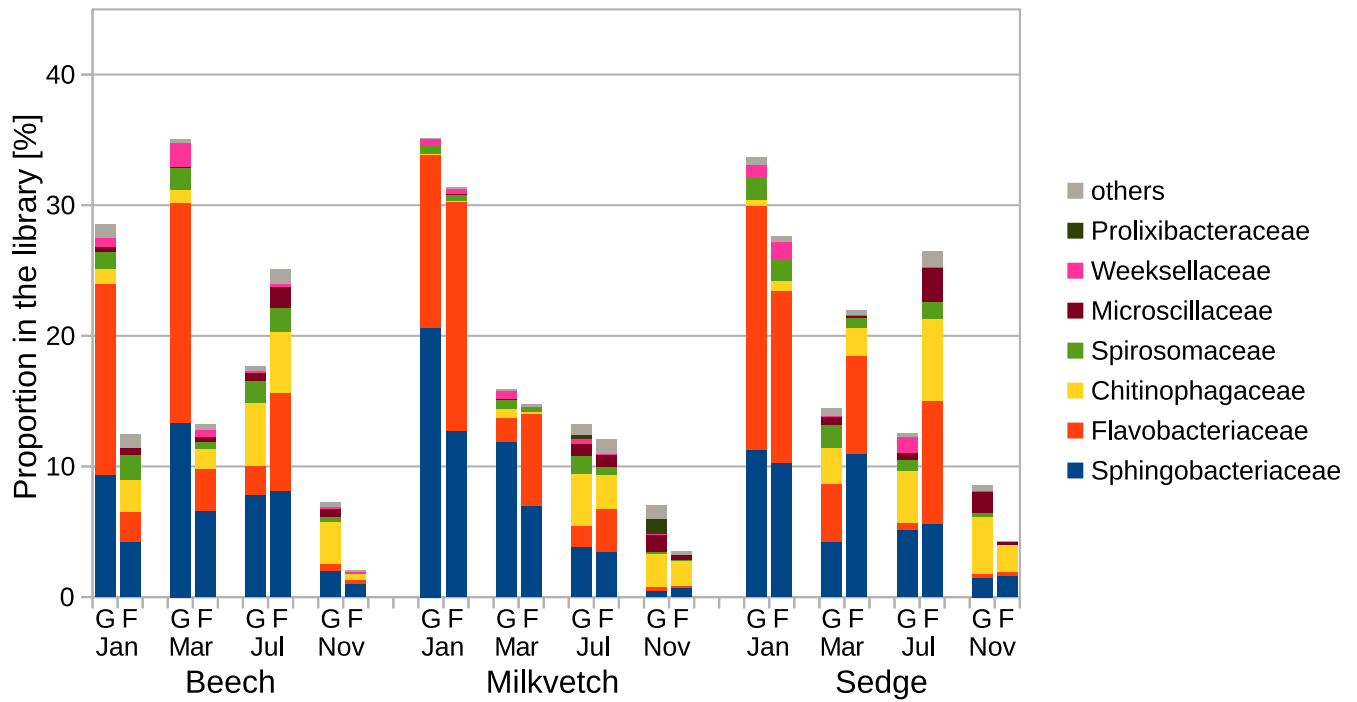


Fig. S6. Average proportions of families within the phylum *Bacteroidetes* in the bacterial 16S rRNA gene amplicon sequence libraries (5 replicates).

Labels at the horizontal axis indicate type of sampled plant litter (beech, milkvetch, and sedge), sampling time (Jan - Nov, i.e. after 2 - 12 months), and experimental site (G - grassland, F - forest).

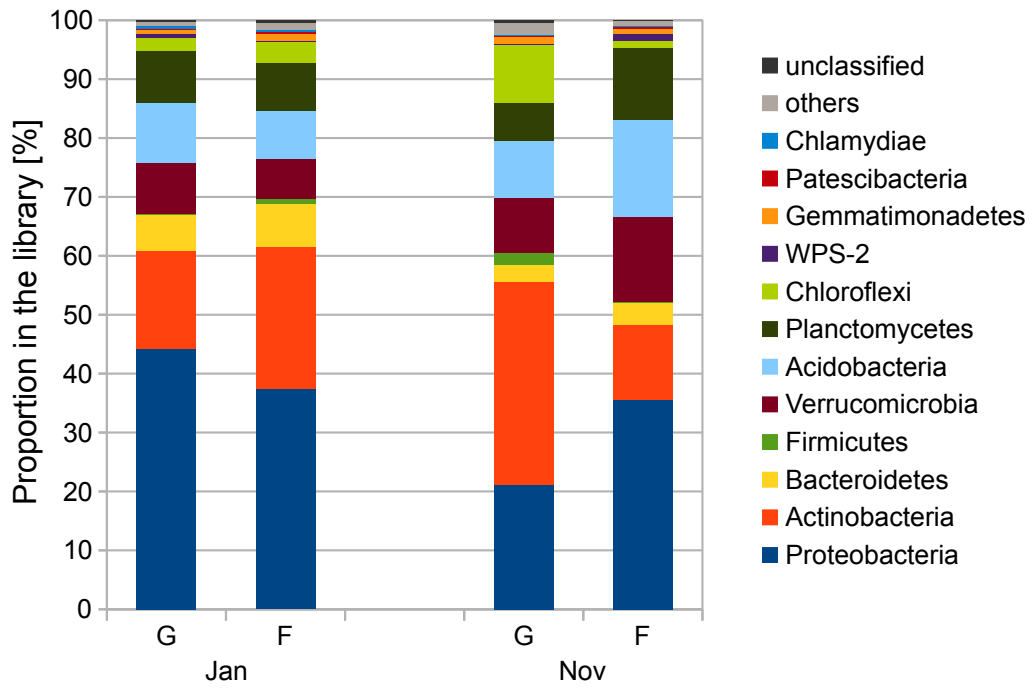


Fig. S7. Average proportions (5 replicates) of phyla in the bacterial 16S rRNA gene amplicon sequence libraries from the soil sampled at the experimental sites (G - grassland, F - forest) during the first (Jan) and the sixth (Nov) litter sampling.

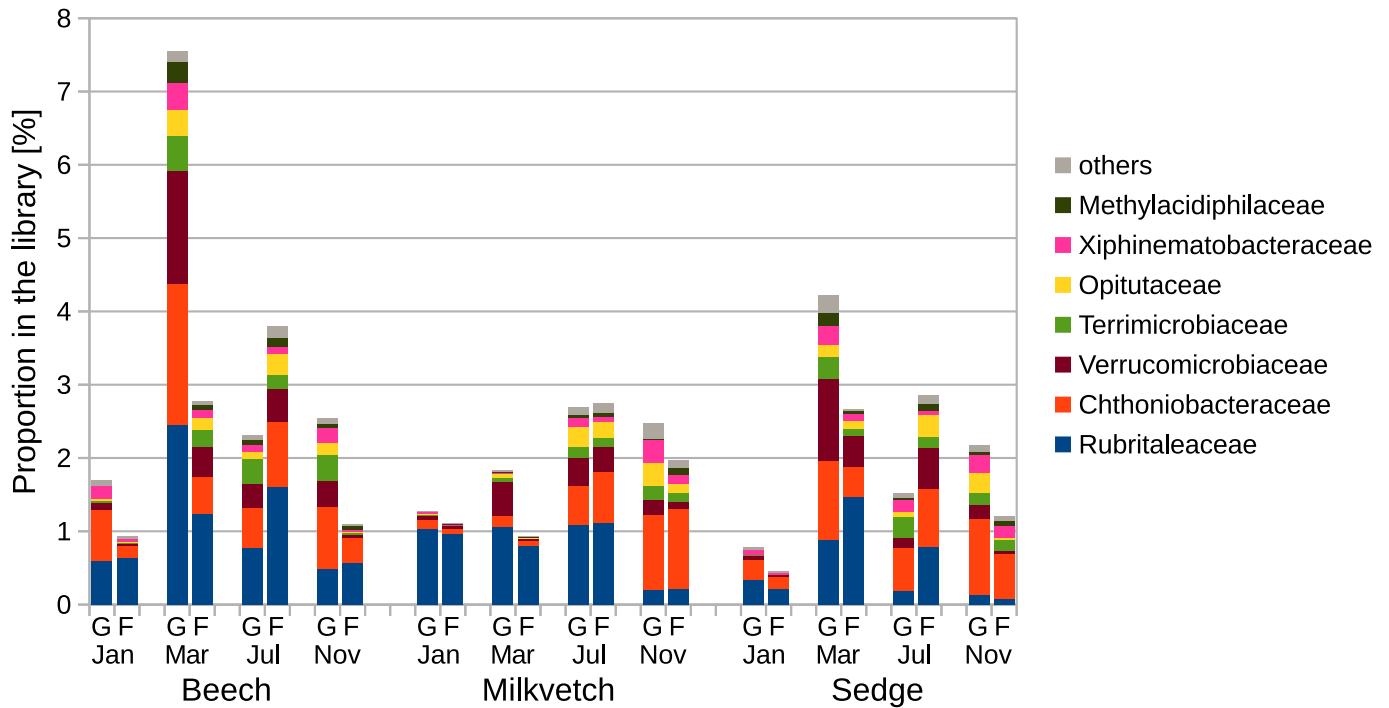


Fig. S8. Average proportions of families within the phylum *Verrucomicrobia* in the bacterial 16S rRNA gene amplicon sequence libraries (5 replicates).

Labels at the horizontal axis indicate type of sampled plant litter (beech, milkvetch, and sedge), sampling time (Jan - Nov, i.e. after 2 - 12 months), and experimental site (G - grassland, F - forest).

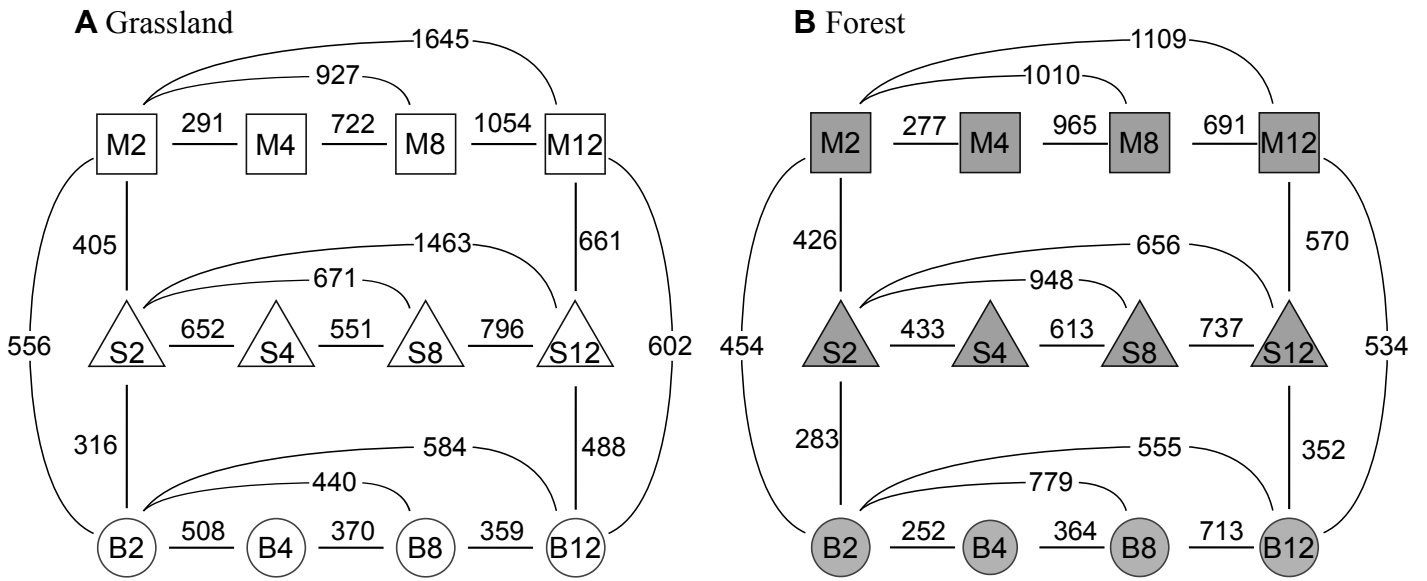


Fig. S9. Changes of composition of bacterial communities during plant litter decomposition assayed by Illumina amplicon sequencing at the grassland (A, open symbols) and the forest (B, grey symbols) sites. Numbers indicate the OTUs significantly contributing to the difference between samples in pairwise comparison (Metastats, $p < 0.05$).

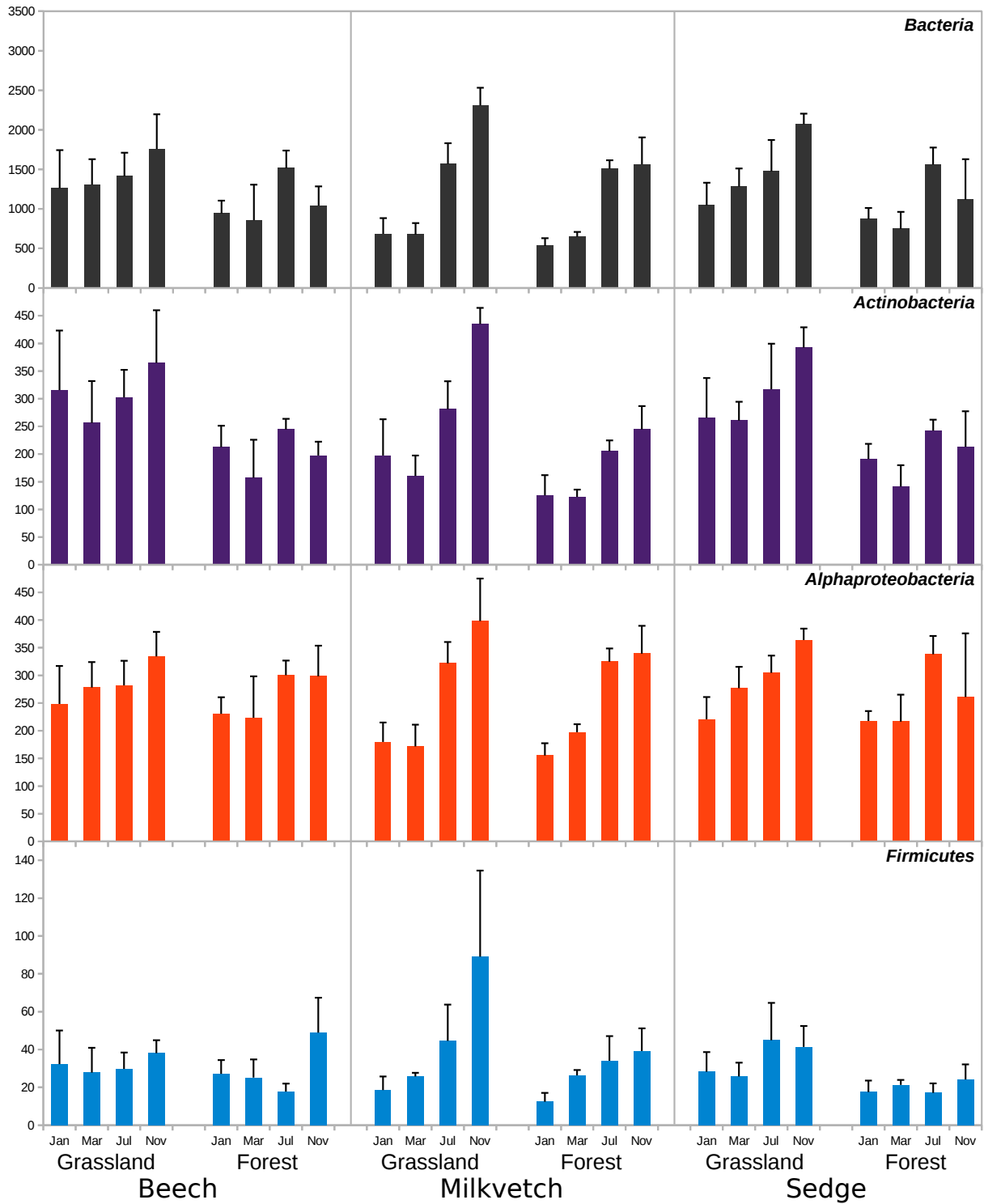


Fig. S10. Rarefaction analysis of 16S rRNA gene amplicon sequence libraries. The columns represent areas below the rarefaction curves \pm SD (5 replicates) for the entire bacterial libraries and for the subsets of *Actinobacteria*, *Alphaproteobacteria* and *Firmicutes*. The x axis indicates sampling time (Jan - Nov, i.e. litterbag samplings after 2 - 12 months).

Table S1. Primers used for qPCR and for MiSeq Illumina sequencing

Experiment	Primer	Sequence [5'-3']	Target	Conc.	Annealing temp.	Ref.
qPCR	EUB518 ^a	ATTACCGCGGCTGCTGG	Bacteria, 16S rRNA	0.2 μM	56 °C	[6]
	Act235	CGCGGCCTATCAGCTTGTTG	Actinobacteria, 16S rRNA	0.2 μM	56 °C	[7]
	S-C-aProt-0528-a-S-19	CGGTAATACGRAGGGRGYT	Alphaproteobacteria, 16S rRNA	0.4 μM	61 °C	[9]
	S-C-aProt-0689-a-A-21	CBAATATCTACGAATTTCACCT	Alphaproteobacteria, 16S rRNA	0.4 μM	61 °C	[9]
	S-P-Firm-0352-a-S-18	CAGCAGTAGGGAATCTTC	Firmicutes, 16S rRNA	0.2 μM	57 °C	[9]
	S-P-Firm-0525-a-A-18	ACCTACGTATTACCGCGG	Firmicutes, 16S rRNA	0.2 μM	57 °C	[9]
	FF390	CGATAACGAACGAGACCT	Fungi, 18S rRNA	0.6 μM	50 °C	[8]
	FR1	AICCATTCAATCGGTAIT	Fungi, 18S rRNA	0.6 μM	50 °C	[8]
Sequencing	CS1-515F	ACACTGACGACATGGTTCTACAGTGCCAGCMGCCGCGGTAA	Bacteria, 16S rRNA			[10]
	CS2-806R	TACGGTAGCAGAGACTTGGTCTGGACTACHVGGGTWTCTAAT	Bacteria, 16S rRNA			[10]

^aEub518 was used as a reverse primer for Act235.

Table S2. Pairwise quantitative comparison of the experimental sites (F – forest, G – grassland) and plant substrates (B – beech, M – milkvetch, S – sedge) assayed by ANOVA using linear model with the additive effects, correlation coefficients of profiles determined by PERMANOVA using distance matrices (P-permanova) and variability of the profiles assayed by testing for homogeneity of multivariate dispersions using dissimilarity measures (P-disp).

	ANOVA		CORRELATION COEFFICIENT	
	Sites	Plant substrates	P-permanova	P-disp
Dry weight loss	G < F***	M > S***, M > B***, S > B***	0.00	0.382
N	G < F***	M > B***, S***	0.002	0.000
C	G < F***	-	0.140	0.383
P	G > F**	M > S***, M > B***, S > B*	0.000	0.005
Actinobacteria	G > F***	-	0.021	0.387
Fungi	-	M**, S*** > B	0.000	0.505
Alphaproteobacteria ^a	G > F**	M > B***, S***	0.029	0.002
Firmicutes	-	M > B***, S***	0.852	0.006
β - Glucosidase	G < F***	M > B***, S***	0.651	0.932
Cellobiohydrolase	G < F**	M > S**, M > B***, S > B***	0.278	0.867
β - Xylosidase	G < F***	M > S*, M > B***, S > B***	0.213	0.001
N-acetylglucosaminidase (Chitinase)	G < F***	M***, S*** > B	0.005	0.914
Glucuronidase	G < F**	M***, S*** > B	0.125	0.000
Acid Phosphatase	G < F***	M > B***, S***	0.067	0.208
Arylsulphatase	G < F***	M***, S*** > B	0.004	0.052
α - Glucosidase	G < F**	M***, S*** > B	0.191	0.018
Laccase	G < F**	S > B**	0.009	0.796
Mn - peroxidase	-	-	0	0.385

For ANOVA: * P < 0.05; ** P < 0.01; *** P < 0.001

For correlation coefficient: Bonferroni-corrected critical P value < 0.0035

^aonly for the first two sampling points (from November to January)

Table S3. Differences (indicated by P – values) of low-molecular-weighted compounds at beech (B), milkvetch (M) and sedge (S) between experimental sites (Forest and grassland) at sampling times (January 2011 – January 2012) assayed by non-parametric multivariate analysis using distance matrix.

	B	M	S	OVERALL
January 2011	0.008	0.000	0.000	<0.001
March	0.002	0.001	0.001	<0.001
May	0.004	0.001	0.001	<0.001
July	0.001	0.001	0.001	<0.001
September	0.003	0.001	0.001	<0.001
November	0.030	0.009	0.018	<0.001
January 2012	0.005	NA	0.008	<0.001

Bonferroni-corrected threshold P value < 0.016

Table S4. Differences (indicated by P – values) of bacterial community at beech (B), milkvetch (M) and sedge (S) between experimental sites (forest and grassland) at sampling times (January 2011 – January 2012) assayed by non-parametric multivariate analysis using Yue-Clayton distance matrix.

	B	M	S	OVERALL
January 2011	0.098	0.009	0.418	0.002
March	0.092	0.008	0.161	<0.001
July	0.008	0.064	0.006	<0.001
November	0.009	0.039	0.009	<0.001

Bonferroni-corrected threshold P value < 0.016

Table S5. AMOVA analysis of differences in composition of bacterial communities at beech (B), milkvetch (M) and sedge (S) at the forest and the grassland sites (F-values).

Grassland				Forest			
	df	M	S		df	M	S
B	1	4.39381*	1.09189	B	1	2.67483*	1.29985
M	1		4.56859*	M	1		3.05833*

* P < 0.016 (Bonferroni-corrected threshold)

References for supplementary text citations

1. Sagova-Mareckova M, Omelka M, Cermak L, Kamenik Z, Olsovska J, Hackl E, Kopecky J, Hadacek F. 2011. Microbial communities show parallels at sites with distinct litter and soil characteristics. *Appl Environ Microbiol* 77:7560–7567.
2. Baldrian P. 2009. Microbial enzyme-catalyzed processes in soils and their analysis. *Plant, Soil Environ* 55:370–378.
3. Bourbonnais R, Paice MG. 1990. Oxidation of non-phenolic substrates. *FEBS Lett* 267:99–102.
4. Šnajdr J, Cajthaml T, Valášková V, Merhautová V, Petránková M, Spetz P, Leppänen K, Baldrian P. 2011. Transformation of *Quercus petraea* litter: Successive changes in litter chemistry are reflected in differential enzyme activity and changes in the microbial community composition. *FEMS Microbiol Ecol* 75:291–303.
5. Sagova-Mareckova M, Cermak L, Novotna J, Plhackova K, Forstova J, Kopecky J. 2008. Innovative methods for soil DNA purification tested in soils with widely differing characteristics. *Appl Environ Microbiol* 74:2902–2907.
6. Muyzer G, de Waal EC, Uitterlinden AG. 1993. Profiling of complex microbial populations by denaturing gradient gel electrophoresis analysis of polymerase chain reaction-amplified genes coding for 16S rRNA. *Appl Environ Microbiol* 59:695–700.
7. Stach JEM, Maldonado LA, Ward AC, Goodfellow M, Bull AT. 2003. New primers for the class Actinobacteria: Application to marine and terrestrial environments. *Environ Microbiol* 5:828–841.
8. Prévost-Bouré CN, Christen R, Dequiedt S, Mougel C, Lelièvre M, Jolivet C, Shahbazkia HR, Guillou L, Arrouays D, Ranjard L. 2011. Validation and application of a PCR primer set to quantify fungal communities in the soil environment by real-time quantitative PCR. *PLoS One* 6.
9. Kozich JJ, Westcott SL, Baxter NT, Highlander SK, Schloss PD. 2013. Development of a dual-index sequencing strategy and curation pipeline for analyzing amplicon sequence data on the miseq illumina sequencing platform. *Appl Environ Microbiol* 79:5112–5120.
10. Quast C, Pruesse E, Yilmaz P, Gerken J, Schweer T, Yarza P, Peplies J, Glöckner FO. 2012. The SILVA ribosomal RNA gene database project:

- improved data processing and web-based tools. *Nucleic Acids Res* 41:D590–D596.
11. Rognes T, Flouri T, Nichols B, Quince C, Mahé F. 2016. VSEARCH: a versatile open source tool for metagenomics. *PeerJ* 4:e2584.
 12. Yilmaz P, Parfrey LW, Yarza P, Gerken J, Pruesse E, Quast C, Schweer T, Peplies J, Ludwig W, Glöckner FO. 2014. The SILVA and “all-species Living Tree Project (LTP)” taxonomic frameworks. *Nucleic Acids Res* 42:643–648.
 13. Edgar RC. 2013. UPARSE: highly accurate OTU sequences from microbial amplicon reads. *Nat Methods* 10:996–998.
 14. Yue JC, Clayton MK. 2005. A similarity measure based on species proportions. *Commun Stat - Theory Methods* 34:2123–2131.
 15. Martin AP. 2002. Phylogenetic Approaches for Describing and Comparing the Diversity of Microbial Phylogenetic Approaches for Describing and Comparing the Diversity of Microbial Communities. *DNA Seq* 68:3673–3682.
 16. White JR, Nagarajan N, Pop M. 2009. Statistical Methods for Detecting Differentially Abundant Features in Clinical Metagenomic Samples. *PLoS Comput Biol* 5:e1000352.
 17. R Core Team. 2018. R Core Team, R : A language and environment for statistical computing. R Found Stat Comput Vienna, Austria R Foundation for Statistical Computing.

Paper III: Litter chemical quality and bacterial community structure influenced decomposition in acidic forest soil

1 **Litter chemical quality and bacterial community structure influenced decomposition in acidic forest**
2 **soil**

3

4 **Authors**

5 Andrea Buresova ^{1,3,4}, Vaclav Tejnecky ², Jan Kopecky ¹, Ondrej Drabek ², Pavla Madrova ¹, Nada
6 Rerichova ², Marek Omelka ⁵, Petra Krizova ², Karel Nemecek ², Thomas B. Parr ⁶, Tsutomu Ohno ⁷,
7 Marketa Sagova-Mareckova ⁸

8

9 Corresponding author: Vaclav Tejnecky, email: tejnecky@af.czu.cz

10

11 ¹ Epidemiology and Ecology of Microorganisms, Crop Research Institute, Drnovska 507, Prague, Czech
12 Republic

13 ² Department of Soil Science and Soil Protection, Faculty of Agrobiolgy, Food and Natural Resources,
14 Czech University of Life Sciences Prague, Kamycka 129, Prague, Czech Republic

15 ³ Department of Ecology, Faculty of Science, Charles University in Prague, Vinicna 7, Prague, Czech
16 Republic

17 ⁴ Microbial Ecology, University Claude Bernard Lyon 1, UMR CNRS 5557, INRA 1418, Villeurbanne,
18 France

19 ⁵ Department of Probability and Mathematical Statistics, Faculty of Mathematics and Physics, Charles
20 University in Prague, Sokolovska 68, Prague 8, Czech Republic

21 ⁶ Department of Biology, University of Oklahoma, 730 Van Vleet Oval, Norman, OK, USA

22 ⁷ School of Food and Agriculture, University of Maine, 5763 Rogers Hall, Orono, ME, USA

23 ⁸ Department of Microbiology, Dietetics and Nutrition, Faculty of Agrobiolgy, Food and Natural
24 Resources, Czech University of Life Sciences Prague, Kamycka 129, Prague, Czech
25 Republic

26

27

28

29 **Abstract**

30 The study was designed to see if naturally occurring beech forests uptake different nutrients than
31 artificially planted spruce forests and if the structure of microbial communities participating in
32 decomposition corresponds to the soil types developed under the respective tree species. This corresponds
33 to previous observations that the soil under spruce forest is typically dominated by podzol, while the soil
34 under beech forest undergoes higher mineralization, which leads to moder humus and the development of
35 cambisol. A litterbag experiment was performed with beech and spruce litter placed respectively to beech
36 and spruce forests. In the beech forest, the observed litter decomposition rate reached the exponential faze
37 after 15 months, while in the spruce forest a steeper decrease was noted only 29 months after the litter
38 burial. Thus, the study focused on the period between 15 and 29 months to observe the exponential stages
39 of recalcitrant organic matter transformation. In this period, the chemical composition of two litters was
40 distinguished by higher contents of Mn and Ca in beech and higher content of Fe, S, N and P in spruce.
41 On top of that, the beech litter released higher amount of dissolved organic carbon and its associated
42 bacterial community was enriched with r-selected taxa, that correlated positively with organic acids and
43 cations. In contrast, the more acidic spruce litter was dominated by K-selected acidophilic community and
44 its turnover rate was slower, resulting in increased carbon sequestration. The higher pH and humus quality
45 of beech cambisol also correlates with its observed higher resilience to disturbances by acidification, pests
46 or climate change in mountainous environments.

47

48 **Keywords**

49 Soil type, Humus, Elemental composition, DOC, Bacteria, Fungi

50

51

52 **1. Introduction**

53 Human-introduced spruce forests are more vulnerable to environmental changes than natural beech
54 forests in the Czech Republic. The spruce forests vulnerability is even increased in acidic soils, which are
55 limited by availability of nutrients [1] and potential mobilization of toxic forms of Al [2,3]. In such
56 environments, the litter represents a major source of Ca, K, Mg, P and organic carbon (OC) in the upper
57 layer of soil [4].

58 The precise chemical composition of litter depends mostly on the requirements of particular plant
59 species and its nutrient uptake and allocation to tissues [5,6]. The nutrient content and composition of
60 organic compounds in litter further establish the microbial community corresponding to the litter type [7].
61 Microbial decomposers return the litter nutrients back to soil by activities mostly regulated by soil
62 chemistry, but also by local climate, i.e. precipitation, which have further impact on soil development and
63 environmental stability [8].

64 In particular, the elevated concentration of some litter components may speed up [9] or slow down
65 the decomposition rate [10]. For example, N and P stimulate decomposition rate in earlier stages but inhibit
66 its rate in later stages due to formation of complexes, which are recalcitrant for microbes [10,11]. Litter
67 decomposition is further dependent on the amount of dissolved organic carbon (DOC) released from litter
68 and its character, as the low level of DOC with its elevated aromaticity (A_{254} ; absorbance at 254 nm) and
69 complexity of organic compounds increase the litter recalcitrance [12]. Finally, the decomposition is also
70 predicted by humification index (HIX) of the decomposed litter, which determines how the particular litter
71 contributes to the humus formation [13].

72 Decomposition process over time may be illustrated as an asymptotic function. The upper
73 threshold of the function - limit value of decomposition – represents the phase, when the substrate is no
74 longer decomposed and remains stabilized in the soil [14]. The lag-time shows how long it takes a litter

75 to enter the exponential stage of decomposition. The long lag-time eventually implicates that old organic
76 matter is not necessarily stabilized and recalcitrant but that other mechanisms keep it from the
77 decomposition [15]. Later stages of litter decomposition are typically less explored due to longer time
78 required for experiments. Yet, they are needed mostly to evaluate chemical traits of recalcitrant litter and
79 its contribution to humus and soil formation.

80 Consequently, the contribution of different biotic and abiotic factors to low limit value or long lag-
81 time of recalcitrant litter is not well studied, although it is important for understanding which mechanism
82 and microbial decomposers participate on the release of sequestered nutrients. Furthermore, it is not
83 known, what is the role of different tree species in creating specific soil chemical conditions, and their
84 further influence on the composition and response of the decomposing microbial community [16,17].

85 Bacteria are generally less studied decomposers in forest soils compared to fungi, particularly in
86 later stages of decomposition [18]. That might be due to the previous association of bacterial
87 decomposition with readily degradable nutrient rich litter. However, some recent studies found that after
88 the initial stage of decomposition, bacterial community showed increased diversity and different structure
89 than in the early stages of decomposition [19]. Moreover, bacterial phyla *Actinobacteria* and *Firmicutes*,
90 which represent K-selected decomposers, dominated in stages characterized by high proportion of a
91 recalcitrant organic matter [20].

92 Thus, our study aimed in evaluating differences between chemical conditions and microbial
93 communities of native beech and introduced spruce litter during the decomposition stage following the
94 initial stage in two forests soils. The forests are located next to each other in the Jizera Mountains, Czech
95 Republic. They share an acid bedrock (porphyric granite) and mountainous climate with intense
96 precipitation of 800–1700 mm per year [16,21]. We hypothesized that the beech litter will promote faster
97 decomposition with a more abundant and diverse microbial community. In contrast, the spruce litter will

98 be preserved against decomposition by relatively high acidity and sequestered C, which will support less
99 abundant decomposers possibly dominated by a few taxa. The comparison consisted of detailed litter
100 chemical analyses (DOC, HIX, A_{254}), low molecular mass organic acids (LMMOA), N, P, Ca, Mn, Fe
101 together with the observation of the microbial succession on beech leaves and spruce needles using
102 quantification of bacteria (16S rRNA, ddPCR) and fungi (ITS region, ddPCR) and bacterial community
103 composition (16S rRNA, Illumina MiSeq) after months 15, 19 and 29 of decomposition. That knowledge
104 was further applied to resolve factors which support higher decomposition rate and more diverse microbial
105 community in the beech forest soil and to find the basis of the humus quality and soil type formation at
106 the two sites.

107 2. Materials and Methods

108 2.1. Litter bag experiment

109 The litterbag experiment was carried out in a beech forest (European beech, *Fagus sylvatica* L.)
110 and a spruce forest (Norway spruce, *Picea abies* [L.] Karst.), which grow next to each other on the Palicnik
111 hill located in the Jizera Mountains (Czech Republic; 50.8673125N, 15.2544103E), affected by
112 acidification in the past [16]. The altitude of studied plots ranged from 635 (bottom limit) to 680 m a.s.l.
113 (upper limit). The bedrock of both forest types is a medium-grained porphyric granite and granodiorite of
114 the Upper Carboniferous age. The soil under spruce was classified as the Entic and Haplic Podzols and
115 the soil under beech as the Aluminic Cambisol [22]. Mor or moder are respectively the prevailing types
116 of humus [23]. Mean annual temperatures 7.33 °C, 9 °C and 8.7 °C and mean annual precipitations 922
117 mm, 683 mm and 696 mm were measured in years 2013, 2014 and 2015, respectively, in Liberec region,
118 where the experiment was conducted [24]. Diameter at breast height of living trees was 534.6 (\pm 153.4)
119 mm in beech forest and 405.8 (\pm 112.4) mm in spruce forest, canopy closure was 87 % in beech and 40 %
120 in spruce forest and total area of rock was 811.9 m² in beech forest and 10.9 m² in spruce forest [23]. The
121 experimental layout is showed in Supplementary Fig. S1.

122 Soil samples were collected from the surface litter (L), fermentation (F), humified (H) organic and
123 organo-mineral (humic, A) horizons. Samples from subsurface B horizons (cambic or spodic) were also
124 collected. Each sample was thoroughly mixed. The soil samples were analyzed in a “fresh” state
125 representing actual soil moisture and in dry and sieved (< 2mm) state. In total, 8 beech and 7 spruce soil
126 pits were described and sampled in September 2015.

127 Newly fallen spruce needles and beech leaves were collected in November 2011. Part of the
128 collected litter was directly used for chemical analysis (denoted as the initial litter). Overall, 120 bags
129 were made of polyamide with 99 μ m mesh size and 50 μ m fibre diameter were filled with 5 g of dry beech

130 (BL) or spruce (SL) litter. Sixty bags with BL were placed in the beech forest and sixty with SL in the
131 spruce forest 1 m apart between litter (L) and fermentation (F) organic horizons in April 2013. Three
132 litterbags from each litter type were collected during each sampling period in May 2013, June 2013, July
133 2013, August 2013, September 2013, October 2013, November 2013, July 2014, November 2014 and
134 September 2015 (i.e. months 1, 2, 3, 4, 5, 6, 7, 15, 19 and 29 from the start of the experiment). After the
135 collecting, samples were weighed and frozen for further analysis. Mass loss of litter and chemical analyses
136 were assessed for all samples but only samples collected in months 15, 19 and 29 were chosen for further
137 microbiological analysis because at those dates, an increased rate of decomposition was observed. The
138 stage was thus termed exponential.

139

140 **2.2. Chemical analysis**

141 **2.2.1. Soil analysis**

142 Fresh soil samples were extracted by deionised water and pH and DOC were measured according
143 to Tejnecky et al. [16,17]. Cation exchange capacity (CEC) and exchangeable elements (Ca_{ex} , Al_{ex} , H^+_{ex})
144 were determined according to Cools and De Vos [25] and base saturation (BS in %) was calculated as a
145 ratio between CEC and base cations (Na^+ , K^+ , Ca^{2+} and Mg^{2+}).

146

147 **2.2.2. Litter analyses**

148 Water extracts were made from each defrosted sample (1 g of thawed sample with 30 ml deionized
149 H_2O). Water extraction represents easily available elements or substances and preserves sample matrices
150 [26]. The suspension was then centrifuged at 4000 g for 15 min; finally, extracts were filtered through a
151 0.45 μm nylon membrane filter (Sigma-Aldrich, MO, USA). In aqueous extracts, the following chemical

152 parameters were determined: pH, main inorganic anions (NO_3^- w, NO_2^- w, SO_4^{2-} w and PO_4^{3-} w, Cl^- w, F^- w)
153 and low-molecular mass organic acids (LMMOA, lactate w, acetate w, formate w and oxalate w) by means
154 of ion chromatography (IC, ICS 1600; Dionex; CA, USA) with suppressed conductivity. Cations (NH_4^+
155 w, K^+ w, Mg^{2+} w, Na^+ w, Ca^{2+} w) were determined by means of ion chromatography (ICS 90, Dionex; CA,
156 USA) and the contents of selected elements (P w, Al w, Fe w, K w, Ca w, Mn w) by inductively coupled
157 plasma-optical emission spectrometer (ICP-OES, DUO iCap 7000; Thermo Scientific, MA, USA). The
158 contents of N_{tot} , C_{tot} , S_{tot} were determined by Elementary Analyzer Flash 2000 NCS (Thermo Scientific,
159 UK). For C_{tot} , S_{tot} , N_{tot} , 9 replicates were used for SL but 7 replicates were used for BL. The respective
160 part of each sample was oven dried (40°C), homogenized and digested in Teflon vessels with the addition
161 of HNO_3 (0.5 g of samples and 5-10 ml 65 % HNO_3). In the obtained solution, the contents of selected
162 elements (P_{tot} , Ca_{tot} , Mg_{tot} , K_{tot} , Al_{tot} , Fe_{tot} and Mn_{tot}) were determined by ICP-OES (DUO iCap 7000,
163 Thermo Scientific, MA, USA). Quality of digestion and analysis were controlled using standard reference
164 materials (NIST SRM 1575a Pine Needles and NCS DC 73351 Tea). The contents of elements and
165 substances were calculated to dry mass.

166 Dissolved organic carbon (DOC), absorbance at 254 nm (A_{254}) and humification index (HIX) were
167 determined in water extracts of litter- using 0.2500 g of homogenized litter mixed with 12.5 ml of
168 deionized water incubated for 24 h at 4°C on an orbital shaker. The 4°C condition was selected to
169 minimize microbial DOM alteration during extraction [27]. Suspensions were centrifuged at 3000 g for
170 25 min before vacuum filtering through $0.4\ \mu\text{m}$ polycarbonate membrane filter (Whatman, England). The
171 DOC concentration in the extracts was determined by high temperature catalytic oxidation using a
172 Shimadzu TOC-V analyzer (Kyoto, Japan). UV A_{254} was obtained using a Shimadzu UV-1800
173 spectrophotometer and a 1-cm quartz cuvette.

174 All litter extracts were diluted with deionized water to set the absorbance at 254 nm to 0.10 to
175 minimize inner-filtration effects in obtaining the fluorescence spectra [28]. Fluorescence spectra were
176 obtained using a Hitachi F-4500 spectrofluorometer (Tokyo, Japan). The instrumental parameters were:
177 excitation (EX) and emission (EM) slits, 5 nm; response time, 0.5 s; and scan speed, 2400 nm min⁻¹. The
178 EM spectra were obtained using 240 nm for EX and EM recorded from 300 to 600 nm. Correction factors
179 were applied according to the manufacturer's instructions, emission scans were blank subtracted, then
180 Raman Normalized, and then corrected for dilution in R 3.5.0 [29]. The HIX was calculated as ratio of the
181 sum of fluorescence intensities from 435 to 480 nm divided by sum of intensities from 300 to 345 nm and
182 435 to 480 nm [28].

183 From initial litter samples, total contents of Ca_{tot}, Mn_{tot}, Fe_{tot}, K_{tot}, Mg_{tot}, Na_{tot}, Al_{tot}, DOC, A₂₅₄ and
184 HIX were assessed.

185

186 **2.3. DNA extraction and amplicon sequencing**

187 DNA was extracted from 0.1 g of homogenized plant litter by method described in Sagova-
188 Mareckova et al. [30]. The method is based on bead-beating and phenol/chloroform extraction. The
189 samples were purified by incubation with acetyltrimethylammonium bromide followed by chloroform
190 extraction and incubation with CaCl₂. DNA samples were finally cleaned with GeneClean Turbo kit (MP
191 Biomedicals, CA, USA) and afterwards stored at -70 °C until further analysis. Fragments of the bacterial
192 16S rRNA gene including the variable region V3-V4 were amplified from the DNA samples by PCR,
193 using bacteria specific forward primer 341F (CCTACGGGAGGCAGCAG) and universal reverse primer
194 806R (GGA CTACHVGGGTWTCTAAT). Construction of amplicon libraries and sequencing using
195 MiSeq sequencer (Illumina, San Diego, USA) were done at the DNA Services Facility, Research
196 Resources Center, University of Illinois (Chicago, USA).

197

198 **2.4. Processing of sequence data**

199 The resulting paired sequence reads were merged, filtered, aligned using reference alignment from
200 the Sylva database [31], and chimera checked using integrated Vsearch tool[32] following the MiSeq
201 standard operation procedure (Miseq SOP, February 2018; [33]) in Mothur v. 1.39.5 software [34]. A
202 taxonomic assignment of sequence libraries was performed in Mothur using the recreated SEED database
203 subset of Sylva Small Subunit rRNA Database, release 132 [35] adapted for use in Mothur
204 (https://mothur.org/w/images/a/a4/Sylva.seed_v132.tgz) as the reference database.

205 Sequences of plastids, mitochondria, and those not classified in the domain *Bacteria* were discarded. The
206 sequence library was clustered into operational taxonomic units (OTUs) using the Uparse pipeline in
207 Usearch v10.0.240 software [36], and the OTU table was further processed using tools implemented in
208 the Mothur software. Rarefaction curves were used to detect observed OTUs for respective sequence
209 numbers. Bray-Curtis distance matrices describing the differences in bacterial community composition
210 between individual samples were calculated. The Illumina MiSeq 16S rRNA gene amplicon sequences
211 were deposited in the NCBI Sequence Read Archive (www.ncbi.nlm.nih.gov/sra) as BioProject No.:
212 PRJNA494609.

213

214 **2.5. Quantification of bacteria and fungi**

215 Quantification of bacteria (16S rRNA genes) and fungi (ITS region) from extracted DNA were
216 done by droplet digital PCR (ddPCR). For gene amplification primers 16Seu27f
217 (AGAGTTTGATCMTGGCKCAG) [37] and mixture of 783r-a, (CTACCAGGGTATCTAATCCTG),
218 783r-b (CTACCGGGGTATCTAATCCCG) and 783r-c (CTACCGGGGTATCTAATCCGG) [38] were

219 used for quantification of a bacterial 16S rRNA gene and primers ITS1F
220 (CTTGGTCATTTAGAGGAAGTAA) [39] and ITS4 (TCCTCCGCTTATTGATATGC) [40] were used
221 for quantification of a fungal ITS region. Reactions were prepared with QX200 EvaGreen Digital PCR
222 Supermix (Bio-Rad Laboratories, CA, USA) with 400 μ M final concentration of forward and reverse
223 primers. After generating droplets in QX200™ Droplet Generator (Bio-Rad Laboratories, CA, USA) the
224 PCR amplifications were performed (annealing temperatures: 56°C for bacteria and 54°C for fungi) and
225 droplets were detected fluorescently in Droplet Reader (Bio-Rad Laboratories, CA, USA). Results were
226 analyzed in QuantaSoft 1.7.4.0917 (Bio-Rad Laboratories, CA, USA).

227

228 **2.6. Statistical analysis**

229 Based on the observation of increased rate of decomposition, samples from months 15, 19 and 29
230 of each litter (n = 9) were used for statistical analysis (except for several analyses of mass loss and a few
231 selected chemical traits in the Supplementary Material). The effect of litter type and time during the whole
232 course of the experiment (from months 1 to 29) on mass loss was calculated by two-way ANOVA. Pair-
233 wise differences in mass loss between each month of decomposition for BL and SL were separately
234 calculated by ANOVA and Tukey's post-hoc test. Mass loss, chemical and microbiological variables
235 (abundance of bacteria 16S rRNA and fungi ITS region) from the three months of exponential stage
236 decomposition period on the BL (n = 9) and SL (n = 9) litter and chemical variables from the initial litter
237 (n = 3) were compared by Welch version of the two-sample t-test [41], which does not require equal
238 variances for both groups. The effect of time was not statistically analyzed.

239 Rarefaction analysis was used to demonstrate bacterial diversity expressed as the number of observed
240 OTUs with sequence numbers. Analysis of molecular variance (AMOVA) was calculated based on a
241 matrix of Bray-Curtis distances [42]. Metastats [43] analysis was used to show differences between

242 bacterial communities of BL and SL and to detect the differentially represented OTUs between the two
243 litter types. The outcome was also visualized as heat maps. Maximum-likelihood phylogram of the OTU
244 representative sequences was constructed using FastTree 2 [44]. Figures were created using Interactive
245 Tree of Life online tool (<http://itol.embl.de>; [45], and Inkscape (v0.92; <http://www.inkscape.org>). The
246 Bray-Curtis distance matrix was plotted by non-metric multidimensional scaling [46] using the Mass
247 package v. 7.3-51.5 [47]. Vectors of environmental variables which significantly correlated to bacterial
248 community were fitted to the nmDS plot in R using function envfit from the package vegan v. 2.5-6 [48].
249 All statistical calculations were done in the R computing environment [29] or in Mothur v. 1.39.5 software
250 [34]. Figures were plotted with the help of vegan package [49].

251 **3. Results**

252 **3.1. Soil chemical characteristics**

253 Spruce forest soils were more acidic ($\text{pH} = 3.82 \pm 0.29$) than beech forest soils ($\text{pH} = 4.08 \pm 0.27$)
254 except for F horizons, where pH were not statistically different (Table 1). H^+_{ex} represents exchangeable
255 pool of H^+ and significantly differed between beech and spruce soil profile except the B horizon (Table
256 1). In the uppermost L horizon, the content of $\text{Ca}^{2+}_{\text{ex}}$, base saturation (BS), cation exchange capacity (CEC)
257 and dissolved organic carbon (DOC) were significantly higher in the beech forest (Table 1). $\text{Al}^{3+}_{\text{ex}}$ was
258 the lowest in L horizon and did not differ between the two forest soils (Table 1). Litter (L) organic horizons
259 thickness under beech was on average 2.7 cm and 1.8 cm under spruce and bulk density under beech was
260 0.015 g.cm^{-3} and 0.048 g.cm^{-3} under spruce.

261 **Table 1.** Spruce and beech soil horizons (L - litter, F - fermentation, H - humic, A - organic and organo-
 262 mineral and B - subsurface cambic or spodic horizon) differences in pH, dissolved organic carbon (DOC),
 263 base saturation (BS), cation exchange capacity (CEC) and exchangeable cations (H+ex, Al³⁺+ex, Ca²⁺+ex).
 264 Average values and standard deviations (SD), degrees of freedom (Df), t-values and p-values are indicated
 265 (t-test).

	Horizon	Beech		Spruce		T- test		
		Average	SD	Average	SD	Df	t - value	p - value
pH	L	4.99	0.21	4.59	0.12	13	4.39	< 0.001
	F	4.20	0.29	3.90	0.43	13	1.62	0.129
	H	4.15	0.22	3.79	0.11	13	3.96	0.002
	A	4.32	0.19	3.93	0.08	12	5.10	< 0.001
	B	4.51	0.10	4.32	0.09	12	3.77	0.003
DOC [mg kg ⁻¹]	L	69.43	20.20	34.36	38.42	13	2.26	0.042
	F	678.0	358.1	473.8	250.8	13	1.26	0.230
	H	305.8	115.5	461.4	132.4	13	-2.43	0.030
	A	143.6	58.99	218.1	73.42	12	-2.10	0.058
	B	57.80	17.41	27.30	15.36	12	3.48	0.005
CEC [meq kg ⁻¹]	L	185.3	27.6	115.3	6.962	13	6.50	< 0.001
	F	135.0	18.2	148.5	6.515	13	-1.85	0.087
	H	100	11.44	122.5	12.64	13	-3.64	0.003
	A	80.58	14.36	84.81	7.703	12	-0.69	0.505
	B	46.72	10.65	50.49	9.712	12	-0.69	0.502
BS [%]	L	84.73	4.13	74.62	6.44	13	3.67	0.003
	F	47.29	14.71	40.60	5.99	13	1.12	0.283
	H	14.71	2.17	15.40	2.15	13	-0.62	0.548
	A	9.753	2.007	9.943	2.106	12	-0.17	0.866
	B	9.589	3.210	8.644	3.079	12	0.56	0.585
H ⁺ _{ex} [meq kg ⁻¹]	L	3.924	0.906	15.76	2.57	13	-12.23	< 0.001
	F	13.80	6.073	31.37	2.96	13	-6.95	< 0.001
	H	9.080	2.566	21.03	2.59	13	-8.95	< 0.001
	A	5.913	1.589	14.63	1.56	12	-10.37	< 0.001
	B	2.833	0.463	3.270	0.891	12	-1.15	0.270
Al ³⁺ _{ex} [meq kg ⁻¹]	L	2.899	6.388	7.916	5.171	13	-1.65	0.122
	F	46.30	17.44	47.37	11.30	13	-0.14	0.892
	H	70.19	9.06	73.10	10.20	13	-0.59	0.568
	A	62.70	11.71	54.15	7.97	12	1.59	0.137
	B	37.84	9.21	40.57	7.97	12	-0.59	0.565
Ca ²⁺ _{ex} [meq kg ⁻¹]	L	125.4	21.51	60.36	12.24	13	7.04	< 0.001
	F	47.10	22.68	39.09	10.36	13	0.86	0.407
	H	6.063	1.531	6.055	1.784	13	0.01	0.992
	A	2.668	0.582	2.238	0.732	12	1.218	0.247
	B	1.651	0.506	0.949	0.187	12	3.48	0.005

266

3.2. Litter mass loss

267

268

269

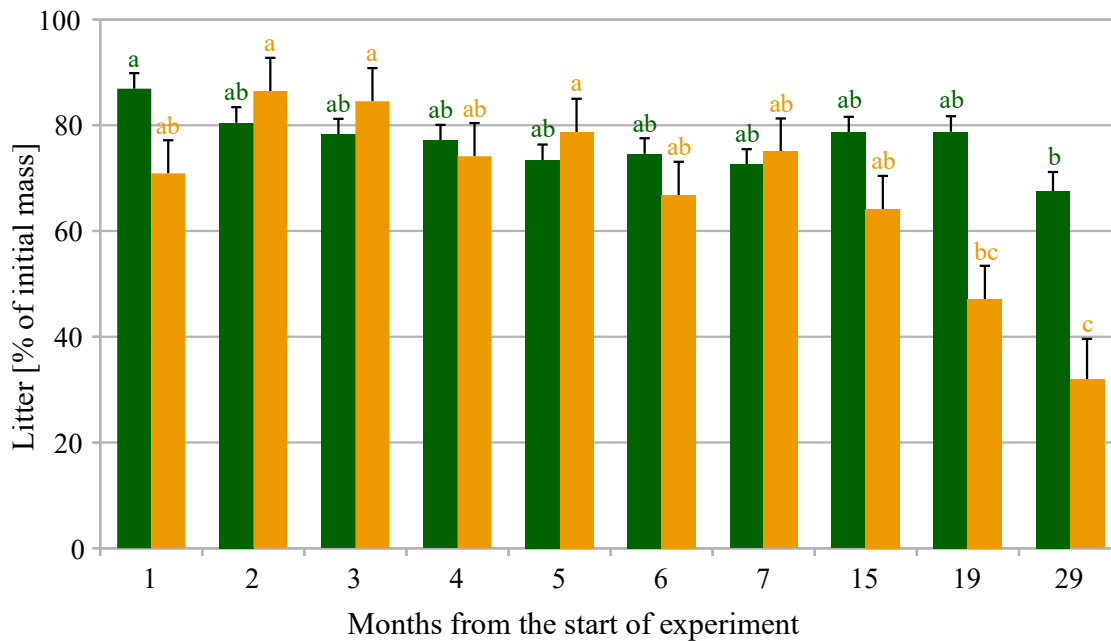
270

271

272

273

Litter mass loss was affected by factors of time as well as litter type (Table S1.) The average litter mass decreased from month 1 to month 29 by about 22.4 % in beech and 12.4 % in spruce forests ($p < 0.001$, Fig 1). In month 15, beech litter (BL) entered the exponential decomposition rate with the highest differences in mass loss between beech and spruce (SL) litter recorded in the last month 29 (Fig. 1). The mass loss most significantly differed from previous months in months 19 and 29 for BL and in month 29 for SL (Fig. 1). The mass loss was significantly different between BL and SL in months 15 to 29 (Table S2 A).



274

275

Fig. 1. The average residual mass loss (\pm SD) of beech (yellow) and spruce (green) during litter bag decomposition experiment ($n = 3$). The x axe indicates sampling time.

276

3.3. Litter chemical characteristics

277

278

279

In the initial litter, significantly higher contents of Ca_{tot} , Mn_{tot} , K_{tot} , Mg_{tot} and Na_{tot} were measured for BL, while higher, Al_{tot} , S_{tot} , N_{tot} , C_{tot} were measured for SL (Table S2 B). Differences for selected elements (N_{tot} , S_{tot} , P_{tot} , Fe_{tot} , Ca_{tot} , Mn_{tot}) from month 1 to month 29 were specific for each litter type (Fig.

280 S2; Table S3). A particularly fast decrease of Ca and Mn was observed in beech, and P in spruce in the
281 beginning of the decomposition process (Fig. S2).

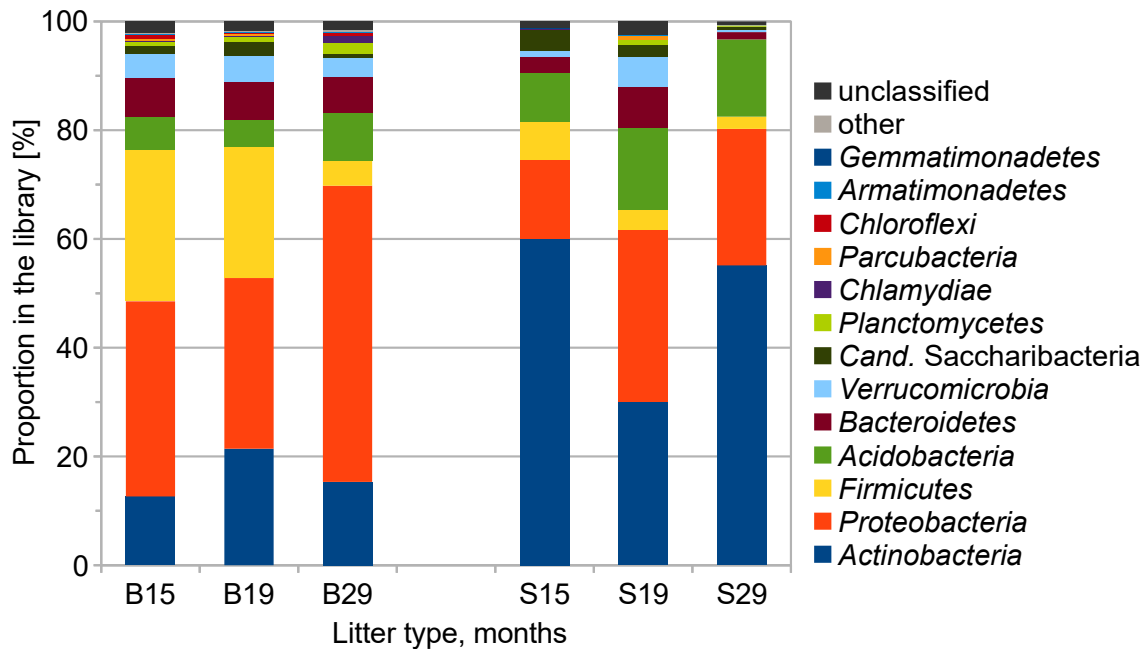
282 In the exponential stage litter, (month 15, 19 and 29) contents of Ca_{tot} , Mn_{tot} and pH were
283 significantly higher for BL, while Fe_{tot} , Fe_{w} , P_{tot} , S, N were significantly higher for SL (Table S2 A). Yet,
284 most of the studied chemical parameters ($\text{NO}_3^-_{\text{w}}$, $\text{NO}_2^-_{\text{w}}$, $\text{SO}_4^{2-}_{\text{w}}$, $\text{PO}_4^{3-}_{\text{w}}$, Cl^-_{w} , F^-_{w} , $\text{NH}_4^+_{\text{w}}$, K^+_{w} , $\text{Mg}^{2+}_{\text{w}}$,
285 Na^+_{w} , $\text{Ca}^{2+}_{\text{w}}$, lactate_w, acetate_w, formate_w, oxalate_w, P_{w} , Al_{w} , Al_{tot} , Mn_{w} , Ca_{w} , K_{w} , K_{tot} , DOC, HIX) did
286 not significantly differ between the two litter types throughout the experiment (Table S2 A).

287

288 **3.4. Microbial characteristics**

289 Abundances of bacteria (16S rRNA gene copies) and fungi (ITS region gene copies) did not
290 significantly differ between BL and SL in months 15, 19 and 29 of decomposition (Table S2 A) but
291 composition of bacterial communities (Illumina MiSeq) differed significantly between BL and SL (Table
292 S4).

293 More specifically, the bacterial community composition was analyzed using a total of 665,606 16S
294 rRNA gene sequence reads were mapped to 2052 OTUs. Bacterial communities were represented by
295 highest proportions of *Proteobacteria*, followed by *Actinobacteria*, *Firmicutes*, *Acidobacteria* and
296 *Bacteroidetes* on BL and by *Actinobacteria*, followed by *Proteobacteria*, *Acidobacteria*, *Firmicutes* and
297 *Bacteroidetes* on SL (Fig. 2). Proportions of *Acidobacteria*, *Actinobacteria*, *Bacteroidetes*, *Firmicutes*,
298 *Patescibacteria* and *Proteobacteria* significantly differed between BL and SL (Table S4.)



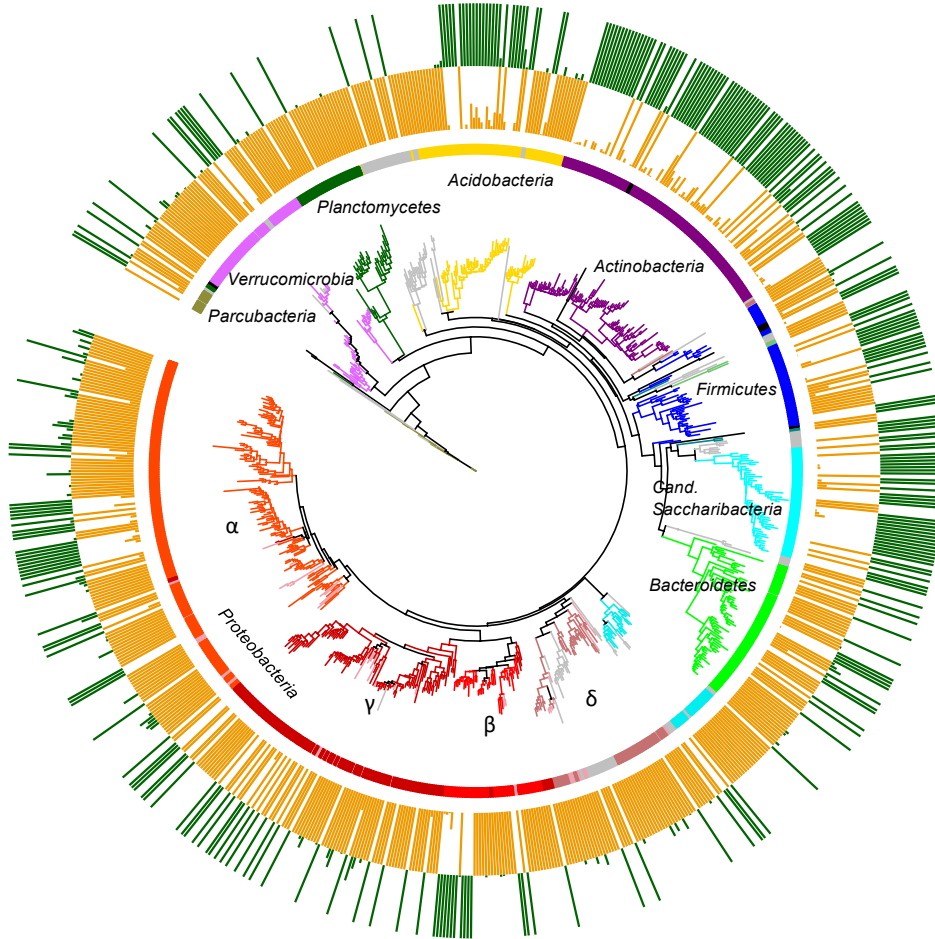
299 **Fig. 2.** Average proportions of phyla in the bacterial 16S rRNA gene amplicon sequence libraries on beech
 300 (B) and spruce (S) litter (n = 3) in different sampled time points.

301

302 Proportions of *Proteobacteria* families *Acetobacteraceae* and *Burkholderiaceae* were higher on
 303 SL than on BL, while *Bradyrhizobiaceae* and unclassified *Gammaproteobacteria* were higher on BL than
 304 on SL (Fig. S3). Proportions of all *Actinobacteria* families were higher on SL than on BL (Fig. S4).
 305 Highest proportions of *Solirubrobacteraceae*, followed by Trebon clade, *Mycobacteriaceae*, were found
 306 on both litter types, but proportionally lower were on BL (Fig. S4). Proportions of *Firmicutes* families
 307 decreased in the following period with both litter types, while they were overall higher (especially in
 308 month 15 and in month 29) on BL than on SL. The family *Bacillaceae 1* followed by *Bacillaceae 2*,
 309 *Paenibacillaceae 1* and unclassified *Bacillales* dominated on BL, while *Alicyclobacillaceae* dominated
 310 on SL (Fig. S5).

311 The phylogenetic tree was built from 839 OTUs differing significantly between communities
 312 associated with SL and BL (Metastats, $p < 0.05$). Out of those, proportions of 294 OTUs were higher on

313 SL and 545 OTUs on BL. OTUs corresponding to *Actinobacteria*, *Acidobacteria*, *Firmicutes* and *Cand.*
314 *Saccharibacteria* were proportionally higher on SL, while *Proteobacteria*, *Bacteroidetes*,
315 *Verrucomicrobia*, *Planctomycetes* and *Parcubacteria* on BL (Fig. 3).



316 **Fig. 3.** Phylogenetic tree of OTUs that significantly differed between the communities associated with
317 beech (yellow) and spruce (green) litter after 15, 19 and 29 months of decomposition (Metastats, $p < 0.05$,
318 $n = 9$). The phylogeny was inferred by maximum likelihood analysis of representative sequences of each
319 OTU.

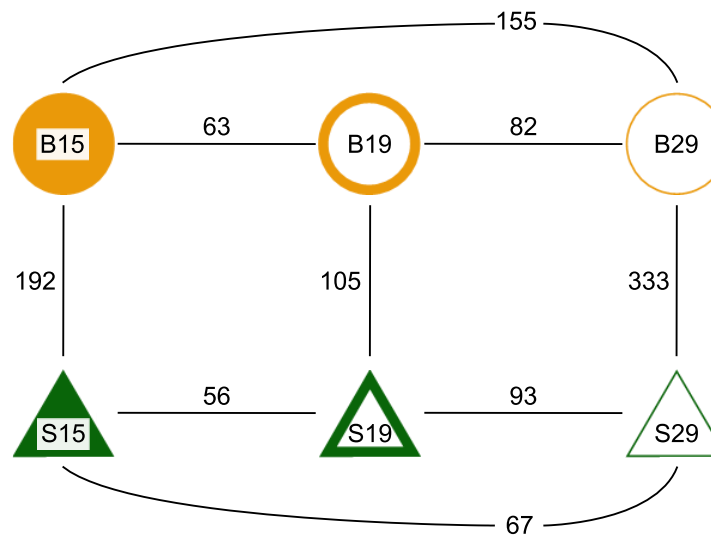
320

321 Changes in the composition of bacterial communities showed that higher number of OTUs
322 significantly contributing to differences between months 15 and 29 were found on BL (Metastats, $p <$
323 0.05 , Fig. 4). The number of OTUs significantly contributing to differences between litter types was the
324 highest in month 29 and the lowest in month 19 (Metastats, $p < 0.05$). Rarefaction curves demonstrated

325 that bacterial diversity was higher for the BL than the SL in months 15 and 19 (Fig. S6).

326

327 Heat maps (supported by Metastats) showed differences between BL and SL between months 15
328 and 29 (Table S5 A, B). On BL proportions of 155 OTUs differed (Metastats, $p < 0.05$), out of which 123
329 OTUs proportions increased and 32 OTUs decreased. On SL, proportions of only 67 OTUs differed, out
330 of which 30 increased and 37 decreased during that period. The most abundant bacterial groups separating
331 samples from month 15 and month 29 were on BL especially *Actinobacteria*, *Proteobacteria*,
332 *Acidobacteria*, *Verrucomicrobia*, *Bacteroidetes*, *Firmicutes* and *WPS-2* (Table S5 A), while on SL it was
333 *Acidobacteria*, *Actinobacteria*, *Proteobacteria*, *Patescibacteria* and *Firmicutes* (Table S5 B).



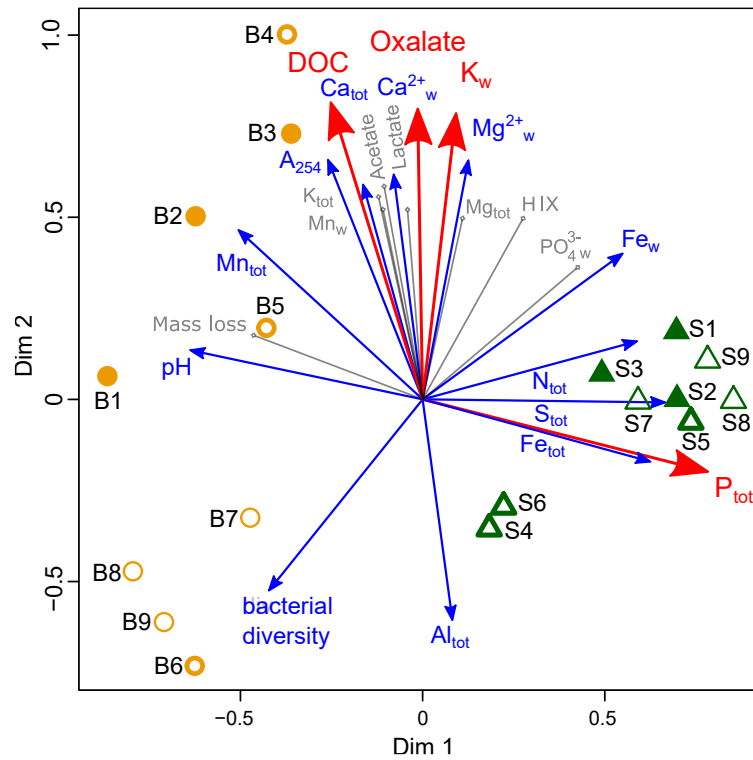
334 **Fig. 4.** Changes of composition of bacterial communities during plant litter decomposition on beech (B,
335 yellow circle) and spruce (S, green triangle) after months 15, 19 and 29 assayed by Illumina amplicon
336 sequencing. Numbers indicate the OTUs significantly contributing to the difference between samples in
337 pairwise comparison (Metastats, $p < 0.05$, $n = 3$).

338 3.5. NMDS analysis

339 NMDS distinguished bacterial communities into two groups corresponding to BL and SL (Fig. 5).
340 The bacterial community on BL most strongly positively correlated to DOC, oxalate, K_w , followed by
341 A_{254} , Mn_{tot} , pH, Ca_{tot} , Ca_w , Mg^{2+}_w and bacterial diversity (Fig. 5). The bacterial community on SL most

342 strongly positively correlated to P_{tot} , followed by Fe_w , N_{tot} , S_{tot} , Fe_{tot} (Fig. 5).

343 Composition of bacterial communities at both sites significantly correlated to pH, Ca_{tot} , Ca^{2+}_w ,
344 Mg^{2+}_w , Fe_{tot} , Fe_w , Mn_w , Mn_{tot} , P_{tot} , $PO_4^{3-}_w$, K_{tot} , K^+_w , N_{tot} , S_{tot} , Al_{tot} , DOC, A_{254} , Acetate_w, Oxalate_w, HIX,
345 mass loss and bacterial diversity (Table S6).



346

347 **Fig. 5.** Sammon's projection showing distance and relationship between bacterial communities on beech
348 (yellow circle) and spruce (green triangle) after months 15 (full symbol), 19 (empty symbol outlined by a
349 thick line) and 29 (empty symbol outlined by a thin line) of decomposition. Linear vectors represent
350 chemical and microbiological variables significantly correlating with the structure of bacterial community
351 ($p < 0.001$ red vectors; $0.001 < p < 0.01$ blue vectors; $0.01 < p < 0.05$ grey vectors). A_{254} indicates
352 aromaticity, HIX humification index and DOC dissolved organic carbon.

353

354

355 **4. Discussion**

356 Abundances of bacteria and fungi did not differ between beech (BL) and spruce litter (SL) but
357 different bacterial communities were established on the two litter types after 15, 19 and 29 months of
358 decomposition, when it reached the exponential stage. The litter mainly differed by the length of time to
359 reach the exponential stage but also by chemistry of litter and its changes over the following period. That
360 complied with previous findings that the succession of bacterial communities rather than abundance
361 reflected chemical differences between litter types [50,51] and that this was transferred to situations of the
362 later decomposition stage [52,53].

363 More specifically, beech was typical by accumulation of Ca and Mg in leaves, which led to
364 concentration of those elements in shallow soil layers and consequently to improvement of soil quality.
365 That activity is called the base-pump strategy, which describes how trees selectively uptake certain
366 nutrients from lower horizons by their roots and via litter fall increase their concentration in top soil
367 horizons [5]. In contrast, spruce needles accumulated N and S, which probably originated in anthropogenic
368 acidification (in form of HNO_3^- and SO_4^{2-} , respectively) occurring in the past [16]. Also, the fresh needles
369 were enriched in Fe and Al, possibly due to preferential uptake of those elements from the granite bedrock
370 by spruce [21,54].

371 On beech litter, bacterial communities were most strongly correlated to DOC, oxalate and K_w .
372 Total DOC increased after the initial stage of decomposition and exposed higher degree of aromatic
373 compounds (A_{254}) [12]. Therefore, the correlation of BL community to DOC demonstrates the litter
374 degradability, which enables microbes to utilize released C specific to a given stage of decomposition.
375 The positive correlation between LMMOA (low molecular mass organic acids), especially oxalate and
376 Ca^{2+} to BL community can be explained by microbe solubilization of Ca from poorly dissolved
377 biominerals e.g. calcium oxalate [55]. Additionally, BL bacterial community correlation to Mn_{tot} may

378 reflect the activity of manganese peroxidase, since Mn^{2+} is an essential component of this ligninolytic
379 enzyme [4,9]. The positive relationship of organic compounds such as DOC, A_{254} and LMMOA with the
380 BL community together with higher weight loss supports the observed more complete decomposition of
381 this substrate and confirms that BL was subjected to a more advanced stage of decay probably entering
382 the exponential stage of decomposition [15].

383 On spruce litter, a positive relationship of SL bacterial community to P, Fe, N and S showed that
384 these elements were not only higher there but also available to bacterial inhabitants. More precisely, P
385 was probably not precipitated by basic cations as it happened in the BL [17] and was intensively depleted
386 from SL over time. Similarly, Fe often occurs in organo-mineral complexes [56] or complexes with P-
387 PO_4^{3-} [57], which are resistant to degradation. However, the correlation of SL community to both Fe and
388 P suggests that the community may be enriched with bacteria, which can solubilize those complexes
389 possibly using organic acids or siderophores [58]. It is typical for activities of *Actinobacteria*, which
390 indeed dominated SL. A positive correlation to N may reflect either increased N litter concentration or
391 possibly also N fixation by specialized bacteria [59]. Nitrogen and P typically promote decomposition in
392 earlier stages, and thus their relatively high content may enable a gradual shift of SL into the exponential
393 decomposition stage, which was already partially noticeable [10]. Above that, N together with S belong
394 among the main agents causing soil acidification and thus, might explain the community shift towards
395 acidophilic taxa, such as a proportional increase of *Acidobacteria* [16,18].

396 Interestingly, no effect of Al on bacterial communities was determined on either litter type,
397 suggesting that bacterial communities may be protected from its toxicity by three different processes; i.e.
398 while acidic SL might release Al to lower organic horizons, Al on BL might be bound by cations, inorganic
399 anions (SO_4^{2-} , F^-) and organic compounds (e.g. fulvic acid, DOC and organic acids) [60,61], which
400 function as natural complexation agents eliminating Al toxicity [3] or that the bacteria are adapted by

401 resistance developed over the time of exposure [62].

402 Differing content and availability of nutrients of the two litter types corresponded to bacterial
403 functional groups represented by typical taxa. *Proteobacteria*, *Bacteroidetes*, *Verrucomicrobia* dominated
404 on BL. Especially, *Betaproteobacteria* and *Bacteroidetes* are considered r-selected, preferentially utilizing
405 easily accessible substrates in balanced environment [63]. SL was typical by higher proportion of
406 *Actinobacteria*, *Acidobacteria* and *Firmicutes*. *Actinobacteria* and *Firmicutes* are typical K-selected litter
407 decomposers [64] and *Acidobacteria* are a group, which preferentially inhabits low pH forest soils [18,65].

408 The most pronounced differences between the communities on the two studied litter types were
409 found in *Firmicutes*, of which *Bacillaceae* and *Paenibacillaceae* had higher proportions on BL, while
410 *Alicyclobacilales* dominated on SL. Out of those, *Bacilli* and *Paenibacilli* are highly abundant in organic
411 soil horizons, where they participate at decomposition of calcareous substrates. They are also involved in
412 the N cycle, including N fixation and P solubilization in soil [66]. In comparison, the family
413 *Alicyclobacillaceae* suggests shifting of the SL community towards acidophilic members since its
414 members were described as thermo-acidophilic [67]. However, *Bacillaceae* as well as *Alicyclobacillaceae*
415 significantly decrease over the exponential stage on BL and SL suggesting a correlation with nutrients
416 typical for each litter type.

417 Other important exponential stage decomposers were *Actinobacteria*. *Actinobacteria* may promote
418 availability of some limiting nutrients because they produce an array of enzymes, organic acids and
419 siderophores, which participate in solubilization of organic matter and soil complexes [68]. In particular,
420 a higher proportion of *Solirubrobacteraceae* was observed on SL and they belong among plant growth
421 promoting bacteria [69]. Additionally, Trebon clade, a new clade of *Actinobacteria* occurring in acidic
422 soils [70] had higher relative abundance on SL.

423 The different modes of pedogenesis observed under spruce or beech [16] resulted from both litter

424 chemistry and bacterial community composition, which together provide a particular potential for
425 decomposing activities and explain the diverging decomposition rates [71]. Furthermore, on the BL,
426 higher litter Ca_{tot} positively correlated to soluble C, C turnover and diversity of soil microbes, which may
427 further improve the development of soil horizons [72]. In contrast, SL with lower amounts of Mn and Ca,
428 higher amounts of Fe_{tot} , S_{tot} , N_{tot} and P_{tot} and low pH, reduced the rate of microbial decomposition,
429 resulting in higher accumulation of lower quality litter in the soil. More specifically, lower pH in SL can
430 lead to increased mobility of Al, Mn and Fe, which leach from the L horizon to deeper parts of soil profile
431 causing the differentiation of soil profiles – creating podzol (e.g. Sauer et al. [73]). It has been observed
432 previously that even small differences between the quality of humus and soil chemistry (pH) led to
433 increasing podsolization process in cambisols [74]. Similar observation was previously reported from the
434 Giant Mountains (Czechia) [75]. Thus, soils with different characteristics are developed under the two
435 tree species and their different microbial communities and decomposition rate may have consequences in
436 the stability and resilience of beech and spruce forests.

437

438 **5. Conclusions**

439 Our study compared the litter decomposition rate of beech litter (BL) and spruce litter (SL). The
440 BL displayed lower C accumulation and higher release of aromatic DOC after 15, 19 and 29 months of
441 decomposition, while SL showed lower pH and higher amount of Fe, S, N and P, resulting in accumulation
442 of organic matter and thus, C sequestration in the soil.

443 The BL had the lag-time of decomposition delayed until month 15 but after that period the
444 decomposition was relatively fast and supported by readily available compounds, while promoting the
445 growth of r-selected taxa. On the contrary, SL was described as an oligotrophic environment typical with

446 K-selected taxa, which together with acidic conditions caused that the SL substrate to remain in the lag-
447 phase during the entire experiment.

448 The litter chemical quality and specific decomposition pathways determined by the presence of
449 soil microorganisms with different life strategies lead to a consequent transformation of litter to humus
450 with different quality in beech and spruce forests. Finally, that process results to the development of soils,
451 which undergo podsolization under spruce but not beech.

452 **6. Funding**

453 Research was supported by the Czech University of Life Sciences Prague (internal project n.
454 21130/1312/3131), Ministry of Education, Youth and Sports of the CR (projects No.
455 CZ.02.1.01/0.0/0.0/16_019/0000845 and LTC17075), Czech Science Foundation (grant no. 15-01312S),
456 and Ministry of Agriculture of the CR (Institutional Project RO 0418).

457 **References**

- 458 [1] K.C. Rice, J.S. Herman, Acidification of Earth: An assessment across mechanisms and scales, *Appl.*
459 *Geochemistry*. 27 (2012) 1–14. <https://doi.org/10.1016/J.APGEOCHEM.2011.09.001>.
- 460 [2] T. Fukami, I.A. Dickie, J. Paula Wilkie, B.C. Paulus, D. Park, A. Roberts, P.K. Buchanan, R.B.
461 Allen, Assembly history dictates ecosystem functioning: evidence from wood decomposer
462 communities, *Ecol. Lett.* 13 (2010) 675–684. <https://doi.org/10.1111/j.1461-0248.2010.01465.x>.
- 463 [3] L. Borůvka, A. Nikodem, O. Drábek, P. Vokurková, V. Tejnecký, L. Pavlů, Assessment of soil
464 aluminium pools along three mountainous elevation gradients, *J. Inorg. Biochem.* 103 (2009) 1449–
465 1458. <https://doi.org/10.1016/j.jinorgbio.2009.07.022>.
- 466 [4] B. Berg, Litter decomposition and organic matter turnover in northern forest soils, *For. Ecol.*
467 *Manage.* 133 (2000) 13–22. [https://doi.org/10.1016/S0378-1127\(99\)00294-7](https://doi.org/10.1016/S0378-1127(99)00294-7).
- 468 [5] G. van der Heijden, E. Dambrine, B. Pollier, B. Zeller, J. Ranger, A. Legout, Mg and Ca uptake by
469 roots in relation to depth and allocation to aboveground tissues: results from an isotopic labeling
470 study in a beech forest on base-poor soil, *Biogeochemistry*. 122 (2015) 375–393.
471 <https://doi.org/10.1007/s10533-014-0047-2>.
- 472 [6] Z. Wang, A. Gottlein, G. Bartonek, Effects of growing roots of Norway spruce and European beech
473 on rhizosphere soil solution chemistry, *J. Plant Nutr. Soil Sci.* 164 (2001) 35–41.
- 474 [7] J. Rousk, S.D. Frey, Revisiting the hypothesis that fungal-to-bacterial dominance characterizes
475 turnover of soil organic matter and nutrients, *Ecol. Monogr.* 85 (2015) 457–472.
476 <https://doi.org/10.1890/14-1796.1>.
- 477 [8] A. Bani, S. Pioli, M. Ventura, P. Panzacchi, L. Borruso, R. Tognetti, G. Tonon, L. Brusetti, The
478 role of microbial community in the decomposition of leaf litter and deadwood, *Appl. Soil Ecol.* 126
479 (2018) 75–84. www.elsevier.com/locate/apsoil (accessed April 10, 2018).

- 480 [9] B. Berg, B. Erhagen, M.-B. Johansson, M. Nilsson, J. Stendahl, F. Trum, L. Vesterdal, Manganese
481 in the litter fall-forest floor continuum of boreal and temperate pine and spruce forest ecosystems -
482 A review, *For. Ecol. Manage.* 358 (2015) 248–260. <https://doi.org/10.1016/j.foreco.2015.09.021>.
- 483 [10] X. Ge, L. Zeng, W. Xiao, Z. Huang, X. Geng, B. Tan, Effect of litter substrate quality and soil
484 nutrients on forest litter decomposition: A review, *Acta Ecol. Sin.* 33 (2013) 102–108.
485 <https://doi.org/10.1016/j.chnaes.2013.01.006>.
- 486 [11] P.M. Vitousek, S. Porder, B.Z. Houlton, O.A. Chadwick, Terrestrial phosphorus limitation:
487 mechanisms, implications, and nitrogen–phosphorus interactions, *Ecol. Appl.* 20 (2010) 5–15.
488 <https://doi.org/10.1890/08-0127.1>.
- 489 [12] S.L. Mosier, E.S. Kane, D.L. Richter, E.A. Lilleskov, M.F. Jurgensen, A.J. Burton, S.C. Resh,
490 Interactive effects of climate change and fungal communities on wood-derived carbon in forest
491 soils, *Soil Biol. Biochem.* 115 (2017) 297–309. <https://doi.org/10.1016/J.SOILBIO.2017.08.028>.
- 492 [13] A. Don, K. Kalbitz, Amounts and degradability of dissolved organic carbon from foliar litter at
493 different decomposition stages, *Soil Biol. Biochem.* 37 (2005) 2171–2179.
494 <https://doi.org/10.1016/J.SOILBIO.2005.03.019>.
- 495 [14] B. Berg, A.V. De Santo, F.A. Rutigliano, A. Fierro, G. Ekbohm, Limit values for plant litter
496 decomposing in two contrasting soils - Influence of litter elemental composition, *Acta Oecologica.*
497 24 (2003) 295–302. <https://doi.org/10.1016/j.actao.2003.08.002>.
- 498 [15] M. Kleber, P.S. Nico, A. Plante, T. Filley, M. Kramer, C. Swanston, P. Sollins, Old and stable soil
499 organic matter is not necessarily chemically recalcitrant: Implications for modeling concepts and
500 temperature sensitivity, *Glob. Chang. Biol.* 17 (2011) 1097–1107.
501 <https://escholarship.org/content/qt8q25s86p/qt8q25s86p.pdf> (accessed October 2, 2018).

- 502 [16] V. Tejnecký, M. Bradová, L. Borůvka, K. Němeček, O. Šebek, A. Nikodem, J. Zenáhlíková, J.
503 Rejzek, O. Drábek, Profile distribution and temporal changes of sulphate and nitrate contents and
504 related soil properties under beech and spruce forests, *Sci. Total Environ.* 442 (2013) 165–171.
505 <https://doi.org/10.1016/j.scitotenv.2012.10.053>.
- 506 [17] V. Tejnecký, N. Rerichová, M. Brandová, K. Němeček, H. Santrůvková, C. Ash, O. Drábek, Litter
507 decomposition as a source of active phosphates in spruce and beech mountainous forests affected
508 by acidification, *Procedia Earth Planet. Sci.* 10 (2014) 130–132.
509 <https://doi.org/10.1016/j.proeps.2014.08.043>.
- 510 [18] S. Lladó, R. López-Mondéjar, P. Baldrian, Forest Soil Bacteria: Diversity, Involvement in
511 Ecosystem Processes, and Response to Global Change, *Microbiol. Mol. Biol. Rev.* 81 (2017)
512 e00063-16. <https://doi.org/10.1128/MMBR.00063-16>.
- 513 [19] V. Tlaskal, J. Voříšková, P. Baldrian, Bacterial succession on decomposing leaf litter exhibits a
514 specific occurrence pattern of cellulolytic taxa and potential decomposers of fungal mycelia, *FEMS*
515 *Microbiol. Ecol.* 92 (2016) fiw177. <https://doi.org/10.1093/femsec/fiw177>.
- 516 [20] A. Buresová, J. Kopecký, V. Hrdinková, Z. Kameník, M. Omelka, M. Šagová-Marečková,
517 Succession of microbial decomposers is designated by litter type, but site conditions drive
518 decomposition rates., *Appl. Environ. Microbiol.* (2019). <https://doi.org/10.1128/AEM.01760-19>.
- 519 [21] J. Chaloupský, J. Cervenka, J. Jetel, F. Kralík, J. Libalová, E. Pichová, J. Pokorný, K. Posmourný,
520 J. Sekyra, O. Šrbený, K. Salanský, J. Šrámek, J. Vacl, *Geologie Krkonos a Jizerských hor*, 1.,
521 Moravské tiskarské závody, 1989.
- 522 [22] I.W.G. WRB, World reference base for soil resources 2006, *World Soil Resour. Reports.* 103
523 (2006). <http://www.fao.org> (accessed February 11, 2019).

- 524 [23] M. Bradová, V. Tejnecký, L. Borůvka, K. Němeček, C. Ash, O. Šebek, M. Svoboda, J. Zenáhlíková,
525 O. Drábek, The variations of aluminium species in mountainous forest soils and its implications to
526 soil acidification, *Environ. Sci. Pollut. Res.* 22 (2015) 16676–16687.
527 <https://doi.org/10.1007/s11356-015-4855-2>.
- 528 [24] Czech Hydrometeorological Institute, Historical data - Territorial air temperature and precipitation,
529 (n.d.). <http://portal.chmi.cz/historicka-data/pocasi/zakladni-informace?l=en>.
- 530 [25] N. Cools, B. De Vos, Sampling and Analysis of Soil. In: UNECE ICP Forests Programme
531 Coordinating Centre (ed.): Manual on methods and criteria for harmonized sampling, assessment,
532 monitoring and analysis of the effects of air pollution on forests, Thünen Institute of Forest
533 Ecosystems, Eberswalde, Germany, 2016. <https://doi.org/10.1063/1.2761021>.
- 534 [26] P. Hubova, V. Tejnecky, C. Ash, L. Boruvka, O. Drabek, Low-Molecular-Mass Organic Acids in
535 the Forest Soil Environment, *Mini. Rev. Org. Chem.* 14 (2017) 75–84.
536 <https://www.ingentaconnect.com/contentone/ben/mroc/2017/00000014/00000001/art00010>
537 (accessed October 3, 2018).
- 538 [27] L.X. Zhou, J.W.C. Wong, Microbial Decomposition of Dissolved Organic Matter and Its Control
539 during a Sorption Experiment, *J. Environ. Qual.* 29 (2000) 1852.
540 <https://doi.org/10.2134/jeq2000.00472425002900060017x>.
- 541 [28] T. Ohno, Fluorescence inner-filtering correction for determining the humification index of
542 dissolved organic matter, *Environ. Sci. Technol.* 36 (2002) 742–746.
543 <https://doi.org/10.1021/es0155276>.
- 544 [29] R Core Team, R Core Team, R : A language and environment for statistical computing., R Found.
545 Stat. Comput. Vienna, Austria. (2018) R Foundation for Statistical Computing.

- 546 [30] M. Sagova-Mareckova, L. Cermak, J. Novotna, K. Plhackova, J. Forstova, J. Kopecky, Innovative
547 methods for soil DNA purification tested in soils with widely differing characteristics, *Appl.*
548 *Environ. Microbiol.* 74 (2008) 2902–2907. <https://doi.org/10.1128/AEM.02161-07>.
- 549 [31] C. Quast, E. Pruesse, P. Yilmaz, J. Gerken, T. Schweer, P. Yarza, J. Peplies, F.O. Glöckner, The
550 SILVA ribosomal RNA gene database project: improved data processing and web-based tools,
551 *Nucleic Acids Res.* 41 (2012) D590–D596. <https://doi.org/10.1093/nar/gks1219>.
- 552 [32] T. Rognes, T. Flouri, B. Nichols, C. Quince, F. Mahé, VSEARCH: a versatile open source tool for
553 metagenomics, *PeerJ.* 4 (2016) e2584. <https://doi.org/10.7717/peerj.2584>.
- 554 [33] J.J. Kozich, S.L. Westcott, N.T. Baxter, S.K. Highlander, P.D. Schloss, Development of a dual-
555 index sequencing strategy and curation pipeline for analyzing amplicon sequence data on the miseq
556 illumina sequencing platform, *Appl. Environ. Microbiol.* 79 (2013) 5112–5120.
557 <https://doi.org/10.1128/AEM.01043-13>.
- 558 [34] P.D. Schloss, S.L. Westcott, T. Ryabin, J.R. Hall, M. Hartmann, E.B. Hollister, R.A. Lesniewski,
559 B.B. Oakley, D.H. Parks, C.J. Robinson, J.W. Sahl, B. Stres, G.G. Thallinger, D.J. Van Horn, C.F.
560 Weber, Introducing mothur: Open-source, platform-independent, community-supported software
561 for describing and comparing microbial communities, *Appl. Environ. Microbiol.* 75 (2009) 7537–
562 7541. <https://doi.org/10.1128/AEM.01541-09>.
- 563 [35] P. Yilmaz, L.W. Parfrey, P. Yarza, J. Gerken, E. Pruesse, C. Quast, T. Schweer, J. Peplies, W.
564 Ludwig, F.O. Glöckner, The SILVA and “all-species Living Tree Project (LTP)” taxonomic
565 frameworks, *Nucleic Acids Res.* 42 (2014) 643–648. <https://doi.org/10.1093/nar/gkt1209>.
- 566 [36] R.C. Edgar, UPARSE: highly accurate OTU sequences from microbial amplicon reads, *Nat.*
567 *Methods.* 10 (2013) 996–998. <https://doi.org/10.1038/nmeth.2604>.

- 568 [37] L. Čermák, J. Kopecký, J. Novotná, M. Omelka, N. Parkhomenko, K. Plháčková, M. Ságová-
569 Marečková, Bacterial communities of two contrasting soils reacted differently to lincomycin
570 treatment, *Appl. Soil Ecol.* 40 (2008) 348–358. <https://doi.org/10.1016/j.apsoil.2008.06.001>.
- 571 [38] M. Sakai, A. Matsuka, T. Komura, S. Kanazawa, Application of a new PCR primer for terminal
572 restriction fragment length polymorphism analysis of the bacterial communities in plant roots, *J.*
573 *Microbiol. Methods.* 59 (2004) 81–89. <https://doi.org/10.1016/J.MIMET.2004.06.005>.
- 574 [39] M. Gardes, T.D. Bruns, ITS primers with enhanced specificity for basidiomycetes - application to
575 the identification of mycorrhizae and rusts, *Mol. Ecol.* 2 (1993) 113–118.
576 <https://doi.org/10.1111/j.1365-294X.1993.tb00005.x>.
- 577 [40] T.J. White, T. Bruns, S. Lee, J.W. Taylor, Amplification and direct sequencing of fungal ribosomal
578 RNA genes for phylogenetics, *Acad. Press. Inc., New York.* (1990) 315–322.
579 https://scholar.google.cz/scholar?hl=cs&as_sdt=0%2C5&q=White+TJ%2C+Bruns+T%2C+Lee+S+%26+Taylor+J+%281990%29+PCR+protocols.+Amplification+and+Direct+Sequencing+of+Fungal+Ribosomal+RNA+Genes+for+Phylogenetics+%28Innins+MA%2C+Gelfand+DH%2C+S+ninsky+JJ+%26+Whi (accessed February 5, 2019).
- 583 [41] B.L. Welch, On the comparison of several mean values: an alternative approach, *Biometrika.* 38
584 (1951) 330–336. <https://doi.org/10.1093/biomet/38.3-4.330>.
- 585 [42] A.P. Martin, Phylogenetic Approaches for Describing and Comparing the Diversity of Microbial
586 Communities, *DNA Seq.* 68 (2002) 3673–3682. <https://doi.org/10.1128/AEM.68.8.3673>.
- 587 [43] J.R. White, N. Nagarajan, M. Pop, Statistical methods for detecting differentially abundant features
588 in clinical metagenomic samples., *PLoS Comput. Biol.* 5 (2009) e1000352.
589 <https://doi.org/10.1371/journal.pcbi.1000352>.

- 590 [44] M.N. Price, P.S. Dehal, A.P. Arkin, FastTree 2 - Approximately maximum-likelihood trees for
591 large alignments, *PLoS One*. 5 (2010) e9490. <https://doi.org/10.1371/journal.pone.0009490>.
- 592 [45] I. Letunic, P. Bork, Interactive tree of life (iTOL) v3: an online tool for the display and annotation
593 of phylogenetic and other trees, *Nucleic Acids Res.* 44 (2016) W242–W245.
594 <https://doi.org/10.1093/nar/gkw290>.
- 595 [46] W.N. Venables, B.D. Ripley, Random and Mixed Effects, in: *Mod. Appl. Stat.* with S. Springer,
596 New York, NY, Springer, New York, NY, 2002: pp. 271–300. https://doi.org/10.1007/978-0-387-21706-2_10.
- 598 [47] B. Ripley, B. Venables, D.M. Bates, K. Hornik, A. Gebhardt, D. Firth, Package “MASS,” 2019.
599 <http://www.stats.ox.ac.uk/pub/MASS4/> (accessed April 2, 2020).
- 600 [48] J. Oksanen, F.G. Blanchet, M. Friendly, R. Kindt, P. Legendre, D. Mcglinn, P.R. Minchin, R.B.
601 O’hara, G.L. Simpson, P. Solymos, M. Henry, H. Stevens, E. Szoecs, H.W. Maintainer, Package
602 “vegan” Title Community Ecology Package Version 2.5-6, 2019.
- 603 [49] J. Oksanen, F.G. Blanchet, M. Friendly, R. Kindt, P. Legendre, D. Mcglinn, P.R. Minchin, R.B.
604 O’hara, G.L. Simpson, P. Solymos, M. Henry, H. Stevens, E. Szoecs, H.W. Maintainer, Package
605 “vegan” Title Community Ecology Package, 2018.
606 <https://cran.ism.ac.jp/web/packages/vegan/vegan.pdf> (accessed October 5, 2018).
- 607 [50] J.C. Frankland, Fungal succession — unravelling the unpredictable, *Mycol. Res.* 102 (1998) 1–15.
608 <https://doi.org/10.1017/S0953756297005364>.
- 609 [51] M. Sauvadet, M. Chauvat, D. Cluzeau, P.A. Maron, C. Villenave, I. Bertrand, The dynamics of soil
610 micro-food web structure and functions vary according to litter quality, *Soil Biol. Biochem.* 95
611 (2016) 262–274. <https://doi.org/10.1016/j.soilbio.2016.01.003>.

- 612 [52] T. Fukami, Historical Contingency in Community Assembly: Integrating Niches, Species Pools,
613 and Priority Effects, *Annu. Rev. Ecol. Evol. Syst.* 46 (2015) 1–23. [https://doi.org/10.1146/annurev-](https://doi.org/10.1146/annurev-ecolsys-110411-160340)
614 [ecolsys-110411-160340](https://doi.org/10.1146/annurev-ecolsys-110411-160340).
- 615 [53] L.C. Cline, D.R. Zak, Initial colonization, community assembly and ecosystem function: fungal
616 colonist traits and litter biochemistry mediate decay rate, *Mol. Ecol.* 24 (2015) 5045–5058.
617 <https://doi.org/10.1111/mec.13361>.
- 618 [54] J. Kratina, Rozdíly Ve Vlastnostech Horských Lesních Půd Na Kyselých a Bazických Matečných
619 Horninách, *Geol. Výzkumy Na Moravě a ve Slezsku.* 17 (2010).
- 620 [55] J.M. Dauer, S.S. Perakis, Calcium oxalate contribution to calcium cycling in forests of contrasting
621 nutrient status, *For. Ecol. Manage.* 334 (2014) 64–73.
622 <https://doi.org/10.1016/J.FORECO.2014.08.029>.
- 623 [56] J.P. Boudot, A.B. Hadj, R. Steiman, F. Seigle-Murandi, Biodegradation of synthetic organo-
624 metallic complexes of iron and aluminium with selected metal to carbon ratios, *Soil Biol. Biochem.*
625 21 (1989) 961–966. [https://doi.org/10.1016/0038-0717\(89\)90088-6](https://doi.org/10.1016/0038-0717(89)90088-6).
- 626 [57] F. Lang, J. Bauhus, E. Frossard, E. George, K. Kaiser, M. Kaupenjohann, J. Krüger, E. Matzner,
627 A. Polle, J. Prietzel, H. Rennenberg, N. Wellbrock, Phosphorus in forest ecosystems: New insights
628 from an ecosystem nutrition perspective, *J. Plant Nutr. Soil Sci.* 179 (2016) 129–135.
629 <https://doi.org/10.1002/jpln.201500541>.
- 630 [58] R.C. Hider, X. Kong, Chemistry and biology of siderophores, *Nat. Prod. Rep.* 27 (2010) 637–657.
631 <https://doi.org/10.1039/b906679a>.

- 632 [59] D. Finn, K. Page, K. Catton, E. Strounina, M. Kienzle, F. Robertson, R. Armstrong, R. Dalal, Effect
633 of added nitrogen on plant litter decomposition depends on initial soil carbon and nitrogen
634 stoichiometry, *Soil Biol. Biochem.* 91 (2015) 160–168.
635 <https://doi.org/10.1016/J.SOILBIO.2015.09.001>.
- 636 [60] O. Drábek, I. Kipkoech Kiplagat, M. Komárek, V. Tejnecký, L. Borůvka, Study of Interactions
637 between Relevant Organic Acids and Aluminium in Model Solutions Using HPLC and IC, *Orig.
638 Pap. Soil Water Res.* 10 (2015) 172–180. <https://doi.org/10.17221/256/2014-SWR>.
- 639 [61] O. Drabek, L. Mladkova, L. Boruvka, J. Szakova, A. Nikodem, K. Nemecek, Comparison of water-
640 soluble and exchangeable forms of Al in acid forest soils, in: *J. Inorg. Biochem.*, Elsevier Inc.,
641 2005: pp. 1788–1795. <https://doi.org/10.1016/j.jinorgbio.2005.06.024>.
- 642 [62] R. Garciduefias Pifia, C. Cervantes, Microbial interactions with aluminium, *Bio Met.* 9 (1996) 311–
643 316.
- 644 [63] L. Philippot, S.G.E. Andersson, T.J. Battin, J.I. Prosser, J.P. Schimel, W.B. Whitman, S. Hallin,
645 The ecological coherence of high bacterial taxonomic ranks, *Nat. Rev. Microbiol.* 8 (2010) 523–
646 529. <https://doi.org/10.1038/nrmicro2367>.
- 647 [64] F. Bastian, L. Bouziri, B. Nicolardot, L. Ranjard, Impact of wheat straw decomposition on
648 successional patterns of soil microbial community structure, *Soil Biol. Biochem.* 41 (2009) 262–
649 275. <https://www.sciencedirect.com/science/article/pii/S0038071708003696> (accessed April 20,
650 2018).
- 651 [65] M. Štursová, L. Žifčáková, M.B. Leigh, R. Burgess, P. Baldrian, Cellulose utilization in forest litter
652 and soil: identification of bacterial and fungal decomposers, *FEMS Microbiol. Ecol.* 80 (2012) 735–
653 746. <https://doi.org/10.1111/j.1574-6941.2012.01343.x>.

- 654 [66] I. Mandic-Mulec, P. Stefanic, J. Van Elsas, Ecology of Bacillaceae, *Bact. Spore from Mol. to Syst.*
655 (2015) 59–85. <https://doi.org/10.1128/microbiolspec.TBS-0017-2013>.
- 656 [67] E. Ciuffreda, A. Bevilacqua, M. Sinigaglia, M. Corbo, E. Ciuffreda, A. Bevilacqua, M. Sinigaglia,
657 M.R. Corbo, Alicyclobacillus spp.: New Insights on Ecology and Preserving Food Quality through
658 New Approaches, *Microorganisms*. 3 (2015) 625–640.
659 <https://doi.org/10.3390/microorganisms3040625>.
- 660 [68] W. Wang, Z. Qiu, H. Tan, L. Cao, Siderophore production by actinobacteria, *BioMetals*. 27 (2014)
661 623–631. <https://doi.org/10.1007/s10534-014-9739-2>.
- 662 [69] I.H. Franke-Whittle, L.M. Manici, H. Insam, B. Stres, Rhizosphere bacteria and fungi associated
663 with plant growth in soils of three replanted apple orchards, *Plant Soil*. 395 (2015) 317–333.
664 <https://doi.org/10.1007/s11104-015-2562-x>.
- 665 [70] J. Kopecky, M. Kyselkova, M. Omelka, L. Cermak, J. Novotna, G.L. Grundmann, Y. Moënne-
666 Loccoz, M. Sagova-Mareckova, Actinobacterial community dominated by a distinct clade in acidic
667 soil of a waterlogged deciduous forest, *FEMS Microbiol. Ecol.* 78 (2011) 386–394.
668 <https://doi.org/10.1111/j.1574-6941.2011.01173.x>.
- 669 [71] J.A.J. Dungait, D.W. Hopkins, A.S. Gregory, A.P. Whitmore, Soil organic matter turnover is
670 governed by accessibility not recalcitrance, *Glob. Chang. Biol.* 18 (2012) 1781–1796.
671 <https://doi.org/10.1111/j.1365-2486.2012.02665.x>.
- 672 [72] J. Frouz, V. Jílková, T. Cajthaml, V. Pižl, K. Tajovský, L. Háněl, A. Burešová, H. Šimáčková, K.
673 Kolaříková, J. Franklin, J. Nawrot, J.W. Groninger, P.D. Stahl, Soil biota in post-mining sites along
674 a climatic gradient in the USA: Simple communities in shortgrass prairie recover faster than
675 complex communities in tallgrass prairie and forest, *Soil Biol. Biochem.* 67 (2013).
676 <https://doi.org/10.1016/j.soilbio.2013.08.025>.

- 677 [73] D. Sauer, H. Sponagel, M. Sommer, L. Giani, R. Jahn, K. Stahr, Podzol: Soil of the year 2007. A
678 review on its genesis, occurrence, and functions, *J. Plant Nutr. Soil Sci.* 170 (2007) 581–597.
679 <https://doi.org/10.1002/jpln.200700135>.
- 680 [74] V. Brahy, H. Titeux, B. Delvaux, Incipient podzolization and weathering caused by complexation
681 in a forest Cambisol on loess as revealed by a soil solution study, *Eur. J. Soil Sci.* 51 (2000) 475–
682 484. <https://doi.org/10.1046/j.1365-2389.2000.00324.x>.
- 683 [75] S. Dlouhá, L. Borůvka, L. Pavlů, V. Tejnecký, O. Drábek, Comparison of Al speciation and other
684 soil characteristics between meadow, young forest and old forest stands., *J. Inorg. Biochem.* 103
685 (2009) 1459–64. <https://doi.org/10.1016/j.jinorgbio.2009.07.024>.
- 686

Supplementary Information for

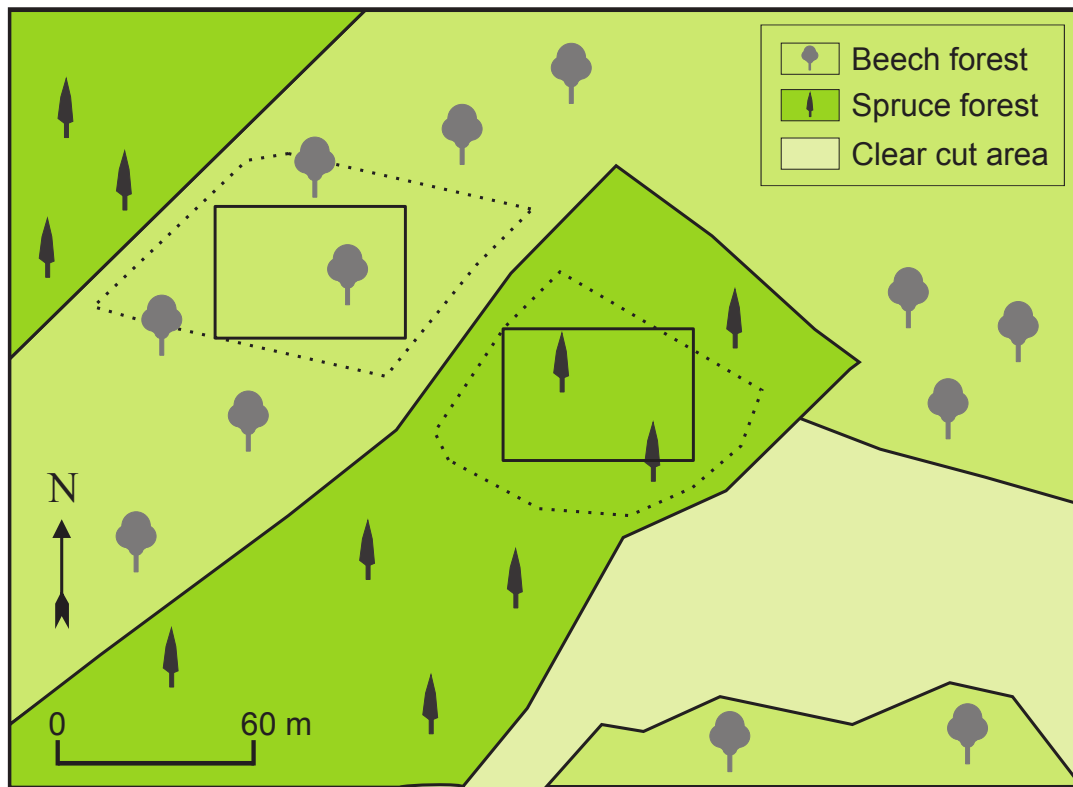
**Litter chemical quality and bacterial community structure influenced decomposition
in acidic forest soil**

Andrea Buresova, Vaclav Tejnecky, Jan Kopecky, Ondrej Drabek, Pavla Madrova, Nada Rerichova, Marek Omelka, Petra Krizova, Karel Nemecek, Thomas B. Parr, Tsutomu Ohno, Marketa Sagova-Mareckova

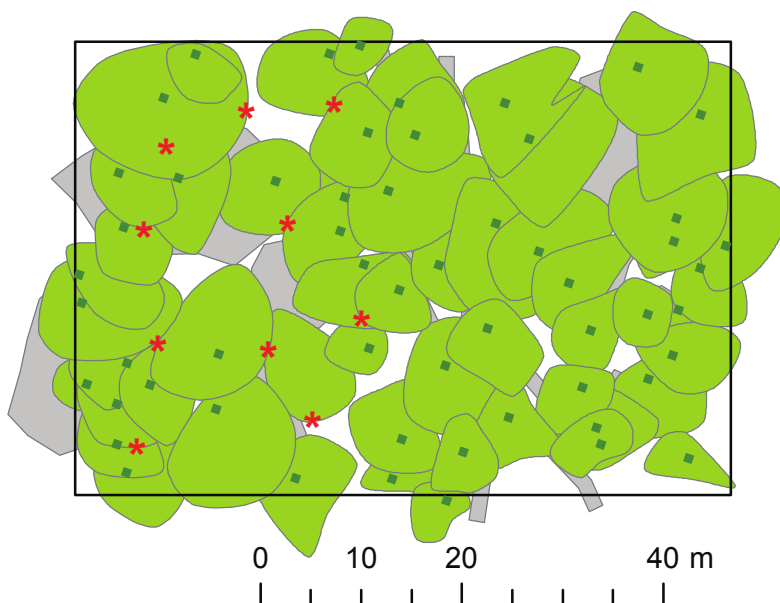
Corresponding author: Vaclav Tejnecky,
Email: tejnecky@af.czu.cz

This PDF file includes:
Figs. S1 to S6
Tables S1 to S6

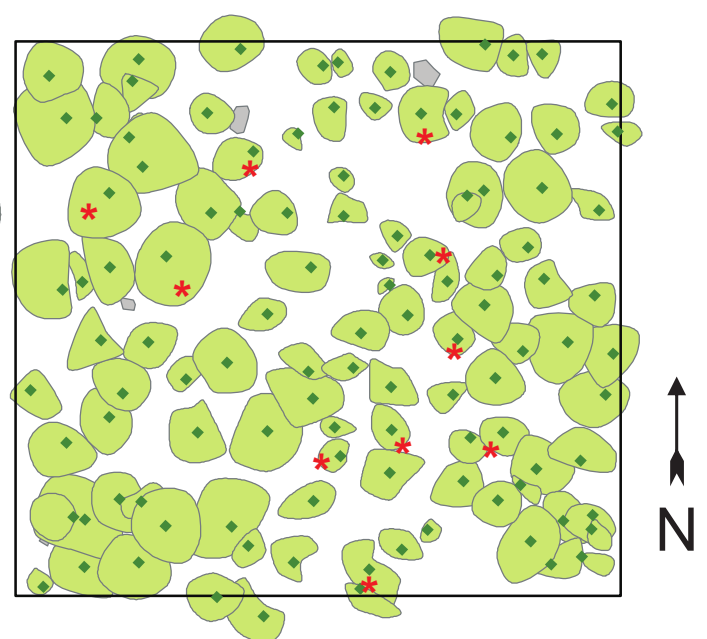
Supplementary Figure S1. Spruce and beech experimental forest sites located at Palicnik hill (635 - 680 a.s.l.) in Jizera mountains in the Czech Republic. The size of the investigated area was 2925 m² in beech and 3300 m² in spruce forest. 60 bags filled with beech litter were placed to beech forest and 60 bags filled with spruce litter were placed to spruce forest. DBH of living trees was 534.6 (±153.4) in beech forest and 405.8 (±112.4) in spruce forest, total area of rock was 811.9 m² in beech forest and 10.9 m² in spruce forest and canopy closure was 87% in beech and 40% in spruce forest.



Beech forest

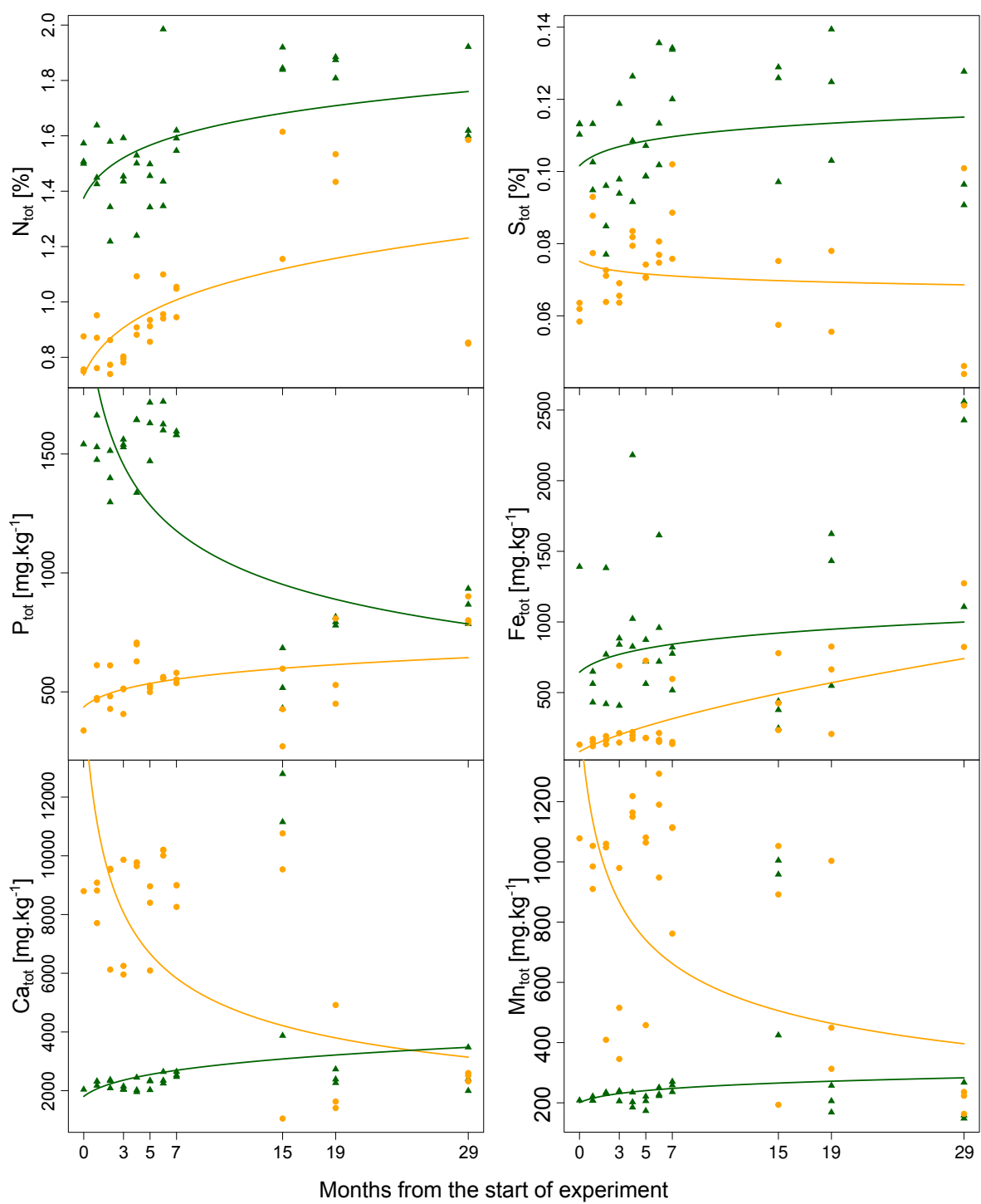


Spruce forest

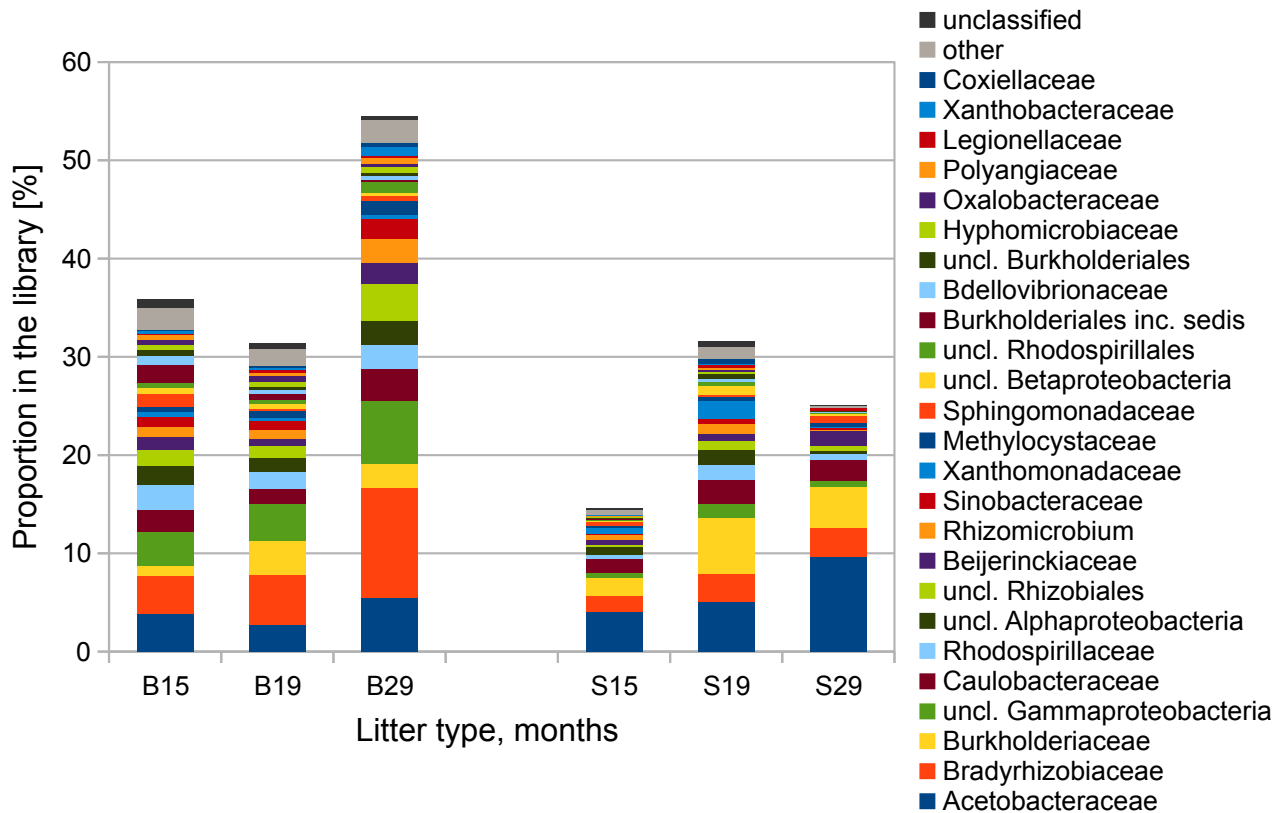


- ◆ Tree
- * Litter bags position
- Rock and surface runoff
- Crown projection

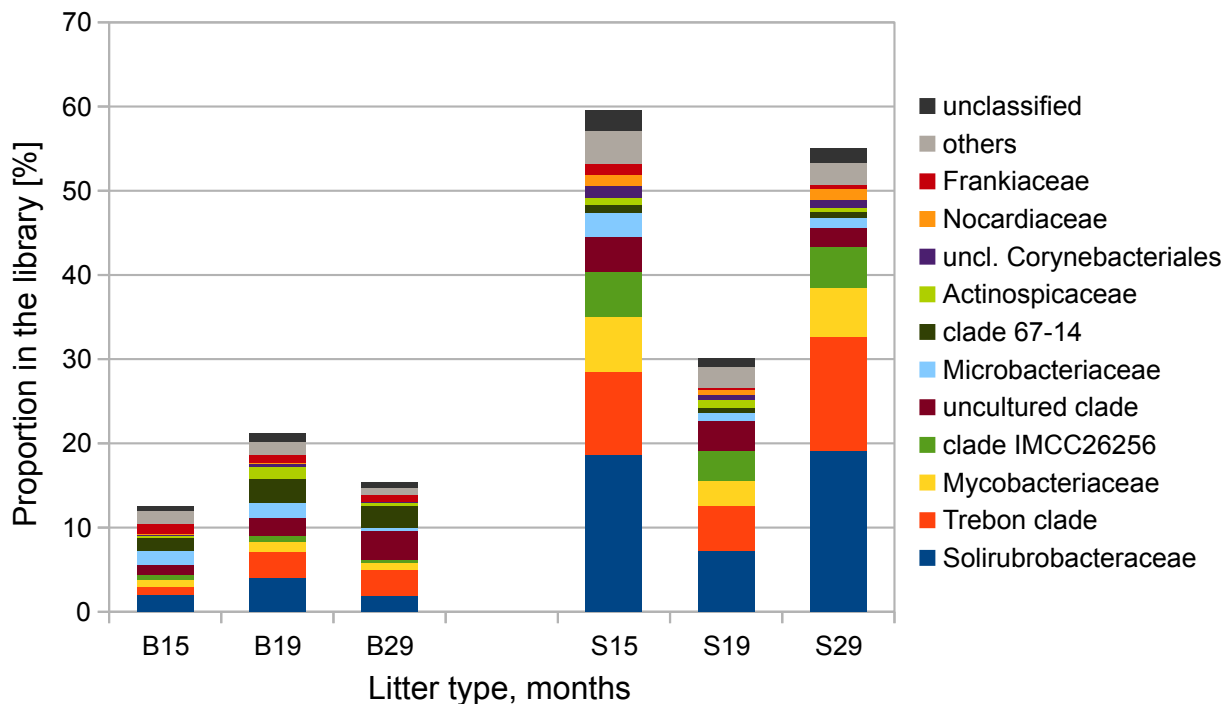
Supplementary Figure S2. Changes in the contents of selected elements in course of beech (yellow) and spruce (dark green) litter decomposition.



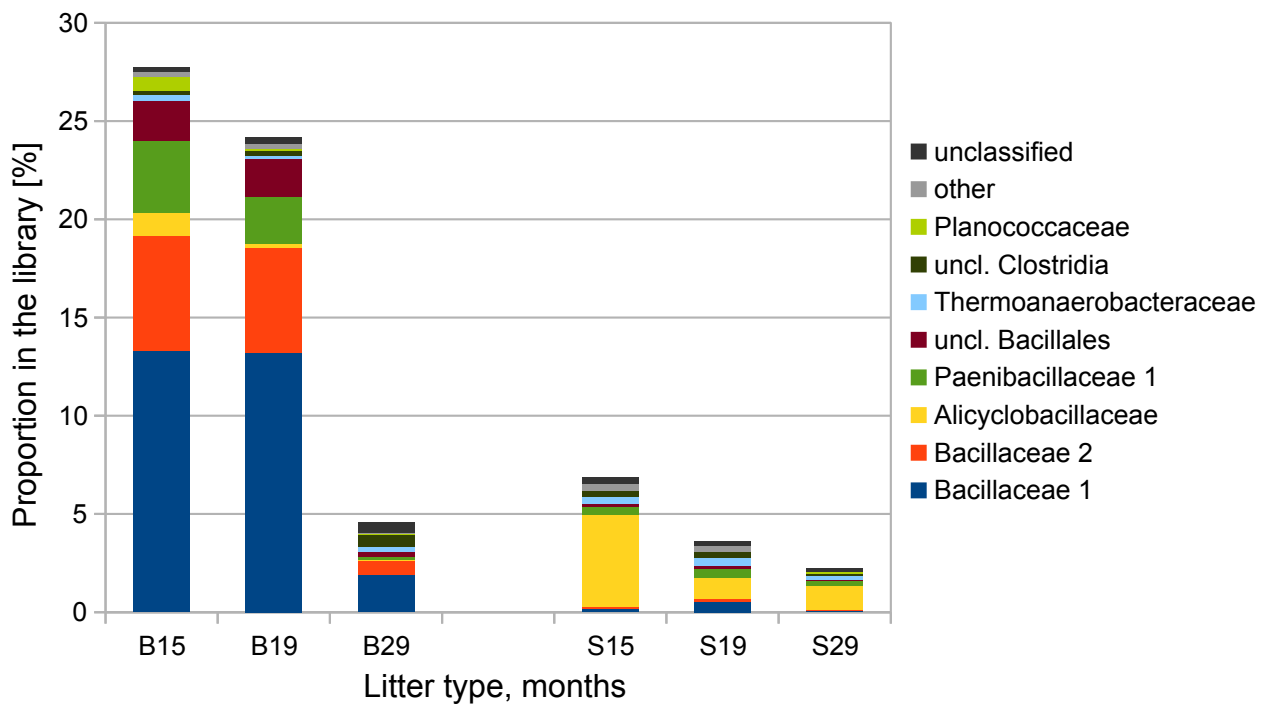
Supplementary Figure S3. Average proportions of groups at the family level within the phylum *Proteobacteria* in the bacterial 16S rRNA gene amplicon sequence libraries (n=3).



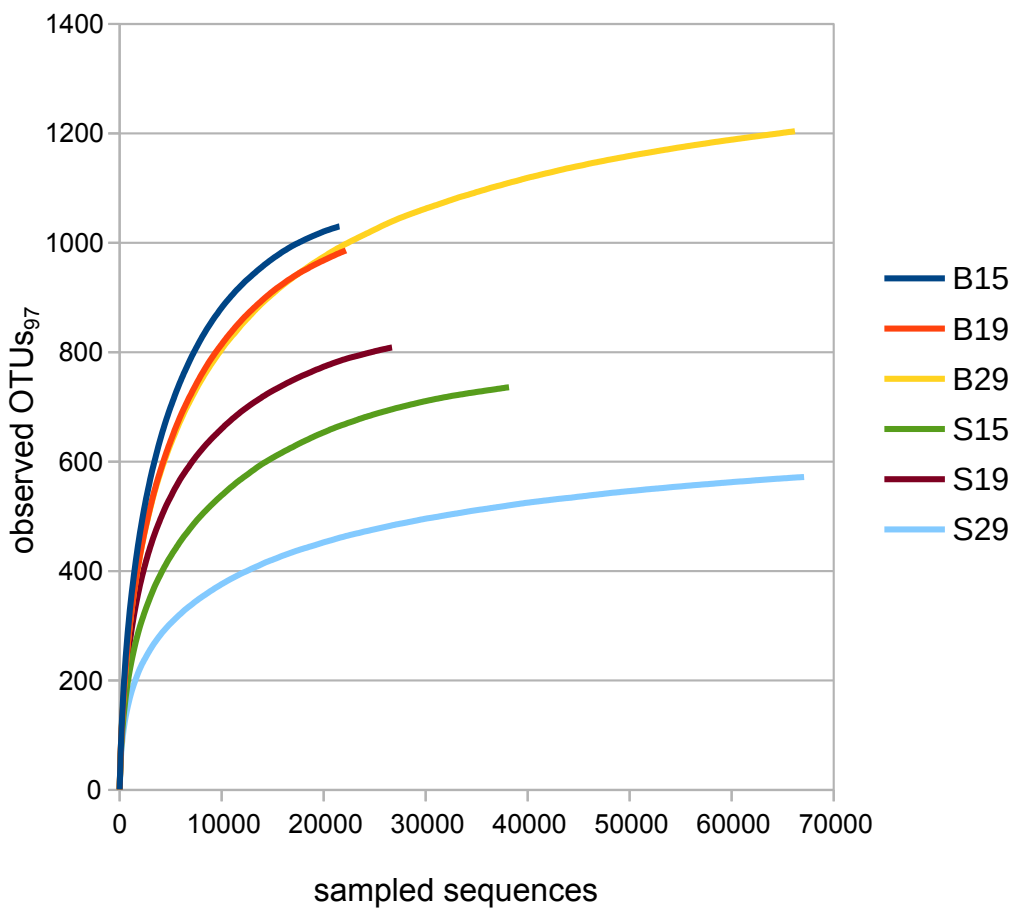
Supplementary Figure S4. Average proportions of groups at the family level within the phylum *Actinobacteria* in the bacterial 16S rRNA gene amplicon sequence libraries (n=3).



Supplementary Figure S5. Average proportions of groups at the family level within the phylum *Firmicutes* in the bacterial 16S rRNA gene amplicon sequence libraries (n=3).



Supplementary Figure S6. Rarefaction analysis of the sequence libraries (n=3).



Supplementary Table S1. Results of two-way ANOVA calculating the influence of factor of time and litter type (beech and spruce litter), and their interactions on mass loss (degrees of freedom (df), F and p value are indicated).

	Sum of sqrs	df	Mean square	F-value	p-value
Time:	9429	10	942.9	15.13	<0.001
Litter:	1070	1	1070	17.17	<0.001
Interaction:	3309	10	330.9	5.31	<0.001
Within:	2741	44	62.3		
Total:	16548	65			

Supplementary Table S2A. Results of t-test (degrees of freedom (Df), t-values and p-values) comparing total and water extractable content of selected elements and compounds, pH, dissolved organic carbon (DOC), aromaticity (A_{254}), humification index (HIX) and mass loss (average values and standard deviations are indicated) between beech and spruce litter in months 15, 19 and 29 of decomposition.

			Beech	Spruce	T-test		
					Df	t-value	p-value
Mass loss	[% of initial mass]	Average SD	49.69 20.18	75.92 8.278	14	-3.39	0.004
C_{tot}	[%]	Average SD	45.64 1.701	45.78 0.978	13	-0.23	0.823
N_{tot}	[%]	Average SD	1.289 0.336	1.812 0.12	13	-4.36	0.001
S_{tot}	[%]	Average SD	0.0653 0.0204	0.115 0.0179	13	-5.17	<0.001
P_{tot}	[mg.kg ⁻¹]	Average SD	523.9 160.1	829.7 51.24	10.04	-5.47	<0.001
Fe_{tot}	[mg.kg ⁻¹]	Average SD	466.7 231.7	1592 754.4	9.54	-4.27	0.002
Mn_{tot}	[mg.kg ⁻¹]	Average SD	699.1 381.7	203.2 49.87	8.27	4.26	0.003
Ca_{tot}	[mg.kg ⁻¹]	Average SD	6348 4000	2522 384.2	8.12	2.43	0.041
K_{tot}	[mg.kg ⁻¹]	Average SD	667.7 309.0	479.6 164.4	11.69	1.49	0.163
Al_{tot}	[mg.kg ⁻¹]	Average SD	1542 1447	1103 328.4	8.49	0.7	0.500
Mg_{tot}	[mg.kg ⁻¹]	Average SD	250.3 137.7	238.3 72.45	12.27	0.24	0.811
$PO_4^{3-}_w$	[μ mol.kg ⁻¹]	Average SD	5758 3968	9602 2608	15.55	-2.02	0.061
Fe_w	[μ mol.kg ⁻¹]	Average SD	207.1 95.48	386.0 106.9	15.96	-3.44	0.003
Mn_w	[μ mol.kg ⁻¹]	Average SD	2175 2045	638.2 375.1	8.38	1.87	0.097
Ca^{2+}_w	[μ mol.kg ⁻¹]	Average SD	11744 8737	5381 2007	8.60	1.68	0.129
K^+_w	[μ mol.kg ⁻¹]	Average SD	7124 3390	6387 1509	11.13	0.48	0.644

SO ₄ ²⁻ _w	[μmol.kg ⁻¹]	Average SD	1012 630.0	956.1 382.4	14.14	0.24	0.814
Al _w	[μmol.kg ⁻¹]	Average SD	1133 803.8	1157 476.4	10.79	-0.06	0.950
Mg ²⁺ _w	[μmol.kg ⁻¹]	Average SD	1733 1524	1229 580.5	9.51	0.76	0.464
Cl _w	[μmol.kg ⁻¹]	Average SD	1340 971.0	848.7 210.7	9.26	1.46	0.177
NH ₄ ⁺ _w	[μmol.kg ⁻¹]	Average SD	6586 3528	10311 5019	12.74	-1.32	0.212
NO ₃ ⁻ _w	[μmol.kg ⁻¹]	Average SD	343.0 398.8	343.3 330.6	15.76	0	0.999
F _w	[μmol.kg ⁻¹]	Average SD	1199 765.1	953.1 451.0	12.05	0.46	0.657
Oxalate _w	[μmol.kg ⁻¹]	Average SD	283.7 172.2	196.9 60.90	9.51	1.24	0.244
Acetate _w	[μmol.kg ⁻¹]	Average SD	3231 2875	1549 1501	12.58	1.12	0.284
Lactate _w	[μmol.kg ⁻¹]	Average SD	482.7 291.7	335.2 203.9	12.40	0.8	0.439
Formate _w	[μmol.kg ⁻¹]	Average SD	3138 2197	2914 2949	15.86	0.19	0.852
LMMOA _w	[μmol.kg ⁻¹]	Average SD	7657 4673	5260 3582	11.96	0.98	0.346
pH		Average SD	4.446 0.261	4.041 0.133	12.48	4.08	0.001
DOC	[mmol.kg ⁻¹]	Average SD	852.0 298.7	619.8 46.59	8.31	2.05	0.073
A ₂₅₄		Average SD	0.201 0.092	0.116 0.0125	8.29	2.34	0.047
HIX		Average SD	0.648 0.165	0.719 0.032	8.5	-1.07	0.316
Bacteria	[gene copies.ng DNA ⁻¹]	Average SD	37221 17719	37003 7704	13.87	0.03	0.977
Fungi	[gene copies.ng DNA ⁻¹]	Average SD	5700 3655	7112 3364	15.97	-0.77	0.451

Supplementary Table S2B. Results of t-test (degrees of freedom (Df), t-values and p-values) comparing the total content of selected elements, dissolved organic carbon (DOC), aromaticity (A_{254}) and humification index (HIX) in initial beech and spruce litter.

		Beech		Spruce		T-test		
		Average	SD	Average	SD	Df	t-value	p-value
N_{tot}	[%]	0.793	0.0714	1.527	0.040	4	-15.489	0.0001
C_{tot}	[%]	46.39	0.328	47.49	0.258	4	-4.583	0.010
S_{tot}	[%]	0.061	0.003	0.112	0.002	4	-24.99	<0.001
Mn_{tot}	[mg.kg ⁻¹]	1079	36.55	206.3	10.23	4	39.83	<0.001
Fe_{tot}	[mg.kg ⁻¹]	131.2	3.139	1438	310.9	4	-7.280	0.001
Ca_{tot}	[mg.kg ⁻¹]	8709	507.3	2042	2.840	4	22.77	<0.001
Mg_{tot}	[mg.kg ⁻¹]	649.4	11.74	232.2	12.91	4	41.41	<0.001
K_{tot}	[mg.kg ⁻¹]	2312	2.896	852.8	60.86	4	41.50	<0.001
Na_{tot}	[mg.kg ⁻¹]	152.4	0.240	64.96	7.547	4	20.06	<0.001
Al_{tot}	[mg.kg ⁻¹]	132.7	1.119	961.4	115.0	4	-12.48	<0.001
DOC	[mmol.kg ⁻¹]	9333	174.8	11458	575.5	4	-6.118	0.004
A_{254}		0.096	0.001	0.112	0.002	4	-9.260	<0.001
HIX		0.350	0.001	0.513	0.012	4	-21.95	<0.001

Supplementary Table S3. Chemical variables changes over the time (from the 1st to 29th month of decomposition). B_0 indicates average value for time 0 and b_1 indicates average percentual increase/decrease if the time from the beginning increase twice. P value indicates if the value of the precedent month is not significantly different.

	SL			BL		
	b_0	b_1	p-value	b_0	b_1	p-value
N_{tot}	1.37	3.5	0.001	0.73	7.6	< 0.001
C_{tot}	46.48	-0.2	0.553	46.22	-0.3	0.202
S_{tot}	0.1	1.8	0.176	0.08	-1.3	0.478
Ca_{tot}	1804	9.7	0.027	15424	-20.1	< 0.001
Fe_{tot}	643.9	6.4	0.281	81.89	36.5	< 0.001
Mn_{tot}	200.6	5	0.244	1488	-17.1	0.001
P_{tot}	2224	-13.7	< 0.001	435.7	5.7	0.024

Supplementary Table S4. Analysis of molecular variance (AMOVA) between composition of bacterial communities and subcommunities of individual phyla on beech and spruce litter in months 15, 19 and 29 of the decomposition. F - statistic and p - values are indicated (Df = 17).

	F-stat.	P-value
Bacterial communities	11.8	<0.001
<i>Acidobacteria</i>	5.93	<0.001
<i>Actinobacteria</i>	9.41	<0.001
<i>Bacteroidetes</i>	6.36	<0.001
<i>Firmicutes</i>	52.4	<0.001
<i>Patescibacteria</i>	3.98	<0.001
<i>Proteobacteria</i>	7.85	<0.001

Supplementary Table S5. Average frequencies (n = 3) of selected OTUs significantly contributing to separation of bacterial communities in the samples collected after 15 and 29 months.

A. The most abundant OTUs significantly separating the beech litter samples B15 and B29 (Metastats, p < 0.05).

OTU	B15	B19	B29	Phylum	Class	Order	Family	Genus
OTU1	4.030	5.903	12.883	Proteobacteria	Alphaproteobacteria	Rhizobiales	Xanthobacteraceae	uncl.
OTU12	1.337	1.177	3.363	Proteobacteria	Alphaproteobacteria	Rhizobiales	Beijerinckiaceae	Roseiarcus
OTU17	0.430	1.220	2.227	Actinobacteria	Acidimicrobiia	uncult.		
OTU26	0.113	0.260	1.443	Proteobacteria	Alphaproteobacteria	Rhizobiales	Xanthobacteraceae	uncult.
OTU35	0.203	0.747	1.290	Bacteroidetes	Bacteroidia	Chitinophagales	Chitinophagaceae	uncult.
OTU62	0.507	0.593	1.420	Proteobacteria	Gammaproteobacteria	JG36-TzT-191	uncl.	
OTU140	0.163	0.400	1.063	Proteobacteria	Alphaproteobacteria	Acetobacterales	Acetobacteraceae	uncult.
OTU76	0.087	0.220	0.823	Acidobacteria	Acidobacteriia	Solibacterales	Solibacteraceae Subgroup 3	Bryobacter
OTU172	0.027	0.400	0.667	Actinobacteria	Actinobacteria	Trebon clade	uncl.	uncl.
OTU82	0.100	0.170	0.657	Acidobacteria	Acidobacteriia	Solibacterales	Solibacteraceae Subgroup 3	Cand. Solibacter
OTU24	0.450	0.537	0.937	Actinobacteria	Acidimicrobiia	uncult.		
OTU93	0.007	0.077	0.447	WPS-2	uncl.			
OTU100	0.030	0.153	0.453	Proteobacteria	Deltaproteobacteria	Myxococcales	Polyangiaceae	Pajaroellobacter
OTU65	0.040	0.110	0.427	Actinobacteria	Thermoleophilia	Solirubrobacterales	Solirubrobacteraceae	uncult.
OTU51	0.367	0.220	0.747	Proteobacteria	Alphaproteobacteria	Caulobacterales	Caulobacteraceae	uncult.
OTU124	0.073	0.107	0.400	Acidobacteria	Acidobacteriia	Acidobacteriales	Koribacteraceae	Cand. Koribacter
OTU121	0.007	0.087	0.273	Acidobacteria	Acidobacteriia	Solibacterales	Solibacteraceae Subgroup 3	Bryobacter
OTU228	0.193	0.103	0.450	Proteobacteria	Alphaproteobacteria	Caulobacterales	Caulobacteraceae	uncl.
OTU63	0.063	0.237	0.307	Acidobacteria	Acidobacteriia	Solibacterales	Solibacteraceae Subgroup 3	Cand. Solibacter
OTU129	0.243	0.193	0.477	Proteobacteria	Alphaproteobacteria	Rhizobiales	Beijerinckiaceae	Roseiarcus
OTU41	0.027	0.233	0.260	Actinobacteria	Acidimicrobiia	uncult.		
OTU220	0.023	0.127	0.243	Proteobacteria	Alphaproteobacteria	Acetobacterales	Acetobacteraceae	uncult.
OTU149	0.000	0.117	0.207	Acidobacteria	Acidobacteriia	Acidobacteriales	Acidobacteriaceae Subgroup 1	Acidicapsa
OTU171	0.007	0.000	0.213	WPS-2	uncl.			
OTU233	0.023	0.037	0.223	Proteobacteria	Alphaproteobacteria	Rhizobiales	Xanthobacteraceae	uncult.
OTU135	0.000	0.010	0.180	Planctomycetes	Planctomycetacia	Isosphaerales	Isosphaeraceae	uncl.
OTU130	0.013	0.050	0.170	Acidobacteria	Acidobacteriia	Solibacterales	Solibacteraceae Subgroup 3	uncl.
OTU174	0.000	0.013	0.147	Proteobacteria	Gammaproteobacteria	uncl.		
OTU1513	0.007	0.000	0.153	Actinobacteria	Acidimicrobiia	uncult.		
OTU637	0.037	0.087	0.177	Proteobacteria	Alphaproteobacteria	Acetobacterales	Acetobacteraceae	uncult.
OTU178	0.003	0.123	0.143	Planctomycetes	Planctomycetacia	Isosphaerales	Isosphaeraceae	Aquisphaera
OTU103	0.000	0.190	0.133	Acidobacteria	Acidobacteriia	Subgroup 2	uncl.	
OTU97	0.037	0.203	0.167	Actinobacteria	Actinobacteria	Trebon clade	uncl.	uncl.
OTU289	0.003	0.023	0.127	Acidobacteria	Acidobacteriia	Solibacterales	Solibacteraceae Subgroup 3	Bryobacter
OTU269	0.007	0.120	0.130	Proteobacteria	Alphaproteobacteria	Elsterales	uncult.	
OTU247	0.020	0.150	0.143	Acidobacteria	Acidobacteriia	Acidobacteriales	Acidobacteriaceae Subgroup 1	Occallatibacter
OTU184	0.000	0.023	0.123	Acidobacteria	Acidobacteriia	Subgroup 2		
OTU518	0.020	0.133	0.140	Actinobacteria	Acidimicrobiia	uncult.		
OTU344	0.043	0.060	0.153	Proteobacteria	Alphaproteobacteria	Acetobacterales	Acetobacteraceae	uncult.
OTU290	0.000	0.040	0.100	Bacteroidetes	Bacteroidia	Sphingobacteriales	Sphingobacteriaceae	Mucilagininibacter

OTU71	0.117	0.017	0.017	Proteobacteria	Alphaproteobacteria	Caulobacterales	Caulobacteraceae	uncult.
OTU306	0.120	0.157	0.007	Patescibacteria	Saccharimonadia	Saccharimonadales	uncl.	
OTU529	0.153	0.080	0.033	Proteobacteria	Alphaproteobacteria	Rickettsiales	SM2D12	
OTU482	0.130	0.230	0.000	Proteobacteria	Gammaproteobacteria	Enterobacteriales	Enterobacteriaceae	Escherichia-Shigella
OTU54	0.173	0.330	0.027	Bacteroidetes	Bacteroidia	Sphingobacteriales	Sphingobacteriaceae	Mucilaginibacter
OTU243	0.217	0.163	0.010	Bacteroidetes	Bacteroidia	Chitinophagales	Chitinophagaceae	uncult.
OTU163	0.243	0.073	0.033	Proteobacteria	Alphaproteobacteria	Rhodospirillales	uncult.	
OTU267	0.223	0.040	0.003	Acidobacteria	Acidobacteriia	Acidobacteriales	Acidobacteriaceae Subgroup 1	Terriglobus
OTU177	0.253	0.097	0.030	Verrucomicrobia	Verrucomicrobiae	Methylacidiphilales	Methylacidiphilaceae	uncult.
OTU203	0.320	0.210	0.087	Verrucomicrobia	Verrucomicrobiae	Chthoniobacterales	Chthoniobacteraceae	Chthoniobacter
OTU78	0.477	0.903	0.207	Bacteroidetes	Bacteroidia	Sphingobacteriales	Sphingobacteriaceae	Mucilaginibacter
OTU37	0.593	0.263	0.303	WPS-2	uncl.			
OTU49	0.387	0.080	0.090	Acidobacteria	Acidobacteriia	Acidobacteriales	Acidobacteriaceae Subgroup 1	Granulicella
OTU57	0.367	0.090	0.060	Proteobacteria	Alphaproteobacteria	Sphingomonadales	Sphingomonadaceae	Sphingomonas
OTU6	0.580	0.490	0.157	Actinobacteria	Actinobacteria	Corynebacteriales	Mycobacteriaceae	Mycobacterium
OTU86	0.710	0.050	0.220	Proteobacteria	Alphaproteobacteria	Sphingomonadales	Sphingomonadaceae	Novosphingobium
OTU2012	0.673	0.540	0.173	Actinobacteria	Actinobacteria	Micrococcales	Microbacteriaceae	uncl.
OTU55	0.557	0.570	0.053	Verrucomicrobia	Verrucomicrobiae	Pedosphaerales	Pedosphaeraceae	uncl.
OTU2	22.287	18.457	3.007	Firmicutes	Bacilli	Bacillales	Bacillaceae	Bacillus

B. The most abundant OTUs significantly separating the spruce litter samples S15 and S29 (Metastats, $p < 0.05$).

OTU	S15	S19	S29	Phylum	Class	Order	Family	Genus
OTU3	2.227	2.773	6.557	Proteobacteria	Alphaproteobacteria	Acetobacterales	Acetobacteraceae	uncult.
OTU1	1.927	3.357	3.540	Proteobacteria	Alphaproteobacteria	Rhizobiales	Xanthobacteraceae	uncl.
OTU10	1.007	1.987	2.430	Acidobacteria	Acidobacteriia	Acidobacteriales	Acidobacteriaceae Subgroup 1	Granulicella
OTU83	0.570	0.993	1.587	Proteobacteria	Gammaproteobacteria	Betaproteobacteriales	Burkholderiaceae	Burkholderia-Caballeronia-Paraburkholderia
OTU22	0.430	0.287	1.413	Acidobacteria	Acidobacteriia	Solibacterales	Solibacteraceae Subgroup 3	Bryobacter
OTU36	0.173	0.413	0.807	Proteobacteria	Gammaproteobacteria	Betaproteobacteriales	Burkholderiaceae	Burkholderia-Caballeronia-Paraburkholderia
OTU522	0.300	0.210	0.827	Acidobacteria	Acidobacteriia	Solibacterales	Solibacteraceae Subgroup 3	Bryobacter
OTU64	0.217	0.373	0.660	Acidobacteria	Acidobacteriia	Acidobacteriales	Acidobacteriaceae Subgroup 1	Acidipila
OTU61	0.147	0.217	0.510	Proteobacteria	Alphaproteobacteria	Rhizobiales	Beijerinckiaceae	uncult.
OTU148	0.007	0.053	0.323	Proteobacteria	Gammaproteobacteria	Betaproteobacteriales	Burkholderiaceae	Burkholderia-Caballeronia-Paraburkholderia
OTU1768	0.333	0.127	0.637	Actinobacteria	Thermoleophilia	Solirubrobacterales	Solirubrobacteraceae	Conexibacter
OTU88	0.200	0.077	0.500	Proteobacteria	Alphaproteobacteria	Acetobacterales	Acetobacteraceae	Acidiphilium
OTU75	0.207	0.093	0.490	Actinobacteria	Acidimicrobiia	IMCC26256	uncl.	uncl.
OTU46	0.167	0.230	0.447	Proteobacteria	Alphaproteobacteria	Rhizobiales	Beijerinckiaceae	Methylocapsa
OTU156	0.043	0.160	0.213	Acidobacteria	Acidobacteriia	Acidobacteriales	Acidobacteriaceae Subgroup 1	Acidipila
OTU172	0.230	0.110	0.353	Actinobacteria	Actinobacteria	Trebon clade	uncl.	uncl.
OTU219	0.017	0.030	0.127	Acidobacteria	Acidobacteriia	Acidobacteriales	Acidobacteriaceae Subgroup 1	uncl.
OTU543	0.037	0.020	0.143	Acidobacteria	Acidobacteriia	Acidobacteriales	Acidobacteriaceae Subgroup 1	uncl.
OTU769	0.123	0.147	0.020	Patescibacteria	Saccharimonadia	Saccharimonadales	uncl.	uncl.
OTU1674	0.187	0.577	0.077	Proteobacteria	Alphaproteobacteria	Micropepsales	Micropepsaceae	uncult.
OTU432	0.130	0.030	0.017	Actinobacteria	Thermoleophilia	Solirubrobacterales	67-14	uncl.
OTU128	0.187	0.470	0.073	Patescibacteria	Saccharimonadia	Saccharimonadales	uncl.	uncl.
OTU703	0.133	0.060	0.007	Patescibacteria	Saccharimonadia	Saccharimonadales	uncl.	uncl.
OTU482	0.127	0.160	0.000	Proteobacteria	Gammaproteobacteria	Enterobacteriales	Enterobacteriaceae	Escherichia-Shigella
OTU147	0.263	0.180	0.117	Actinobacteria	Acidimicrobiia	IMCC26256	uncl.	uncl.
OTU351	0.210	0.073	0.047	Firmicutes	Bacilli	Bacillales	Alicyclobacillaceae	Alicyclobacillus
OTU278	0.410	0.137	0.150	Actinobacteria	Thermoleophilia	Solirubrobacterales	Solirubrobacteraceae	Conexibacter
OTU296	0.380	0.110	0.093	Actinobacteria	Actinobacteria	Corynebacteriales	Mycobacteriaceae	Mycobacterium
OTU32	1.227	0.700	0.830	Actinobacteria	Actinobacteria	Trebon clade	uncl.	uncl.
OTU68	0.617	0.637	0.177	Proteobacteria	Alphaproteobacteria	Micropepsales	Micropepsaceae	uncult.
OTU19	1.403	1.130	0.887	Acidobacteria	Acidobacteriia	Acidobacteriales	Acidobacteriaceae Subgroup 1	Granulicella
OTU72	0.863	0.717	0.047	Patescibacteria	Saccharimonadia	Saccharimonadales	uncl.	uncl.
OTU167	1.633	0.590	0.643	Actinobacteria	Thermoleophilia	Solirubrobacterales	Solirubrobacteraceae	Conexibacter
OTU8	5.317	1.053	1.057	Firmicutes	Bacilli	Bacillales	Alicyclobacillaceae	Alicyclobacillus

Supplementary Table S6. Statistical correlations (coefficient of determination (R^2) and p - values) of total and water extractable content of selected elements and compounds, pH, dissolved organic carbon (DOC), aromaticity (A_{254}), humification index (HIX), abundance of bacteria, fungi and bacterial diversity (Bact. div) with bacterial communities on beech and spruce litter after months 15, 19 and 29 of decomposition (number of permutations = 99999).

	C_{tot}	N_{tot}	S_{tot}	P_{tot}	Fe_{tot}	Mn_{tot}	Ca_{tot}	K_{tot}	Al_{tot}	Mg_{tot}
R^2	0.310	0.473	0.591	0.629	0.535	0.601	0.476	0.422	0.476	0.338
p-value	0.062	0.008	0.002	0.001	0.004	0.002	0.009	0.017	0.006	0.046

	$PO_4^{3-}_w$	Fe_w	Mn_w	Ca^{2+}_w	K^+_w	$SO_4^{2-}_w$	Mg^{2+}_w	Cl^-_w	$NH_4^+_w$	$NO_3^-_w$
R^2	0.408	0.589	0.370	0.493	0.602	0.189	0.569	0.084	0.172	0.226
p-value	0.016	0.001	0.032	0.007	0.001	0.207	0.002	0.526	0.242	0.142

	Oxalate _w	Acetate _w	Lactate _w	Formate _w	LMMOA _w
R^2	0.613	0.460	0.356	0.017	0.195
p-value	0.001	0.011	0.037	0.883	0.198

	pH	DOC	A_{254}	HIX	Bacteria	Fungi	Bact. div.	Mass loss
R^2	0.542	0.702	0.638	0.421	0.301	0.091	0.578	0.376
p-value	0.003	< 0.001	0.001	0.015	0.069	0.487	0.002	0.030

**Paper IV: Litter traits and rainfall reduction alter microbial
litter decomposers: the evidence from three Mediterranean
forests**

RESEARCH ARTICLE

Litter traits and rainfall reduction alter microbial litter decomposers: the evidence from three Mediterranean forests

S. Pereira¹, A. Burešová^{2,3,4}, J. Kopecký⁵, P. Mádrová⁵, A. Aupic-Samain¹, C. Fernandez¹, V. Baldy^{1,*} and M. Sagova-Mareckova⁵

¹Aix Marseille Univ, Avignon Université, CNRS, IRD, IMBE UMR 7263, Marseille, France, ²Department of Ecology, Faculty of Science, Charles University in Prague, Vinicna 7, Prague, Czech Republic, ³Ecologie Microbienne, Université Claude Bernard Lyon 1, UMR CNRS 5557, INRA 1418, Villeurbanne, France, ⁴Laboratory for Diagnostics and Epidemiology of Microorganisms, Crop Research Institute, Drnovska 507, CZ-16106 Prague 6, Ruzyně, Czech Republic and ⁵Czech University of Life Sciences, Faculty of Agrobiology, Food and Natural Resources, Department of Microbiology, Nutrition and Dietetics, Kamýcká 129, 165 00 Praha 6 - Suchbát, Czech Republic

*Corresponding author: Aix Marseille Univ, Avignon Université, CNRS, IRD, IMBE UMR 7263, Marseille, France. E-mail: virginie.baldy@imbe.fr

One sentence summary: This study addresses the impact of climate change, forest sites and tree species on microbial communities and litter decomposition process in three Mediterranean forests.

Editor: Taina Pennanen

ABSTRACT

The objective of the study was to evaluate changes in microbial communities with the predicted arrival of new species to Mediterranean forests under projected intensification of water stress conditions. For that, litter from three Mediterranean forests dominated respectively by *Quercus pubescens* Willd., *Quercus ilex* L. and *Pinus halepensis* Mill. were collected, and placed to their 'home' forest but also to the two other forests under natural and amplified drought conditions (i.e. rainfall reduction of 30%). Quantitative PCR showed that overall, actinobacteria and total bacteria were more abundant in *Q. pubescens* and *Q. ilex* than in *P. halepensis* litter. However, the abundance of both groups was dependent on the forest sites: placement of allochthonous litter to *Q. pubescens* and *P. halepensis* forests (i.e. *P. halepensis* and *Q. pubescens*, respectively) increased bacterial and fungal abundances, while no effect was observed in *Q. ilex* forest. *P. halepensis* litter in *Q. pubescens* and *Q. ilex* forests significantly reduced actinobacteria (A/F) and total bacteria (B/F) to fungi ratios. The reduction of rainfall did not influence actinobacteria and bacteria but caused an increase of fungi. As a result, a reduction of A/F ratio is expected with the plant community change towards the dominance of spreading *P. halepensis* under amplified drought conditions.

Keywords: litter decomposition; fungi; actinobacteria; Mediterranean forest; climate change

INTRODUCTION

Microorganisms are key actors in nutrient cycling and carbon turnover during litter decomposition (Gessner et al. 2010;

Garcia-Pausas and Paterson 2011). At a global scale, it is estimated that the soil C coming from soil microbial biomass is about 16.7 Pg C, which represents approximately 2.3–2.4% of total organic C found in soil in the top 30 cm (Xu, Thornton

Received: 15 December 2018; Accepted: 23 October 2019

© FEMS 2019. All rights reserved. For permissions, please e-mail: journals.permissions@oup.com

and Post 2013). Heterotrophic respiration resulting from microbial litter decomposing activity can account for 10–90% of the CO₂ efflux from soils and substantially affect the atmospheric CO₂ concentration (Manzoni et al. 2012). However, annual reduction of rainfall by up to 30% predicted for the Mediterranean basin (Giorgi and Lionello 2008; IPCC 2014; Hertig and Trambly 2017) may significantly impact microbial abundance and structure, and thus, also the overall C dynamics (Wardle and Putten 2002).

Studies have already demonstrated shifts in plant community composition in response to the changed climatic conditions (Morales et al. 2007; Bertrand et al. 2011; Guiot and Cramer 2016). In southern France, dominating downy oak (*Quercus pubescens* Willd.) is expected to be replaced by more drought tolerant species: the sclerophylls' evergreen holm oak (*Quercus ilex* L.) and Aleppo pine (*Pinus halepensis* Mill.) (Barbero et al. 1990; Fortunel et al. 2009). Additionally, the increase of water stress may induce the synthesis of plant secondary metabolites (e.g. phenolics) known for their phytotoxic activities and anti-appetizing effects, which limit leaf consumption by fauna (Chomel et al. 2014). This investment in defence mechanisms over primary metabolic processes may result on the one hand to the decrease of primary productivity (Ogaya and Peñuelas 2007) and thus litter inputs, and on the other hand, in the reduction of litter quality through the increase of recalcitrant organic compounds (i.e. lignin, wax, polyphenolics) (Ormeño et al. 2006; Hättenschwiler and Jørgensen 2010; Sagova-Mareckova et al. 2011). Moreover, the reduction of moisture level may induce physiological stress and limit dispersal of microorganisms, enzymatic activities and substrate diffusion (Bouskill et al. 2013). Thus, the reduction of moisture levels and aboveground litter quality and quantity may impose new community dynamics belowground (Lunghini et al. 2013; Cleveland et al. 2014) and lead to a shift of soil microbial communities to more drought tolerant species, capable of using recalcitrant C sources and resistant to desiccation (Yuste et al. 2011; Peñuelas et al. 2012; Allison et al. 2013). Actinobacteria are known to thrive in low resource environments (Fierer, Bradford and Jackson 2007) and low soil moisture conditions (Yuste et al. 2011; De Vries and Shade 2013; Acosta-Martinez et al. 2014) reaching high abundance in arid soils (Okoro et al. 2009). They are well protected by a strong, thick interlinked peptidoglycan cell wall, which explains their high resistance to low osmotic potential conditions (Davet 2004). They produce enzymes able to degrade a wide range of biopolymers, whose building blocks including aromatic compounds (McCarthy and Williams 1992) have a vital role in organic matter turnover and humus formations (Anandan, Dharumadurai and Manogaran 2016). They produce a variety of secondary metabolites (Anandan et al. 2016), through which they interact with other microbial groups (Lewin et al. 2016). However, little is known about how microbial communities and actinobacteria in particular, would be affected by future reduction of rainfall, both directly by decrease of moisture level and indirectly through the plant species shift. In general, litter types sharing a common history with local microbial communities (autochthonous) have faster decomposition rates than litter types coming from distant (allochthonous) habitats (Gholz et al. 2000; Strickland et al. 2009). Consequently, changes in biochemical composition of local litter with the arrival of new species may constrain microbial activity and impact negatively litter decomposition (Schimel, Balsler and Wallenstein 2007).

In here, we examine how reduction of rainfall and change in plant species may affect belowground microbial community's (actinobacteria, fungi and total bacteria) abundance and

structure and consequently also the litter decomposition process. For that, we performed a litter transplanting experiment between three main Mediterranean forests (*Q. pubescens* Willd., *Q. ilex* L., and *P. halepensis* Mill.) occurring in Southeast of France, under natural and amplified drought conditions for simulating the 30% rainfall reduction. We hypothesised that the arrival of new litter under amplified drought conditions will have a negative impact on microbial abundance and litter decomposition.

MATERIALS AND METHODS

Sites description

This study was conducted at the three forest sites in the Mediterranean region in southern France: the *Q. pubescens* forest at Oak Observatory at the 'Observatoire de Haute Provence' (O₃HP; Santonja et al. 2015a), the *Q. ilex* forest at Puéchabon (Limousin et al. 2008) and the mixed *P. halepensis* forest at Font-Blanche (Table 1). During the study period, the mean annual temperature was 12.1°C, 13.7°C and 14.0°C, and the cumulative annual precipitation was 609 mm, 794 mm and 632 mm, respectively (Table 1; Supplementary Figure 1, Supporting Information). There were no significant differences between sites in the mean annual temperature and cumulative annual precipitation during the study period (One-way ANOVA, $P < 0.05$). Each site included a control plot (natural drought—ND) and a rain exclusion plot (amplified drought—AD) to mimic the future reduction of rainfall predicted by the climatic model for the Mediterranean Region (about -30% yearly; Table 1 and Supplementary Figure 2, Supporting Information).

Experimental design and sample processing

In 2014, senescent leaves were collected in the control plot of the three forests. For that, litter traps were used during the abscission period that occurred from October to November for the broadleaves (*Q. ilex* and *Q. pubescens*) and from June to September for the needles (*P. halepensis*). Leaves and needles were air dried and stored at room temperature in paper boxes until the beginning of the experiment.

Litter decomposition was assessed by using the litter bag method (Swift et al. 1979). Four-mm mesh litter bags (20 × 20 cm) containing 10 g (air-dried) of the senescent material were used to perform the experiment. Litter transplants were made between each site for the three species considered, i.e. a litter bag containing the litter of each species placed on each forest site, under two drought conditions: natural (ND) and amplified (AD) (see Supplementary Figure 3, Supporting Information).

Thus, the experiment consisted in 18 modalities corresponding to the 3 forests *Q. ilex*, *Q. pubescens* and *P. halepensis* × 3 plant species (*Q. ilex*, *Q. pubescens* and *P. halepensis*) × 2 drought conditions (ND and AD). In total, 126 litter bags (18 modalities × 1 sampling date × 7 replicates) were analysed. Litter bags were placed perpendicularly to the gutters system in Aleppo pine and holm oak forests and under the rain exclusion device in the downy oak forest, by using a transect in blocks (7 columns × 6 lines), equidistantly one from each other (1 m distance between the 7 columns and 0.6 m between the 6 lines). Transects were E-W oriented. They were disposed in the ground floor after the removal of litter layer and fixed to the soil with galvanised nails to prevent movement by animals or wind. Litter layer was then replaced over the litterbags.

Litter bags were retrieved after 1 year (December 2015). Litterbags were placed in zipped plastic bags to prevent the loss of

Table 1. Main characteristics of the three forest sites selected for this study (for the study period: December 2014 to December 2015).

Forests	<i>Q. pubescens</i> Willd. Oak Observatory at the Observatoire de Haute Provence	<i>Q. ilex</i> L. Puéchabon	Mixed <i>P. halepensis</i> Mill. Font-Blanche
Location	43° 56' 115" N, 050 42' 642" E	43° 44' 29"N, 3°35' 45"E	43° 14'27" N, 5°40'45" E
Altitude a.s.l. (m)	650	270	425
MAT (Mean Annual Temperature) (°C)	12.25	13.71	14.01
MAP (Mean Annual Precipitation) (mm)	609	794	632
Soil type	pierric calcosol	rhodo-chromic luvisol	leptosol
Soil texture	clay	clay loam	clay
Soil pH	6.76	6.6	6.8
Surface rocks cover (%)	23	75	50
Dominant tree species	<i>Q. pubescens</i> Willd.	<i>Q. ilex</i> L.	mixed <i>P. halepensis</i> Mill./ <i>Q. ilex</i> L.
Other dominant plant species	<i>Acer monspessulanum</i> L. <i>Cotinus coggygria</i> Scop.	<i>Buxus sempervirens</i> L. <i>Phyllirea latifolia</i> L. <i>Pistacia terebinthus</i> L. <i>Juniperus oxycedrus</i> L.	<i>Quercus coccifera</i> L. <i>Phyllirea latifolia</i> L.
Tree density (stems/ ha)	3503	4500	3368
Forest structure	even-age (70 years)	even-age (74 years)	uneven-age (61 years)
Rain exclusion system dimensions (m ²)	300	140	625
Rain exclusion (%)	33	30	30

biological material. In the laboratory, the soil and other debris were removed from the litter bags. Then, they were freeze-dried (Lyovac GT2) for 72 hours and the remaining dry mass (%) was calculated. A 1 g of dry mass aliquote was collected, grounded to powder (Retsch® MM400, 30 Hz during 30s) and kept at -20°C for posteriori microbial DNA analysis.

Initial litter chemical characteristics

At the beginning of the experiment, 5 replicates from each leaf species collected from trees in control plots were grounded to powder (Retsch® MM400, 30 Hz during 30s). Carbon (C) and nitrogen (N) were determined by thermal combustion on a Flash EA 1112 series C/N elemental analyser (Thermo-Scientific, U.S.A). Phosphorus (P) and cations (Ca, K, Mg and Na) were extracted from 80 mg of ground litter sample with 8 ml of nitric acid and 2 ml of H₂O₂ at 175°C for 40 min using a microwave digestion system (Ethos One, Milestone SRL, Sorisole, Italy). After the mineralisation, each sample was adjusted to 50 ml with demineralised water. Phosphorus concentration was measured at 720 nm using a microplate reader (Victor, Perkin Elmer, Waltham, MA, USA). Cations were determined using an atom absorption spectrometer (AAS, iCE 3000 series, Thermo-Scientific, China). Leaf structural compounds (lignin, cellulose and hemicellulose) and water-soluble compounds (WSC) concentrations were determined according to the van Soest extraction protocol (Van Soest and Wine 1967), using a fiber analyser (Fibersac 24; Ankom®, Macedon, NJ, USA). Total phenolic concentrations were measured by colorimetry according to the method of Peñuelas et al. (1996) using gallic acid as standard. Aqueous extracts were made by dissolving 0.25 g of litter powder in 20 ml of 70% aqueous methanol solution with shaking for 1 hour and filtered (0.45 µm). A total of 25 ml of extracts obtained were then mixed with 0.25 ml of Folin-Ciocalteu reagent (Folin and Denis 1915), 0.5 ml of saturated aqueous Na₂CO₃ (to stabilize the colorimetric reaction) and 4 ml of distilled water. After 60 min, the reaction was completed and the concentration of phenolics was measured at 765 nm using a UV / Vis spectrophotometer (Thermoscientific, U.S.A.).

To determine the water holding capacity (WHC), twenty-one freshly abscised leaves (3 species x 5 replicates) were soaked in distilled water for 24 hours, drained and weighted (wet weight). The dry weight was measured after drying the samples for 48 hours at 60°C. Water holding capacity (in %) was calculated according to the formula: (wet weight/dry weight) × 100 (Santonja et al. 2015b). Specific leaf area (SLA) was determined by using the Image J software (<https://imagej.nih.gov/ij/>, MA, USA). Specific leaf area was calculated as the ratio between leaf area and leaf dry weight.

DNA extraction

Environmental DNA from leaf litter samples was extracted with the NucleoSpin® soil kit (Macherey-Nagel, Düren, Germany), following the standard protocol with a slight adjustment. In brief, approximately 250 mg of dry litter was added to the NucleoSpin Bead tubes. Lysis conditions were performed by using buffer SL1 (700 µl, vortex for 5 min, room temperature, 11 000 x g for 2 min), and buffer SL3 (150µl, vortex 5 min, 0–4°C, 14 000 g for 1 min). This procedure was repeated twice using the same sample to optimise the DNA extraction. The filtration of the supernatant was performed in the NucleoSpin Inhibitor Removal Column followed by 11 000 x g for 1 min. DNA binding was done in the Nucleo Spin Soil column after adding 250 µl of Buffer SB to the supernatant followed by 11 000 x g for 1 min. A series of successive DNA washing was performed: 500 µl buffer SB (11 000 x g, 3 sec), 550 µl buffer SW1 (11 000 x g, 3 sec), 700 µl SW2 (2 sec vortex, 11 000 x g, 3 sec). At each step, flow-through were discarded. Finally, DNA was eluted in 30 µl of Buffer SE followed by incubation at room temperature for 1 min and 11 000 x g for 30 seconds and kept at -20°C until further analysis. DNA quantification was performed in the ND-1000 spectrophotometer (Nanodrop Technology, Wilmington, DE).

Quantitative real-time PCR analysis

Abundances of total bacteria, actinobacteria and fungi were assessed using a quantitative real-time PCR analysis (qPCR)

Table 2. Initial leaf litter quality of each litter species: *Q. pubescens*, *Q. ilex* and *P. halepensis*, the values are mean \pm SE (n = 5) and the results of the one-way ANOVA to test differences between initial litter species are indicated (* P < 0.05, ** P < 0.01, *** P < 0.001 and different letters denote significant differences among species with a>b>c.)

	df	<i>Q. pubescens</i>		<i>Q. ilex</i>		<i>P. halepensis</i>		F-ratio	
Carbon	2	462.6 \pm 2.65	c	478.1 \pm 1.4	b	516.1 \pm 1.6	a	198.80	***
Nitrogen	2	6.4 \pm 0.2	b	9.6 \pm 0.2	a	5.4 \pm 0.1	c	146.30	***
Phosphorus	2	1.9 \pm 0.1	b	3.5 \pm 0.2	a	1.6 \pm 0.1	b	64.6	***
Calcium	2	32.9 \pm 0.8	a	25.1 \pm 0.6	b	18.4 \pm 0.2	c	168.1	***
Potassium	2	0.8 \pm 0.01	c	1.8 \pm 0.1	a	0.95 \pm 0.01	b	370.7	***
Magnesium	2	2.8 \pm 0.2	a	1.4 \pm 0.01	b	1.5 \pm 0.02	c	104.8	***
Sodium	2	0.04 \pm 0.00	b	0.11 \pm 0.00	a	0.11 \pm 0.00	a	149.6	***
Total phenolics	2	40.8 \pm 2.6	a	32.9 \pm 1.58	b	38.6 \pm 1.2	ab	4.7	*
Lignin	2	273.3 \pm 9.0	b	337.4 \pm 5.5	a	302.6 \pm 10.6	b	13.8	***
Cellulose	2	159.1 \pm 8.0	b	205 \pm 4.2	a	150.8 \pm 12.9	b	10.3	**
Hemicellulose	2	274.2 \pm 22.5	a	270.0 \pm 16.2	ab	206.6 \pm 10.4	b	4.7	*
Water-soluble compounds	2	293.4 \pm 12.1	b	187.6 \pm 10.2	c	340.0 \pm 7.1	a	60.9	***
Specific leaf area	2	133.1 \pm 0.4	a	51.5 \pm 0.9	c	83.5 \pm 2.2	b	690.7	***
Water holding capacity	2	146.9 \pm 1.0	a	137.2 \pm 1.0	b	113.9 \pm 1.03	c	285.5	***

method. Microbial abundance was quantified as copy number of a target gene. Partial 16S rRNA gene sequences were amplified from the total bacteria using primers COM1 (5'-CAG CAGCCGCGTAATAC-3') and 769R (5'-ATCCTGTTGMTMCCC CRC-3', annealing temperature 59°C) (Dorn-In et al. 2015), and from actinobacteria using primers S-P-Acti-1154-a-S-19 (5'-GRD ACYGCCGGGTAACT-3' annealing temperature 59°C) and S-P-Acti-1339-a-A-18 (5'-TCWGCATTACTAGCGAC-3') (Pfeiffer et al. 2014). Partial 18S rRNA genes from fungi were amplified with primers FF390 (5'-CGATAACGAACGAGACCT-3') and FR1 (5'-A ICCATTCAATCGTAIT-3', annealing temperature 50°C) (Vainio and Hantula 2000). All PCR reactions were done 15 μ l total volume containing 1 \times SYBR® Green Gotaq PCR Master Mix (Promega), primers at 600 nM for total bacteria and fungi, and 200 nM for actinobacteria, and 0.2–2 ng environmental DNA. The cycling parameters were: 10 min at 95°C followed by 45 cycles at 95°C (15 sec), 59°C (30 sec), 72°C (30 sec). Melting curves were recorded to ensure qPCR specificity, and gel electrophoresis analyses were performed to confirm the expected size of amplified products. All qPCR reactions were run in triplicate on StepOne Plus Real-Time PCR System (Applied Biosystems, Foster City, CA). To quantify the target gene copy numbers, standard dilution curves of known concentrations of previously cloned standards of the target genes were determined. Baseline and threshold calculations and data analysis were performed with the StepOne v. 2.2.2 software.

The primer pair recommended by Dorn-In et al. (2015) for amplification of bacterial 16S rRNA gene fragment from plant samples, Com1/769R (Rastogi et al. 2010; Fredriksson, Hermansson and Wilén 2013) was used for quantitative real-time PCR analysis of the total bacteria. The primer pair does not amplify 16 rRNA genes from chloroplasts, however, consequently also its coverage of the domain Bacteria is incomplete. In silico analysis using TestPrime 1.0 (Klindworth et al. 2013) against the Silva database, release 132 (www.arb-silva.de), showed 75% overall coverage of Bacteria with varying representation of the phyla, e.g. 88% Proteobacteria, 81.9% Firmicutes, 93.6% Bacteroidetes, but only 56.2% Actinobacteria, 20.5% Acidobacteria and 17.5% Verrucomicrobia. Therefore, the results can be used as a proxy of bacterial abundance when comparing between samples, but not to compare with qPCR quantification of individual bacterial phyla or lower taxonomic units using group-specific primers.

Statistical analysis

All statistical analyses were performed in R v.3.1.3 software (R Development Core Team 2017). One-way analysis of variance (ANOVA) was used to determine differences between the initial parameters of litter plant species and between forest sites for each litter species and microbial group. Three-way ANOVA was also used to test the effects of forest sites (S), litter species (L) and drought treatment (D) on litter mass loss and microbial abundance (total bacteria (B), actinobacteria (A), fungi (F) and the respective B/F and A/F ratios, followed by post-hoc Tukey tests. Microbial abundance was log-transformed to fit the assumption of normality and homoscedasticity.

RESULTS

Initial litter composition

Initial litter characteristics varied significantly among species (Table 2, One-way ANOVA, P < 0.05). *Quercus ilex* showed a significantly higher N (9.62 mg g⁻¹) and P (3.48 mg g⁻¹) contents than the two other species, particularly *P. halepensis* (5.36 mg g⁻¹ and 1.56 mg g⁻¹), which resulted in a lowest C/N and C/P ratio for *Q. ilex* and highest ratios for *P. halepensis* (Table 2). Regarding the cations, *Q. pubescens* showed significantly higher content of Ca (32.90 mg g⁻¹) and Mg (2.83 mg g⁻¹), and lower content of K (0.84 mg g⁻¹) and Na (0.04 mg g⁻¹) than the two other species. Concerning the structural compounds of the leaves, *Q. ilex* had higher lignin (337.38 mg g⁻¹) and cellulose content (204.99 mg g⁻¹) than the two other species. Finally, *Q. pubescens* showed higher total phenolics content compared to *Q. ilex*, and the highest specific leaf area (133.13 mg g⁻¹) and water holding capacity (146.90 mg g⁻¹). *Pinus halepensis* showed higher water-soluble compounds (340.02 mg g⁻¹) and lower water holding capacity (113.89 mg g⁻¹).

Litter mass loss

After 357 days of decomposition, litter mass loss was statistically different among sites and plant species with interaction effects (Table 3). On average, significantly higher mass loss occurred at *Q. pubescens* forest (36.94%) in comparison with *Q. ilex* forest (33.88%) and *P. halepensis* forest (33.80%). Regarding the litter, *P. halepensis* (36.81%) and *Q. ilex* (35.07%) lost significantly

Table 3. ANOVA table of F-Ratio and P-values for the effects of forest sites (S), litter species (L) and drought conditions (D) on the mass loss, microbial biomass (actinobacteria, bacteria and fungi) and actinobacteria/fungi (A/F) and bacteria/fungi (B/F) ratios.

	df	Mass loss		Actino (A)		Bacteria (B)		Fungi (F)		A/F		B/F	
		F	P	F	P	F	P	F	P	F	P	F	P
Sites (S)	2	8.81	0.0008	33.92	<0.0001	8.86	0.0003	30.38	<0.0001	6.11	0.0030	11.78	<0.0001
Litter species (L)	2	8.11	0.0022	16.31	<0.0001	4.58	0.0122	2.41	0.0945	53.55	<0.0001	11.34	<0.0001
Drought (D)	1	3.70	0.0571	0.09	0.7602	1.91	0.1688	6.20	0.0143	12.08	0.0007	11.70	0.2828
SxL	4	7.03	<0.0001	5.69	0.0003	20.56	<0.0001	21.01	<0.0001	7.67	<0.0001	11.49	<0.0001
SxD	2	0.43	0.6488	3.00	0.0539	7.25	0.0011	3.82	0.0251	0.18	0.8368	5.43	0.0056
LxD	2	0.14	0.8724	3.83	0.0246	1.36	0.2593	1.12	0.3313	3.34	0.0392	0.11	0.8973
SxLxD	4	0.10	0.9839	1.11	0.3540	2.72	0.0335	1.45	0.2229	2.12	0.0836	1.17	0.3293

higher mass than *Q. pubescens* (32.72%). Concerning interactions, *P. halepensis* lost most of its mass at *Q. pubescens* and *P. halepensis* forests compared to the *Q. ilex* forest (Fig. 1A). No significant effect of rain exclusion was found on the litter mass loss (Table 3).

Microbial abundance and structure

Abundances of actinobacteria, total bacteria and fungi differed significantly according to forest sites, when control and amplified drought conditions were combined (Table 3, Fig. 1) The highest abundances of all microbial groups were observed at *P. halepensis* forest and lowest at *Q. ilex* forest. However, it differed according to plant litter species producing a site x species interaction effect (Table 3; Fig. 1). Actinobacteria and total bacteria had the highest abundance in *Q. ilex* litter and lowest in *P. halepensis* at *Q. ilex* and *P. halepensis* forests, respectively (Fig. 1B and C). Roughly, higher abundance of fungi was observed in *P. halepensis* litter at *Q. pubescens* forest, *Q. ilex* litter at *Q. ilex* forest and *Q. pubescens* litter at *P. halepensis* forest (Fig. 1D). Regarding the actinobacteria to fungi (A/F) ratio, it was significantly higher in *Q. pubescens* and *Q. ilex* litter and lower in *P. halepensis* litter at *Q. pubescens* and *Q. ilex* forests (Fig. 1E). Total bacteria to fungi (B/F) ratio was significantly higher in *Q. ilex* litter and lowest in *P. halepensis* litter, at *Q. ilex* and *P. halepensis* forests (Fig. 1F).

Overall, there was a significant increase of fungal abundance and a decrease of A/F ratio under amplified drought (AD) in comparison with natural conditions (Table 3). No main effect of drought conditions was observed for actinobacteria, total bacteria and bacteria to fungi (B/F) ratio (Table 3). However, an interaction effect was observed between site and drought conditions for total bacteria, fungi and total bacteria to fungi ratio (Table 3; see Supplementary Table 1, Supporting Information). Thus, we observed a significant increase of total bacterial (Fig. 2A) and fungal abundance (Fig. 2B) under AD conditions at the *P. halepensis* forest, and a decrease of B/F ratio in *Q. pubescens* forest (Fig. 2C).

DISCUSSION

In this study, we evaluated how reduction of rainfall and change in plant species may affect belowground microbial community's abundance and structure and consequently the litter decomposition process in three dominant Mediterranean forests of southern France. Our findings are that (i) actinobacteria and total bacteria were more affected by changes of plant species than by the decrease of water availability; (ii) fungi were positively impacted by the reduction of rainfall and (iii) the future arrival of *P. halepensis* litter to *Q. pubescens* and *Q. ilex* forest and rainfall

reduction could alter the relative proportion of fungi and bacteria in the community hence having implication in microbial decomposers activity.

Effects of litter quality on microbial communities and mass loss

Our results showed the importance of leaf litter initial litter with respect to microbial composition and litter mass loss dynamics. We observed higher abundance of actinobacteria and total bacteria in oak litter than in pine. This is in line with previous studies, which showed a preference of bacteria for high quality litter (i.e. low C/N, C/P, lignin: P and lignin/N ratio) (Hodge, Robinson and Fitter 2000; De Boer et al. 2005; Romani et al. 2006). Both oaks *Q. pubescens* and *Q. ilex* are characterised by high N and P content, which are efficiently utilised by bacterial enzymes (Romani et al. 2006) and then are consistently considered key factors in litter decomposition and good predictors of litter mass loss (Moro and Domingo 2000; Garcia-Pausas, Casals and Romanya 2004; Güsewell and Gessner 2009). However, our results only partially corroborate with this by showing that *Q. ilex* and *P. halepensis* litter had higher mass loss than *Q. pubescens*. That is possibly due to higher initial content of total phenolics determined in *Q. pubescens* compared to *Q. ilex*, which are known to inhibit litter microbial communities and N mineralisation, during the early stage of decomposition (Lambers 1993; Souto, Chiapusio and Pellissier 2000; Ormeño et al. 2006; Chomel et al. 2014). This may explain the lower mass loss of its litter in comparison with *Q. ilex* and *P. halepensis*. The high mass loss of *P. halepensis* litter may be also explained by the leaching of high content of water-soluble compounds (Tripathi and Singh 1992; Kaushal et al. 2012) and high Na content (Gressel et al. 1995), which both are known to positive correlated litter decay. Gressel et al. (1995) observed that salt accumulation in *P. halepensis* needles enhanced their breakdown compared to *Q. coccifera* leaves in a typical Mediterranean mixed woodland.

Effects of litter-site interaction on litter decomposition processes

The influence of plant species on litter decomposition varied according to the forest sites as shown by strong litter-site interaction. At *Q. pubescens* forest, we observed the highest abundance of fungi associated with *P. halepensis* litter, associated to a reduction of the A/F ratio. This is consistent with the findings by Hodge et al. (2000) and Wardle et al. (2004) who showed that fungi are favoured by litter with high C/N ratio. In addition, fungi

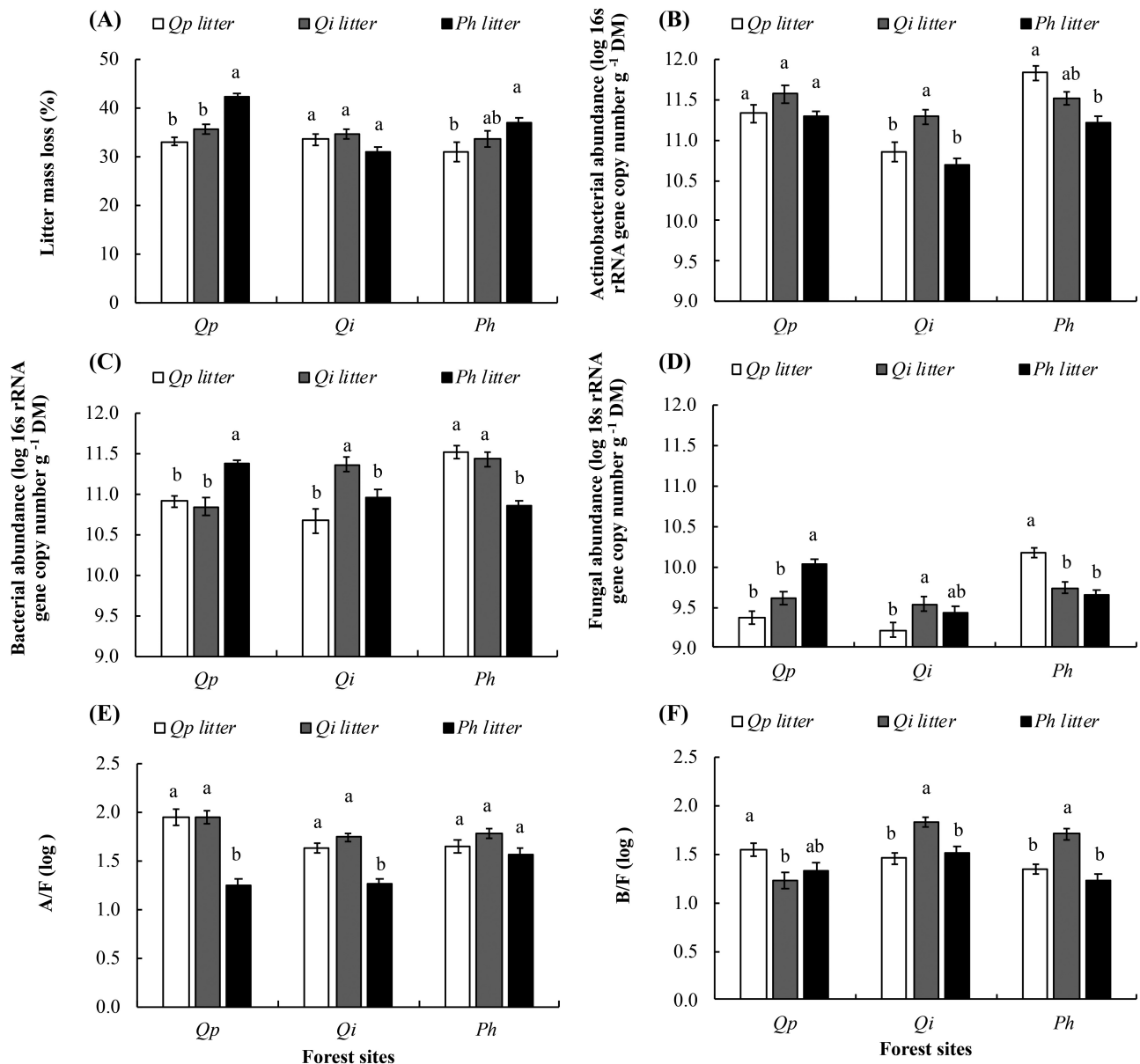


Figure 1. Leaf litter mass loss (A) and associated leaf litter microbial decomposers abundances (actinobacteria (B), bacteria (C), fungi (D)), actinobacteria to fungi (E) and bacteria to fungi (F) ratios, for the three forests and litter species (control and amplified drought conditions were combined). Values are mean \pm SE (n = 14). Different letters denote significant differences between litter species within forest sites (e.g. both drought conditions combined), with a > b > c. DM = litter dry mass. *Qp* = *Q. pubescens*, *Qi* = *Q. ilex*, *Ph* = *P. halepensis*.

are rather considered specialists and are more equipped enzymatically to assimilate recalcitrant material than more generalist bacteria (Møller, Miller and Kjølner 1999; Romaní et al. 2006). The high abundance of total bacteria observed in *P. halepensis* litter may be explained by the synergistic relationship between bacteria and fungi because bacteria may benefit by the presence of fungi, which may provide them resources that bacteria were not able to acquire on their own (Romaní et al. 2006). At *Q. ilex* forest, microorganisms were more numerous with *Q. ilex* litter in comparison with the two other species, which suggests the high specificity of decomposers for decomposing the autochthonous litter in this forest (Ayres et al. 2009). However, this difference in microbial abundance did not lead to a significant difference in mass loss of *Q. ilex* litter in its own forest

compared to the two other forests. This may due to the presence of decomposers able to use different sources of carbon. Decomposers can also develop preferences for some resources they are not used to (St John et al. 2011). Taking into account the three litter species, our results showed that *P. halepensis* forest had generally higher microbial abundance (actinobacteria, total bacteria and fungi) than other sites, possibly because this is the only mixed woodland out of the three studied forests and it was demonstrated that an increase of plant diversity promotes litter microbial growth (Chapman and Newman 2010; Santonja et al. 2017). Indeed, litter dissimilarity may decrease resource competition between functional groups and thus increase the abundance, activity, and hence efficiency of decomposers (Barbe et al. 2017).

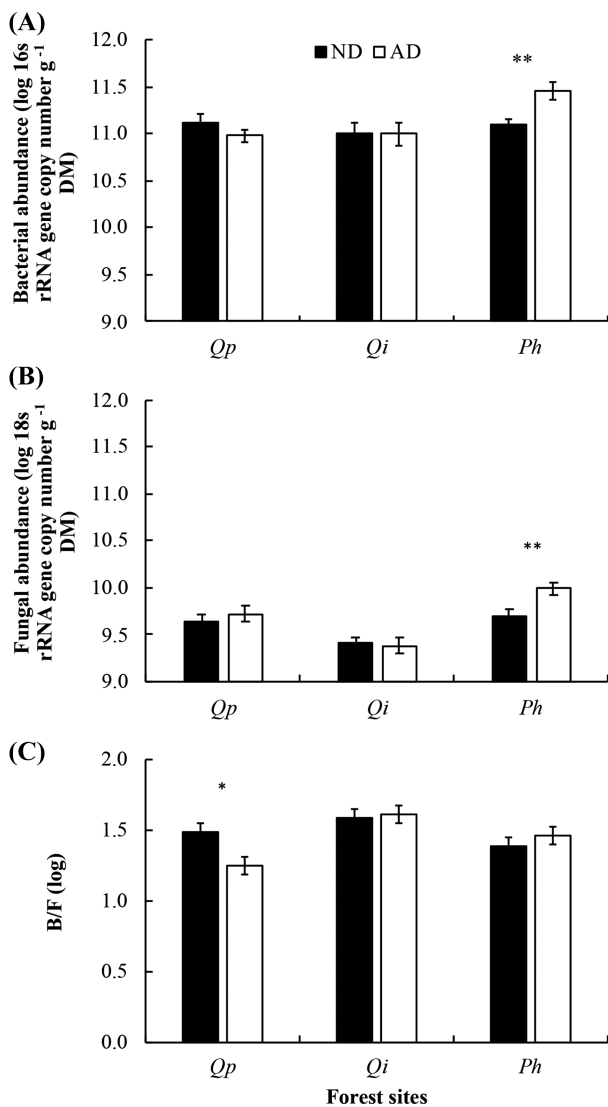


Figure 2. Effects of the two drought conditions (ND = natural drought; AD = amplified drought) on the total bacterial (A), fungal (B) abundances and bacteria to fungi ratio (C). Barplots are mean \pm SE. Significant effects are indicated with respective symbols * for $P < 0.05$ and ** for $P < 0.01$. *Qp* = *Q. pubescens*, *Qi* = *Quercus ilex*, *Ph* = *P. halepensis*.

Effects of rainfall reduction on litter mass loss and microbial community

Contrary to our expectations, amplified drought conditions (AD) had no effect on litter mass loss after 1 year of decomposition. This may be explained by the extremely dry year during which the study was performed (Saunier et al. 2018). Actinobacteria were not directly affected by AD conditions, contrary to previous studies (Bouskill et al. 2013; Felsmann et al. 2015). Nevertheless, a reduction in the A/F ratio was observed, probably due to the positive effect of AD conditions on fungal abundance. The increase of fungal abundance under drier conditions was also observed in other Mediterranean forests (Hawkes et al. 2011; Sherman, Sternberg and Steinberger 2012; Allison et al. 2013; Alster et al. 2013). It is well recognised that fungi are more resistant to drought than bacteria (De Vries and Shade 2013; Guhr et al. 2015) and might get competitive advantage over bacteria during dry periods (Six 2012; Yuste et al. 2011). Moreover, the

expansion of fungal hyphae reported by some studies under drought periods (Allison et al. 2013; Zeglin et al. 2013) may result from the reduction of predatory pressure (i.e. grazers activity or number) under water stressed conditions (Davet 2004; Bapiri, Bååth and Rousk 2010; Barnard, Osborne and Firestone 2013). The observed decrease of the A/F ratio under AD conditions in *Q. pubescens* litter was possibly related to the persistence of phenolics due to the decrease of leaching processes under AD conditions, which delayed microbial colonisation by decomposers in that litter (Chomel et al. 2014). Contrary to fungi, total bacteria were not affected by changes in drought conditions. Bacterial biomass stability under drought was also observed by Hartmann et al. (2017), and it was explained by independence of bacteria on water film for dispersal (Mohammadipanah and Wink 2016). Nevertheless, those results varied according to forest site and litter type. For example, in the *P. halepensis* forest, an increase of total bacteria biomass was observed under AD conditions, which may be explained by (i) natural selection of the most drought-tolerant bacterial groups (Barnard, Osborne and Firestone 2013) and/or (ii) bacteria resilience to drought resulting from their predominating r-selected life strategy, which enables rapid recovery after a period of disturbance (i.e. drought) (Barnard, Osborne and Firestone 2013; Meisner, Rousk and Bååth 2015).

CONCLUSIONS

Our results showed that microbial litter decomposers respond differently to intensification of water stress conditions in the Mediterranean forests. Actinobacteria and total bacteria were more negatively affected by plant litter changes (*Q. ilex* and *Q. pubescens* higher than *P. halepensis*) than by the direct rainfall reduction. In contrary, fungal communities seemed to be more tolerant and even favored to water limitation. Also, the potential resilience of bacterial communities was proposed, while fungal response seemed to reflect a higher degree of adaptation to decreased water availability. Finally, the arrival of *P. halepensis* litter to a *Q. pubescens* and *Q. ilex* forest may change litter microbial communities, leading to a decrease of A/F and B/F ratios and promoting fungi and certain groups of bacteria, which are more capable of using complex carbon sources. Therefore, the intensification of drought conditions in Mediterranean forest may introduce a fungi dominated community over bacteria, by either the capability of degrading more recalcitrant litter or/and tolerance to future climate conditions.

SUPPLEMENTARY DATA

Supplementary data are available at [FEMSEC](https://www.femsec.org/) online.

ACKNOWLEDGMENTS

We thank all the people that contributed in the set-up of the experiment and in the field campaigns especially to Sylvie Dupouyet, Jean-Philippe Orts and Jean-Marc Ourcival. We thank to Anne Haguenaer from Endoume Marine Station (Marseille, France) for her efficient orientation in the lab and whole team of CRI—Crop Research Institute (Prague, Czech Republic)—for their unconditional help and support. The three experimental sites were annually supported by the research infrastructure AnaEE-France (ANR-11-INBS-0001) and by Allenvi through the SOERE F-ORE-T. We acknowledge the use of the COOPERATE database (Reiter IM, Castagnoli G, Rotureau A 2015 "Cooperate database", <https://cooperate.obs-hp.fr/db>) run by the CNRS

FR3098 ECCOREV and OSU-Pytheas with support from the Labex OT-Med. We also thank the French Region PACA and Europe for the PhD grant attributed to Susana Pereira.

AUTHOR CONTRIBUTIONS

SP, MM and VB wrote the manuscript. VB and CF conceived and designed the experiments. SP, AB, AA, and PM performed the experiments. SP, JK, MM, and VB analysed the data.

FUNDING

This research was financially supported by the Agence Nationale pour la Recherche (ANR) with the project SecPriMe2 (ANR-12-BSV7-0016-01), the BioDivMeX Mistrals program and partially by the Ministry of Education, Youth and Sports of the Czech Republic, European Regional Development Fund-Project No. CZ.02.1.01/0.0/0.0/16.019/0000845 and grant No. LTC17075 and Ministry of Agriculture of the Czech Republic, institutional support MZE-RO0418.

This work is a contribution to Labex OT-Med (ANR-11-LABX-0061) and has received funding from Excellence Initiative of Aix-Marseille University—A*MIDEX, a French 'Investissements d'Avenir' programme.

Conflict of interest. None declared.

REFERENCES

- Acosta-Martinez V, Cotton J, Gardner T et al. Predominant bacterial and fungal assemblages in agricultural soils during a record drought/heat wave and linkages to enzyme activities of biogeochemical cycling. *Appl Soil Ecol* 2014;**84**:69–82.
- Allison SD, Lu Y, Weihe C et al. Microbial abundance and composition influence litter decomposition response to environmental change. *Ecology* 2013;**94**:714–25.
- Alster CJ, German DP, Lu Y et al. Microbial enzymatic responses to drought and to nitrogen addition in a southern California grassland. *Soil Biol Biochem* 2013;**64**:68–79.
- Anandan R, Dharumadurai D, Manogaran GP. An introduction to actinobacteria. In: *Actinobacteria - Basics and Biotechnological Applications*. Intech, 2016.
- Ayres E, Steltzer H, Berg S et al. Soil biota accelerate decomposition in high-elevation forests by specializing in the breakdown of litter produced by the plant species above them. *J Ecol* 2009;**97**:901–12.
- Bapiri A, Bååth E, Rousk J. Drying–rewetting cycles affect fungal and bacterial growth differently in an arable soil. *Microb ecol* 2010;**60**:419–28.
- Barbe L, Jung V, Prinzing A et al. Functionally dissimilar neighbors accelerate litter decomposition in two grass species. *New Phytologist* 2017;**214**:1092–102.
- Barbero M, Bonin G, Loisel R et al. Changes and disturbances of forest ecosystems caused by human activities in the western part of the mediterranean basin. *Vegetatio* 1990;**87**:151–73.
- Barnard RL, Osborne CA, Firestone MK. Responses of soil bacterial and fungal communities to extreme desiccation and rewetting. *The ISME journal* 2013;**7**:2229.
- Bertrand R, Lenoir J, Piedallu C et al. Changes in plant community composition lag behind climate warming in lowland forests. *Nature* 2011;**479**:517.
- Bouskill NJ, Lim HC, Borglin S et al. Pre-exposure to drought increases the resistance of tropical forest soil bacterial communities to extended drought. *The ISME journal* 2013;**7**:384.
- Chapman SK, Newman GS. Biodiversity at the plant–soil interface: microbial abundance and community structure respond to litter mixing. *Oecologia* 2010;**162**:763–9.
- Chomel M, Fernandez C, Bousquet-Mélou A et al. Secondary metabolites of *Pinus halepensis* alter decomposer organisms and litter decomposition during afforestation of abandoned agricultural zones. *J Ecol* 2014;**102**:411–24.
- Cleveland CC, Reed SC, Keller AB et al. Litter quality versus soil microbial community controls over decomposition: a quantitative analysis. *Oecologia* 2014;**174**:283–94.
- Davet P. *Microbial Ecology of Soil and Plant Growth*. Boca Raton: CRC Press, 2004.
- De Boer W, Folman LB, Summerbell RC et al. Living in a fungal world: impact of fungi on soil bacterial niche development. *FEMS Microbiol Rev* 2005;**29**:795–811.
- De Vries FT, Shade A. Controls on soil microbial community stability under climate change. *Front microbiol* 2013;**4**:265.
- Dorn-In S, Bassitta R, Schwaiger K et al. Specific amplification of bacterial DNA by optimized so-called universal bacterial primers in samples rich of plant DNA. *J microbiol meth* 2015;**113**:50–6.
- Felsmann K, Baudis M, Gimbel K et al. Soil bacterial community structure responses to precipitation reduction and forest management in forest ecosystems across Germany. *PLOS ONE* 2015;**10**:e0122539.
- Fierer N, Bradford MA, Jackson RB. Toward an ecological classification of soil bacteria. *Ecology* 2007;**88**:1354–64.
- Folin O, Denis WA. Colorimetric method for the determination of phenols (and phenol derivatives) in urine. *J Biol Chem* 1915;**22.2**:305–8.
- Fortunel C, Garnier E, Joffre R et al. Leaf traits capture the effects of land use changes and climate on litter decomposability of grasslands across Europe. *Ecology* 2009;**90**:598–611.
- Fredriksson NJ, Hermansson M, Wilén B-M. The choice of PCR primers has great impact on assessments of bacterial community diversity and dynamics in a wastewater treatment plant. *PLOS ONE* 2013;**8**:e76431.
- Garcia-Pausas J, Casals P, Romanya J. Litter decomposition and faunal activity in Mediterranean forest soils: effects of N content and the moss layer. *Soil Biol Biochem* 2004;**36**:989–97.
- Garcia-Pausas J, Paterson E. Microbial community abundance and structure are determinants of soil organic matter mineralisation in the presence of labile carbon. *Soil Biol Biochem* 2011;**43**:1705–13.
- Gessner MO, Swan CM, Dang CK et al. Diversity meets decomposition. *Trends ecol evol* 2010;**25**:372–80.
- Gholz HL, Wedin DA, Smitherman SM et al. Long-term dynamics of pine and hardwood litter in contrasting environments: toward a global model of decomposition. *Glob Change Biol* 2000;**6**:751–65.
- Giorgi F, Lionello P. Climate change projections for the Mediterranean region. *Global Planet Change* 2008;**63**:90–104.
- Gressel N, Inbar Y, Singer A et al. Chemical and spectroscopic properties of leaf litter and decomposed organic matter in the Carmel Range, Israel. *Soil Biol Biochem* 1995;**27**:23–31.
- Guhr A, Borken W, Spohn M et al. Redistribution of soil water by a saprotrophic fungus enhances carbon mineralization. *P Natl A Sci* 2015;**112**:14647–51.
- Guiot J, Cramer W. Climate change: the 2015 paris agreement thresholds and Mediterranean basin ecosystems. *Science* 2016;**354**:465–8.
- Güsewell S, Gessner MO. N:P ratios influence litter decomposition and colonization by fungi and bacteria in microcosms. *Funct Ecol* 2009;**23**:211–9.

- Hartmann M, Brunner I, Hagedorn F et al. A decade of irrigation transforms the soil microbiome of a semi-arid pine forest. *Mol ecol* 2017;**26**:1190–206.
- Hawkes CV, Kivlin SN, Rocca JD et al. Fungal community responses to precipitation. *Glob Change Biol* 2011;**17**:1637–45.
- Hertig E, Trambly Y. Regional downscaling of Mediterranean droughts under past and future climatic conditions. *Global Planet Change* 2017;**151**:36–48.
- Hodge A, Robinson D, Fitter A. Are microorganisms more effective than plants at competing for nitrogen? *Trends plant sci* 2000;**5**:304–8.
- Hättenschwiler S, Jørgensen HB. Carbon quality rather than stoichiometry controls litter decomposition in a tropical rain forest. *J Ecol* 2010;**98**:754–63.
- IPCC. *Climate Change 2013 - The Physical Science Basis*. Cambridge: Cambridge University Press, 2014.
- Kaushal R, Verma KS, Chaturvedi OP et al. Leaf litter decomposition and nutrient dynamics in four multipurpose tree species. *Range Manag Agrofor* 2012;**33**:20–7.
- Kindworth A, Pruesse E, Schweer T et al. Evaluation of general 16S ribosomal RNA gene PCR primers for classical and next-generation sequencing-based diversity studies. *Nucleic acids res* 2013;**41**:e1–e1.
- Lambers H. Rising CO₂, secondary plant metabolism, plant-herbivore interactions and litter decomposition. In: *CO₂ and Biosphere*. Dordrecht: Springer, 1993, 263–71.
- Lewin GR, Carlos C, Chevrette MG et al. Evolution and ecology of Actinobacteria and their bioenergy applications. *Annu rev microbiol* 2016;**70**:235–54.
- Limousin JM, Rambal S, Ourcival JM et al. Modelling rainfall interception in a Mediterranean *Quercus ilex* ecosystem: lesson from a throughfall exclusion experiment. *J Hydrol* 2008;**357**:57–66.
- Lunghini D, Granito VM, Di Lonardo DP et al. Fungal diversity of saprotrophic litter fungi in a Mediterranean maquis environment. *Mycologia* 2013;**105**:1499–515.
- Manzoni S, Schimel JP, Porporato A. Responses of soil microbial communities to water stress: results from a meta-analysis. *Ecology* 2012;**93**:930–8.
- McCarthy AJ, Williams ST. Actinomycetes as agents of biodegradation in the environment: a review. *Gene* 1992;**115**:189–92.
- Meisner A, Rousk J, Bååth E. Prolonged drought changes the bacterial growth response to rewetting. *Soil Biol Biochem* 2015;**88**:314–22.
- Mohammadipanah F, Wink J. Actinobacteria from arid and desert habitats: diversity and biological activity. *Front microbiol* 2016;**6**:1541.
- Morales P, Hickler T, Rowell DP et al. Changes in European ecosystem productivity and carbon balance driven by regional climate model output. *Global Change Biol* 2007;**13**:108–22.
- Moro MJ, Domingo F. Litter decomposition in four woody species in a Mediterranean climate: weight loss, N and P dynamics. *Ann Bot* 2000;**86**:1065–71.
- Møller J, Miller M, Kjølner A. Fungal-bacterial interaction on beech leaves: influence on decomposition and dissolved organic carbon quality. *Soil Biol Biochem* 1999;**31**:367–74.
- Ogaya R, Peñuelas J. Tree growth, mortality, and above-ground biomass accumulation in a holm oak forest under a five-year experimental field drought. *Plant Ecol* 2007;**189**:291–9.
- Okoro CK, Brown R, Jones AL et al. Diversity of culturable actinomycetes in hyper-arid soils of the Atacama Desert, Chile. *Anton van Lee* 2009;**95**:121–33.
- Ormeño E, Baldy V, Ballini C et al. Effects of environmental factors and leaf chemistry on leaf litter colonization by fungi in a Mediterranean shrubland. *Pedobiologia* 2006;**50**:1–10.
- Peñuelas J, Estiarte M, Kimball BA et al. Variety of responses of plant phenolic concentration to CO₂ enrichment. *J Exp Bot* 1996;**47**:1463–7.
- Peñuelas J, Rico L, Ogaya R et al. Summer season and long-term drought increase the richness of bacteria and fungi in the foliar phyllosphere of *Quercus ilex* in a mixed Mediterranean forest. *Plant Biol* 2012;**14**:565–75.
- Pfeiffer S, Pastar M, Mitter B et al. Improved group-specific primers based on the full SILVA 16S rRNA gene reference database. *Environ Microbiol* 2014;**16**:2389–407.
- Rastogi G, Tech JJ, Coaker GL et al. A PCR-based toolbox for the culture-independent quantification of total bacterial abundances in plant environments. *J Microbiol Meth* 2010;**83**:127–32.
- R Core Team. R: A language and environment for statistical computing. 2017. <https://www.R-project.org/>
- Romaní AM, Fischer H, Mille-Lindblom C et al. Interactions of bacteria and fungi on decomposing litter: differential extracellular enzyme activities. *Ecology* 2006;**87**:2559–69.
- Sagova-Mareckova M, Omelka M, Cermak L et al. Microbial communities show parallels at sites with distinct litter and soil characteristics. *Appl Environ Microbiol* 2011;**77**:7560–7.
- Santonja M, Baldy V, Fernandez C et al. Potential shift in plant communities with climate change: outcome on litter decomposition and nutrient release in a Mediterranean oak forest. *Ecosystems* 2015b;**18**:1253–68.
- Santonja M, Fernandez C, Gauquelin T et al. Climate change effects on litter decomposition: intensive drought leads to a strong decrease of litter mixture interactions. *Plant and Soil* 2015a;**393**:69–8.
- Santonja M, Rancon A, Fromin N et al. Plant litter diversity increases microbial abundance, fungal diversity, and carbon and nitrogen cycling in a Mediterranean shrubland. *Soil Biol Biochem* 2017;**111**:124–34.
- Saunier A, Ormeño E, Havaux M et al. Resistance of native oak to recurrent drought conditions simulating predicted climatic changes in the Mediterranean region. *Plant Cell Environ* 2018;**41**:2299–312.
- Schimel J, Balsler TC, Wallenstein M. Microbial stress-response physiology and its implications for ecosystem function. *Ecology* 2007;**88**:1386–94.
- Sherman C, Sternberg M, Steinberger Y. Effects of climate change on soil respiration and carbon processing in Mediterranean and semi-arid regions: an experimental approach. *Eur J Soil Biol* 2012;**52**:48–58.
- Six J. Fungal friends against drought. *Nat Clim Change* 2012;**2**:234–5.
- Souto XC, Chiapusio G, Pellissier F. Relationships between phenolics and soil microorganisms in spruce forests: significance for natural regeneration. *J Chem Ecol*. 2000;**26**:2025–34.
- St. John MG, Orwin KH, Dickie IA. No “home” versus “away” effects of de-composition found in a grassland-forest reciprocal litter transplant study. *Soil Biol Biochem* 2011;**43**:1482–9.
- Strickland MS, Lauber C, Fierer N et al. Testing the functional significance of microbial community composition. *Ecology* 2009;**90**:441–51.
- Swift MJ, Heal OW, Anderson JM et al. *Decomposition in Terrestrial Ecosystems*. Berkeley: University of California Press, 1979.

- Tripathi SK, Singh KP. Nutrient immobilization and release patterns during plant decomposition in a dry tropical bamboo savanna, India. *Biol Fert Soils* 1992;**14**:191–9.
- Vainio EJ, Hantula J. Direct analysis of wood-inhabiting fungi using denaturing gradient gel electrophoresis of amplified ribosomal DNA. *Mycol Res* 2000;**104**:927–36.
- Van Soest PJ, Wine RH. Use of detergents in the analysis of fibrous feeds: IV. Determination of plant cell-wall constituents. *J of official analytical chemists* 1967;**50**: 50–5.
- Wardle DA, Bardgett RD, Klironomos JN et al. Ecological linkages between aboveground and belowground biota. *Science* 2004;**304**:1629–33.
- Wardle DA, Van der Putten WH. Biodiversity, ecosystem functioning and above-ground-below-ground linkages. *Biodiversity and Ecosystem Functioning: Synthesis and Perspectives* 2002.
- Xu X, Thornton PE, Post WM. A global analysis of soil microbial biomass carbon, nitrogen and phosphorus in terrestrial ecosystems. *Global Ecol Biogeogr* 2013;**22**:737–49.
- Yuste JC, Peñuelas J, Estiarte M et al. Drought-resistant fungi control soil organic matter decomposition and its response to temperature. *Global Change Biol* 2011;**17**:1475–86.
- Zeglin LH, Bottomley PJ, Jumpponen A et al. Altered precipitation regime affects the function and composition of soil microbial communities on multiple time scales. *Ecology* 2013;**94**:2334–45.

1 **Supplementary information for**

2

3 **Litter traits and rainfall reduction alter microbial litter decomposers: the evidence from**
4 **three Mediterranean forests**

5

6 S. Pereira¹, A. Burešová^{2,3,4}, J. Kopecký⁵, P. Mádrová⁵, A. Aupic-Samain¹,

7 C. Fernandez¹, V. Baldy¹, and M. Sagova-Mareckova⁵

8

9 ¹Aix Marseille Univ, Avignon Université, CNRS, IRD, IMBE UMR 7263, Marseille, France,

10 ²Department of Ecology, Faculty of Science, Charles University in Prague, Vinicna 7, Prague,
11 Czech Republic,

12 ³Ecologie Microbienne, Université Claude Bernard Lyon 1, UMR CNRS 5557, INRA 1418,
13 Villeurbanne, France,

14 ⁴Laboratory for Diagnostics and Epidemiology of Microorganisms, Crop Research Institute,
15 Drnovska 507, CZ-16106 Prague 6, Ruzyně, Czech Republic and

16 ⁵Czech University of Life Sciences, Faculty of Agrobiolgy, Food and Natural Resources,
17 Department of Microbiology, Nutrition and Dietetics, Kamýcká 129, 165 00 Praha 6 -
18 Suchbátka, Czech Republic

19

20

21

22

23

24

25

26 **Supplementary Table 1** - Summary table of microbial abundance (expressed as 10^{10} gene
27 copy number g^{-1} litter dry mass) for each litter species at each forest site and drought condition
28 (ND = Natural drought; AD = amplified drought). One-way ANOVAs were performed for
29 differences among litter species per drought condition and forest site. F-Ratio are indicated and
30 P-values with the respective symbols * for $P < 0.05$, ** for $P < 0.01$, and *** for $P < 0.001$.
31 Different letters denote significant differences among litter species with $a > b$. T-tests was
32 performed to test the effect of drought conditions for each species at each forest site. T-test are
33 indicated and significant P-values ($P < 0.05$) are denoted in bold.

34

35

36

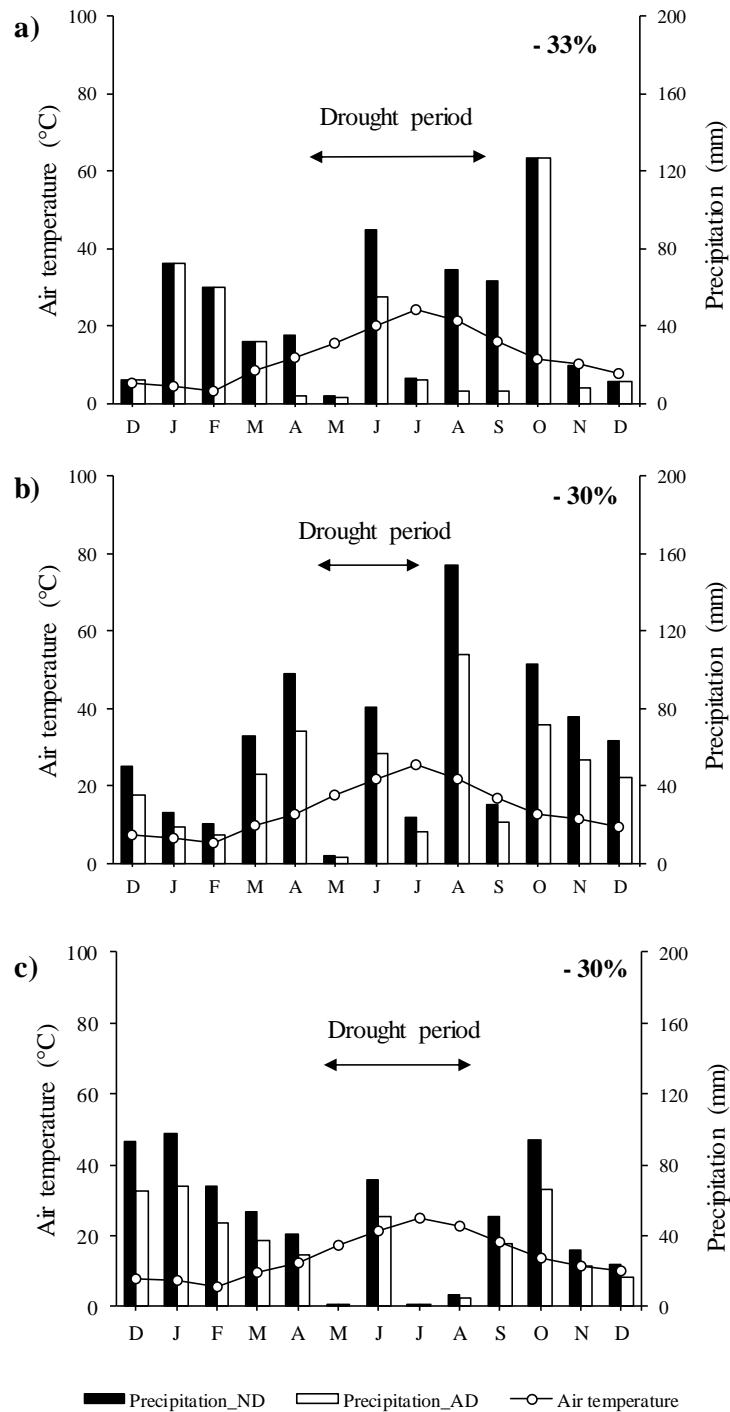
37

Little species

		Forest sites						
		<i>Q. pubescens</i>	<i>Q. ilex</i>	<i>P. halepensis</i>	F	P		
<i>Quercus pubescens</i>	Actinobacteria	ND	49.55 ± 17.89 ab	15.52 ± 4.23 b	74.75 ± 17.67 a	6.05	**	
		AD	17.27 ± 5.13 b	7.15 ± 2.94 b	85.62 ± 14.22 a	19.95	***	
		<i>t-test</i> <i>p-value</i>	-2.1757 ns	-1.9232 ns	0.93659 ns			
	Bacteria	ND	11.86 ± 3.10 a	10.41 ± 2.76 a	24.58 ± 4.25 a	33.51	ns	
		AD	8.12 ± 1.92 b	6.73 ± 3.94 b	53.70 ± 8.17 a	19.54	***	
		<i>t-test</i> <i>p-value</i>	-0.65657 ns	-1.3221 ns	2.7689 0.0176			
	Fungi	ND	0.30 ± 0.09 b	0.26 ± 0.05 b	1.08 ± 0.17 a	13.91	***	
		AD	0.33 ± 0.13 b	0.16 ± 0.05 b	2.26 ± 0.23 a	33.35	***	
		<i>t-test</i> <i>p-value</i>	0.089708 ns	-1.559 ns	4.1807 0.0018			
	Ratio A/F	ND	171.78 ± 40.21 a	58.32 ± 10.71 b	71.30 ± 18.25 b	5.60	*	
		AD	62.77 ± 14.26 a	38.00 ± 5.39 a	37.91 ± 5.47 a	2.34	ns	
		<i>t-test</i> <i>p-value</i>	-3.391 0.0054	-1.6586 ns	-1.5571 ns			
	Ratio B/F	ND	24.48 ± 4.57 a	48.18 ± 10.46 a	35.92 ± 6.42 a	1.91	ns	
		AD	32.56 ± 5.13 a	29.48 ± 7.56 a	23.59 ± 2.65 a	0.67	ns	
		<i>t-test</i> <i>p-value</i>	-0.91979 ns	-0.83125 ns	0.16864 ns			
	<i>Quercus ilex</i>	Actinobacteria	ND	63.26 ± 18.05 a	30.64 ± 8.66 a	28.44 ± 6.39 a	0.94	ns
			AD	39.9 ± 10.89 ab	19.45 ± 5.14 b	50.03 ± 8.88 a	5.33	*
			<i>t-test</i> <i>p-value</i>	-0.47229 ns	-0.63645 ns	1.8596 ns		
Bacteria		ND	18.66 ± 12.96 a	35.92 ± 9.87 a	17.00 ± 2.31 a	0.01	ns	
		AD	7.27 ± 1.92 b	24.97 ± 5.84 b	55.01 ± 11.58 a	15.89	***	
		<i>t-test</i> <i>p-value</i>	-0.56905 ns	-0.44153 ns	3.4846 0.0061			
Fungi		ND	0.47 ± 0.14 a	0.47 ± 0.12 a	0.39 ± 0.06 a	29.61	ns	
		AD	0.54 ± 0.09 a	0.41 ± 0.14 a	0.90 ± 0.17 a	4.00	*	
		<i>t-test</i> <i>p-value</i>	0.9151 ns	-0.34763 ns	3.2994 0.0073			
Ratio A/F		ND	129.45 ± 22.32 a	63.52 ± 9.21 b	72.76 ± 11.76 b	38.21	*	
		AD	70.58 ± 12.05 a	53.67 ± 5.53 a	59.00 ± 6.49 a	0.83	ns	
		<i>t-test</i> <i>p-value</i>	-2.2672 0.0445	-0.78997 ns	-0.45703 ns			
Ratio B/F		ND	29.55 ± 10.32 b	77.12 ± 15.33 a	46.96 ± 7.00 ab	7.28	**	
		AD	12.96 ± 2.31 b	73.53 ± 14.96 a	64.72 ± 12.05 a	27.71	***	
		<i>t-test</i> <i>p-value</i>	-1.9048 ns	-0.19647 ns	1.2028 ns			
<i>Pinus halepensis</i>		Actinobacteria	ND	17.53 ± 5.56 a	5.57 ± 1.79 b	17.98 ± 4.8 a	5.73	*
			AD	27.18 ± 2.79 a	6.58 ± 1.44 b	23.74 ± 7.53 a	14.48	***
			<i>t-test</i> <i>p-value</i>	1.5554 ns	0.43757 ns	0.64576 ns		
	Bacteria	ND	32.19 ± 4.07 a	6.59 ± 1.86 b	5.77 ± 0.89 b	29.41	***	
		AD	19.02 ± 1.91 a	17.52 ± 3.94 a	10.85 ± 0.82 a	29.38	ns	
		<i>t-test</i> <i>p-value</i>	-2.88 0.0185	2.7371 0.0228	2.5945 0.0291			
	Fungi	ND	1.01 ± 0.1 a	0.23 ± 0.05 b	0.41 ± 0.07 b	15.48	***	
		AD	1.47 ± 0.41 a	0.41 ± 0.07 b	0.59 ± 0.08 b	9.75	**	
		<i>t-test</i> <i>p-value</i>	0.97788 ns	2.1384 ns	1.7302 ns			
	Ratio A/F	ND	17.56 ± 5.16 b	22.63 ± 1.88 ab	45.56 ± 9.66 a	7.50	**	
		AD	24.90 ± 5.37 a	16.79 ± 3.51 a	43.48 ± 13.61 a	30.13	ns	
		<i>t-test</i> <i>p-value</i>	0.98631 ns	-1.4713 ns	-0.1249 ns			
	Ratio B/F	ND	32.42 ± 3.27 a	28.16 ± 3.91 ab	19.43 ± 6.12 b	4.24	*	
		AD	18.67 ± 5.31 b	44.85 ± 7.37 a	19.67 ± 3.29 b	6.13	**	
		<i>t-test</i> <i>p-value</i>	-2.2045 ns	2.0002 ns	0.034746 ns			

40

41



42

43 **Supplementary Figure 1** – Ombrothermic diagrams at a) O₃HP, b) Puéchabon and c) Font-

44 Blanche study sites between December 2014 to December 2015. Bar represents the mean

45 monthly precipitation (mm) in black (ND= natural drought) and in white (AD = amplified

46 drought). The curve represents the mean monthly temperature (°C). At each forest site, drought

47 period is indicated by the horizontal arrow and the percentage represents the proportion of
48 excluded rain compared to the natural drought plot.

49

50

51

52

53

54

55

56

57

58

59

60

61

62

63

64

65

66

67

68

69

a)



b)



c)



70

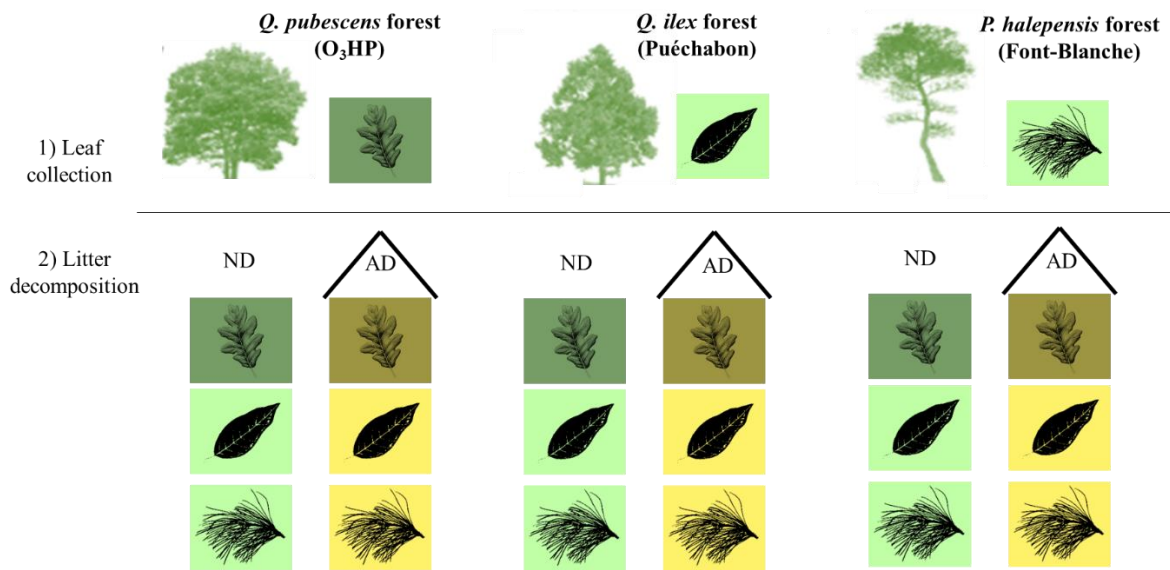
71 **Supplementary Figure 2** – Rain exclusion devices in the three forest studies (a) *Q.*

72 *pubescens* forest at O₃HP, (b) *Quercus ilex* at Puéchabon and (c) *P. halepensis* at Font-

73 Blanche.

74

75



76

77

78 **Supplementary Figure 3** - Litterbags experimental design: 1) leaf litter of the three tree
 79 species (*Q. pubescens*, *Q. ilex* and *P. halepensis*) coming from natural drought (ND) were
 80 redistributed and placed 2) in the three different forests (O₃HP, Puéchabon and Font-Blanche,
 81 respectively), under natural drought (ND) and amplified drought (AD) conditions .

82

83

84

Appendix

Curriculum vitae Mgr. Ing. Andrea Burešová

Date of birth: 28th May, 1991

Contact: Něvská 583, Praha 9, 196 00, Czech Republic

Phone: +420 775 931 831

E-mail: Andrea.Buresova@seznam.cz

Current positions

- **Young researcher** at research team Epidemiology and Ecology of Microorganisms
Crop Research Institute in Prague
Czech Republic
- **Ph.D. student** (Cotutelle)
Charles University in Prague and University Claude Bernard Lyon 1

Education

September 2015 - February 2021: PhD. in Microbial Ecology (Cotutelle)

Thesis title: Actinobacteria communities in natural and anthropogenic environments

Department of Ecology, Faculty of Science, Charles University in Prague (CZ)

Supervisor: RNDr. Marketa Sagova-Mareckova, PhD.

Microbial Ecology, doctoral school Evolution, Ecosystèmes, Microbiologie et Modélisation, University Claude Bernard Lyon 1 (FR)

Supervisor: Prof. Veronica Rodriguez-Nava

September 2013 – May 2016: M.Sc. in Waste Use and Management

Czech University of Life Sciences in Prague

Thesis Title: The effect of sulfur compounds on mercury mobility and activity of microorganisms in soil

Supervisor: prof. Ing. Jiřina Száková, CSc.

September 2013 – May 2015: M.Sc. in Ecology, Department of Ecology

Faculty of Science, Charles University in Prague

Thesis Title: Composition and activity of microbial community during decomposition of plant litter on two contrasting localities

Supervisor: RNDr. Marketa Sagova-Mareckova, PhD.

September 2010 – September 2013: B.Sc. in Soil science in Ecology and Environmental protection

Faculty of Science, Charles University in Prague

Thesis Title: Bioturbation and its role in soil formation

Supervisor: Prof. Ing. Mgr. Jan Frouz, CSc

Scholarships

- **May 2017** - French Government scholarship for Cotutelle studies
- **April 2016** – French Government scholarship for scientific internship
- **December 2014** – Merit scholarship at Charles University in Prague

Publications

2019

Buresova A., Kopecky J., Hrdinkova V., Kamenik Z., Omelka M. and Sagova-Mareckova M., (2019), Succession of Microbial Decomposers Is Determined by Litter Type, but Site Conditions Drive Decomposition Rates, *Applied and Environmental Microbiology*, 85 (24): e01760-19

Pereira S., **Buresova A.**, Kopecky J., Madrova P., Aupic-Samain A., Fernandez C., Baldy V. and Sagova-Mareckova M., (2019), Litter traits and rainfall reduction alter microbial litter decomposers: the evidence from three Mediterranean forests, *FEMS Microbiology Ecology*, 95 (12): fiz168

2016

Sagova-Mareckova M, Zádorová T, Penížek V, Omelka M, Tejnecký V, Pruchova P, Chuman T, Drábek O, **Burešová A**, Vaněk A, Kopecky J, (2016), The structure of microbial communities along two vertical profiles of a deep colluvial soil, *Soil Biology and Biochemistry*, 101, 65-73

Száková J, **Burešová A**, Praus L, García-Sánchez M, Holečková Z, Gabriel J, Sysalová J, Komárek J, Grohová J, Tlustoš P, (2016), The response of mercury (Hg) transformation in soil on sulfur and sulfur-rich biowaste application, *Environmental Earth Sciences*, 75:584

2013

Frouz J, Jílková V, Cajthaml T, Pižl V, Tajovský K, Háněl K, **Burešová A**, Šimáčková H, Kolaříková K, Franklin J, Nawrot J, Groninger JW, Stahl PD. 2013. Soil biota in post-mining sites along a climatic gradient in the USA: Simple communities in shortgrass prairie recover faster than complex communities in tallgrass prairie and forest, *Soil Biology and Biochemistry*, 57, 212 – 225.

Contributions at scientific meetings and conferences

December 2020: Poster presentation at international conference ACTINO 2020 (online conference)

June 2019: Poster presentation at international conference FEMS 2019 in Glasgow, Scotland

May 2017: Oral presentation at ISME Meeting of Young Soil Microbial Ecologists, Prague

December 2015: Poster presentation at international conference Ecology of Soil Microorganisms, Prague, Czech Republic

Scientific internship

October 2017 - December 2017: Ben-Gurion University of the Negev, Israel

Research topic: Bacterial response to altered precipitation regimes in desert soil

June 2016 – July 2016: Microbial Ecology, Université Claude Bernard Lyon 1, France

Research topic: Phylogenetic diversity of *Actinobacteria* colonizing Paleolithic wall paintings of Lascaux Cave, France

Main research interests

- Ecology of terrestrial *Actinobacteria* (soil, caves)
- Microbial decomposition of organic matter and extracellular enzyme production in soil

Methods experience

DNA, RNA extraction, PCR, qPCR, ddPCR, cloning, sequencing, primer design

Extracellular hydrolytic and oxidative enzyme activity assessment in soil and plant substrate

Working with microbial cultures, *Actinobacteria* isolation

Fumigation and microbial biomass carbon extraction

Extraction of low molecular weight substances for HPLC analysis

Bioinformatic analysis of microbial community: next-generation sequencing, taxonomic database design, molecular markers evaluation, phylogenetic analysis (Mothur, UPARSE, MEGA, Galaxy)

Statistical data analysis (STATISTICA, Past, Canoco, R)

Other qualifications

Languages: English (B2)

French (B1)

Driving license B category